THE PROCEEDINGS OF THE PHYSICAL SOCIETY

VOL. 51, PART 2 1 March 1939 No. 284

CONTENTS

	PAGE
L. C. TYTE. The rate of viscous flow of metals. Part 2: lead	203
G. P. BARNARD. The spectral sensitivity of selenium rectifier photoelectric cells	222
R. JACKSON and A. G. QUARRELL. Apparatus for electron-diffraction at high temperatures	237
D. BROWN. Acoustic spectra obtained by the diffraction of light from sound films	244
M. BOUND and D. A. RICHARDS. A study of the atmospheric oxidation of metals and alloys at different temperatures by electron-diffraction	256
R. F. BARROW. Ultra-violet band systems of silicon monoselenide and monotelluride	267
W. W. BARKAS. Analysis of light scattered from a surface of low gloss into its specular and diffuse components	274
D. KEMPERER and W. D. WRIGHT. The investigation of electron lenses	296
C. W. OATLEY. The adsorption of oxygen and hydrogen on platinum and the removal of these gases by positive-ion bombardment	318
H. G. HOWELL and G. D. ROCHESTER. The band spectrum of antimony fluoride (SbF)	329
L. F. BROADWAY and A. F. PEARCE. Emission of negative ions from oxide cathodes	335
J. R. BRISTOW. The conductivity of thin films of thallium on a pyrex glass surface	349
R. L. SEN GUPTA. The scattering of fast β particles by xenon nuclei	355
Discussion on electroacoustics	359
Discussion: The investigation of electron lenses	376
Reviews of books	378

Price to non-Fellows 7/- net; post free 7/5

Annual subscription 35/- post free, payable in advance

Published by

THE PHYSICAL SOCIETY

1 Lowther Gardens, Exhibition Road

London, S.W.7

Printed at

THE UNIVERSITY PRESS, CAMBRIDGE

THE PHYSICAL SOCIETY

OFFICERS OF THE SOCIETY, 1938–39:

President:—A. FERGUSON, M.A., D.Sc., F.Inst.P.

Hon. Secretaries:
W. JEVONS, D.Sc., Ph.D., F.Inst.P. (*Business*).
J. H. AWBERY, B.A., B.Sc., F.Inst.P. (*Papers*).

Office of the Society:—1 *Lowther Gardens, Exhibition Road, London, S.W.7.*

Hon. Foreign Secretary:—Prof. O. W. RICHARDSON, M.A., D.Sc., F.R.S.

Hon. Treasurer:—C. C. PATERSON, O.B.E., D.Sc., M.I.E.E., F.Inst.P.

Hon. Librarian:—J. H. BRINKWORTH, D.Sc., A.R.C.S., F.Inst.P.

Editor of the Proceedings:—Capt. C. W. HUME, M.C., B.Sc.,
284 *Regent's Park Road, Finchley, N.3.*

Assistant Secretary:—Miss J. I. DENNIS.

All communications, other than those to the Editor, should be sent to the office of the Society, viz. 1 Lowther Gardens, Exhibition Road, London, S.W.7.

INSTRUCTIONS TO AUTHORS

NOTE. The acceptance of a paper for publication in the Proceedings rests with the Council, advised by its Editing Committee. The high cost of printing renders it imperative to exclude matter that is not novel and not of importance to the understanding of the paper.

Authors offering original contributions for publication in the Proceedings should observe the following directions; failure to comply with these may cause considerable delay in publication.

Manuscript.—A clear and concise style should be adopted, and the utmost brevity consistent with effective presentation of the original subject-matter should be used. The copy should be easily legible, preferably typewritten and double-spaced. It should receive a careful final revision before communication, since alterations are costly when once the type has been set up. Mathematical expressions should be set out clearly, in the simplest possible notation.

References.—In references to published papers the author's initials and name followed by the title of the journal in italics, volume, page and year should be given thus: *Proc. Phys. Soc.* **43**, 199 (1931). The abbreviations given in the *World List of Scientific Periodicals* should be employed.

Drawings and tables.—Diagrams must be carefully drawn in Indian ink on white paper or card. Their size and thickness of line must be sufficient to allow of reduction. *Lettering and numbering should be in pencil,* to allow of printing in a uniform style. The number of diagrams should be kept down to the minimum. Photographs of apparatus are not ordinarily accepted. Data should in general be presented in the form of either curves or tables, but not both. Footlines descriptive of figures, and headlines indicative of contents of tables, should be supplied. *Sheets should not be larger than foolscap.*

Abstracts.—Every paper must be accompanied by an abstract in duplicate, brief but sufficient to indicate the scope of the paper and to summarize all novel results.

Proofs.—Proofs of accepted papers will be forwarded to authors. They should be returned promptly with errors corrected, but additions to or other deviations from the original copy should be avoided.

Reprints.—Fifty copies of printed papers will be supplied gratis. Extra copies may be purchased at cost price.

Contributions by non-Fellows.—Papers by non-Fellows must be communicated to the Society through a Fellow.

Republication.—Permission to reproduce papers or illustrations contained therein may be granted by the Council on application to the Hon. Secretaries.

THE PROCEEDINGS OF THE PHYSICAL SOCIETY

VOL. 51, PART 2 1 *March* 1939 NO. 284

THE RATE OF VISCOUS FLOW OF METALS. PART 2: LEAD

BY L. C. TYTE, B.SC., PH.D., F.INST.P.
Ballistics Directorate, Research Department, Woolwich

Received 9 *August* 1938. *Read in title* 25 *November* 1938

ABSTRACT. Experiments previously reported for tin have been extended to lead. It has been found that for very small extensions the velocity of viscous flow v is not completely independent of time. However, as soon as the non-viscous flow ceases to have appreciable effect, the velocity of viscous flow is connected with the stretching load P by an exponential relation for any given temperature and with the absolute temperature T by an exponential relation for any given load.

Relationships of the form

$$v = \delta e^{\beta PT - \alpha P + \gamma T},$$

where α, β, γ and δ are constants, have been obtained, from the {flow, load} curves, for the rate of viscous flow of lead, and the relations are probably of the type

$$v = K\{e^{\beta (P+P_0)(T-T_0)} - 1\},$$

where K, β, P_0 and T_0 are constants. Four sets of constants have been obtained, which can be attributed to (1) single or double glide in untwinned crystals, (2) single or double glide in twinned crystals, (3) extension during the recrystallization period and production of annealing twins and (4) extension when strain hardening is considerably diminished by self-annealing. The elastic limit, transition and breaking loads have been shown to be connected with the corresponding temperatures by hyperbolic expressions. Finally, the general behaviour of the lead wire has been shown to be in agreement with that for tin, and to be in line with the results obtained from single crystals.

§ 1. INTRODUCTION

THE earlier work on the present subject has already been indicated in a previous paper[1] describing experiments on tin. Andrade[2] has investigated the extension with time of lead, which occurs in three parts: (1) an immediate extension on loading, (2) an initial rate of flow (called the β flow), which decreases with time, and (3) the viscous flow, which remains constant. He found the relation between length and time to be

$$l = l_0 (1 + \beta t^{1/3}) e^{kt},$$

where l was the length at any time t, l_0 the immediate length on loading of unit

length and k and β constants. Experiments were performed for various loads and temperatures from $-180°$ C. to $162°$ C. At a given temperature, with increasing stress the constant β was found to tend to a constant value, while the constant k increased at a rate which itself increased to a constant value. Further, it appeared that the limit to which β tended with stress did not increase with the temperature.

Shoji[3] examined the flow of lead at air temperatures and found that the velocity of flow was a function of time, the initial velocity gradually falling to a final steady value. Both rates of flow satisfied the equation

$$v = a\,(P - P_0)\,e^{b\,(P-P_0)},$$

where P_0 was the elastic limit. In collaboration with Mashiyama the experiments were extended to $160°$ C.

The work described in the present paper is supplementary to the work on tin, and was undertaken to see if the same general type of phenomena occurred for other materials.

§ 2. EXPERIMENTAL METHOD

The apparatus used in this series of experiments was the same as that used for tin, with a single modification, which was necessary because with very large extensions the mirror-bearing lever became fixed between the rods. This difficulty was overcome by making the table P on the standard wire in the form of a cylindrical nut U working on a screw thread, figure 1 : thus the table could be raised or lowered as required while the lever was always maintained in a horizontal position.

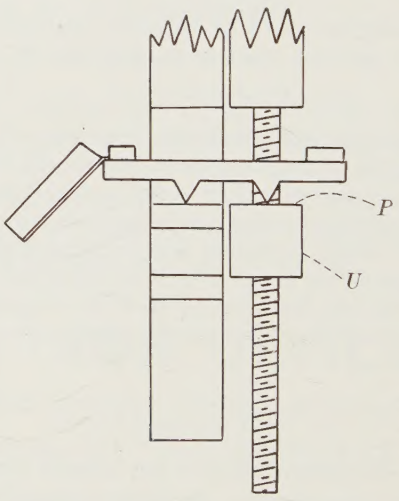

Figure 1.

The general outline of the method has already been given. Stretching experiments were performed on wire of 16 s.w.g. from air temperatures up to $300°$ C. at intervals of approximately $25°$ C., with load-increments of 100 g. from air temperature to $150°$ C. and of 50 g. from $175°$ C. to $300°$ C. For each load, extension readings were taken every 2 min.

The apparatus was capable of measuring variations in the length of the specimen to approximately four parts in a million, a scale deflection of 1 cm. being equivalent to an extension of the specimen of 0·001807 cm. The initial length of the specimen was 4·99 cm.

§ 3. EXPERIMENTAL RESULTS

The lead wire used was of density 11·15 g./cm.^{3} To anneal the wire it was suspended in the furnace with a load of 200 g. to keep it taut. It was then heated to 200° C. for a few minutes and allowed to cool slowly.

It was found that, as with tin at air temperature, a small load could be applied to the wire without causing any measurable viscous flow, but with loads exceeding a certain value viscous flow could be observed, the rate of flow increasing rapidly with further increase of load. With increasing temperature this critical load decreased until at 313° C. the wires collapsed under a weight of 51 g.

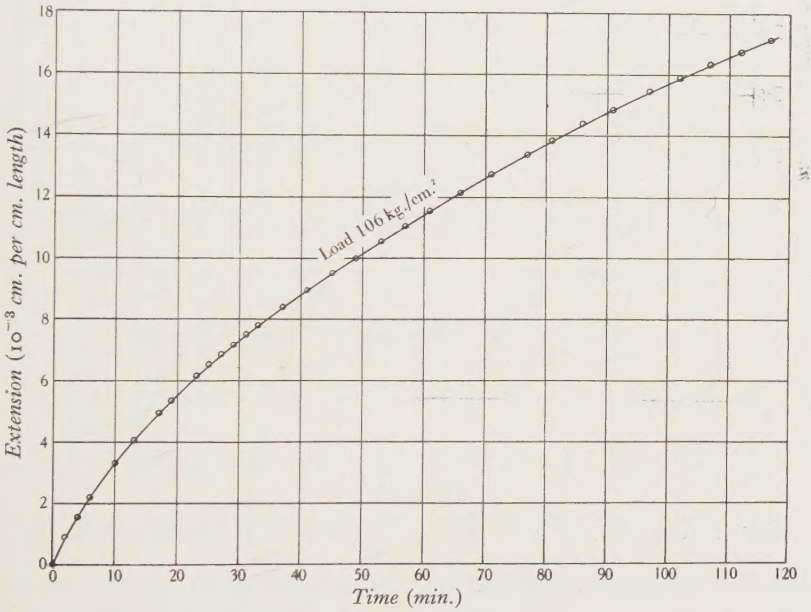

Figure 2. {Extension, time} curve for lead at air temperature.

The following three types of extension were obtained: (1) immediate elongation on loading, (2) subsequent flow decreasing with time, and (3) viscous extension. A few experiments were performed on lead at air temperatures over long time periods; a typical {extension, time} curve obtained for a load of 106 kg./cm.^{2} is given in figure 2. For large values of the time, the expression

$$l = l_0 (1 + \beta t^{1/3}) e^{kt}$$

reduces approximately to

$$l = Ae^{kt}$$

or, velocity of flow

$$v = \frac{dl}{dt} = kAe^{kt},$$

which agrees with the work of Geiss[4], who found from experiments on single crystals that the velocity of flow v can be expressed by the formula

$$v = Ae^{B(P-P_s)t}[e^{C(P-P_e)} - 1],$$

where P is the load, P_e the elastic limit, P_s the breaking load and A, B and C constants. This is of the form

$$v = Ke^{kt}$$

and the relation between $\log_{10} v$ and t should be linear. This conclusion is confirmed by figure 3 for the latter part of the curve when the β flow had died out. It must be remembered that the present experiments were made under constant load, while Andrade's were made under constant stress.

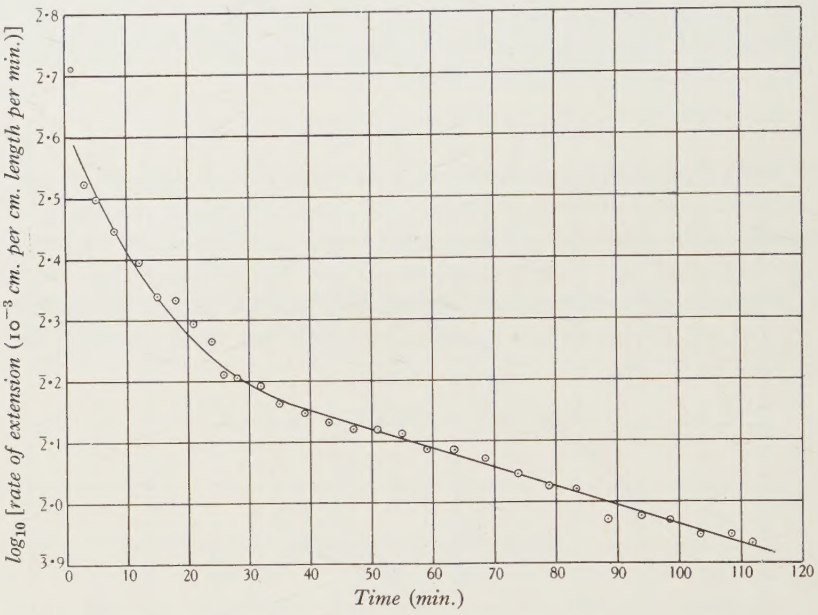

Figure 3. $\{\log_{10} v, t\}$ curve for lead at air temperature and load of 106 kg./cm.²

Although it has been established that the velocity of flow decays (or increases) exponentially with time as soon as the non-viscous flow has died out, it can be taken as linear without introducing serious error with regard to the main object of the experiments, which was to investigate the dependence of the velocity of flow on the load and temperature. This step was necessary because such comprehensive observations for each load as those mentioned above were impracticable in view of the time occupied by them. Thus in the normal mode of procedure the wire was loaded with the smallest load to be used and {time, extension} readings were taken for 20 min. after the rate of extension had become constant, and this rate was noted. The load was then increased and the experiment was repeated, these operations being continued until the wire broke.

The general type of {extension, time} curve obtained is shown in the following figures 4 and 5 for the experiment at 178° C., with the times as abscissae and the

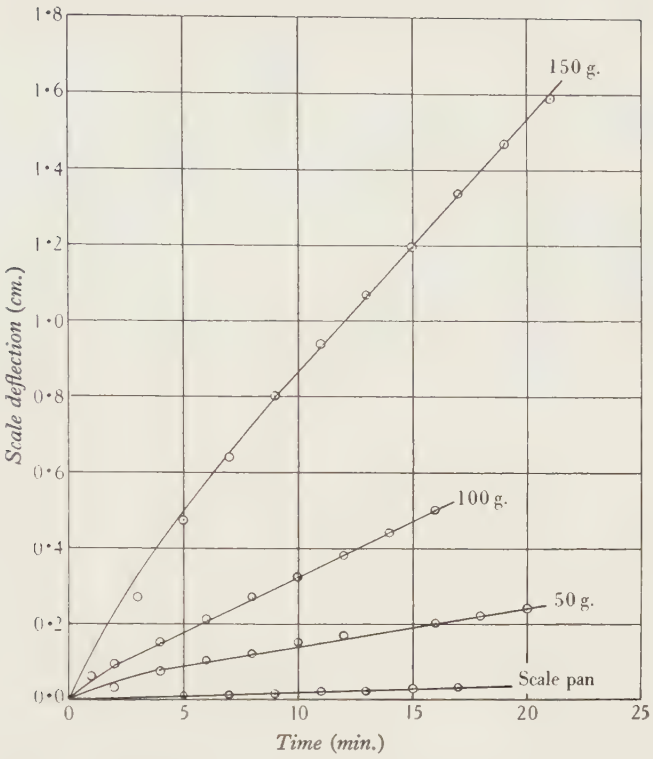

Figure 4. {Extension, time} curves at 178° C. for loads up to 150 g.

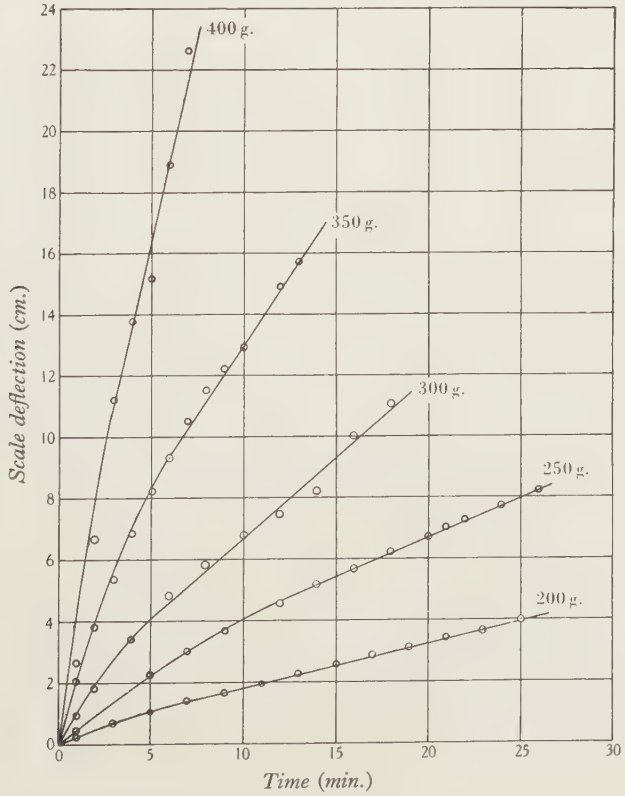

Figure 5. {Extension, time} curves at 178° C. for loads of 200 to 400 g.

extensions, in scale divisions, as ordinates. The curves show how quickly the flow dies out leaving the linear portion of the curve.

The diameter of each specimen was measured but it was found that the deviation of each specimen from the mean value for the series was so small that the mean values could be used for calculating the original cross-sectional area and the stress per unit area for any given load.

In table 1 the results are given for the experiments between air temperature and 150° C., and in table 2 for the experiments between 150° C. and 300° C. The load applied (g.), the stress (kg./cm^2) and the rate of viscous flow (cm./sec. per cm. of length) of the wire are given for each of the temperatures investigated.

Table 1

Exp. temp. (° C.)		18	50	77	99	126	148
Load (g.)	Stress (kg./cm^2)	Rate of extension (10^{-8} cm./sec. per cm. length)					
250	12·34	—	—	—	—	1·64	3·01
350	17·28	—	—	1·12	1·81	3·30	12·0
450	22·21	—	—	1·86	3·61	6·16	69·3
550	27·15	—	1·55	3·10	5·25	27·1	415
650	32·09	1·01	1·86	4·65	22·1	123	2126
750	37·03	1·32	3·10	7·75	85·5	276	9469
850	41·96	1·63	4·96	18·6	148	621	
950	46·90	2·26	6·20	77·5	342	1397	
1050	51·84	3·76	21·7	242	783		
1150	56·77	13·6	99·2	415			
1250	61·70	24·0	161	754			
1350	66·63	35·2	248	1497			
1450	71·57	52·8	465				
1550	76·50	111	744				
1650	81·46	142	1302				
1750	86·38	194	1762				
1850	91·33	326					

Table 2

Exp. temp. (° C.)		178	206	227	262	281	296
Load (g.)	Stress (kg./cm^2)	Rate of extension (10^{-8} cm./sec. per cm. length)					
150	7·40	1·50	3·01	9·04	21·7	72·9	169
200	9·87	6·02	7·05	31·0	95·2	389	1033
250	12·34	17·5	21·1	111	422		
300	14·81	40·2	64·4	391	1879		
350	17·28	85·6	144				
400	19·71	157	783				
450	22·21	310	1687				
500	24·68	548	7348				
550	27·15	1499					

If the rate of flow is plotted against the corresponding load for each temperature examined, the resulting curves show all the general characteristics found previously for tin and are more regular as no complications are introduced by allotropic changes.

§4. THE RELATION BETWEEN VELOCITY OF FLOW AND LOAD

In order to verify the expression

$$v = Ae^{BP},$$

where v is the velocity of flow at constant temperature under a load P in kg./cm.^{2}, A and B being constants, which satisfied the tin observations, $\log_e v$ is plotted as ordinate against the load P as abscissa in figure 6. The curves for the lower temperatures consist of three straight lines, the portions for the smallest and greatest loads having slopes approximately equal with an intermediate portion of much greater

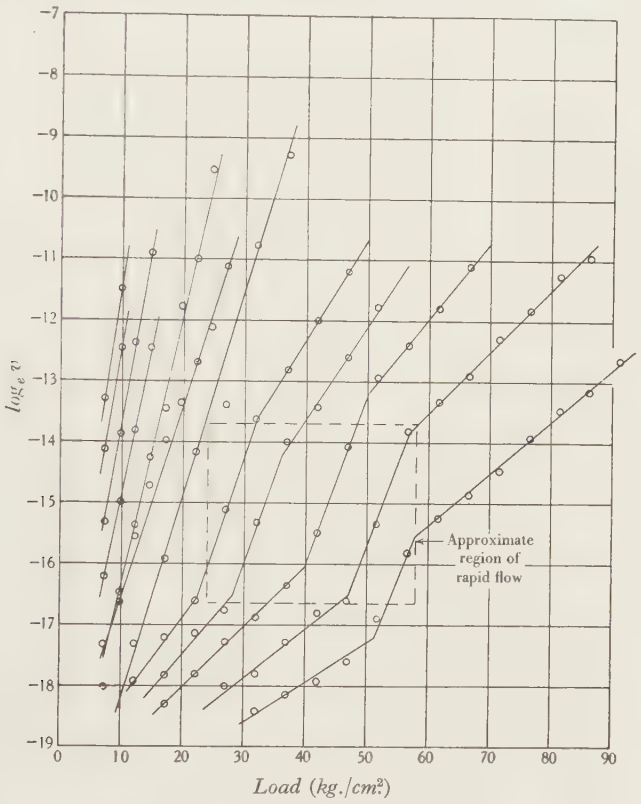

Figure 6. Curves relating $\log_e v$ with load.

slope. These changes of slope are most noticeable at air temperature, becoming gradually less marked with increase of temperature until at 148° C. the results are best represented by a single straight line, which remains a satisfactory representation up to the highest temperatures examined. These straight-line plots justify the extension of the exponential relation to the results obtained for lead.

The straight lines can be represented by the relation

$$\log_e v = \log_e A + BP$$

and the values of the slopes B, and the intercepts $\log_e A$, from which the constants A

are calculated, determined for each slope of the multiple- and the single-slope curves respectively.

In figure 7 the values of the slopes B are plotted as ordinates against the centigrade temperatures as abscissae. The values for each series of slopes B lie on a straight line, which can be represented by

$$B = \beta T + \alpha,$$

the values of the constants β and α being given in table 3.

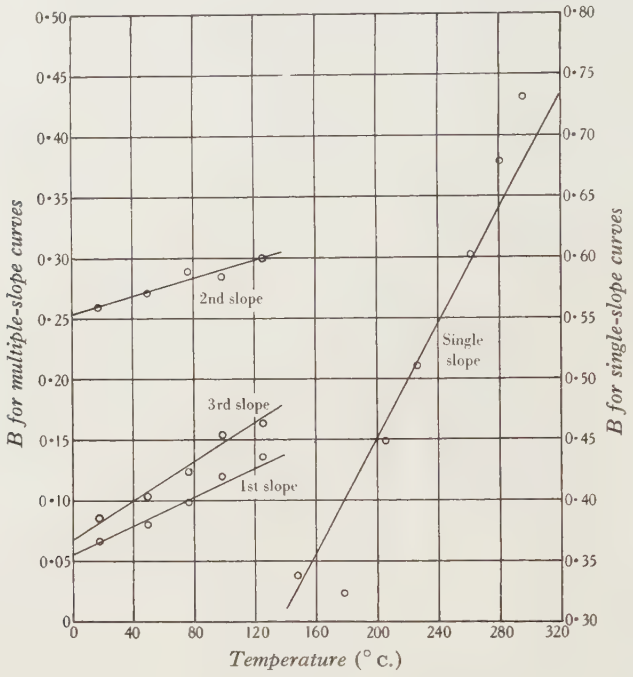

Figure 7. Curves relating B with temperature.

Table 3

		δ	β	α	γ
Multiple-slope curves	First slope	$8{\cdot}00 \times 10^{-11}$	$6{\cdot}24 \times 10^{-4}$	$11{\cdot}86 \times 10^{-2}$	$9{\cdot}17 \times 10^{-3}$
	Second slope	$1{\cdot}78 \times 10^{-23}$	$3{\cdot}75 \times 10^{-4}$	$-15{\cdot}10 \times 10^{-2}$	$7{\cdot}30 \times 10^{-2}$
	Third slope	$4{\cdot}86 \times 10^{-11}$	$7{\cdot}93 \times 10^{-4}$	$14{\cdot}90 \times 10^{-2}$	$11{\cdot}81 \times 10^{-3}$
Single-slope curves		$1{\cdot}07 \times 10^{-12}$	$23{\cdot}52 \times 10^{-4}$	$66{\cdot}0 \times 10^{-2}$	$15{\cdot}10 \times 10^{-3}$

The values of the constant A do not give a linear relation with the load, but by plotting $\log_e A$ against the load straight lines are obtained for each series of values as shown in figure 8. The relation can be expressed as

$$\log_e A = \gamma T + \log_e \delta,$$

the values of the constants γ and δ also being given in table 3.

This confirmation for lead of the expression connecting velocity of flow and load would seem to imply that the relation

$$v = A' e^{B'T},$$

connecting the velocity of flow v with the absolute temperature T at constant load, would also be followed. As, however, there are comparatively few points for each load the direct experimental verification of this relation is not possible.

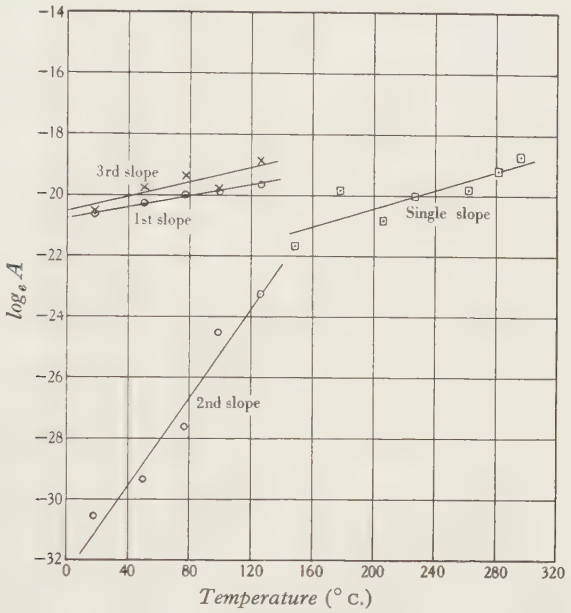

Figure 8. Curves relating $\log_e A$ with the temperature.

§ 5. EMPIRICAL REPRESENTATION OF RESULTS

The expressions for v obtained from the $\{\log_e v, P\}$ series of curves show that for any temperature T and load P the resulting rate of flow is given by the general formula

$$v = \delta e^{\beta PT - \alpha P + \gamma T},$$

where α, β, γ and δ are constants. The values of the constants calculated from the curves are given in table 3.

As in the case of tin, the empirical relation can be written in the form

$$v = K e^{\beta (P+P_0)(T-T_0)},$$

where P_0, T_0 and K are given by

$$P_0 = \gamma/\beta,$$

$$T_0 = \alpha/\beta,$$

and

$$K = \delta e^{\alpha\gamma/\beta},$$

T_0 being the temperature below which the particular type of flow concerned cannot occur and P_0 the corresponding critical load. These constants are given in table 4.

Table 4

		P_0, viz. γ/β (kg./cm²)	T_0, viz. α/β (° K.)	$\beta \times 10^4$	$\alpha\gamma/\beta$	$K = \delta e^{\alpha\gamma/\beta}$
Multiple-slope curves	First slope	14·7	190·1	6·24	1·74	$4{\cdot}57 \times 10^{-10}$
	Second slope	194·6	−403	3·75	−29·40	$3{\cdot}04 \times 10^{-36}$
	Third slope	14·9	187·9	7·93	2·22	$4{\cdot}47 \times 10^{-10}$
Single-slope curves		6·42	280·5	23·52	4·24	$7{\cdot}40 \times 10^{-11}$

To make v equal to 0 for the critical values of P and T the expression must be written

$$v = K\{e^{\beta(P+P_0)(T-T_0)} - 1\},$$

but this makes only a negligible difference.

The lowest rate of flow observed, for which $P = 32{\cdot}1$ kg./cm.² and $T = 291°$ K., gives

$$\exp\{\beta(P+P_0)(T-T_0)\} = 19{\cdot}3$$

leading to the value

$$v = 0{\cdot}88 \times 10^{-8} \text{ cm./sec. per cm. of length}$$

if the unity term is neglected, and

$$v = 0{\cdot}84 \times 10^{-8} \text{ cm./sec. per cm. of length}$$

if it is taken into account.

The difference is $0{\cdot}04 \times 10^{-8}$ cm./sec. per cm. of length, and as the apparatus is only sensitive to changes per unit length of four in a million the difference between the two cases must be regarded as negligible. It may be remarked that the difference introduced by the unity factor is very much less for lead than for tin.

It must be noted that this modification of the empirical expression gives $v = 0$ at temperatures differing from T_0 only when $P = -P_0$, i.e. at a negative tension, which shows that the temperature is the essential condition for plastic flow. The same conclusion was arrived at from the experiments on tin.

§6. THE RELATIONS BETWEEN THE CRITICAL LOADS AND TEMPERATURE

For the lower temperatures the curves for $\log_e v$ and P change their slopes at critical values, tabulated below; P_{12} and P_{23} denote the loads causing changes from the first to the second, and the second to the third slopes respectively.

The wires were always loaded to fracture and the values of the maximum stress P_B, which are approximately the breaking loads, are given. For the lower temperatures the least load P_E causing flow is also given in table 5 as an approximate value of the elastic limit.

The relations between the temperature and the breaking load and elastic limit appear to be hyperbolic in form, and suggest that

$$(P-P_c)(T-T_c)=C.$$

The {transition, load} curves are also hyperbolic but their curvature has the opposite sign.

Table 5

Temperature (° C.)	Temperature (° K.)	P_{12} (kg./cm²)	P_{23} (kg./cm²)	P_B (kg./cm²)	P_E (kg./cm²)
18	291	51·6	57·7	96·3	32·1
50	324	47·3	56·7	86·4	27·2
77	350	40·0	50·4	66·6	17·3
99	372	27·8	36·2	56·8	17·3
126	399	22·5	31·3	46·9	12·3
148	421	—	—	37·0	—
178	451	—	—	27·2	—
206	479	—	—	24·7	—
227	500	—	—	17·3	—
262	535	—	—	14·8	—
281	554	—	—	12·3	—
296	569	—	—	9·9	—

The usual method was employed to obtain straight-line plots, from which were calculated the values of P_c, T_c and C given in table 6.

The agreement between the observed values of the loads and those calculated for the known temperatures by means of these constants is shown in figure 9, where the curves are drawn from the calculated data.

Table 6

	P_c (kg./cm²)	T_c (° K.)	C
Breaking load	−28·9	198	$1{\cdot}45\times10^4$
Elastic limit	−27·5	103	$1{\cdot}17\times10^4$
Transition P_{12}	64·6	432	$1{\cdot}92\times10^3$
Transition P_{23}	70·4	431	$1{\cdot}64\times10^3$

The {breaking-load, temperature} curve confirms the results of Ingall[5]. The temperature T_c below which fracture would occur across as well as along the grain boundaries is 180° K. The continuity of the curve in the region corresponding to change from the threefold to the single curves leads to the conclusion that allotropic modifications or changes of phase do not occur for lead in the region examined.

The {elastic-limit, temperature} curve follows, as was anticipated, a path similar to the breaking-load curve, and 103° K. is the temperature T_c below which no viscous flow would occur even when the wire was loaded to fracture.

The breaking-load and transition-load curves confirm the hyperbolic expressions found for tin; however, the latter have curvature of opposite sign, which is demanded

by the absence of the threefold curves above a critical temperature, their agreement for the values of T_c being very good.

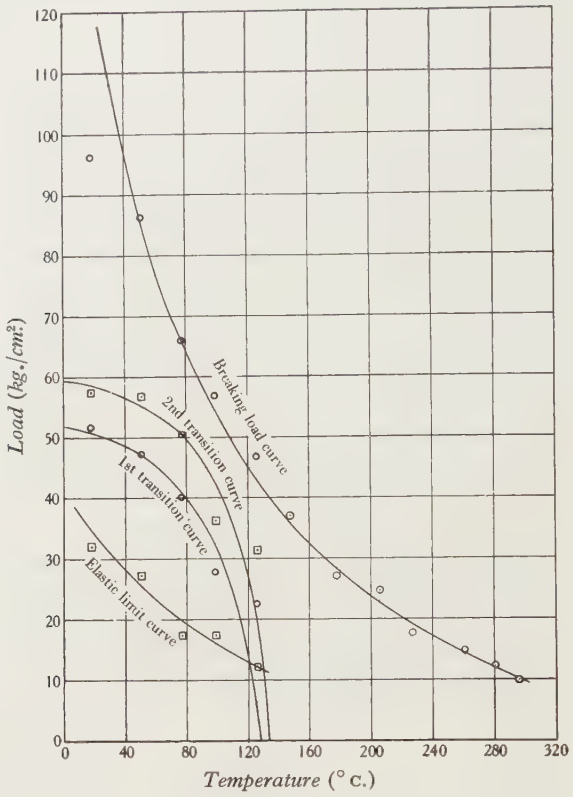

Figure 9. {Critical-load, temperature} curves.

§7. GENERAL DISCUSSION OF RESULTS

Lead[6] belongs to the series of metals which crystallize in the cubic hexa-isoctahedral system with space groups o_h^4; o_h^5. They have a face-centred cubic lattice, which can be represented with orthogonal cubic axes $\Gamma_c :| \mathfrak{A}_1 | = a_w$ and the basis $4\mathrm{Pb}\begin{pmatrix} 0\,0\,0 \\ \frac{1}{2}\,\frac{1}{2}\,0 \end{pmatrix}$ or as a simple lattice with axes

$$\Gamma_c' :| \mathfrak{A}_i | = a_w/\sqrt{2},\ (\mathfrak{A}_i\, \mathfrak{A}_k) = a_w^2/4.$$

Each atom is surrounded, at a distance d equal to $a_w/\sqrt{2}$, by twelve neighbours in rhombicdodecahedral grouping. The values of the constants for lead are

$$a_w = 4{\cdot}92 \times 10^{-8}\ \text{cm.}, \quad \text{and} \quad d = 3{\cdot}48 \times 10^{-8}\ \text{cm.}$$

Recent work by Taylor and Elam[7, 8] has shown that, for single crystals of aluminium, distortion under tension is, in the early stages, by slip on a single octahedral {111} plane in a [110] direction, but during the last stages by slip on two planes. These results have been confirmed for compressive[9, 10, 11] and alternating stress[12, 13].

Elam[14] has shown that in copper, silver and gold, the behaviour is similar to that in aluminium and is due to slip on an octahedral {111} plane in the direction of the pole of one of the three {110} planes.

As far as the author is aware, no recent observations have been made on lead single crystals, but behaviour similar to that for aluminium, copper, silver and gold would be expected; this view receives support from Humphrey's[15] microscopic examination of slip bands in single crystals of lead. He says that "it may be concluded that lead tends to slip along planes perpendicular to the octahedral axes of the crystals and there would, therefore, be at least four possible directions in which slip could occur." Four systems of slip lines had already been noted in strained lead by Ewing and Rosenhain[16,17].

If a metal is subjected to preliminary heating to remove strain, strained a small critical amount, and then heated to a critical temperature, crystal growth occurs, and if suitable conditions prevail the whole specimen can be converted into a single crystal. For a given value of this final temperature no growth occurs below a certain critical strain, just above which maximum crystal growth takes place, and for larger strains the crystal-size diminishes very rapidly at first and more slowly subsequently. Figure 10 shows the effect of heating at 800° C. for 6 hr. on the crystal growth of slightly strained copper, according to Carpenter and Tamura[18]. Precisely similar results were obtained by Seligman and Williams[19] and Carpenter and Elam[20] for aluminium, and by Rüder[21] for silicon steel.

It has been found that the strain required to produce crystal growth is lower, the higher the recrystallizing temperature. Figure 11 shows the relation between the critical strain and recrystallizing temperature for copper found by Carpenter and Tamura[18]. Below the curve no growth occurs, while above it is the region of growth, and the largest crystal-size is obtained near the curve. Similar results were found by Carpenter and Elam[20] for aluminium and by Ewing and Rosenhain[16,17] for lead, with which, under severe strain, crystal growth occurred at air temperature. It has, however, been found impossible to produce large crystals of metals possessing face-centred cubic structure, without also forming annealing twins, whose production Carpenter and Tamura[22] have shown to be intimately connected with crystal growth. The exception is aluminium, for which special reasons are cited.

From these general considerations it is possible to explain the results of the present experiments, which can be discussed best from the $\{\log_e v, P\}$ curves in figure 6.

The initial stage of the multiple-slope curves corresponds to glide on an octahedral {111} plane in a [110] direction. The incidence of single or double gliding will depend on the orientation of the individual crystallites, and both types of glide will undoubtedly be present in the aggregate. This type of glide ceases for critical values of the load P_{12} and temperature, which are plotted in figure 9. This can be considered as the recrystallization curve and has been shown to be a hyperbola

$$(P_{12}-64{\cdot}6)\,(T_{12}-432)=1{\cdot}92\times10^3,$$

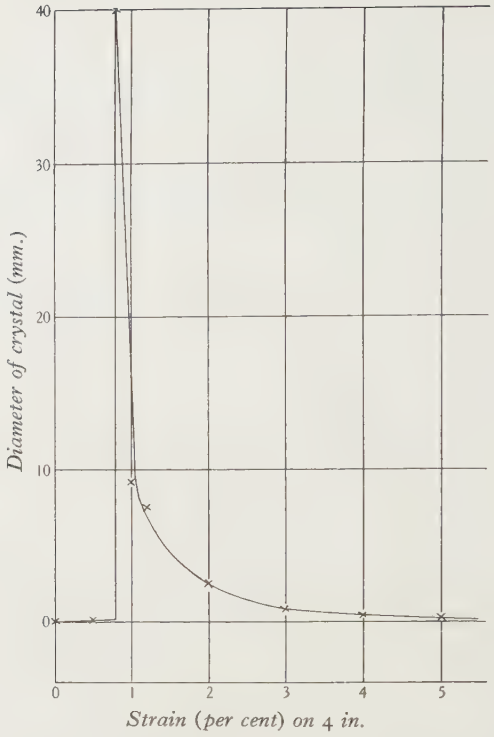

Figure 10. The effects of heating at 800° C. for 6 hr. on the crystal growth of slightly strained copper.

Reproduced by kind permission of the Royal Society.

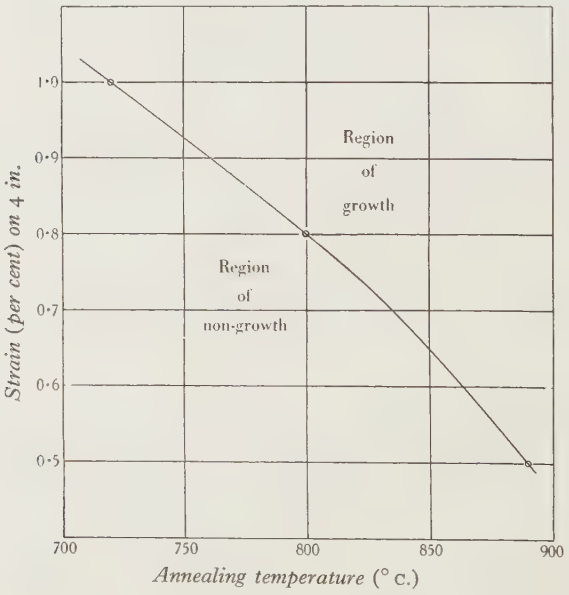

Figure 11. Curve showing the region of growth and non-growth in strained copper.

Reproduced by kind permission of the Royal Society.

which gives the relation between the critical temperature and stress required to produce crystal growth. When $P_{12}=0$, $T_{12}=402°$ K. or 129° C., which is the temperature above which very active crystal growth occurs without preliminary strain—that is, complete annealing takes place. This temperature agrees with the experimental transition from multiple-slope to single-slope curves. The curve for lead is very similar to the recrystallization curve for copper, figure 11, and agrees with the observations of Ewing and Rosenhain[17].

For higher values of the load and temperature, crystal growth occurs, accompanied by the formation of annealing twins. Extension can occur by this recrystallization and formation of twins without lattice distortion, and hence with much less resistance and consequently greater velocity of flow, giving the suddenly increased slope of the middle portion of the curves. That the annealing twins are responsible for this increase is supported by the experiments on tin, since white tin possessing a lattice structure incapable of producing annealing twins[22] under conditions suitable to recrystallization showed no such phenomena.

Examination of the constants in table 3 offers further evidence of the difference in the character of the flow for this second slope, the value of the temperature coefficient γ being some seven times greater than the glide values (first and third slopes), while the value of the load coefficient α, though of the same magnitude as for glide, is opposite in sign.

Reference to figure 10 shows that the size of the crystals produced falls very rapidly with increasing strain (and therefore stress) in consequence of the great increase in the number of possible centres of growth, and the whole mass of the wire quickly becomes recrystallized. The multiplication of the grain-boundaries causes a decrease in the amount of distortion which can be produced by any individual twin, and this method of deformation becomes impossible, so that a second transition stage ensues and gives critical values of the load P_{23} and temperature. These are shown in figure 9 and, though less regular than the values for the first transition stage, are represented by the hyperbola

$$(P_{23}-70{\cdot}4)\,(T_{23}-431)=1{\cdot}64\times10^3.$$

When $P_{23}=0$, $T_{23}=408°$ K. or 135° C., which gives very close agreement with the recrystallization temperature of 129° C. obtained from the $\{P_{12},\ T_{12}\}$ relation.

For the final stage a very close return must be made to the initial conditions. The distortion will again take place by single or double gliding on an octahedral {111} plane in a [110] direction. However, as a result of the production of annealing twins in the second stage of the distortion, twinned crystallites will exist with their lattices inclined at the twinning angle; thus gliding will occur as though there were two glide directions and two glide planes.

Now, assuming as before[1] that the flowability in any direction for given temperature and load conditions is proportional to the atomic density in that direction, and therefore inversely proportional to the distance apart of the atoms, the flowability in the [110] direction can be written as $f(PT)/d_{[110]}$, where $f(PT)$ is a function of the temperature and load conditions. For glide in a simple untwinned

crystal the flowability F_S in the direction of load can be written as $kf(PT)/d_{[110]}$, where k is a constant depending on the orientation of the [110] direction with respect to the direction of loading.

For glide in a twinned crystal, the flowability F_T in the direction of load can be written as

$$kf(PT)\left[\frac{1}{d_{[110]}}+\frac{1}{d_{[110]}}\cos 70^\circ 32'\right],$$

where $70^\circ 32'$ is the angle between the [110] directions in the twinned lead crystal[22]. Hence the ratio of flowability for twinned and simple crystals can be expressed thus:

$$\frac{F_T}{F_S}=\frac{kf(PT)\frac{1}{d_{[110]}}\{1+\cos 70^\circ 32'\}}{kf(PT)\frac{1}{d_{[110]}}}$$

$$=1+\cos 70^\circ 32'$$

$$=1{\cdot}33.$$

Now the velocity of flow is given by the expression

$$v=ke^{\beta PT-\alpha P+\gamma T},$$

and the ratios of the constants α, β and γ taken from the $\{\log_e v, P\}$ curves for twinned crystals (third slope of the multiple curves) and untwinned crystals (first slope of the multiple curves) are given in the following table 7.

Table 7

	Third slope	First slope	Ratio
α	$14{\cdot}90\times10^{-2}$	$11{\cdot}86\times10^{-2}$	1·26
β	$7{\cdot}93\times10^{-4}$	$6{\cdot}24\times10^{-4}$	1·27
γ	$11{\cdot}81\times10^{-3}$	$9{\cdot}17\times10^{-3}$	1·29

The agreement of these values with the calculated figure of 1·33 gives support to this hypothesis. Additional evidence of the similarity of the behaviour represented by the first and third portions of the multiple-slope curves is offered by a comparison of the values of P_0 and T_0 being 14·7 and 14·9 kg./cm^2, and 190·1 and 187·9° K. respectively.

The single-slope curves present a fresh problem, as for these the temperature is high enough to cause complete recrystallization without subjecting the material to strain. Distortion will proceed by single or double glide on simple and twinned crystals but the slightest incidence of strain in any individual crystal will be sufficient to cause very rapid recrystallization of that unit. Thus with this continual self-annealing, the effect of strain hardening is very materially diminished and may become zero. Hence it is to be expected that the velocity of flow will be dependent on the load to a much higher degree than for glide in crystals subject to the normal limitations of strain hardening. Now the rate of flow depends concurrently on the independent variables load and temperature, and it is not to be anticipated that the

change in the {flow, load} relationship will affect the {flow, temperature} relation, except for the secondary influence on the release of strain hardening.

These conclusions are confirmed by an examination of the coefficients in table 3. The value of γ (the temperature coefficient) is of the same order and sign as for simple and twinned glide, but the value of α (the load coefficient, consequently a function of strain hardening) is some six times greater than for glide in simple or twinned crystals. The coefficient β is also some three times greater than for the first and third slopes of the multiple-slope curves.

§8. GRAPHICAL REPRESENTATION OF RESULTS

The results can be represented qualitatively by the graphical method shown in figure 12. Loads are plotted as abscissae and temperatures as ordinates. {Load,

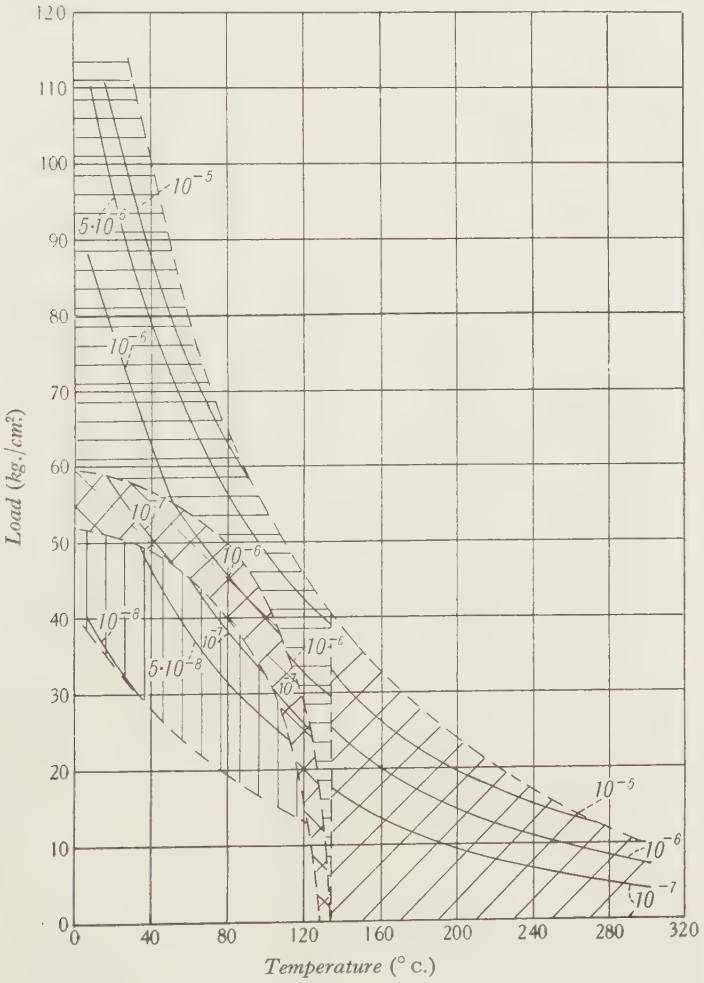

Figure 12. The rates of flow are given in cm./sec. per cm. length.

temperature} curves are then drawn for certain values of the rate of extension. The breaking-load curve ABC, the elastic-limit curve EF and the transition curves GH and JD are dotted in. The vertical line BD is then drawn at the temperature above which recrystallization occurs spontaneously without preliminary strain. All points lying above and to the right of the {breaking-load, temperature} curve correspond to immediate fracture. The area below and to the left of the breaking-load curve is divided by the line BD into two portions. The region to the left can be divided further into four portions—(1) the region below the elastic-limit curve in which no slip occurs; (2) the area EFG, denoted by vertical hatching, in which single or double glide occurs in simple untwinned crystals; (3) the area $JDHG$, denoted by double cross-hatching, in which recrystallization and considerable deformation occur in association with the production of annealing twins, and (4) the area $ABDJ$, denoted by horizontal hatching, in which single and double glide take place in twinned crystals. In the region to the right, denoted by cross-hatching, self-annealing (recrystallization) largely eliminates the effect of strain hardening, with the result that distortion by glide proceeds, producing a much greater rate of extension than that which would occur under more normal conditions.

§9. SUMMARY OF RESULTS

(1) It has been shown that the rate of viscous flow is not independent of the time, and that its value, as soon as the non-viscous flow has ceased, is connected with the load for constant temperature, and with the temperature for constant load, by exponential relations.

(2) The following experimental relationships were obtained between the velocity of flow v, the load P and the absolute temperature T:

for single or double glide in untwinned crystals

$$v_1 = 4{\cdot}57 \times 10^{-10} \exp\{6{\cdot}24 \times 10^{-4}\,(P+14{\cdot}7)\,(T-190)\} \text{ cm./sec. per cm. length,}$$

for single or double glide in twinned crystals

$$v_3 = 4{\cdot}47 \times 10^{-10} \exp\{7{\cdot}93 \times 10^{-4}\,(P+14{\cdot}9)\,(T-188)\} \text{ cm./sec. per cm. length,}$$

for extension during the recrystallization period and production of annealing twins

$$v_2 = 3{\cdot}04 \times 10^{-36} \exp\{3{\cdot}75 \times 10^{-4}\,(P+194{\cdot}6)\,(T+403)\} \text{ cm./sec. per cm. length,}$$

and for extension when strain hardening is considerably diminished by self-annealing

$$v_4 = 7{\cdot}40 \times 10^{-11} \exp\{23{\cdot}52 \times 10^{-4}\,(P+6{\cdot}4)\,(T-280)\} \text{ cm./sec. per cm. length.}$$

(3) The results are best expressed in the form

$$v = K\,[e^{\beta\,(P+P_0)\,(T-T_0)} - 1],$$

where K, β, P_0 and T_0 are constants and probably would be brought into line for time variations by multiplying by the Geiss term $e^{B\,(P-P_B)t}$, where t is the time, P_B the breaking load and B a constant.

(4) The elastic limit, transition, and breaking loads have been shown to be connected with the corresponding temperatures by hyperbolic expressions.

(5) The general behaviour has been shown to be in agreement with that found in tin, and with the results obtained for single crystals.

§ 10. ACKNOWLEDGEMENTS

I am indebted to Prof. C. H. Lees for facilities for carrying out this investigation in the Physical Laboratories of the Queen Mary College, and for his interest during its progress. I desire also to express my thanks to Dr A. D. Crow and the Ordnance Committee for permission to publish this paper, and to Prof. Sir H. H. C. Carpenter and the Royal Society for permitting the reproduction of figures 10 and 11.

REFERENCES

(1) Tyte. *Proc. Phys. Soc.* **50**, 153 (1938).
(2) Andrade. *Proc. Roy. Soc.* A, **84**, 1 (1910); **90**, 329 (1914).
Andrade and Chalmers. *Proc. Roy. Soc.* A, **138**, 348 (1932).
(3) Shoji. *Sci. Pap. Inst. Phys. Chem. Res., Tokyo*, nos. 57 and 58.
(4) Geiss. *Z. Phys.* **29**, 78 (1924).
(5) Ingall. *J. Inst. Met.* **30**, 171 (1923); **32**, 41 (1924); **34**, 171 (1925).
(6) Landolt and Börnstein. *Phys. Chem. Tabn.* 5 Auf. 1 Ergd. 392.
(7) Taylor and Elam. *Proc. Roy. Soc.* A, **102**, 643 (1923).
(8) Taylor and Elam. *Proc. Roy. Soc.* A, **108**, 28 (1925).
(9) Farren and Taylor. *Proc. Roy. Soc.* A, **107**, 422 (1925).
(10) Taylor and Farren. *Proc. Roy. Soc.* A, **111**, 529 (1926).
(11) Taylor. *Proc. Roy. Soc.* A, **116**, 16 (1927).
(12) Gough, Hanson and Wright. *Philos. Trans.* A, **226**, 1 (1926).
(13) Gough, Hanson and Wright. *J. Inst. Met.* **36**, 173 (1926).
(14) Elam. *Proc. Roy. Soc.* A, **112**, 289 (1926).
(15) Humphrey. *Philos. Trans.* A, **200**, 225 (1903).
(16) Ewing and Rosenhain. *Philos. Trans.* A, **193**, 353 (1899).
(17) Ewing and Rosenhain. *Philos. Trans.* A, **195**, 279 (1900).
(18) Carpenter and Tamura. *Proc. Roy. Soc.* A, **113**, 28 (1927).
(19) Seligman and Williams. *J. Inst. Met.* **20**, 162 (1918).
(20) Carpenter and Elam. *Proc. Roy. Soc.* A, **100**, 329 (1921).
(21) Rüder. *Trans. Amer. Inst. Min. Engrs*, **47**, 569 (1913).
(22) Carpenter and Tamura. *Proc. Roy. Soc.* A, **113**, 161 (1927).

THE SPECTRAL SENSITIVITY OF SELENIUM RECTIFIER PHOTOELECTRIC CELLS

By G. P. BARNARD, B.Sc., A.Inst.P., Grad.I.E.E.

Received 17 *October* 1938. *Read in title* 13 *January* 1939

ABSTRACT. It is shown that the spectral distribution curve of sensitivity of the selenium rectifier cell is determined by the external-circuit resistance, the output and the temperature; consequently the course of the {sensitivity, output} curve is determined by the quality of the incident radiation, the external-circuit resistance and the temperature. Further, the observed temperature coefficient of sensitivity is determined by the external-circuit resistance, the quality of the incident radiation and, to a smaller extent, the quantity of the incident radiation.

§ 1. INTRODUCTION

The dependence of the response of rectifier photoelectric cells upon the spectral composition of the incident radiation is of great importance even when a comparatively low precision, of only a few per cent, is desired in the use of these cells for photometric measurement. The spectral sensitivity has, of course, been studied by many investigators, and the published results reveal substantial differences between the various types of commercial selenium cells. More disturbing is the work of Marchal and Marton[1], and of König[2], indicating that the effects of independent beams of light of different quality are not strictly additive. It follows that a full investigation is necessary before any method is adopted to correct the spectral sensitivity curves (obtained by means of a spectrophotometer) to the response curve of the average human eye. Fortunately, results so far published tend to show that cells of any one type are reasonably uniform in their spectral response. In fact, work at the National Physical Laboratory on commercial cells and cells of National Physical Laboratory construction has shown that, with sufficient control upon the various manufacturing stages, it is not difficult to maintain general uniformity in spectral response amongst cells of a given type.

Hence the work detailed in this paper deals primarily with the various factors upon which the spectral sensitivity depends, and secondarily with the possible methods of colour correction.

§ 2. EXPERIMENTAL METHODS AND APPARATUS

As a source of illumination, a 1000-w., 100-v. gas-filled projection lamp was used; this lamp was operated at 50 v., with a colour temperature of 2360° k., to give a candle-power of 209 in a known direction perpendicular to the plane of the filament, and was used on a 5-metre photometer bench. A 30-w., uniplanar, tungsten-fila-

ment vacuum lamp also was available for low illumination measurements; operated at 102 v., at a colour temperature of 2360° k., it had a candle-power of 22·0.

For most of the work on spectral sensitivity two standard coloured glasses were used; these had previously been measured with the visual spectrophotometer. One was a selective blue-green glass (C.F. 6), and the other a selective red glass (C.F. 14); the spectral transmission curves of these glasses are given in figure 1.

The spectral sensitivity curves given in this paper were obtained by use of the photoelectric spectrophotometer designed by Preston and Cuckow[3]. A vacuum photoelectric cell was used to measure the energy at each wave-length step, the cell

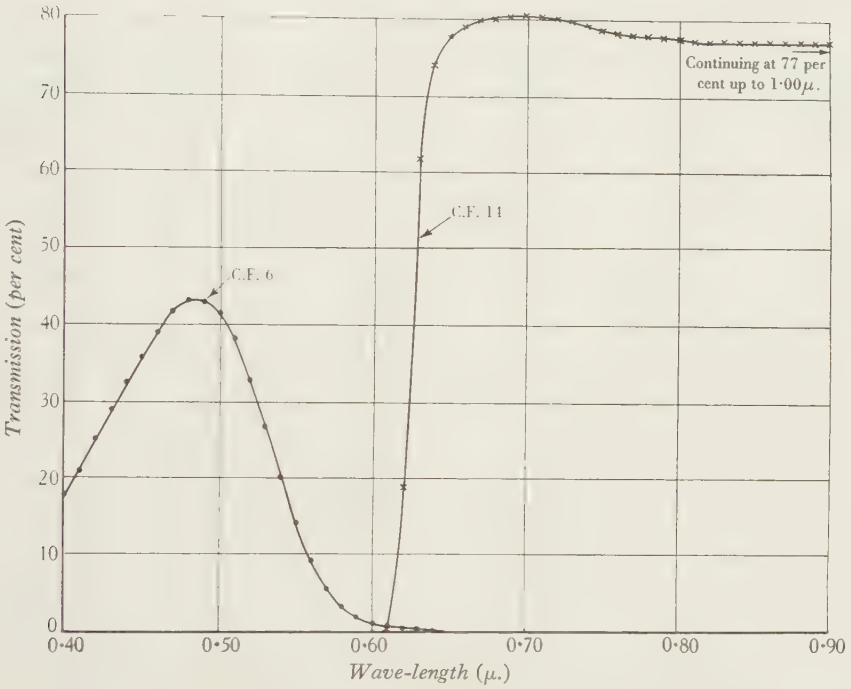

Figure 1. Spectral transmission for blue-green glass (C.F. 6) and selenium red glass (C.F. 14).

having previously been calibrated against a linear thermopile; its spectral sensitivity was known to be independent of output and temperature within the normal operating ranges. Stray-light filters were used, but no slit-width corrections were made, errors arising from slit-width being considered to be less than the experimental errors. Spectrophotometer measurements were made from 0·40 to 0·70μ. All curves given are referred to a constant-energy spectrum but not obtained with it; in each case the output of the rectifier cell with an external-circuit resistance of 100 Ω. varied considerably throughout the spectrum with a maximum range of 0·5 to 4·0μa.

A calibrated potentiometer was in all cases used to measure the output of the rectifier cell; for the measurement of short-circuit output, the circuit shown in figure 2[4] was used, a correction for the potentiometer resistance being made to

obtain an absolute measure of the short-circuit current. In the measurement of output a precision better than $\pm 0{\cdot}5$ per cent was obtained at the lowest values of output.

To facilitate examination of rectifier photoelectric cells with a view to noting changes of or differences in spectral sensitivity, the cells were mounted on the 5-metre photometer bench and used to measure the integral transmission ratios of the two selective coloured glasses (C.F. 6 and C.F. 14). The visual integral transmission ratio of a coloured glass is given by the quotient

$$\int_0^\infty T_\lambda E_\lambda k_\lambda d\lambda \Big/ \int_0^\infty E_\lambda k_\lambda d\lambda,$$

where T_λ represents the transmission of the glass at wave-length λ, E_λ the relative energy of the source at wave-length λ, and k_λ the visibility function at wave-length λ. Let T_{vB} denote the visual integral transmission ratio of the blue-green glass, and T_{vR} the visual integral transmission ratio of the red glass. With a source operating

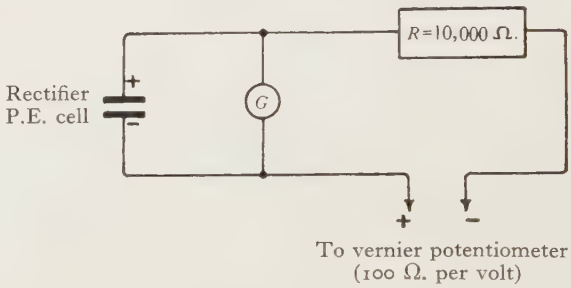

Figure 2. Circuit used for the measurement of short-circuit output from rectifier photoelectric cell.

at a colour temperature of 2360° K. and a glass temperature of 20° C., the ratio T_{vR}/T_{vB} was found to be 1·041.

Let T_{cB} denote the integral transmission ratio of the blue-green glass as determined by the cell, and T_{cR} the integral transmission ratio of the red glass as determined by the cell. By adjusting the position of the lamp on the bench the output of the cell was maintained constant for the open reading with white light, for the lamp with blue glass, or for the lamp with red glass; and hence the glass transmission was given by the ratio of the inverse squares of the distances from the light-centre of the lamp to the cell with the filter out and with the filter in, respectively. It was not possible to maintain this output constant from cell to cell owing to widely varying sensitivities; hence it was decided to keep the initial illumination with white light constant, and to keep the output, so set, constant for each cell during the coloured-glass measurements. Such experiments gave for each cell at a definite value of the output the ratio T_{cB}/T_{cR}.

It is seen that for a cell whose spectral sensitivity conforms to the internationally agreed visibility curve $(T_{cB}/T_{cR})/(T_{vB}/T_{vR})$ is equal to unity.

The converse, of course, is not necessarily true, i.e. a value of unity for this expression by no means necessarily implies that a cell has a spectral distribution of

sensitivity in complete conformity with the visibility curve. This is merely another way of saying that measurements on two coloured glasses do not suffice to describe the cell's performance. Nevertheless, for any cell this expression gives conveniently an empirical ratio of blue-green sensitivity to red sensitivity for constant output. This sensitivity ratio shows the performance of the cell in relation to that of the ideal cell having a spectral sensitivity in conformity with the visibility curve. It affords therefore a convenient method of revealing differences between cells of different types, and changes in the same cell under varying experimental conditions.

Henceforth the expression $(T_{cB}\ T_{cR})\ (T_{rB}/T_{rR})$ will be referred to simply as the ratio of blue-green sensitivity to red sensitivity, S_B/S_R.

It is considered that while such tests may in general be unnecessarily severe, so long as cells are used only for the measurement of light-sources having continuous spectra, they are actually less severe than is necessary to determine the behaviour of cells with sources having discontinuous spectra.

§ 3. CONTROL OF SPECTRAL SENSITIVITY DURING CONSTRUCTION OF CELL

Measurements of the ratio $S_B\ S_R$ for a number of well-known commercial cells are given in table 1.

Table 1. External-circuit resistance, 100 Ω.; glass temperature and cell temperature, 20° C.

Cell*	S_B/S_R
1. Weston Photronic	0·197
2. Electrocell	0·391
3. S.A.F.	0·550
4. Tungsram	0·579

* The maker's name is given here for convenience. Although cells of each type were obtained in the ordinary way on the open market it is not known whether the manufacturers would regard them as typical of their products.

The wide variation between these different types of selenium rectifier cells indicates that considerable control of the resultant spectral sensitivity should be possible during the construction of a cell. This is, in fact, the case.

Seven selenium-sulphur rectifier cells were constructed according to the general method described in an earlier paper[5], and in addition one cell (P in table below) made of pure selenium[6] was obtained. Particular details in the constructional stages were, however, altered to produce cells of different types. These details are given in table 2, which also gives the corresponding values of the ratio S_B/S_R.

It is seen from table 2 that (1) except in the case of cell no. 1*c* the addition of sulphur generally increases the blue-green sensitivity with respect to the red; (2) reduction of the time of annealing for Se-S cells increases the blue-green sensitivity with respect to the red; (3) with the other constructional details unaltered, rapid cooling of the selenium-sulphur film from the annealing temperature results in the final product in a definite increase of red sensitivity with respect to the blue-green;

(4) change of metal sputtered with the other constructional details unaltered has, for the three metals used (platinum, silver, gold), no effect on the ratio of blue-green sensitivity to red sensitivity; (5) abrasion of the semi-conductor surface definitely increases the red sensitivity as compared with the blue-green.

Table 2. Except for P, the thickness of the Se-S film was constant and approximately 0·05 to 0·1 mm. External-circuit resistance, 100 Ω.; glass temperature and cell temperature, 20° C.

Cell no.	Temperature of annealing (° C.)	Time (min.)	Cooled from annealing temperature	Metallic film	S_B/S_R
P	200	45	Slowly	Sputtered Pt	0·435
1	165 to 170	180	,,	,,	0·609
1*a*	165 to 170	180	,,	Sputtered Au	*
1*b*	165 to 170	180	,,	Sputtered Ag	*
1*c*	165 to 170	180	,,	Graphite by polishing	0·421
2	165 to 170	75	,,	Sputtered Pt	0·773
2*a*	165 to 170	75	Rapidly	,,	0·541
3	170 to 175	30	Slowly	,,	0·859

* The ratio S_B/S_R for 1*a* and 1*b* was not sensibly different from that for 1.

While there appears to be no difficulty in reproducing a cell of a given type, it is seen that much may be done by modification of the constructional details to bring about a closer approach of the spectral sensitivity curve to the visibility curve. So long as a colour-correction filter is required for precise adjustment of the spectral sensitivity curve to the standard visibility curve, there is little to be gained by modification of the constructional details; when, however, for reasons of overall sensitivity or in consequence of the obliquity of the incident light, a colour-correction filter cannot be used, modifications calculated to bring about a closer approach of the spectral sensitivity curve to the visibility curve may be very desirable.

It may be added here that the rise of blue-green sensitivity as compared with the red sensitivity consequent upon reduction in the time of annealing is a feature which has frequently been observed in experiments on the selenium photo-conducting cell[7].

§ 4. DEPENDENCE OF SPECTRAL SENSITIVITY UPON OUTPUT AND EXTERNAL-CIRCUIT RESISTANCE

The dependence of the ratio S_B/S_R upon output and upon external-circuit resistance was determined for a number of cells, and representative results are plotted in figure 3 for a selenium-sulphur cell of National Physical Laboratory make.

S_B or S_R was determined for various outputs with external-circuit resistances of 0 Ω., 100 Ω., 1000 Ω. and 10,000 Ω. and on open circuit. The sensitivity S_B or S_R for any external-circuit resistance plotted against the corresponding short-circuit output with the blue-green or the red glass respectively in combination with the

light-source then permitted the determination of the ratio S_B/S_R for any external-circuit resistance corresponding to the same values of short-circuit output with red or with blue light.

Figure 3 shows that the spectral sensitivity for chosen constant conditions of illumination is markedly dependent upon the external-circuit resistance, an increase of which results in a definite increase of blue-green sensitivity with respect to red. Figure 3 also reveals a dependence of S_B S_R upon output, and this becomes more marked with increase of external-circuit resistance. It is only possible here to give

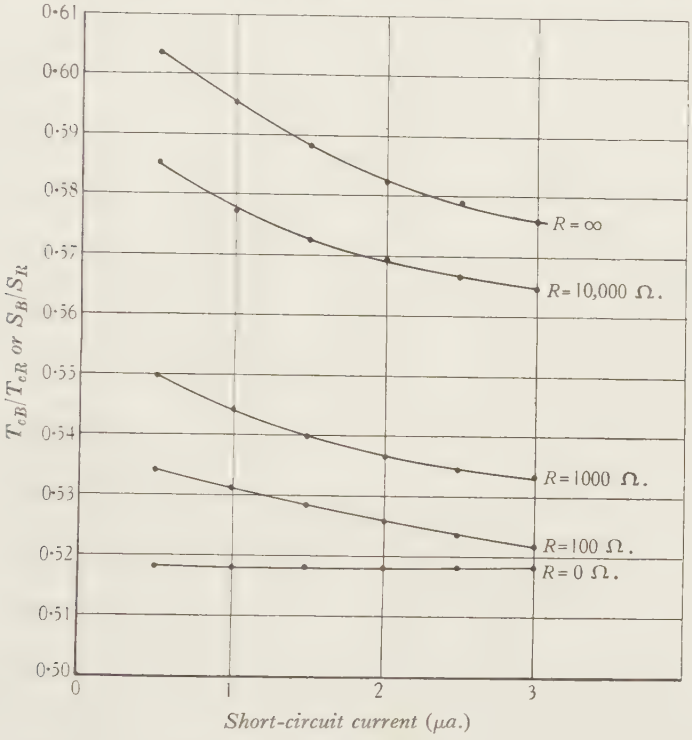

Figure 3. Dependence of S_B/S_R upon output and upon external-circuit resistance R for selenium-sulphur cell, made at National Physical Laboratory. $T = 23{\cdot}5°$ C.

the change of S_B/S_R for a range of 6·1 in short-circuit output, for considerable care has to be taken to avoid heating the coloured glasses by the lamp radiation; but it should not therefore be inferred that the value of S_B S_R for short circuit remains invariable for a greater range than that represented here. The work carried out, in fact, proves that the appearance of non-linearity for white light results not from a simple and uniform proportional change of absolute sensitivity throughout the spectrum but from a change in shape of the spectral distribution curve of sensitivity with output; it is to be noted here that even for the best cells on short circuit the range of output over which the sensitivity is precisely constant is quite definitely limited. Hence it is seen that the departure from a linear relation between response and illumination for any given light-source must depend not only upon the external-

circuit resistance (this, of course, is well known), but also upon the quality of the light received by the cell from that source.

A fall of S_B/S_R with rising output has been found to be the combined result of either (1) a fall of S_B and a rise of S_R with output, or (2) a fall of S_B with output while S_R is constant, or (3) a fall of both S_B and S_R with output, the fall of S_B being greater than that of S_R.

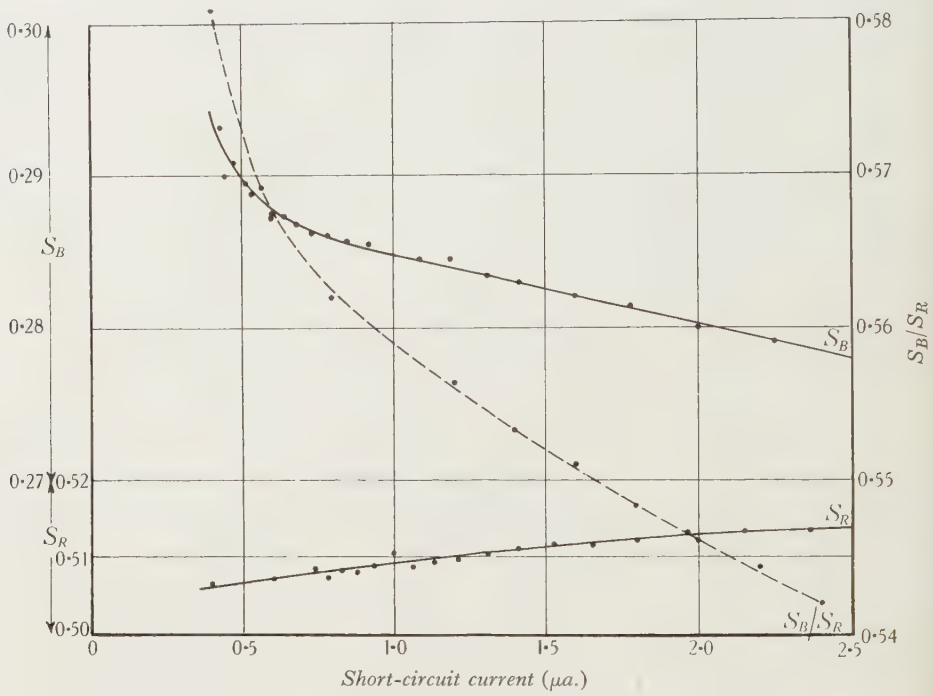

Figure 4. Dependence of S_B, S_R and S_B/S_R upon output for selenium-sulphur cell, made at National Physical Laboratory, on short circuit. $T = 20{\cdot}3°$ C.

Figure 4 gives the results for a second cell on short circuit and shows a small increase of S_R and a much larger decrease of S_B with output; the fall of S_B/S_R with output is given also. Where, however, the rise of S_R is more pronounced than the fall of S_B with output, the cell will show a rise instead of the usual small fall of sensitivity with illumination, when the cell is calibrated with a source whose energy is mainly in the red, for instance a tungsten source operating at 2360° K. A curve for such a cell is given in figure 5. Similar curves have been obtained for Tungsram and other cells by other workers[1]. It is interesting to compare here the results obtained by Preston[8] for vacuum emission photoelectric cells. The change of spectral sensitivity with output will be referred to again in § 6.

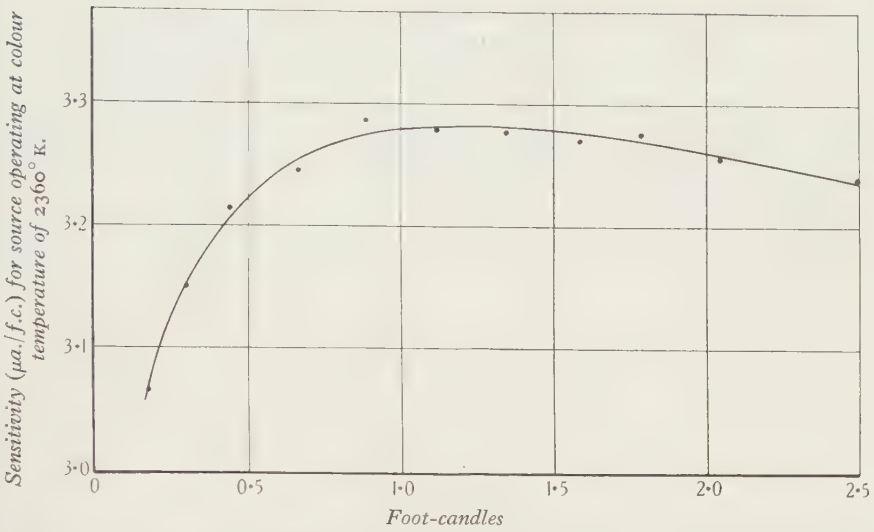

Figure 5. {Sensitivity, illumination} curve for selenium-sulphur cell, made at National Physical Laboratory. $T = 18{\cdot}5°$ C.

§ 5. DEPENDENCE OF THE SPECTRAL SENSITIVITY UPON TEMPERATURE

While no attempt has been made to undertake a separate investigation into the effect of temperature on the spectral sensitivity, very many tests using coloured light have been made over a period of about eighteen months on a number of cells with a maximum range in room temperature of from 16 to 24° C. The results obtained prove that the distribution of spectral sensitivity depends upon the temperature of the cell. Care must, of course, be taken to ensure that the proper correction is applied for the change in transmission with temperature of the coloured glass used. The results plotted in figure 6 were obtained for cell no. 1, table 2, with an external-circuit resistance of 100 Ω. To determine the temperature coefficient of transmission of the orange and red coloured glasses, the distribution curve of spectral sensitivity given in figure 7 for cell no. 1 and obtained by use of the photoelectric spectrophotometer (see § 2) may be used with sufficient accuracy.

If S_λ denote the spectral sensitivity of the cell at wave-length λ, then the effective change of the integral transmission ratio with change of glass temperature may be determined by performing the integrations to give the quotient

$$\int_0^\infty T_{\lambda t} E_\lambda S_\lambda d\lambda \Big/ \int_0^\infty E_\lambda S_\lambda d\lambda$$

at each of two temperatures sufficiently far apart to cover the experimental range; $T_{\lambda t}$ represents the transmission through the glass at wave-length λ and temperature $t°$ C.

The results plotted in figure 6 for the orange glass and for the red glass have been corrected to allow for the dependence of transmission upon temperature in the case

of these two coloured glasses. In the case of the blue glass the dependence of transmission upon temperature was found to be negligible. It is seen from the curves that the sensitivity for red light shows a positive temperature coefficient of about 0·5 per cent per °C., that for orange light a negative temperature coefficient of about 0·4 per cent per °C., and that for blue-green light a negative temperature coefficient of about 0·55 per cent per °C. Hence, when account is also taken of the results given in § 4, it is seen that the spectral distribution curve of sensitivity is determined by (*a*) the temperature of the cell, (*b*) the external-circuit resistance, and/or (*c*) the output. Consequently, the observed temperature coefficient of

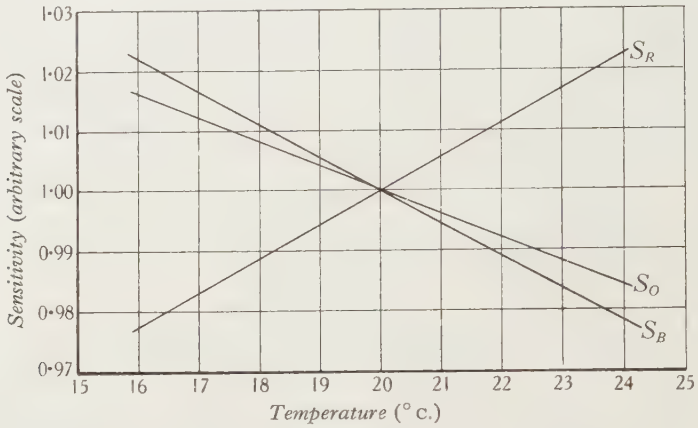

Figure 6. Dependence of sensitivity upon temperature for red light (S_R), for orange light (S_O) and for blue-green light (S_B). External-circuit resistance, 100 Ω.

sensitivity will be determined by (1) the external-circuit resistance, (2) the quality of the incident light, and (3), to a smaller extent, the quantity of the incident light.

The effect of external-circuit resistance has already been substantiated by tests on commercial cells at the National Physical Laboratory and by other workers[9]. The effect of variation of (2) and (3) is likely to be negligibly small for simple tungsten sources; but on the other hand the temperature coefficient of sensitivity observed when the cell is used with a tungsten source may be substantially different (in magnitude or sign or both) from that observed when the source is daylight or one having a discontinuous spectrum.

It is interesting to note here that increase of sensitivity for the red end of the visible spectrum with increase of temperature has often been observed in studies of the inner photoelectric effect in selenium[7].

§ 6. COLOUR CORRECTION

The fact that the spectral sensitivity has been shown not to be independent of the experimental conditions makes it doubtful whether any useful purpose is served by attempting to correct the spectral sensitivity so as to make it coincide with the visibility for the normal eye, for it is seen that unless considerable care is exercised in calibrating the cell under exactly those conditions which prevail during use,

a precision approaching even 1 per cent may be difficult to obtain. On the other hand, the departure from the visibility curve (see tables 1 and 2) is already objectionably large.

Possible methods of correction have been considered in detail, including (1) the deposition by sputtering, on the lacquered surface of the cell, of thin metallic films, and (2) the use of coloured lacquers. However, at present the only practicable method appears to be the use of a liquid colour filter.

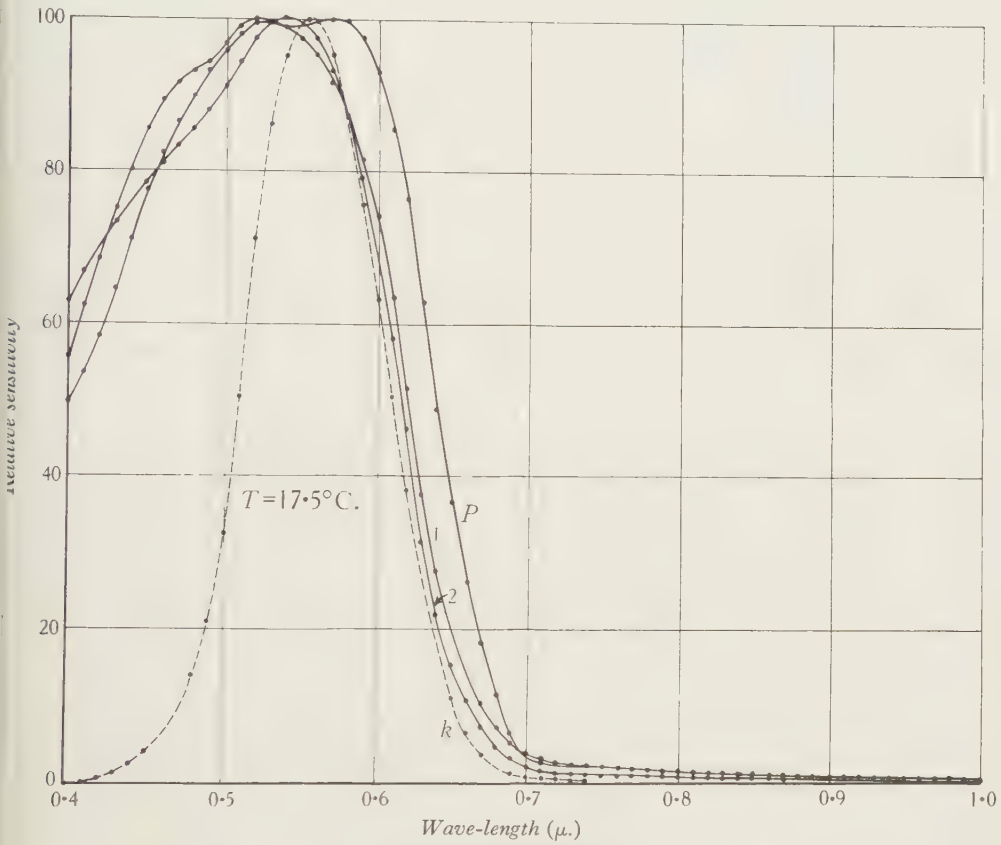

Figure 7. Spectral distribution of sensitivity for cells nos. P, 1 and 2, table 2, external-circuit resistance equal to 100 Ω. The visibility function k is also shown.

Figure 7 gives spectral distribution curves of sensitivity for cells nos. P, 1 and 2, and figure 8 those for the cells listed in table 1. These curves were obtained under the conditions specified in § 2; but in consequence of the falling sensitivity of the vacuum photoelectric cell used, photoelectric spectrophotometer measurements were discontinued at 0·70μ. Except for the Weston Photronic cell, the relative sensitivities of all the cells, for which measurements are given, are not at 0·70μ. greater than about 6 per cent of the maximum sensitivities; in the case of the Weston Photronic cell, the relative sensitivity at 0·70μ. is about 12 per cent of the maximum. There is, however, no evidence that the threshold for the selenium

rectifier photocell is sharply defined. On the contrary, when a cell is used in combination with a saturated solution of copper sulphate, 1 cm. in thickness in a glass cell, there is still appreciable infra-red sensitivity. The threshold appears to lie well out in the infra-red, whence occurs a slow gradual rise in sensitivity with decreasing wave-length down to the beginning of the visible spectrum. Frenkel and Joffé, in fact, believe from theoretical considerations that the contact photoelectric current should actually begin at the same frequency as the inner photoelectric effect.

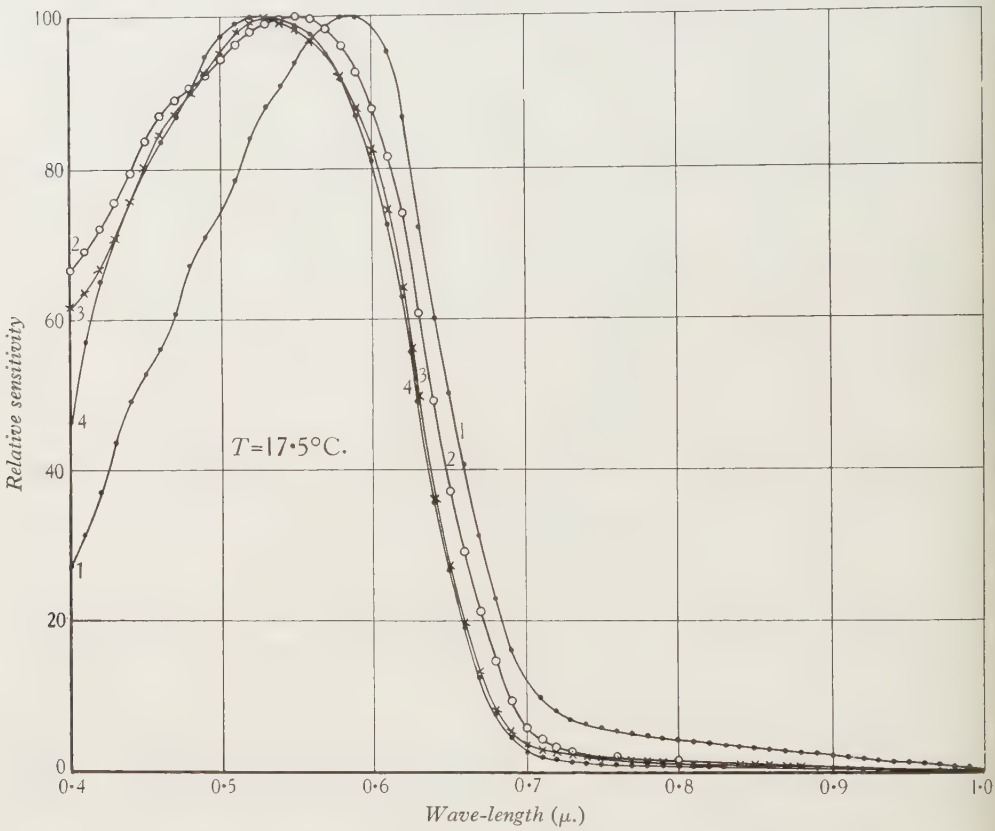

Figure 8. Spectral distribution of sensitivity for cells nos. 1, 2, 3, 4, table 1, external-circuit resistance equal to 100 Ω.

The threshold wave-length for the inner photoelectric effect for selenium lies beyond 1·2 μ.

The general course of any curve given in figures 7 and 8 may, however, be determined from 0·70 to 1·00 μ. with sufficient accuracy by tests with neutral-tint filters. An example will be given for cell no. 1. A Wratten neutral gray filter of mean visible density 2·02 (mean visible transmission 0·95 per cent) has a fairly uniform transmission from 0·40 to 0·72 μ., and hence its integral transmission ratio for the visible region of the spectrum is largely independent of the distribution of sensitivity in this region. From 0·72 μ., however, the filter transmission rises

rapidly to a maximum at 0·90 μ. and remains constant up to 1·00 μ., the transmission being now approximately five times that in the visible spectrum. The assumption is made that the spectral distribution curve of sensitivity of the rectifier cell continues to fall steadily from 0·70 to 1·00 μ., and hence a test with such a filter can be used to determine the gradient of the curve from 0·70 to 1·00 μ. For example, for cell no. 1, yielding constant output with a source operating at a colour temperature of 2360° K., a cell and filter temperature of 17·5° C., and an external-circuit resistance of 100 Ω., the measured density of the Wratten neutral gray filter was found to be 1·880; with the spectral sensitivity curve given in figure 7, the calculated density of the same filter under the same experimental conditions is 1·8794.

From the curves given in figures 7 and 8, values for S_B/S_R with a source operating at a colour temperature of 2360° K. may be calculated. During the photoelectric spectrophotometer measurements the output of the rectifier cell varied over a maximum range of 0·5 to 4·0 μa. with an external-circuit resistance of 100 Ω. The cell-temperature was 17·5° C. Measurements of S_B/S_R for these cells at the same temperature and with the same external-circuit resistance were made on the photometer bench with a source operating at a colour temperature of 2360° K. The output of the cell was maintained constant for the tests on the two filters, but varied from cell to cell as stated in § 2. For all the cells except the Weston Photronic and cell no. 2, the constant values of output were between 3 and 4 μa.; for the two cells mentioned the constant values of output were between 1 and 1·5 μa.

The ratio $(S_B\ S_R)_{\text{calc.}}$ $(S_B\ S_R)_{\text{meas.}}$ for the Weston Photronic cell was found to be 1·000, and for cell no. 2 it was 1 per cent higher. For all the other cells the ratios were found to be all higher than unity by varying amounts up to 15 per cent. In view of the known differences in output between the two methods of determination of $S_B\ S_R$, these results are qualitatively in agreement with the proved dependence of $S_B\ S_R$ upon output. It is thus seen that a representation of the spectral distribution of sensitivity of a rectifier cell means little, or at least is not complete, if the corresponding output of the cell is not also stated for each wave-length. A convenient standard method of representation would be that showing the curve obtained when the output of the cell is constant for all wave-lengths. This may be a matter of difficulty experimentally, and the curve would still not be the correct curve to use in calculating an integral luminosity, for instance, in terms of cell output. Again, the external resistance used and the temperature at which measurements are made are data necessary to complete any representation of the spectral sensitivity of a rectifier cell.

For cell no. 1 at a temperature of 17·5° C., giving a constant output of 3 μa. with an external-circuit resistance of 100 Ω., the ratio $(S_B/S_R)_{\text{calc.}}/(S_B/S_R)_{\text{meas.}}$ was found to be 1·112. When cell no. 1 is combined with a liquid filter having the transmission curve shown in figure 9, the spectral distribution curve of sensitivity of the combination is effectively limited to the region 0·47 to 0·74 μ. At the same temperature and with the same external-circuit resistance, but a constant output of 1·75 μa., the ratio $(S_B/S_R)_{\text{calc.}}/(S_B/S_R)_{\text{meas.}}$ for the combination becomes 1·261. Since in normal circumstances with the cell alone a reduction in output, for the

bench tests, results in an increase of $(S_B/S_R)_{meas.}$ of approximately 1 per cent, which would lead to a slight decrease of the ratio $(S_B/S_R)_{calc.}/(S_B/S_R)_{meas.}$, it is seen that the increase of this ratio obtained by limiting the spectral region of sensitivity to 0·47 to 0·74μ. is very substantial. This would arise if the change of spectral sensitivity with output is most pronounced in the region of the maximum sensitivity, i.e. 0·53 to 0·57μ. Further tests with a very selective sap-green filter in place of the liquid filter provided additional support for this conclusion.

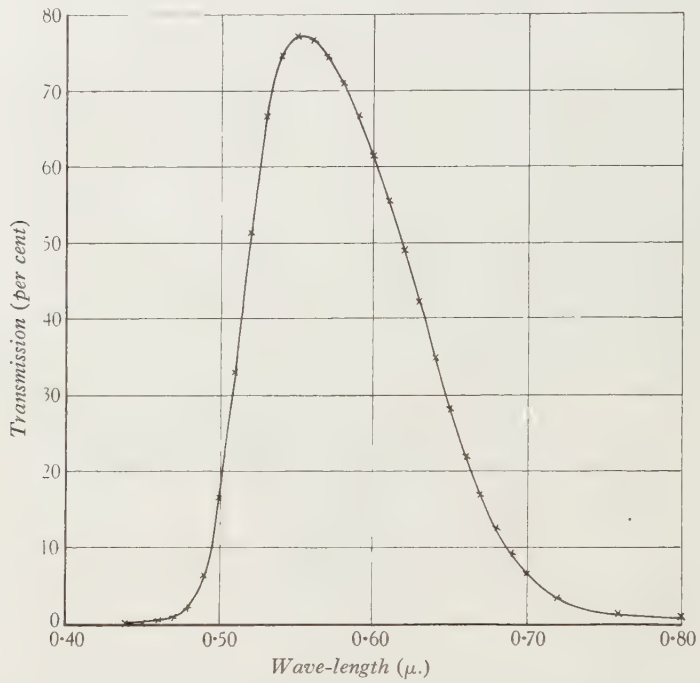

Figure 9. Spectral transmission for liquid filter comprising equal quantities of $(M/66)$ $K_2Cr_2O_7$ and $(M/3)$ $CuSO_4.5H_2O$, 1 cm. in thickness in glass cell. $T = 17{\cdot}5°$ C.

The liquid filter referred to in the above tests was composed of a mixture of equal quantities of $(M/66)$ $K_2Cr_2O_7$ and $(M/3)$ $CuSO_4.5H_2O$, 1 cm. in thickness in a glass cell, M being the molecular weight in grams in 1 litre of distilled water. With a given cell-output, external-circuit resistance, and temperature, this filter was used to correct the spectral distribution curve of sensitivity of cell no. 1, table 2, to the visibility curve for the normal eye; its composition was determined empirically. With the combination of cell and filter the integral transmission ratios of a large number of selective colour filters were measured. The measured integral transmission ratio is denoted by T_m, and the integral transmission ratio according to the visibility function by T_v. Table 3 gives the ratio T_m/T_v for the various filters measured.

By the use of Davis-Gibson standard double-liquid filters in combination with a tungsten lamp, it has been possible to test this combination of cell and filter

throughout the colour-temperature range 2000 to 7000° K. With the experimental conditions as specified in table 3, the sensitivity was found to be constant within ±2 per cent over the entire range.

Table 3. Cell-output, 1·75 μa.; temperature, 17·5° C.; external-circuit resistance, 100 Ω.

Filter no.	Filter	Effective wave-length (μ.)	T_m/T_v
68	Blue-green	0·5288	0·953
6	,,	0·5317	0·972
5	Sap green	0·5509	1·071
9	Cobalt blue	0·5531	1·031
10	Daylight	0·5555	1·038
11	Ortho-green	0·5729	1·028
65	Amber	0·5920	1·055
4	Light orange	0·5950	1·047
3	Dark orange	0·6034	1·037
13	Selenium red	0·6357	1·031
14	,,	0·6432	1·024

It may be mentioned here that by suitable modification of the concentrations of the two components, $K_2Cr_2O_7$ and $CuSO_4$, it is not difficult to obtain satisfactory colour correction for any given set of experimental conditions for any rectifier cell named in this paper[11].

§ 7. DISCUSSION OF RESULTS

The dependence of the spectral distribution curve of sensitivity upon the conditions of measurement here proved for the rectifier photoelectric cell was observed many years ago in the case of the inner photoelectric effect in selenium, and was then ascribed to actual molecular movement of the ionization centres[7]. Since that time, however, many of the properties of semiconductors have been satisfactorily interpreted in terms of A. H. Wilson's theories[10] of conduction in semiconductors. If therefore selenium is considered as an impurity semiconductor, the conduction electrons must be derived entirely from atoms of impurities which although small in quantity are still sufficiently large to mask entirely the natural conductivity of the substance. Hence it is not unlikely, in view of the sparsely distributed impurity states, that ejection of an electron from one of them results in a disturbance of the remaining electronic states, giving rise to a dependence of the spectral distribution curve of sensitivity upon output and temperature. The increase of red sensitivity as compared with blue-green sensitivity for decrease of external-circuit resistance can be ascribed to the same cause, in so far as reduction of external-circuit resistance results in a reduction of the proportion of primary photoelectrons returned to the semiconductor through the contact.

§ 8. ACKNOWLEDGEMENTS

The author is indebted to his colleagues in the photoelectric section of the Photometry Division for the results obtained with the photoelectric spectrophotometer. He particularly wishes to thank Mr J. S. Preston for much valuable criticism in the course of informal discussions on the results obtained.

REFERENCES

(1) Marchal, G. and Marton, L. *Rev. Opt.* (*théor. instrum.*), **15**, 1 (1936).
(2) König, H. *Helv. phys. Acta*, **8**, 505 (1935).
(3) Preston, J. S. and Cuckow, F. W. *Proc. Phys. Soc.* **49**, 189 (1937).
(4) Campbell, N. R. and Freeth, M. K. *J. Sci. Instrum.* **11**, 125 (1934).
Atkinson, J. R., Campbell, N. R., Palmer, E. H. and Winch, G. T. *Proc. Phys. Soc.* **50**, 934 (1938).
(5) Barnard, G. P. *Proc. Phys. Soc.* **47**, 477, 1935.
(6) Preston, J. S. *J. Instn Elect. Engrs*, **79**, 424 (1936).
(7) Barnard, G. P. *The Selenium Cell*, section 35, p. 109 *et seq.* (Constable and Co., Ltd., 1930).
(8) Preston, J. S. *Proc. Phys. Soc.* **46**, 256 (1934).
(9) Illuminating Eng. Soc. (N.Y.). *Report of the Committee on Photoelectric Portable Photometers*, p. 32 (1936).
(10) Wilson, A. H. *Proc. Roy. Soc.* **133**, 458 (1931); **134**, 277–87 (1931–2); **136**, 487–98 (1932).
(11) *Report on Physical Photometry, Comm. Int. de l'Éclairage, C.R.*, p. 231 (1935).

APPARATUS FOR ELECTRON-DIFFRACTION AT HIGH TEMPERATURES

By R. JACKSON and A. G. QUARRELL
Department of Applied Science, University of Sheffield

Received 24 *November* 1938. *Read in title* 13 *January* 1939

ABSTRACT. Apparatus and technique are described by means of which the examination of surfaces by electron-diffraction may be carried out at temperatures up to 1200° C. The diffraction section is water-cooled, and a special feature of the design is that no refractory material is used in the vacuum chamber; this enables a high vacuum to be maintained.

§ 1. INTRODUCTION

HITHERTO the examination of surfaces and thin films by electron-diffraction has been carried out almost entirely at ordinary temperatures, although R. O. Jenkins[1] investigated oxide films on certain molten metals of low melting point. Largely owing to the fact that his specimen-heater was of a porous refractory material, Jenkins was unable to prevent oxidation of the molten metals.

During the course of work on iron-oxide surfaces formed at temperatures up to 1200° C. it became evident that electron-diffraction results were liable to be misleading unless examination was carried out at the temperature of oxidation. Accordingly, a small furnace specimen-holder was made from a densely packed asbestos compound known as "Syndanyo", the heater element being of Kanthal wire. It was found, however, that gas was given off by the refractory during the heating process, and this caused progressive oxidation of the metal surface. Because of this the problem was attacked from a new point of view, based on the principle that no refractory material should be used within the diffraction section.

§ 2. THE SPECIMEN-HEATER

The design finally adopted is shown in figure 1. The specimen *A* is clamped to the closed end of an Immaculate V heat-resisting steel tube *B*, $\frac{3}{4}$ in. in internal diameter and 1 in. in external diameter, and is heated by an arc run between the carbon electrode *C* and the graphite cup *D*. The furnace enters the diffraction section through the standard port *E*, and specimen-adjustment is made possible by the section *F*, which consists essentially of Tombac bellows controlled by the usual system of springs and adjusting screws.

The electrode *C* is held in a brass clamp *G* and insulated by means of a fibre block *H*, the necessary movement for continuous running of the arc being provided by the rack and pinion *I*. A very steady arc may be maintained even on alternating

current, and because of the slow rate of replacement of oxygen along the tube the rate of electrode-consumption is low. Burning of the carbon rod nearer the mouth of the tube is prevented by the silica sheath *J*. Owing to the high temperatures

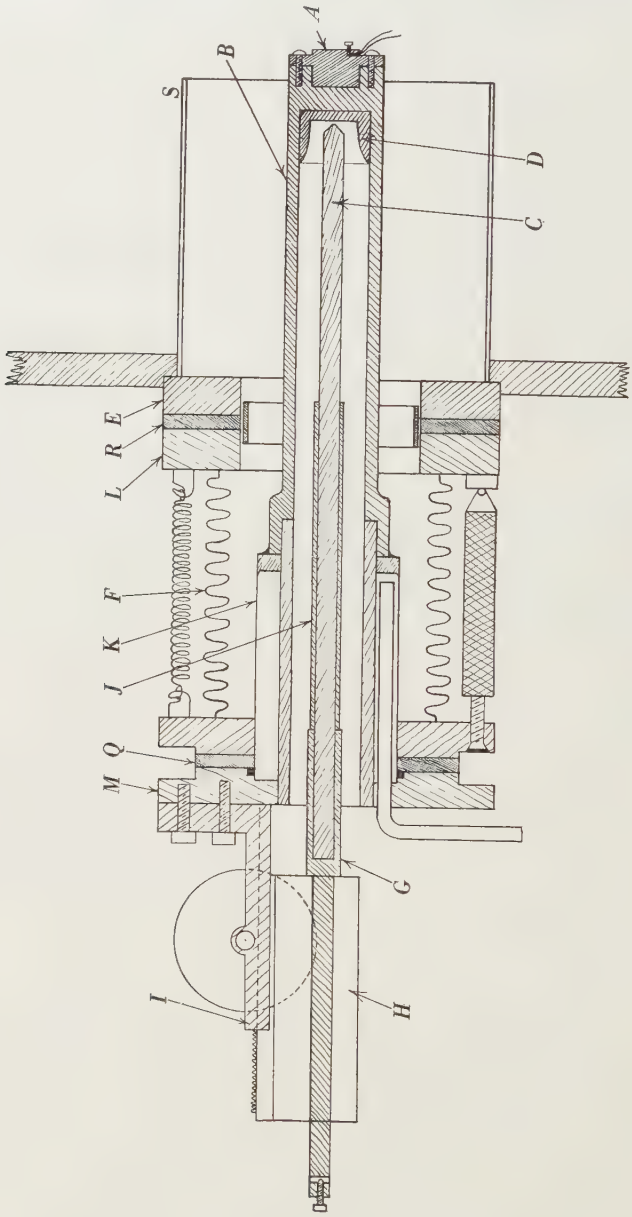

Figure 1. The specimen-heater.

attained by the closed end of the furnace tube, the other end is surrounded by a water jacket *K*, and the block *L* is also water-cooled.

The length of the furnace tube is too great for the tube to be bored with standard

drills, but the following methods of construction have been successfully used. In the first, the specimen-holder was welded to one end of an open tube of suitable length. We have to thank Messrs Accles and Pollock for supplying us with tubes which were made in this way and only failed when the graphite cup slipped out of position and the arc was run between the carbon electrode and the metal. In the second method the tube was in two parts, both of which could be made from the solid black hot-rolled rod with standard drills. The part carrying the specimen holder was enlarged at the open end, and the other part was machined to make a tight press fit in it. The joint was then brazed and the brazing metal was used as a basis for a soft-soldered joint with the water jacket. Similarly, the soldered joint between the mouth of the tube and the block *M* was made possible by depositing a band of brazing metal around the tube.

The difficulty of maintaining vacuum-tight ground surfaces between the various parts of the furnace and its supports was overcome by the introduction of the rubber gaskets *Q* and *R*.

§ 3. THE SPECIMEN

Specimens for use in vacuo at high temperatures must make good thermal contact with the furnace tube and enable accurate thermocouple readings to be taken. The design of specimen indicated in figure 1 was arrived at after several other types had proved unsatisfactory. The specimen is machined to make a good fit in the recess at the end of the furnace tube and is clamped in position with two $\frac{1}{8}$-in. Whitworth screws passing through the specimen flange. A central area $\frac{1}{2}$ in. in diameter projects slightly above the surrounding surface and is the true specimen for electron-diffraction purposes. Owing to the guard-ring effect of the surrounding flange, this central area attains a remarkably uniform temperature. The temperature of the specimen is measured by means of a thermocouple inserted in a hole drilled parallel to the surface and as near to it as possible, good thermal contact being ensured by clamping the junction in position with a 10-B.-A. screw. Since the whole of the specimen near the junction is at a uniform temperature, and the junction is within 1 mm. of the surface, it is believed that the readings obtained are within 5 or 10° C. of the true surface temperature. Bad thermal contact between the thermocouple and the specimen was found to lead to serious errors, but by checking with an optical pyrometer and observing the critical temperatures of the iron specimen it was possible to tell when good thermal contact had been achieved.

At temperatures above 900° C. the specimen and its clamping screws tend to weld to the furnace tube, but this may be avoided by coating with a thin layer of Aquadag colloidal graphite.

§ 4. THE DIFFRACTION SECTION

It was found that the standard diffraction section of the camera[2], which was of the Finch type, was unsatisfactory for work at high temperatures, and accordingly a new diffraction section was made. It consists essentially, figure 2, of a hollow

brass casting whose external dimensions are $9\frac{1}{2}$ in. × 6 in. × 6 in., with a cylindrical inner surface $5\frac{1}{8}$ in. in diameter and $8\frac{1}{2}$ in. long. To avoid the necessity for entirely new specimen-holder and diaphragm-holders, six standard ports were soldered to the machined casting in suitable positions. In addition, a vacuum release valve[3] and a hand port 5 in. in diameter were incorporated. Watercooling ducts, $\frac{3}{8}$ in. in diameter, were drilled lengthways at the four corners and connected in series by channels in the end surfaces of the casting. The whole of the inner and outer surfaces of the casting were tinned to avoid vacuum trouble due to possible porosity.

The furnace-tube port was fitted on the inside with a radiation shield *S* projecting almost to the specimen surface. To the opposite port was fitted an adjustable radiation shield of polished Staybrite, *T*. By means of a suitable screw mechanism

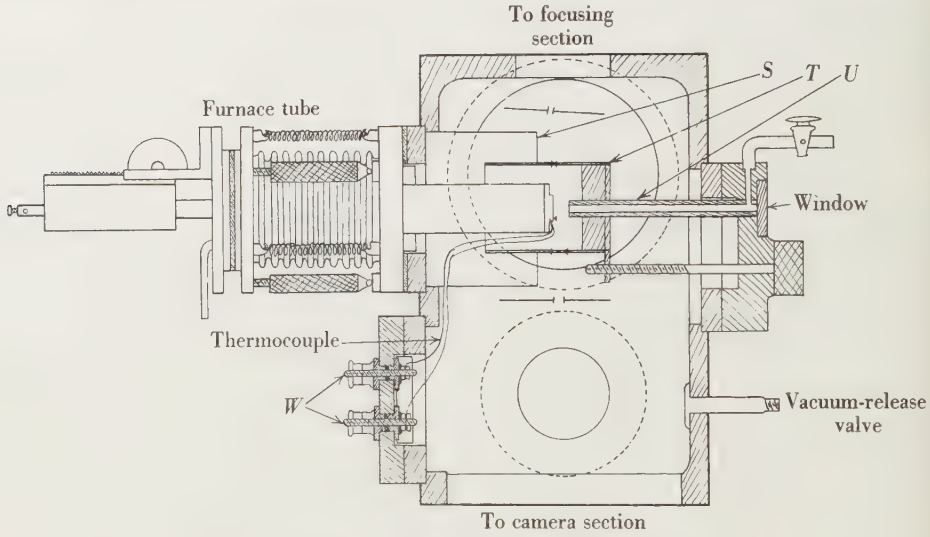

Figure 2. The diffraction section.

this radiation shield could be moved along the tube *U*, which also served as a sighting tube for use with an optical pyrometer and as a means of directing a stream of gas on to the specimen. Holes were made in the shield to permit the passage of the incident and diffracted beams. In order to simplify adjustment, these holes were made larger than was strictly necessary, and two subsidiary diaphragms carried on normal specimen carriers were used to limit the beams more exactly.

The thermocouple, insulated by silica sheathing, was threaded through a hole in the shield *S* and connected to the terminals *W*. These were insulated by ebonite bushes, and a robust vacuum-tight joint was made by packing the space between the bushes with plasticine and tightening the terminal nuts. Adjustment of the thermocouple leads was carried out through the hand port, which also enabled the radiation shields, too large to pass through a standard port, to be placed in position. A 6-v. lamp mounted on one of the lower ports considerably facilitated these adjustments.

§ 5. EXPERIMENTAL PROCEDURE

In using the apparatus for the preparation and examination of oxide films, the following procedure was adopted. A suitable specimen having been placed in position, the camera was evacuated and flushed out several times with argon at a pressure of about 1 mm. Throughout the experiment the leak to the cathode chamber was fed with argon to avoid uncontrolled oxidation of the specimen.

The specimen, radiation shield, and diaphragms were adjusted to give an angle-of-incidence line in a suitable position on the fluorescent screen. Expansion of the furnace tube at high temperatures causes the specimen to move farther into the diffraction section, thus decreasing the angle of incidence for a given setting of the section *F*. The angle of incidence was therefore made sufficiently large to allow for this expansion, in order to avoid adjustment of the specimen at high temperatures, since this was made difficult by light from the red-hot furnace falling on the fluorescent screen.

As the available d.-c. supply was isolated, and since the furnace tube must be earthed, the arc had to be run on a.c. A current of 20 or 25 amp. at 30 or 35 v. sufficed to raise the temperature of the specimen to 1200° c. in 5 or 10 min., the hot zone being confined almost entirely to the last inch of the furnace tube. The temperature of the specimen was measured by means of the thermocouple in conjunction with a Tinsley vernier potentiometer, and the thermocouple readings were checked from time to time by optical measurements and by observing the critical temperatures of the iron specimen. The alternating furnace current caused a pronounced oscillation of the electron beam, and examination whilst the arc was running was rendered impossible. Accordingly no efforts were made to control the arc sufficiently to maintain a steady temperature, but when the specimen reached the required temperature for oxidation the arc was switched off, and simultaneously a small quantity of air or other oxidizing gas was admitted through the tube *U*. Because of the design of the radiation shield this resulted in a temporary local pressure at the specimen surface, causing oxidation, but the normal camera vacuum was soon restored. Thus on admission of 3 cm^3 of air at a pressure of 25 cm. the discharge potential was reduced by about 10 kv. for 10 or 15 sec. For examination of the oxide film at the temperature of formation, the arc was once more switched on and the specimen was reheated to this temperature. The arc was switched off, and the exposure of one half of the photographic plate began when the temperature had reached the required value. Owing to the large heat-capacity and long conduction path of the furnace tube, the rate of fall of temperature was low; initial temperatures of 1050, 850 and 450° c. fell to 990, 820 and 440° c. respectively during exposures of 20 sec. By means of the split-shutter mechanism[4] the other half of the plate could be exposed at some other temperature, or at the same temperature after further treatment of the specimen. In this way structural changes in the film which occurred on cooling or progressive oxidation could be followed.

When it was required to oxidize a new specimen the whole of the furnace tube and radiation shield were thoroughly freed from oxide by being rubbed with

emery paper in order that transfer of oxygen from these parts to the specimen might be avoided.

The FeO patterns of figure 3 were obtained from a steel containing 0·45 per cent of carbon, oxidized at 850° C. with 3 cm^3 of air at a pressure of 25 cm., the exposures being made at 850 to 820° C. and 650 to 625° C. respectively. The two patterns are displaced with respect to each other because no adjustment was made to counterbalance the contraction of the furnace on cooling.

Blackening of the photographic plate by light from the furnace is not appreciable at temperatures below 800° C. At first considerable difficulty was experienced at higher temperatures, the electron-diffraction pattern being almost completely

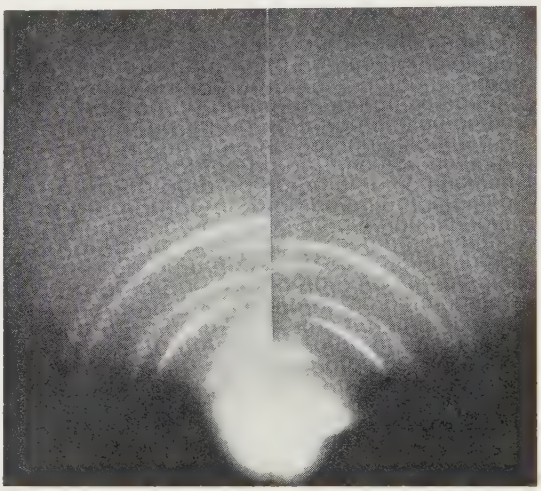

Figure 3. FeO at 850 and 650° C.

masked by the blackening of the plate by light. This was overcome by desensitizing the plates before use with Ilford Desensitol as it was found that the treated plates, after being dried, were still sensitive to electrons but were unaffected by light from the furnace. Finally, however, the trouble was eliminated by reducing the diaphragms below the specimen to the smallest possible size. Under these conditions blackening was inappreciable below 1050° C., and at temperatures up to 1200° C. it was insufficient to cause real difficulty.

Another result of increasing the temperature of the specimen is to increase the amount of incoherent scattering around the undiffracted spot. This effect is not serious below 900° C., but above this temperature it is sufficient to render measurement of the innermost lines difficult. In the particular case of oxide films on specimens of Armco iron it has also been found that repeated heating to high temperatures results in a progressive roughening of the surface, leading to a weakening of the diffraction rings and a further increase in incoherent scattering.

§ 6. LIFE OF THE SPECIMEN-HEATER

Our experience would indicate that the life of the furnace tube is almost unlimited at temperatures below 1000° C., but is much shortened when the tube is used at temperatures in the neighbourhood of 1200° C. The construction is such that replacement of a faulty tube is a relatively simple matter, and therefore there is no reason why the method should not be used even at such high temperatures.

§ 7. CONCLUSION

The apparatus described enables surface films to be examined by electron-diffraction at temperatures up to 1200° C.; it thus opens up a large new field to this method of structural investigation. By suitable adaptation of the furnace tube, thin films could also be examined at high temperatures, and it must be emphasized that the modifications made in the standard camera in no way detract from its suitability for use at ordinary temperatures. Indeed it has been found that since the diffraction section has been water-cooled much less trouble has been given by the ground joints. The design of the diffraction section and the method of attaching the standard ports greatly reduce the restrictions imposed upon the size of diaphragms and other fittings. Moreover, specimens too large to pass through a standard port can be inserted through the hand port and subsequently attached to a normal specimen-carrier.

It is clear that the investigation of changes in surface structure with temperature would be greatly facilitated if a series of exposures could be made instead of the two which alone are possible with the split-shutter plate-holder. For this reason it is hoped that a suitable multiplate camera will be incorporated in the near future.

§ 8. ACKNOWLEDGEMENTS

We wish to express our appreciation of the helpful advice and constructive criticism given us by Prof. J. H. Andrew, D.Sc., in whose laboratories this work was carried out.

REFERENCES

(1) Jenkins, R. O. *Proc. Phys. Soc.* **47**, 109 (1935).
(2) Finch, Quarrell and Wilman. *Trans. Faraday Soc.* **31**, 1077 (1935).
(3) Jackson and Quarrell. *J. Sci. Instrum.* **15**, 208 (1938).
(4) Jackson and Quarrell. *Proc. Phys. Soc.* **50**, 776 (1938).

ACOUSTIC SPECTRA OBTAINED BY THE DIFFRACTION OF LIGHT FROM SOUND FILMS

By D. BROWN, Ph.D.
Auckland University College, New Zealand

Communicated by Prof. P. W. Burbidge 1 *August* 1938. *Read* 25 *November* 1938

ABSTRACT. The theory of diffraction is applied to a generalized form of diffraction grating such as that provided by a variable-density sound film. The results indicate that under certain conditions the different frequency components in the original sound will be uniquely represented by spectral lines in the diffraction pattern, producing an acoustic spectrum. The theory of the method is shown to be of great generality, permitting an analysis of transient as well as of sustained sounds. The analogy between the optical effects and the original sound is developed in some detail, spectral ghosts being identified with the side frequencies which result from amplitude-modulated waves. The latter conception is also found of use in discussing the breadth and fine structure of the spectral lines themselves. Sound films are normally recorded with some form of optical shutter, which transmits light whose intensity is proportional to i, the amplified audio-frequency current, but it is shown that for films intended for acoustic analysis, the light-intensity must vary as i^2. Photographs of records made in this way are reproduced, together with the derived acoustic spectra, which accord with the theory. Finally, the probable value of the method as an addition to existing methods of sound-analysis is discussed.

§ 1. INTRODUCTION

The recording of sound on photographic film by optical means has become one of the most important methods of sound-recording, and one which as a result of much technical research by the sound-film industry is capable of a high degree of fidelity. At the standard film speed of 90 ft./min. frequencies up to 9000 c./sec. can be recorded successfully. The ordinary recording and reproducing processes both make use of a beam of light focused to form a very fine slit image on the moving film; in the former case the film is subjected to an illumination which fluctuates in accordance with the wave-form of the sound, and in the latter the film is the agent which causes similar fluctuations in the transmitted beam. The illumination of the original slit-image can be varied by two alternative methods, the resulting sound-tracks being referred to as "variable-density" or "variable-width" records according to which method is used. The considerations which follow will refer only to the variable-density type, in which the sound-records appear as striations across the film.

It is the purpose of this paper to discuss some optical properties which make these films objects of interest in themselves, quite apart from their normal use as a means of sound-reproduction. Suppose a specimen of such film to be illuminated,

not with a sharply focused beam as in the normal reproducing process, but with a parallel beam of monochromatic light extending over an appreciable length of the film. The film may, for example, be introduced into an ordinary spectroscope in the manner of a diffraction grating. On looking through the instrument, it will usually be found that a number of images of the slit are to be seen on either side of the central image; they are due to beams diffracted from the sound-track itself. If the film is fed through the spectroscope the diffraction images are seen to change in number and in position, being evidently in some way related to the wave-form recorded on the film.

The actual relationship might perhaps be expected to be somewhat remote, as the wave-form of the density-variations will as a rule be compounded of a number of entirely unrelated periodicities. Complicated effects are known to occur with ordinary ruled gratings, when there are any periodic variations in the process of ruling; these are liable to give rise to companion lines or ghosts on either side of the main diffraction lines. If in the present instance each periodicity were to react on every other in this way a great multiplication of lines would ensue, making the diffraction pattern a thing of little physical interest. It is somewhat gratifying to find, as has been briefly reported in an earlier note[1], that the actual relationship is almost the simplest possible, the observed lines virtually constituting an acoustic spectrum of the original sound.

§ 2. HISTORICAL. FOURIER ANALYSIS IN DIFFRACTION PROBLEMS

Michelson[2] in 1905 used a two-dimensional form of Fourier analysis to describe a reciprocal relation between a source and its diffraction pattern. In the following year Porter[3], discussing the theory of microscopic vision, employed the idea of identifying the successive orders of spectra formed by an opacity grating with the Fourier components of the function representing the variation of illumination in the plane of the grating. He showed experimentally that if the abrupt transitions of the grating be replaced by gradual transitions from light to dark, only the lower orders or possibly only the first order appears. Nevertheless, the relationship between the diffraction process and Fourier analysis is not stressed in many subsequent accounts of the theory of optical gratings, although the results of the theory can often be seen to be natural consequences of this relationship. For example, when the opaque and transparent strips are of equal width, the spectra of even order are absent; or when the transparent strips are very narrow compared to their distance apart, the orders decrease very slowly in brightness, since the corresponding Fourier series converges very slowly. In connexion with the diffraction of x rays by crystals, however, the Fourier approach has often been used in recent years, and somewhat similar considerations arise in the diffraction of light by ultrasonic waves, which in the simplest case give rise to a first-order spectrum only. It will be best to consider the case of sound films from first principles, since in many instances the recorded wave-form will lack the regular periodic character which is the basic feature of the various types of grating referred to above.

§ 3. GENERAL THEORY

Suppose a chosen length l of sound film to be illuminated by a parallel beam of light of wave-length λ incident normally as in figure 1. The possibility of grainless photography will be assumed, so that the amount of light transmitted may be treated as a function of the single co-ordinate x, the distance along the film.

Let the amplitude of the light vibration transmitted in the region between x and $x+dx$ be $f(x)$, and introduce the customary assumption that the light diffracted from any point is radiated uniformly in all directions. For present purposes it will be sufficient to discuss the diffracted beams on one side only of the central beam. Then if we consider the resultant at a sufficiently remote point M in the direction θ, we can replace the effect of the whole grating OP by that of the

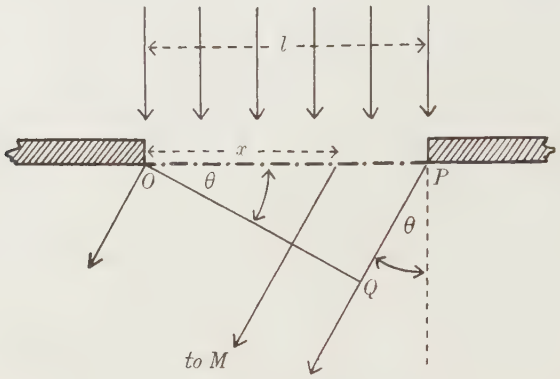

Figure 1.

wave-front OQ, if we allow for the effect of the path-differences upon the phase of the vibrations, and neglect the effect upon the amplitude. As M recedes to infinity the diffraction effect becomes a function of θ only, to be observed with a telescope focused at infinity. In the wave-front OQ a vibration originating from the point x will be retarded in phase by an amount α given by

$$\alpha = \frac{2\pi}{\lambda} x \sin\theta.$$

If we now sum the vibration components which are in the same phase as the undiffracted wave-front OP, or differ from it in phase by $\frac{1}{2}\pi$, we have respectively,

$$C = \int_0^l f(x) \cos\alpha\, dx, \quad S = \int_0^l f(x) \sin\alpha\, dx.$$

Then the aggregate disturbance represented by the diffracted wave-front OQ has an amplitude $\sqrt{(C^2+S^2)}$, and its phase relative to the undiffracted wave-front is

$\tan^{-1}(S/C)$. If now the number of wave-lengths of light in PQ is set equal to n, which is not necessarily an integer, then

$$\frac{l \sin\theta}{\lambda} = n, \qquad \text{.....(1)}$$

$$C = \int_0^l f(x) \cos\frac{2\pi n x}{l}\, dx, \qquad \text{.....(2a)}$$

$$S = \int_0^l f(x) \sin\frac{2\pi n x}{l}\, dx. \qquad \text{.....(2b)}$$

It will be seen from figure 1 that only the portion of the film between $x=0$ and $x=l$ is exposed, the rest of the film being obscured by screens. The function $f(x)$ will thus have zero value for $-\infty < x < 0$ and for $l < x < \infty$, while between 0 and l it may be completely arbitrary, being composed of any number of unrelated periodicities of varying duration. Such a function may be analysed by Fourier's integral, a standard form of which is

$$f(x) = \frac{1}{\pi}\int_0^\infty d\omega \int_0^l f(\xi)\cos\omega(\xi - x)\, d\xi.$$

Here ξ is a running co-ordinate which disappears after the integration has been completed. Expressing this integral in a form more convenient for our purpose, we have

$$\begin{aligned} f(x) &= \frac{1}{\pi}\int_0^\infty d\omega \int_0^l f(\xi)(\cos\omega\xi\cos\omega x + \sin\omega\xi\sin\omega x)\, d\xi \\ &= \frac{1}{\pi}\int_0^\infty \cos\omega x\, d\omega \int_0^l f(\xi)\cos\omega\xi\, d\xi + \frac{1}{\pi}\int_0^\infty \sin\omega x\, d\omega \int_0^l f(\xi)\sin\omega\xi\, d\xi \\ &= \frac{1}{\pi}\int_0^\infty \phi(\omega)\cos\omega x\, d\omega + \frac{1}{\pi}\int_0^\infty \psi(\omega)\sin\omega x\, d\omega \\ &= \frac{1}{\pi}\int_0^\infty A(\omega)\cos(\omega x - \epsilon)\, d\omega. \end{aligned}$$

That is to say, $f(x)$ may be represented by a series of cosine waves of all frequencies from 0 to ∞, where a typical wave has an amplitude proportional to

$$A(\omega) = \sqrt{\{\phi^2(\omega) + \psi^2(\omega)\}},$$

and a phase

$$\epsilon = \tan^{-1}\frac{\psi(\omega)}{\phi(\omega)},$$

these two quantities being determined by the integrals

$$\phi(\omega) = \int_0^l f(\xi)\cos\omega\xi\, d\xi, \qquad \text{.....(3a)}$$

$$\psi(\omega) = \int_0^l f(\xi)\sin\omega\xi\, d\xi. \qquad \text{.....(3b)}$$

The resemblance between these and the integrals for C and S, equations (2a, 2b), is immediately apparent, the two sets becoming identical if we identify ω

with $2\pi\,(n/l)$, so that n is the number of times the corresponding cosine wave is repeated in the length l of the film. The amplitude A of this wave is thus proportional to the amplitude of the light vibration in the beam diffracted in that particular direction for which the path-difference $PQ = n\lambda$.

It may easily be shown that although only one half of the diffraction pattern has been considered, the pattern is symmetrical in appearance about the central line; this symmetry does not, however, extend to the phases of the vibrations in corresponding diffracted beams.

§ 4. DISCUSSION OF THEORY

Pending further discussion in § 5, $f(x)$ will be taken as conforming to the wave-form of the original sound. If V is the film-velocity used in recording, the chosen length l of film will represent a time interval t equal to l/V, which will usually be some fraction of a second. The diffraction pattern may then be regarded as an acoustic spectrum of the original sound averaged over the period t. In deciding upon the value to be given to this period, it would be necessary to bear in mind that the spectrum will obviously be of little significance if t is made very small, or (except in the case of sustained sounds) very large.

Each particular harmonic component in $f(x)$ produces its individual diffracted beam unaffected by any other components which may be present at the same time. The only case where a component of one frequency will react upon another with the formation of what may be termed ghosts, is when the amplitude of the component is caused to vary, or is modulated, at a different frequency. Then sum and difference frequencies will arise, as in the well-known case of the side-bands which occur in wireless theory, and the diffraction pattern will quite properly indicate their presence.

It will be seen that even when the wave-form on the film is known to be compounded of a finite number N of harmonic terms, the function required to represent the length l of the wave-form exposed by the aperture will contain an infinite number of such terms. It is to be expected however that these will be concentrated together into N groups, so as to give rise to N spectral lines on either side of the centre, each of which is more precisely a diffraction maximum with a series of secondary maxima on either side. A particular case in which the full solution is available is that of the traditional diffraction grating composed of equispaced transparent slits, for which it is well known that the total diffraction pattern consists of a series of diffraction maxima or orders, each surrounded by a series of secondary maxima. In this case the orders are spaced according to a regular law, as they correspond to multiples of the fundamental periodicity of the grating. The complete mathematical theory of the secondary maxima is somewhat lengthy, but there is a purely physical justification for the belief that, in the more general case now considered, a similar calculation if carried through would lead to a similar result, except that the N main maxima would not be regularly spaced. This point will be referred to again in § 7.

Reference should be made here to the central image formed by the direct or undiffracted beam. This will be referred to as arising from the constant term of the Fourier expansion for $f(x)$ although it really arises from an infinite number of terms grouped near the value $n=0$. This constant term corresponds to the steady amplitude of the light transmitted by the film in the absence of modulation by sound. It retains the same value, however, in the presence of modulation; that is to say, the light required to form the other lines in the spectrum is not abstracted from the direct beam.

It is well known that it is possible to reproduce sound either from the original (negative) film on which it is recorded, or from positive prints made from the original. If the diffraction pattern formed by a selected length of film is really to constitute an acoustic spectrum of the recorded sound, the spectrum will have to be the same whether the negative or positive be used. That this will be the case may be seen from Babinet's theorem, which states that the diffraction pattern formed by any screen remains unchanged in form (except for the central region) if the opaque and transparent portions are interchanged. The central region corresponds to the constant term of the Fourier expansion, which contributes nothing to the sound as it is reproduced, but causes only a direct-current component in the output of the reproducing photocell.

§ 5. PRACTICAL CONSIDERATIONS

In § 4 it was assumed that the recording was so performed as to make the amplitude $f(x)$ of the light transmitted by the film conform to the wave-form of the original sound. This requirement may be expressed by saying that $f(x)$ must have a profile similar to the wave-form $F(x)$ of the sound, or a relation must exist of the form

$$f(x) \propto k+F(x),$$

where k is some constant.

If we examine the conditions under which sound films are usually made, it will be seen that this is unfortunately not the case. As normally used, a sound film is an agent by which the wave-form of a recorded sound may be reproduced in the wave-form of the current supplied to a loud-speaker. The latter wave-form has a profile similar to that of the current in the photocell of the reproducer, the photoelectric current in its turn being proportional to the intensity of the light which it receives. In the film record, therefore, the intensity and not the amplitude of the light transmitted by the film follows the wave-form $F(x)$ of the sound, so that we shall have

$$f^2(x) \propto k+F(x).$$

This is not the relationship needed for the acoustic analysis here projected, so that ordinary recording apparatus could not be used without some modification of either the electrical or the optical system. It is not difficult theoretically to devise ways in which the various methods of recording now in use could be modified to produce records of the required type, but it will be sufficient to describe as an

illustration one very simple scheme applying to the vibration galvanometer method of recording, in which the light beam is reflected from a small vibrating mirror.

In figure 2 (*a*) the dotted rectangle represents an area of uniform illumination, which is actually the image of an illuminated aperture projected after reflection from the oscillograph mirror, on to the plane of the knife-edge *AB*.

In the absence of modulation by sound the knife-edge obscures half the light patch. Vibrations of the mirror, by varying the distance z, will cause the luminous flux L in the unobstructed portion of the beam to vary in such a way that

$$L \propto z \propto k+F(x),$$

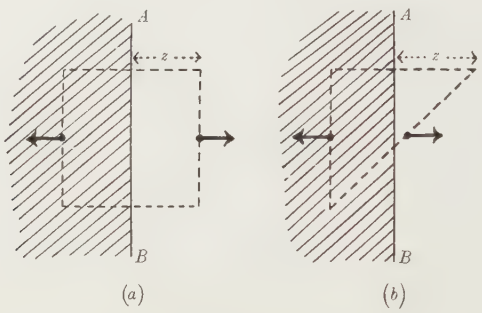

Figure 2.

which is the requirement for normal recording. If we modify this arrangement by using a triangular light-patch as in figure 2 (*b*), we shall now have

$$L \propto z^2 \propto [k+F(x)]^2,$$

or
$$f^2(x) \propto [k+F(x)]^2,$$

or
$$f(x) \propto k+F(x),$$

k being a constant such that the expression on the right-hand side never becomes negative. Thus in this case the condition required for the present type of recording is satisfied, and no modification of the electrical or photographic technique normally used would be necessary.

§ 6. EXPERIMENTAL

In the present paper the experimental aspect must be subsidiary to the theoretical, as a proper sound-film recorder was not available. However, some photographs obtained with improvised apparatus are appended as of interest in bearing out the conclusions reached by theory. The records were made on ordinary panchromatic film, by means of a dynamic loud-speaker movement adapted to swing a small mirror, the modulation of the light-beam being accomplished as in the preceding section. The first experiments were made with groups of organ pipes as affording sounds of approximately known composition. Figure 3 (*a*) shows a portion of the sound-track produced by sounding simultaneously three stopped diapason pipes whose frequencies were approximately 305, 390 and 520 c./sec. Figure 3 (*b*) is the derived diffraction pattern, showing on either side of the rather over-exposed

central image three lines whose displacements are in a ratio agreeing closely with that of the original frequencies. The next photograph is intended to make visible the effect discussed in § 4, the production of side frequencies when a pure wave is subjected to amplitude modulation. For this the source was a modulated oscillator, the oscillation frequency being 305 c. sec. and the modulation frequency 50 c./sec. A record of the wave-form is shown in figure 4 (*a*), and figure 4 (*b*) is the resulting diffraction pattern, in which the main components on either side of the centre are seen to be symmetrically bracketed by the less intense side-frequencies. The occurrence of such symmetrical patterns at any time might be regarded as a strong indication that amplitude modulation had taken place.

§ 7. MODULATION BY SUPERPOSITION OF GRATINGS

An effect similar to the one just described could be produced by taking separate variable-density records of the 305-c./sec. and 50-c./sec. waves, and then superposing the one film on the other. This procedure is not quite the equivalent of the first, however, because the 50-c./sec. wave will modulate not only the 305-c./sec. term, but also the constant term of the density function on which it is superposed. This will cause the central image as well as the lateral images to become bracketed by a pair of 50-c./sec. lines, which does not happen if the 305-c./sec. wave alone is modulated in preparation for recording.

A well-known experiment with ordinary diffraction gratings, in which a coarse grating is superposed upon a finer one, may advantageously be regarded as a similar example of modulation by superposition. Each image formed by the finer grating acquires a set of lines on either side similar to the diffraction pattern formed by the coarse grating itself. This illustration is introduced in view of its bearing on the point raised in § 4 relating to the precise nature of a spectral line. It is significant that the structure of each spectral line produced by an ordinary grating is similar to the diffraction pattern which would be produced by a rectangular aperture of the same dimensions as the ruled surface of the grating. This leads naturally to the view that each spectral line, in so far as it fails to be completely sharp, may be said to have acquired side bands due to modulation by the aperture which limits the grating, or more precisely modulation by the cosine terms present in the Fourier integral representing the aperture. On this view we can safely assume that in the more general type of grating represented by a variable-density sound film, a sound composed of N simple tones will give rise to N spectral lines which, although perhaps irregularly spaced if the tones are unrelated, will otherwise resemble in structure the lines of the various orders of an ordinary grating with the same aperture.

§ 8. TRANSIENT COMPONENTS OF SOUND

If the original wave-form represents a transient sound instead of sustained simple tones, it will require for its expression an infinite number of Fourier terms suitably grouped, even before delimitation by the aperture. Consider as an

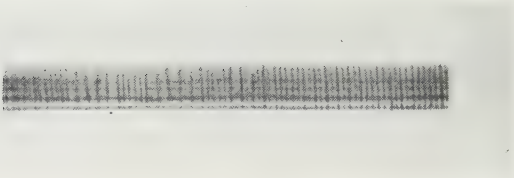

(*a*)

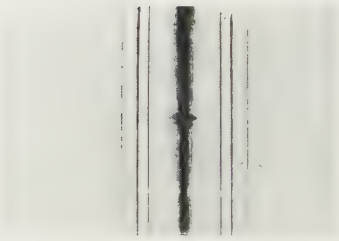

(*b*)

Figure 3.

(*a*)

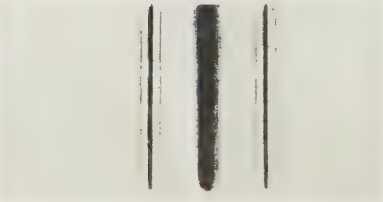

(*b*)

Figure 4.

illustration the case of a sinusoidal wave-train of short duration, represented on the film by n waves of wave-length μ. The main features of such a train can be represented[4] by a group of wave-lengths ranging from $\mu - d\mu$ to $\mu + d\mu$, where $d\mu = \mu/n$, or a group of frequencies ranging from $f + df$ to $f - df$, where $df = f/n$. If the n waves are regarded as a grating of limited resolving power, this is just the range of frequencies which the spectral line will represent, if we consider only its central maximum and neglect the secondary maxima. The diffracted beam then spreads from $\theta - d\theta$ to $\theta + d\theta$, where

$$\lambda = \mu \sin\theta,$$

$$(n+1)\lambda = n\mu \sin(\theta + d\theta),$$

$$\lambda = n\mu\, d(\sin\theta);$$

therefore

$$n = \frac{\lambda}{\mu d(\sin\theta)} = \frac{\sin\theta}{d(\sin\theta)} = \frac{f}{df}.$$

In general the lines of the spectrum will have a lower limit to their width determined by the aperture of the film, but this width may be considerably exceeded if transient components are present.

§ 9. SIGNIFICANCE OF THE WAVE-LENGTH OF THE ILLUMINATION USED

If the light-wave which is used to illuminate the sound film has its wave-length decreased, while the amplitude remains the same, two main effects will be produced, as in a similar problem discussed by Rayleigh[5]. Firstly, the diffraction pattern will contract, the lateral beams moving closer to the direct beam and to each other. Secondly, the beams will increase in intensity, since the intensity is determined by

$$I \propto \frac{C^2 + S^2}{\lambda^2} \propto \frac{A^2}{\lambda^2}.$$

A subsidiary effect is that the diffraction pattern is theoretically more complete, a higher number of terms being included within the maximum angle $\theta = 90°$.

It is to be noted that the present method, in common with other methods of wave-form analysis, is fundamentally an analysis of amplitudes, although when sounds of the same frequency are being compared the intensity of the spectral lines will also be a measure of the intensity of the sounds. When the sensations produced by sounds of different frequencies are being considered we are usually less interested in the amplitudes than in the intensities, which for high-frequency components may be quite large even when the actual amplitudes are small. To find an optical analogy for this, equation (1) may be rewritten in terms of the film-velocity V and the sound frequency f, giving

$$f = \frac{V}{\lambda} \sin\theta.$$

If now the observing telescope be set at some fixed angle θ, and the spectral lines

brought successively into view by varying the wave-length λ of illumination as above, we shall have

$$I \propto \frac{A^2}{\lambda^2} \propto (A^2 f^2).$$

That is to say the intensity of the lines will bear a constant ratio to the intensity of the sound components themselves throughout the frequency range; at the same time the sensation of colour will take the place of the sensation of pitch, giving as it were an optical transformation of sound.

§ 10. CONCLUSIONS

It has been shown that it is possible to resolve a wave-form recorded on variable-density film into its components by making use of the formal resemblance of the equations of diffraction theory to those which occur in Fourier analysis. The main ideas employed have always been implicit in the theory of diffraction, but attention has been called to certain consequences that may be of interest in view of the comparatively new scientific tool provided by the sound film. It remains to give a brief discussion of the possible practical applications. One possibility is that suitable wave-records, which could easily be duplicated, might serve as useful objects for demonstrations in connexion with the theory of waves. More important is it to assess the practicability of developing diffraction into a routine method of wave-analysis; in this connexion a number of difficulties naturally suggest themselves at first. For example, the dispersive power attained is obviously of a low order, so that the lines corresponding to the lower frequencies lie close to the obtrusive central image, the field surrounding which is with most optical systems never completely dark. The dispersion can of course be adjusted to some extent by varying the film-velocity used in recording. Another difficulty is that the film itself is liable to produce aberrations in the image formed by any optical system into which it is introduced, owing to irregularities in the film-surface, so that low dispersion is not readily counteracted by increased magnification. For such reasons the method compares unfavourably with, for example, the electrical wave-analysers which as a result of the investigations of Grützmacher[6], Moore and Curtis[7], and numerous others, have become a very simply operated form of laboratory equipment. With such analysers, even the fainter sound-components become quantitatively measurable in terms of the readings of an output-meter and an adjustable gain-control. If the search frequency which is employed in these methods is varied automatically, they may be used for recording, and Grützmacher[6] has investigated the rapidity with which the acoustic spectrum may be explored with due regard to the necessity of exciting the resonant circuit at each stage. He concludes that at a rate of frequency-change of 300 c./sec^2, the limit is still not necessarily reached. Some limit must exist however to development on these lines, so that other methods must be employed for analysing transient and transitional sounds such as those which occur, for example, in speech. It is in such connexions that the diffraction method might make a useful addition to existing methods of analysis. The technical

difficulties mentioned above do not appear to be insuperable, and there is an attractive generality in the theoretical possibilities which makes it desirable to see how far they can be realized in practice. In conclusion it may be observed that the diffraction method is not restricted to acoustical wave-forms, and could be adapted to deal with much slower vibrations than can be analysed by electrical or resonance methods.

§ 11. A NOTE ON VARIABLE-WIDTH SOUND FILMS

J. F. Schouten has recently reported [8] that he has investigated the corresponding properties of variable-width films, the theory of which is, as might be expected, more complicated than that of the variable-density type. The diffraction patterns, for which a point source must be used, resemble Laue patterns in that they are two-dimensional, and for a single frequency contain spectra of higher order besides the first. If attention is confined, however, to the α axis, for which the angle of diffraction in the vertical direction is zero, the distribution of intensity is found to be the same as that produced by a variable-density film.

REFERENCES

(1) Brown, D. *Nature, Lond.*, **140**, 1099 (1937).
(2) Michelson, A. A. *Phil. Mag.* **9**, 506 (1905).
(3) Porter, A. B. *Phil. Mag.* **11**, 154 (1906).
(4) Thomson, G. P. *The Wave Mechanics of Free Electrons*, p. 124 (McGraw-Hill, 1930).
(5) Rayleigh, Lord. *Scientific Papers*, **111**, 81.
(6) Grützmacher, M. *Elekt. Nachr.-Tech.* **4**, 533 (1927).
(7) Moore, C. R. and Curtis, A. S. *Bell. Syst. Tech. J.* **6**, 217 (1927).
(8) Schouten, J. F. *Nature, Lond.*, **141**, 914 (1938).

DISCUSSION

A discussion on this paper will be published in a future part of the *Proceedings*.

A STUDY OF THE ATMOSPHERIC OXIDATION OF METALS AND ALLOYS AT DIFFERENT TEMPERATURES BY ELECTRON-DIFFRACTION

By M. BOUND, Ph.D.

AND

D. A. RICHARDS, M.Sc., A.R.C.S., D.I.C.

University College of Wales, Aberystwyth

Received 28 *July* 1938. *Read* 13 *January* 1939

ABSTRACT. The atmospheric oxidation of evaporated films of a number of alloys and metals has been studied by electron-diffraction at various temperatures. In a number of cases the protective oxide film formed at room temperatures was not detected even after a month's exposure to air, but in other cases evidence for the oxidation of the metal at room temperatures was obtained.

§ 1. INTRODUCTION

Metals are thermodynamically unstable at room temperatures, and thus the difficulty in connexion with the oxidation of metals is not so much to account for the oxidation as to account for its slow rate. It is generally agreed that metals in bulk are prevented from rapid oxidation by a thin film of oxide on the surface which prevents access of oxygen to the layers beneath.

There is considerable evidence for the existence of this oxide film, and two methods at least have been utilized to determine its rate of formation; one is to note the increase in weight of a film of the metal[8], while the other, due to Tronstad[7], is based on the reflection of polarized light.

The application of electron-diffraction to the study of surface oxide films enables the structure of the films to be determined. In many cases the oxide may be one of several oxides of the metal, and the method enables it to be identified, as the crystal structures are known from x-ray data. The method does not, however, at present lend itself to exact quantitative determination of the rates of oxidation.

In the present work a large number of metals and alloys have been examined by electron-diffraction in order to identify the atmospheric oxidation products formed at room temperatures and at higher temperatures.

§ 2. APPARATUS

The electron-diffraction camera incorporated the high vacuum multiplate camera described by the authors in an earlier paper[1]. The source of electrons was either a cold-cathode discharge tube or a discharge tube of the hot-cathode type; these were

interchangeable on the apparatus. The accelerating voltage used was 30 kv. and the beam was focused by a magnetic lens[2]. The specimen chamber was designed in such a way that specimens could be evaporated, in vacuo, directly on a suitable substrate mounted on the specimen-holder, and a diffraction photograph be obtained before contamination by air, the specimen being subsequently removed for oxidation. Two degrees of freedom could be imparted to the specimen so that reflection and transmission photographs could be obtained. The spacings corresponding to the diffraction rings were obtained by comparison with a standard gold specimen[3].

§ 3. PREPARATION OF FILMS

Films for transmission were obtained by evaporation of a small pellet of the substance placed inside a spiral of tungsten wire, the substrate being collodion.

Films for reflection were prepared in some cases by evaporation on to glass, and in other cases the specimen was cut into blocks measuring 5 cm. × 0·5 cm. × 1 cm. and the surface was prepared by rubbing on 000 emery paper.

Films from melts were obtained by dipping nickel gauze into the molten metal and slowly removing it.

§ 4. RESULTS

Copper. G. P. Thomson has studied thinned films of copper; the oxidation of copper at room temperatures does not seem to have been investigated, but at higher temperatures Preston[5] and Murison[6] have studied the oxidation of copper blocks. Transmission and reflection photographs using evaporated films were obtained, gold being used for comparison purposes; the patterns were found to be due to a face-centred cubic structure for which $a = 3{\cdot}60$ A., in agreement with the X-ray result for copper.

Transmission specimens (copper on collodion) on exposure to air gradually developed extra rings, but even after 9 months' exposure to air the copper rings persist. These extra rings were identified as the 110, 111 and 220 rings of Cu_2O which is cubic with a equal to 4·24 A.

The oxidation of copper at 100° C. was investigated by heating the transmission and reflection specimens in an electric furnace for definite intervals of time. It was found that the film was completely oxidized into Cu_2O in just under an hour. Vernon[8] gives the thickness of the film on copper at 100° C. to be 60 A. after heating for an hour; since the thickness of the films in the present work is probably of the order of 100 A., the rate of oxidation is of the same order as that found by Vernon.

Preston[5] found that specimens of copper which had been polished at room temperatures were covered with Cu_2O; polishing probably raised the temperature of the surface. Beeching[10] found that his evaporated films on glass were Cu_2O, or some other substance which he failed to analyse; the interval between preparation and examination of these films was not stated, and oxidation probably occurred in the interval.

Further heating of the transmission and reflection specimens up to 200° C. produced no change in the transmission patterns, but reflection photographs indicated an orientation with the 110 plane parallel to the surface. After heating at 250° C. for an hour the pattern shown in the table was obtained.

Intensity	Radii (cm.)	Spacing (A.)	x-ray spacing (A.)	Oxide	Indices
f	0·504	3·02	3·01	Cu_2O	110
ff	0·545	2·70	2·75	CuO	011
s	0·620	2·45	2·45	Cu_2O	111
mf	0·663	2·29	2·29	CuO	111
mf	0·720	2·11	2·12	Cu_2O	200
f	0·820	1·84	1·84	CuO	—
ff	0·884	1·72	1·73	Cu_2O	211
f	0·964	1·59	1·59	CuO	$21\bar{1}$
mf	1·018	1·49	1·50	Cu_2O	220
m	1·094	1·39	1·40	CuO	022
m	1·192	1·27	1·28	Cu_2O	311

The pattern is thus a mixture of Cu_2O and tenorite (CuO). Further heating at 300° C. converted the pattern completely into that due to tenorite, which from X-ray data is known to be monoclinic ($a=4{\cdot}66$ A.; $b=3{\cdot}40$ A.; $c=5{\cdot}09$ A.; $\alpha=99°\ 30'$)[11].

No pattern could be obtained from reflection specimens of evaporated copper on glass after they had been heated to 300° C. as they became charged. This fact shows that the film has changed from being a semiconductor Cu_2O and become an insulator, probably CuO. Murison[6] found that blocks of copper heated to high temperatures gave a three-ring pattern; the writers' transmission films did not give this pattern.

Alloys containing copper. (*a*) *Brasses.* Preston[5] has studied the oxidation of brasses at three temperatures, 100° C., 183° C. and 400° C. The present writers have obtained results similar to those of Preston and have used intermediate temperatures.

Three brasses with a nominal composition of 10 per cent, 20 per cent, and 30 per cent zinc, and a bronze containing 5 per cent of tin were found to be covered with Cu_2O at temperatures up to 300° C.; the Cu_2O showed the orientation found on copper at the higher temperatures. A brass containing 38 per cent of zinc gave no pattern below 250° C., but at this temperature a pattern due to ZnO was obtained. Above 300° C. no pattern sufficiently good for analysis was obtained from the bronze or from the brasses containing 10 per cent and 20 per cent of zinc, probably owing to the scaling of the surface; the 30 per cent brasses, however, gave a pattern due to ZnO.

(*b*) 20 *per cent nickel silver* (62 per cent copper, 18 per cent zinc, 20 per cent nickel). This alloy gave patterns analysed to be due to Cu_2O after being heated to temperatures up to 300° C. but above that temperature the nature of the film was not determined.

(*c*) *Ferry* (44 per cent nickel, 56 per cent copper). This alloy gave a very good pattern, figure 1, due to NiO when heated to temperatures around 400° C.

Silver. G. P. Thomson[4] has studied films of silver prepared by thinning silver leaf with nitric acid. Quarrell[12] has recently studied evaporated films of silver on cellulose.

Evaporated films of silver on collodion and glass were prepared in the usual way. The films after exposure to the atmosphere developed extra rings after a week (these rings are additional to the rings due to the face-centred structure of silver). There was a slow increase in the intensity of the extra rings with time, and with some specimens these rings were stronger than the silver rings after six months. A silver-sulphide film was prepared by exposing a silver film to hydrogen sulphide. The X-ray structure for Ag_2S below 180° C. is orthorhombic with a equal to 4·77 A., b to 6·92 A. and c to 6·99 A. This structure may be regarded for practical purposes as pseudotetragonal with a equal to 6·95 A. and an axial ratio of 0·68. The diffraction pattern obtained agreed closely with this structure. The extra rings obtained with the silver films that had been exposed to air, figure 2, agreed in spacing with

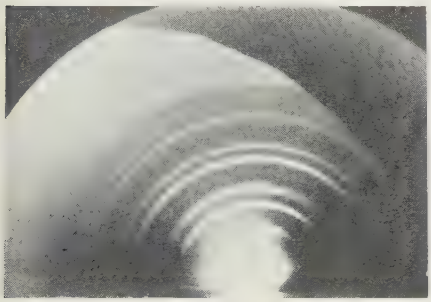

Figure 1.

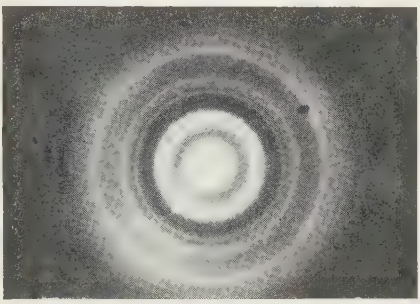

Figure 2.

the strong rings found in the sulphide patterns. Thus with silver the initial corrosion product is the sulphide.

Transmission specimens of silver on collodion were heated to 200° C. within a few hours of their preparation; the films showed a tendency to break, but gave the silver pattern with sharper lines than the original evaporated films. This shows that the crystallites have grown larger and the rupture of the film may be due to that fact. On being further heated to 250° C. the films were completely broken and no pattern could be obtained from them.

Reflection films after being heated to 290° C. appeared granular and gave no diffraction pattern on account of the accumulation of static charge. Examination under the microscope showed that the films were made up of small grains, and the charging up is probably due to the impact of electrons on the exposed surface of the glass between the grains. Thus the crystallites of silver grow rapidly at temperatures above 250° C.

Tin. G. P. Thomson[4] investigated thinned films of tin and obtained patterns consisting of two rings only. The present writers prepared transmission films of tin by evaporation, and the patterns obtained from the unexposed films agree with a

tetragonal structure having axial ratio of 0·54, in agreement with the x-ray data. These films, figure 3, exhibited no preferred orientation.

Photographs of a film of tin taken at intervals up to a month showed no detectable oxidation, a fact which points to the conclusion that the film formed on tin in air is very thin.

After $2\frac{1}{2}$ hours' heating at 100° C. no change was observed in the pattern for tin, but after heating to 190° C. a different pattern was obtained; this was found to be due to a tetragonal structure with a equal to 3·80 A. and c to 4·80 A., the axial ratio being thus 1·27, in agreement with the x-ray data for SnO. This oxide has been found by Jenkins[13] on the melt of tin. The writers found it to be present on the surface of the melt of solder, the oxide exhibiting marked orientation with the 001 planes parallel to the surface, figure 4.

Iron. H. R. Nelson[14] has studied evaporated films of iron by transmission; he has also obtained reflection photographs from blocks of iron abraded with emery paper. In the present work it was found impossible to evaporate iron from a tungsten filament, and the films were prepared by evaporation from a carefully cleaned

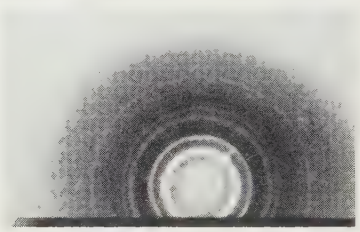

Figure 3.

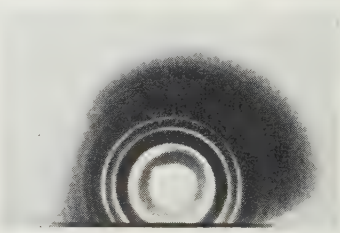

Figure 4.

filament of iron supplied by Johnson and Matthey. Transmission photographs of the specimens taken in situ immediately after preparation and before exposure to the atmosphere gave a body-centred cubic pattern due to αFe together with two diffuse rings having mean spacings of 2·6 A. and 1·5 A. respectively. These rings are probably due to either γFe_2O_3 or Fe_3O_4, since they improve in sharpness when the specimens are heated in air and are strong rings in the structures of the above oxides. It is difficult to account for the presence of the oxide in the films; Nelson appears to have observed the same effect with films which had been exposed to air at pressures not exceeding 10^{-3} mm.

When the films were exposed to air no change took place during 14 days. The data of Tronstad show that the oxide film on iron reaches a maximum thickness of 15 A. or 20 A. on exposure to air, and the writers' patterns indicate that the crystal-size is probably less than 100 A.

Evaporated films of iron (on collodion) showed appreciable oxidation after being heated to 100° C. for an hour. During this heating the rings with spacing of 2·6 A. and 1·5 A. gained in sharpness. The pattern obtained after heating at 150° C. was analysed to be due to a cubic structure with a equal to 8·30 A. γFe_2O_3 and Fe_3O_4 both have cubic structures, and their unit cell lengths are 8·30 A. and 8·37 A. respectively; thus the oxide formed is probably one of these oxides.

Iron alloys. (*a*) *Steel.* Blocks of mild steel heated to temperatures below 300° C. gave no reflection patterns; this may be due to the unsuitability of the surface for reflection below 300° C., for either γFe_2O_3 or Fe_3O_4 would be expected to be formed. At 300° C. faint patterns identical with the patterns obtained at higher temperatures were observed. Good patterns were obtained after heating to 400° C. The spacings of this pattern agree with the X-ray spacings for αFe_2O_3, which is rhombohedral in structure with a equal to 5·41 A., and α to 55° 17′. The pattern indicates that the crystallites are oriented so that the $10\bar{1}$ planes are parallel to the surface; there is a growing tendency to orientation with increase of temperature.

(*b*) *Nickel iron with* 48 *per cent of nickel, and* 52 *per cent of iron.* Blocks of this alloy were treated in the same way as the blocks of steel. After heating to 500° C. good photographs identical with those obtained from steel were obtained. In this case also the oxide film formed on the alloy is αFe_2O_3.

(*c*) *Dullray* (62 *per cent iron*, 34 *per cent nickel*, 4 *per cent chromium*). After heating above 300° C. the pattern obtained from this alloy was identical with that obtained from steel. In this case, however, since the structures of αFe_2O_3 and Cr_2O_3 are very similar, both being rhombohedral with spacings within 1 per cent of one another, it is not possible to say which of the oxides is present on the surface of the heated alloy, although the iron oxide is more to be expected in view of the much greater concentration of iron in the alloy.

Antimony. The only previous work on antimony appears to be that of Kirchner[15], who studied evaporated films of antimony on collodion; the films which he prepared were films which gave diffuse rings. The present writers obtained very beautiful patterns from evaporated antimony on collodion, figure 5. The patterns obtained before the films were exposed to air agreed with the X-ray structure for antimony, which is rhombohedral with a equal to 6·23 A. and α to 87° 24′. It is a deformed face-centred cubic lattice and can be referred to hexagonal axes by means of the usual equations. The films showed no preferred orientation.

No detectable change could be found in the patterns after the antimony films had been exposed to air for a week.

No detectable oxidation was observed with antimony up to a temperature of 250° C. Above this temperature the patterns obtained were found to be due to a cubic structure with a equal to 11·1 A., which is in good agreement with the X-ray data for Sb_2O_3 ($a = 11{\cdot}0$ A.).

Bismuth. Evaporated films of bismuth have been studied by Kirchner[15], but no reference to the oxidation of bismuth has been found in the literature although the oxide film from the melt of bismuth has been studied by Darbyshire and Cooper[16] and by Jenkins[13].

Films of bismuth on collodion were very readily prepared by evaporation from a tungsten filament. The bismuth was of spectroscopic purity supplied by Adam Hilger. Specimens evaporated on glass were also prepared and studied.

Films of bismuth on collodion were examined by transmission in situ immediately after being prepared without being exposed to air. From X-ray data it is known that bismuth has a face-centred rhombohedral structure ($a = 6{\cdot}58$ A., $\alpha = 87°\ 34'$),

i.e. like antimony it has a deformed face-centred cubic structure. It is more convenient however to transform to hexagonal axes which may be done by means of the usual equations.

The films, unlike the films of antimony, which bismuth resembles closely in structure, exhibit a markedly preferred orientation, a specimen inclined to the beam giving an arcked pattern, Fig. 6, while perpendicular to the beam a specimen gave complete rings. The preferred orientation is such that the 111 plane, with reference to rhombohedral axes, is parallel to the surface of the film. This agrees with the orientation found by Kirchner.

A photograph was taken with a bismuth film on collodion which had been exposed to air for 16 hours; it showed a band just outside the 200 ring. Photographs taken at intervals up to 32 days showed no further change in the pattern. This band may possibly be due to the oxide, for when the film was heated in air the band was

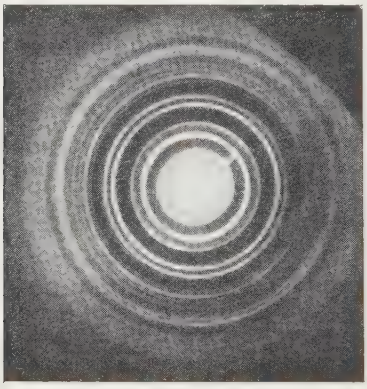

Figure 5.

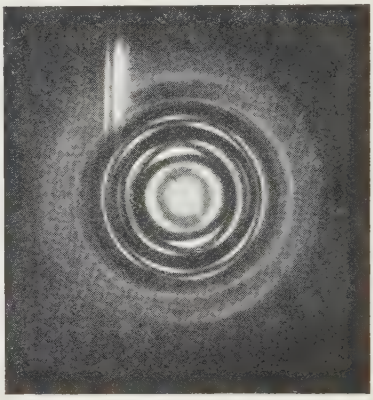

Figure 6.

resolved into rings. If the band is due to an oxide film then the oxide film must be very thin. Reflection specimens on glass behaved in the same way.

A film of bismuth on collodion was heated in order to find whether the film would lose its marked orientation at high temperatures. Photographs were taken with the specimens inclined to the beam. The length of the arcs began to increase at 150° C. and after they had been heated to about 200° C. the preferred orientation was completely absent. During this heating there was no detectable oxidation of the film beyond that found at room temperatures.

The behaviour of transmission specimens of bismuth and that of the reflection specimens on being heated were different. The reflection specimens after being heated to 300° C. for one hour gave poor photographs, which showed a face-centred cubic structure in which $a \fallingdotseq 5{\cdot}7$ A. The accuracy of this result is not very great on account of the poor quality of the photographs. Transmission photographs gave patterns, the strong rings of which agree with a face-centred cubic structure with a equal to 5·50 A., but other faint rings not belonging to a face-centred cubic pattern are also present; in addition the 111 ring is diffuse. This diffuse ring may be due to

amorphous Bi_2O_3 which is known to form a glass with a single band of mean spacing 3·13 A.

Two investigations have been devoted to a study of the oxide film on the melt of bismuth and their results may be compared with those obtained above. Darbyshire and Cooper obtained two types of pattern, one indicating a face-centred structure of unit length 5·43 A. and the other a complex pattern which they found to be due to a body-centred tetragonal structure with *a* equal to 10·85 A. and *c* to 11·28 A. Jenkins found the pattern to be a hexagonal close-packed structure of axial ratio 1·56.

The X-ray structure of Bi_2O_3 has not been studied in detail, but Randall[17] found the X-ray pattern of Bi_2O_3 to indicate a face-centred cubic structure; the complete structure has not been determined "on account of certain lines which are missing from the crystalline pattern of Bi_2O_3. This is due to the fact that the scattering power of bismuth for X rays is very great compared with that of oxygen." He quotes the 111 ring as having a spacing of $3·18_5$ A. which makes *a* equal to 5·51 A.

Darbyshire and Cooper's first type of pattern and the authors' reflection patterns gave the structure expected of Bi_2O_3. The authors' transmission photographs at 300° C. as described above gave a face-centred pattern with faint extra rings and the 111 ring diffuse. Further heating of the films up to 400° C. gave a pattern with sharp rings but the pattern could not then be ascribed to a simple face-centred cubic structure. Since very few of the bismuth compounds have been analysed by X-ray methods it is not possible to discover the nature of the film.

Zinc. A number of investigators have studied evaporated films of zinc, for instance Dixit[18]. The oxide film on the melt of zinc has also been studied by a number of investigators, for instance Finch and Quarrell[19], and Yearian[20].

Evaporated films of zinc were easily prepared by evaporation from a tungsten filament. The patterns obtained before the films had been exposed to air were those expected of zinc, and in addition they showed a preferred orientation with the *c* axis of the crystallites perpendicular to the film; the orientation was, however, not very marked. The high volatility of zinc makes its evaporation in the electron-diffraction camera a nuisance, since it becomes deposited on the mirrors, windows and screens.

A specimen of zinc was then exposed to air and photographed at intervals up to 34 days; the only change in the pattern was the appearance of a faint ring very close to the 102 ring of the zinc pattern, and further this ring does not appear when a photograph of an inclined film is taken. It may be due to grease or have some other origin. It is well known that zinc is difficult to sputter owing probably to the formation of an oxide film, but if the data of Tronstad are valid, the film will only be 5 A. thick after a month.

Films of zinc on collodion when heated to 100° C. gave faint extra rings; after they had been heated at 150° C., 200° C. and 250° C. the 100, 101 and 110 rings of the ZnO pattern were obtained. Further heating at 300° C. gave the complete oxide pattern; any remaining zinc would have evaporated completely at this temperature.

Cadmium. Evaporated films of cadmium on collodion were prepared by evapora-

tion from a tungsten filament. The patterns obtained were found to be due to a hexagonal close-packed structure agreeing closely with the X-ray structure of cadmium, in which a is equal to 2·97 A. and c to 5·61 A. The pattern exhibits arcking, but as yet the orientation has not been completely analysed.

On exposure to air a faint ring of spacing 1·66 A. appeared within a day. This ring gradually increased in intensity, and it agrees with the strongest ring in the CdO pattern. Some of the other strong rings of the CdO pattern were present at the end of a month.

When the films of evaporated cadmium were heated, appreciable oxidation took place at 100° C.; the ring of spacing 1·66 A. was present as a strong ring. On heating to temperatures above 100° C., face-centred cubic patterns were obtained with a equal to 4·72 A. From X-ray data, CdO is cubic with a equal to 4·70 A.; the pattern obtained experimentally denotes a face-centred cubic structure, probably because the scattering power of cadmium is greater than that of oxygen.

Lead. The authors are not aware of any work that has previously been done on evaporated films of lead. These are not easy to prepare by evaporation from a tungsten filament, probably because molten lead does not wet tungsten. The lead used in these experiments was of very high purity. The patterns obtained with the unexposed films denoted the normal face-centred cubic structure expected of lead.

The only change in the pattern when the lead was exposed to air was the appearance of a very faint ring outside the 200 ring; this may be due to an oxide or to grease. No other change took place in the pattern when the films were exposed to air for a month.

No change was observed when the film of lead was heated up to 100° C., but when it was heated above this temperature very poor photographs were obtained, and these were not analysable; on being heated to a temperature above 200° C. the film broke completely.

The oxide film on the melt of lead has been studied by two workers, Bragg[21] and Jenkins[13]. Bragg found the oxide film on the melt to be PbO_2, whilst Jenkins found it to be PbO (orthorhombic). Chemically PbO_2 is impossible, since its dissociation pressure exceeds atmospheric pressure at a temperature below the melting point of lead. Since we had a sample of very pure lead we decided to repeat these experiments. The pure lead gave a pattern due to orthorhombic PbO ($a = 5·50$ A., $b = 4·72$ A., $c = 5·88$ A.) showing a preferred orientation with the 001 planes parallel to the surface of the film, as found by Jenkins. Films were also prepared from a lead melt consisting of impure lead; these films gave a pattern which could not be due to any oxide of lead, but roughly agreed with PbO_2 within about 5 per cent. The pattern is probably due to an impurity in the lead.

Arsenic. Films of arsenic were prepared by evaporation from a tungsten filament, and patterns consisting of only two diffuse rings were obtained from them before they were exposed to air. The pattern did not change on exposure of the films to air for a week. Heating of the films to above 100° C. produced no change in the pattern, but after being heated to 200° C. the material on the film sublimed away; this would appear to indicate that it is As_2O_3 which sublimes at 193° C. in air.

This oxide is also known to form a glass. Probably the sample of arsenic contained the oxide as an impurity.

Aluminium. G. P. Thomson[4] has studied thinned films of aluminium, whilst Beeching[10] has studied evaporated films on glass. The oxide film on the metal has been studied by Preston[9] and Steinheil[22]. With films of aluminium prepared by thinning on potassium hydroxide the authors obtained two types of pattern. Some specimens gave patterns consisting of two strong rings indicating spacings of 2·60 A. and 1·51 A., together with faint unmeasurable rings; other specimens showed the face-centred cubic structure expected of aluminium, and a marked preferred orientation with a cube face parallel to the surface of the film. It has been impossible to find under what conditions the above two distinct patterns are produced.

An evaporated film of aluminium on glass showed the normal face-centred structure, with the same markedly preferred orientation as that found with the thinned films.

A thinned specimen giving the normal face-centred cubic pattern was photographed a month after its preparation and was found to be unaltered. The non-oxidation of thinned films on a collodion base has been observed by Steinheil. The evaporated film of aluminium on glass gradually developed an intense background scattering, and after a year the pattern was unmeasurable. The intense background may be due to the formation of an oxide film.

There is at present conflicting evidence as to the nature of the oxide and the thickness of the oxide film formed on aluminium in air. Tronstad[7] gives the film thickness as 100 A. to 150 A. Beeching found that his thick films on glass did not change in air or when heated to 250° C. in air, and the authors found no change in the normal face-centred aluminium structure on exposure to air for a short while. Steinheil's evaporated films became oxidized completely in a month, to a pattern which he attributed to a new oxide of aluminium and which Beeching suggests is some form of γAl_2O_3. The strong rings in the authors' first type of pattern agree with the strong rings in Steinheil's oxide pattern. Preston found, however, that the oxide film removed from aluminium was amorphous and did not recrystallize until the specimen had been heated to temperatures near the melting point of aluminium. The authors are unable to account for their first type of pattern. Thus further work on the oxide film formed on aluminium in air at room temperatures appears to be necessary.

§ 5. SUMMARY OF RESULTS

With tin, antimony, lead, gold, zinc and aluminium, no change definitely ascribable to the formation of an oxide film at room temperatures was found. Copper, iron and cadmium gave rings which have been analysed as being due to oxides. Silver gave extra rings which are to be ascribed to the sulphide. With bismuth the appearance of a band in the pattern on exposure to air may be due to a thin film of oxide.

The oxide films formed at high temperatures have been found for a number of metals. SnO, Sb_2O_3, Cu_2O, CuO, Fe_2O_3, CdO, NiO, ZnO and Bi_2O_3 have been found on the appropriate metals and alloys.

§ 6. ACKNOWLEDGEMENTS

We wish to thank the British Non-Ferrous Research Association for supplying us with the brasses and lead and Messrs Henry Wiggin and Co. for the nickel alloys. We also wish to thank Dr R. M. Davies for many helpful criticisms, Mr Sulston and Mr D. Owen for help in the construction of the apparatus. One of us (M. B.) also wishes to thank the University of Wales for a University Studentship.

REFERENCES

(1) Richards and Bound. *J. Sci. Instrum.* **14**, 403 (1937).
(2) Tillman. *Phil. Mag.* **18**, 659 (1934).
(3) Finch and Quarrell. *Proc. Phys. Soc.* **46**, 148 (1934).
(4) Thomson. *The Wave Mechanics of Free Electrons*, New York: McGraw Hill Book Co. (1930).
(5) Preston and Bircumshaw. *Phil. Mag.* **20**, 710 (1935).
(6) Murison. *Phil. Mag.* **17**, 97 (1934).
(7) Tronstad and Borgman. *Trans. Faraday Soc.* **30**, 349 (1934).
(8) Vernon. *J. Chem. Soc.* 2273 (1926).
(9) Preston and Bircumshaw. *Phil. Mag.* **22**, 654 (1936).
(10) Beeching. *Phil. Mag.* **22**, 947 (1936).
(11) Miyake. *Institute of Physical and Chemical Research Scientific Papers, Tokio*, **29**, 167 (1936).
(12) Quarrell. *Proc. Phys. Soc.* **49**, 281 (1937).
(13) Jenkins. *Proc. Phys. Soc.* **47**, 109 (1935).
(14) Nelson. *Nature, Lond.* (2 Jan. 1937).
(15) Kirchner. *Z. Phys.* **76**, 755 (1932).
(16) Darbyshire and Cooper. *Trans. Faraday Soc.* **30**, 1038 (1934).
(17) Randall. *J. Soc. Glass. Tech.* **17**, 287 (1933).
(18) Dixit. *Phil. Mag.* **16**, 1057 (1933).
(19) Finch and Quarrell. *Proc. Phys. Soc.* **46**, 148 (1934).
(20) Yearian. *Phys. Rev.* **83**, 632 (1935).
(21) Bragg. *Trans. Faraday Soc.* **28**, 522 (1932).
(22) Steinheil. *Ann. Phys., Lpz.*, **19**, 465 (1934).

ULTRA-VIOLET BAND SYSTEMS OF SILICON MONOSELENIDE AND MONOTELLURIDE

By R. F. BARROW, Departments of Inorganic Chemistry and Physics, Imperial College, London, S.W. 7

Communicated by W. Jevons 26 October 1938. Read in title 13 January 1939

ABSTRACT. Ultra-violet systems of red-degraded bands of SiSe and SiTe have been developed in heavy-current uncondensed discharges through silica tubes containing aluminium selenide and a mixture of aluminium and tellurium powders respectively. The vibrational analyses are described. The SiSe system consists of about thirty-five bands extending from $\lambda 2910$ to $\lambda 3670$ and has its $0 \rightarrow 0$ band at $\lambda 3089{\cdot}3$: the band-heads are approximately represented by

$$\nu = 32448{\cdot}8 + (403{\cdot}4u' - 3{\cdot}24u'^2 + 0{\cdot}141u'^3) - (580{\cdot}0u'' - 1{\cdot}78u''^2 + 0{\cdot}001u''^3),$$

where $u = v + \frac{1}{2}$. For SiTe, twenty-five bands have been measured between $\lambda 3290$ and $\lambda 3900$, the $0 \rightarrow 0$ band being at $\lambda 3496{\cdot}6$, and the band-heads being represented by

$$\nu = 28663{\cdot}5 + (335{\cdot}7u' - 0{\cdot}83u'^2 - 0{\cdot}080u'^3) - (480{\cdot}4u'' - 1{\cdot}16u''^2 - 0{\cdot}008u''^3).$$

In neither case is the $0 \rightarrow 0$ band very intense.

These systems are analogous to the already known systems of SiO and SiS. The data are discussed briefly in relation to the corresponding systems of PbO, PbS, PbSe and PbTe, and other similar molecules of group-IV*b* elements.

§ 1. INTRODUCTION

In a recent paper[1] it was reported that the ultra-violet system of SiS is well developed in a heavy-current discharge through Al_2S_3 in a silica discharge tube, SiS being formed by the interaction of Al_2S_3 and SiO_2 at the high temperature (*c.* 1000° C.) of the positive-column tube. It appeared possible that an analogous method would suffice for the production of the corresponding band systems of SiSe and SiTe. This is, in fact, the case, and preliminary notes on the results obtained have been published[2, 3]. The present paper gives more complete data for the vibrational analyses of these systems obtained by this method and based on results from spectrograms taken under improved experimental conditions.

§ 2. EXPERIMENTAL DETAILS

The sources used for the production of the band systems of SiSe and SiTe were heavy-current uncondensed discharges through a silica tube, as used with Al_2S_3, and described by Barrow and Jevons[1].

For the present purpose, however, the tipping device for the introduction of material into the discharge was omitted, since it was anticipated that the times of

exposure required to photograph the systems on dispersion sufficient to give an accurate vibrational analysis would be relatively short. For the production of the SiSe system, Kahlbaum's aluminium selenide, which had been previously powdered, was used; while for SiTe, a mixture of ordinary chemically pure powdered aluminium and tellurium was found to be satisfactory. In the spectral range covered by these band systems, no "impurities" were found to be introduced to the spectrum by presence of air at low pressures, and this was accordingly used in place of argon as residual gas.

Current for the discharge tube was taken from a pair of 2400-v. 5-kva. transformers whose primaries were connected in parallel to the 230-v. supply of a.c. at 50 c./sec.; and whose secondaries were also connected in parallel. The optimum value of the current through the tube was found to be about 2 amp. With higher currents atomic lines due to impurities in the aluminium selenide and in the tellurium (Ag, Cu, Fe, Ca, Pb and Tl) were greatly increased in intensity, while with smaller currents the temperature of the central tube was too low to allow of the reaction with the silica to take place to any appreciable extent, and the intensity of the SiSe and SiTe systems was accordingly very low. Bands of the ultra-violet systems were photographed against Fe arc lines on Ilford Ordinary plates in a first order of a 2·4-m. concave grating in an Eagle mounting with a dispersion of about 7·42 A./mm. With the optimum current through the tube, the times of exposure were of the order 4 or 5 min.

The discharge in both cases was of a bluish green colour, being predominantly due to intense emission of the Se_2 and Te_2 visible systems. It may be observed here that no evidence for the existence of a second band system corresponding to the near ultra-violet and visible system of SiS described by Barrow and Jevons[1] has been found in the cases of SiSe and SiTe. This result is in exact accordance with the SiS observations, in which the strong system in the ultra-violet was accompanied by the weaker less refrangible bands in the discharge through silicon sulphide itself, but not in that through aluminium sulphide.

§ 3. THE ULTRA-VIOLET BAND SYSTEM OF SILICON MONOSELENIDE

The high-temperature discharge through aluminium selenide in the presence of silica gives rise to an ultra-violet system in the region $\lambda 2914$ to $\lambda 3671$, consisting of apparently single-headed bands degraded to the red. A grating spectrogram is reproduced in plate 1 (*a*). Just beyond the short wave-length end of the system lies the $^1\Pi \rightarrow {}^1\Sigma$ system of SiO, while at the long wave-length end, the weaker bands of the system (with $v'' = 11$, 12 and 13) are obscured by a background of partially unresolved rotational structure; at $\lambda 4225$ and upwards the bands described by Cameron[4] and associated with a silicon oxide, have been observed. Atomic lines present are due to Si, Al, Mg, Cu and Ag. Measurements of the band heads, visual estimates of relative intensities and the assigned values of the vibrational quantum numbers are set out in the Deslandres scheme in table 1. The main Condon curve of intensity-distribution is wide, as would be expected from the

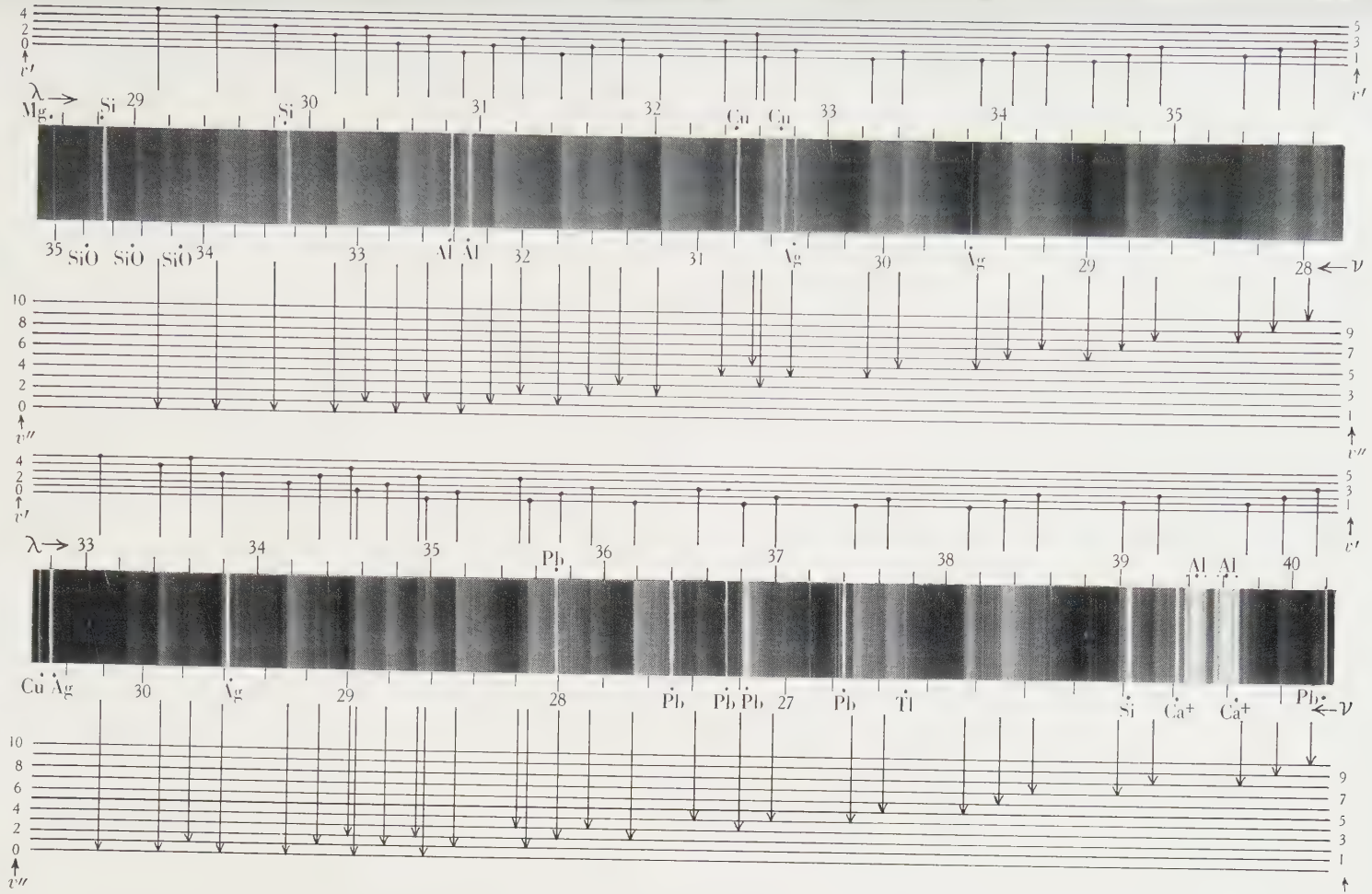

First-order spectrum, taken with 2·4-m. grating, showing the ultra-violet band systems of (*a*) SiSe and (*b*) SiTe.

PLATE I

To face page 268

Table 1. Deslandres' arrangement of data for band-heads of SiSe

Italics in parentheses denote visual estimates of intensities; Italics, wave-lengths in air (I.A.); Large Roman type, wave-numbers in vacuo (cm.$^{-1}$); Small Roman type, wave-number differences (vibrational frequencies in upper and lower electronic states).

v' →	v'' → 0	1	2	3	4	5	6	7	8	9	10	11	12
6		(1) *2930·92* 34109·0											
5	(1) *2914·24* 34304·2												
	383·4												
4	(4) *2947·18* 33920·8											(1) *3599·27* 27775·5	(1) *3670·74* 27234·7
	385·9											385·6	530·8
3	(6) *2981·10* 33534·9	577·0 (1) *3033·29* 32957·9				(1) *3257·69* 30687·8					(4) *3579·44* 27929·4	539·5 (3) *3649·96* 27389·9	
	385·5	384·8									384·1		
2	(7) *3015·77* 33149·4	576·3 (3) *3069·11* 32573·1	571·6 (1) *3123·95* 32001·5	569·8 (4) *3180·58* 31431·7	565·7 (3) *3238·88* 30866·0		(2) *3361·41* 29740·9	554·1 (2) *3425·23* 29186·8	550·8 (3) *3491·12* 28636·0	549·5 (3) *3559·37* 28086·5	541·2 (2) *3629·35* 27545·3		
	391·2	390·9	393·1		389·5		389·0	390·4	390·4				
1	(8) *3051·78* 32758·2	576·0 (9) *3106·41* 32182·2	573·8 (5) *3162·80* 31608·4	*	(2) *3280·27* 30476·5	564·5 (9) *3242·18* 29912·0	560·1 (7) *3405·96* 29351·9	555·5 (4) *3471·66* 28796·4	550·8 (2) *3539·37* 28245·6				
	397·7	398·1	396·6		398·3	396·7			398·7				
0	(1) *3089·29* 32360·5	576·4 (9) *3145·32* 31784·1	572·3 (10) *3202·99* 31211·8	568·1 (10) *3262·38* 30643·7	565·5 (8) *3323·71* 30078·2	562·9 (5) *3387·10* 29515·3			(2) *3590·04* 27846·9				

* Band probably present, but head not measurable on account of (0, 2) band.

rather large difference between the vibrational frequencies in the upper and lower electronic states: it is, however, noteworthy that there is a secondary distribution of intensity falling on a curve inside the main Condon curve. It may also be remarked that the intensity of the $0 \rightarrow 0$ band of the SiSe system is so low as to admit of no accurate measurement of wave-length.

The derivation of an equation which satisfactorily accounts for the observed values of the band-heads has proved difficult, owing to the existence of perturbations in certain of the rotational levels associated with one or more of the vibrational levels having $v' = 2$, 3 or 4. The expression

$$\nu_{\text{head}} = 32448{\cdot}8 + (403{\cdot}4u' - 3{\cdot}24u'^2 + 0{\cdot}141u'^3) - (580{\cdot}0u'' - 1{\cdot}78u''^2 + 0{\cdot}001u''^3),$$

where $u = v + \frac{1}{2}$, involves the assumption of a perturbation in the $v' = 3$ level of the order of 5 cm^{-1}. Apart from this single level, the experimentally determined values are represented to the expected degree of accuracy. It may, however, be remarked that the value for $x_e'\omega_e'$ so obtained, viz. 3·24, is considerably higher than would have been expected from a study of the isoelectronic molecule, GeS, and of the other members of the series of oxides, sulphides, selenides and tellurides of the group-IV*b* elements. Finally, it may be noted that an alternative expression for $G'(v')$, viz. $(403{\cdot}2u' - 3{\cdot}24u'^2)$, is in excellent agreement with observed values for the levels having $v' = 0$, 1, 2 and 3, but leaves considerable residuals $(\nu_{\text{obs.}} - \nu_{\text{calc.}})$ associated with band-heads with v' values 4, 5 and 6.

§ 4. THE ULTRA-VIOLET BAND SYSTEM OF SILICON MONOTELLURIDE

As will be seen from an inspection of the reproduction of a grating spectrogram in plate 1(*b*), this system manifests the same essential features as the SiSe system previously discussed. The high-temperature discharge through the Al and Te in presence of SiO_2 gives rise to an ultra-violet system, extending from $\lambda 3290$ to $\lambda 3901$, and consisting of apparently single-headed bands degraded to the red. Atomic lines present in spectrograms of this source are due to Si, Al, Ca, Ag, Cu, Pb and Tl. Measurements of the band-heads, visual estimates of relative intensities, and the assigned values of the vibrational quantum numbers are set out in table 2.

The band-heads are represented approximately by the expression

$$\nu_{\text{head}} = 28663{\cdot}5 + (335{\cdot}7u' - 0{\cdot}83u'^2 - 0{\cdot}080u'^3) - (480{\cdot}4u'' - 1{\cdot}16u''^2 - 0{\cdot}008u''^3).$$

This expression assumes a perturbation in certain rotational levels associated with the vibrational level $v' = 3$, of the order of 1·2 cm^{-1}. The bands with this value of v' being disregarded, the equation given above represents satisfactorily the experimentally determined values. In this case, the highest value of v'' is 7, as against 12 for SiSe. The curve representing a secondary distribution of intensity and falling inside the main Condon curve is even more manifest in the SiTe system than in the SiSe: several instances of such intensity-distribution are already known, e.g. in P_2[6] and As_2[7], and an explanation on the basis of wave-mechanics has been indicated.

Table 2. Deslandres' arrangement of data for band-heads of SiTe

Italics in parentheses denote visual estimates of intensities; Italics, wave-lengths in air (I.A.); Large Roman type, wave-numbers in vacuo (cm.$^{-1}$); Small Roman type, wave-number differences (vibrational frequencies in upper and lower electronic states).

$v''\rightarrow$	0	1	2	3	4	5	6	7
0	(1) *3290·19* 30384·7							
	313·7							
1	(1) *3324·51* 30071·0							
2	(2) *3306·78* 30232·2							
	320·4							
3	(3) *3342·20* 29911·8		(3) *3452·59* 28955·5					
	324·9		323·0					
5	(5) *3378·91* 29586·9		(3) *3491·54* 28632·5	473·3	(1) *3550·23* 28159·2			
	330·1		329·6		330·0			
7	(7) *3417·03* 29256·8	477·5	(6) *3473·73* 28779·3	476·4	(2) *3532·20* 28302·9	473·7	(4) *3592·33* 27829·2	470·8	(3) *3654·15* 27358·4						(3) *3850·55* 25963·0
	331·5		332·4		332·5										333·3
8	(8) *3456·19* 28925·3	478·4	(10) *3514·32* 28446·9	476·5	(5) *3574·19* 27970·4		*			(8) *3763·91* 26560·6	466·5	(5) *3831·20* 26094·1	464·4	(2) *3900·62* 25629·7
	334·1		334·0		333·2										
9	(4) *3496·58* 28591·2	478·3	(10) *3556·08* 28112·9	475·7	(10) *3617·28* 27637·2	472·9	(9) *3680·26* 27164·3	470·7	(9) *3745·16* 26693·6						

* Band probably present, but head not measurable on account of (0, 2) band.

§ 5. DISCUSSION OF RESULTS

The band systems described above would appear to be analogous to the ultra-violet systems of monoxides and monosulphides of group-IV*b* elements previously discussed[1, 5]. Rotational analyses have shown some of these systems to be due to $^1\Pi \rightarrow {}^1\Sigma$ transitions (for instance the CO fourth positive, CS and SiO systems) and others to $^1\Sigma \rightarrow {}^1\Sigma$ transitions (for instance the GeO, SnO and PbO systems). To which class the SiS, SiSe and SiTe systems belong cannot, of course, be stated, pending rotational analysis. For SiS this is already in progress, but for the other two emitters it would probably be beyond the power of the spectrographs available.

A discussion of the data for the system-origins and vibrational coefficients for analogous band systems of related molecules, together with certain empirical relations between them which appear to be of interest, has recently been published[1]. It is not proposed at this stage to recapitulate this discussion, and only a brief summary of the results of the present investigation is included here. A more complete

survey of the constants for the members of this group is deferred until the establishment of reliable data for all the members. This work also is in progress.

In tables 3 and 4, the values taken by certain functions for the corresponding systems of Si and Pb compounds are set out, I_M and I_X being the ionization potentials (in ev.) of the component atoms. As in the former paper[1], the PbSe and PbTe data used are those for two of the absorption systems recently described by Walker, Straley and Smith[8]. While it is unwise to draw any general conclusions from these figures, two facts are perhaps worthy of attention: (i) the functions $I_M I_X/E_e$ and ω_e'/ω_e'' are of the same orders of magnitude for corresponding systems of a series of compounds containing the same group-IV*b* atom; and

Table 3

Molecule	$I_M I_X/E_e$		ω_e'/ω_e''		D'' (ev.)	
	Si	Pb	Si	Pb	Si	Pb
Oxide	20·8	35·4	0·686	0·690	7·8	4·3
Sulphide	19·4	28·2	0·683	0·659	6·7	4·7
Selenide	19·3	27·1	0·696	0·665	5·8	5·1
Telluride	20·6	27·2	0·699	0·687	6·1	11·6

Table 4

Metal	Electronic states of molecules	Ratio of values of ω_e		
		MS/MO	MSe/MS	MSe/MTe
Silicon	Upper (ω_e')	0·602	0·789	0·832
	Ground (ω_e'')	0·604	0·774	0·828
Lead	Upper (ω_e')	0·568	0·655	0·787
	Ground (ω_e'')	0·592	0·649	0·762

(ii) the ratios shown in table 4 increase through the group in much the same way for the silicon compounds as for the lead compounds, and in the same way for the upper as for the lower electronic states. It can also be stated that the empirical functions discussed in connexion with SiS indicate that the system-origins and vibrational coefficients for SiSe and SiTe are of the expected order, with the single exception of the $x_e'\omega_e'$ for SiSe. To the abnormally high value of this coefficient and to the difficulty of determining it attention has already been drawn in § 3. Moreover, in six of the eight systems examined here, the lower state has been ascertained to be the ground state, and in the light of this discussion it appears probable that the same is true also for the two newly discovered systems, although confirmation by means of a study of the absorption by SiSe and SiTe is, of course, very desirable.

The uninflected curves obtained by plotting $1/\omega_e$ against the number of electrons in the molecule[1] have precisely the same form in the case of SiO, SiS, SiSe and SiTe as they have in the case of the corresponding lead compounds. Only for Si and Pb are data on all four molecules available.

Not only the progressive changes in the system-origins and vibrational coefficients of SiO, SiS, SiSe and SiTe, but also the data for the corresponding systems of molecules isoelectronic to SiSe and SiTe are of value in confirming the identification of the emitters of these systems. This point has already been mentioned in the preliminary note on the SiTe system[3], and the revised values of the constants given in the present paper make the similarity between the expressions for the SiSe and GeS, and SiTe and SnS (B — X) systems, appear no less striking; thus

48-electron emitters:

$$\nu_{SiSe} = 32448{\cdot}8 + (403{\cdot}4u' - 3{\cdot}24u'^2 + 0{\cdot}141u'^3) - (580{\cdot}0u'' - 1{\cdot}78u''^2 + 0{\cdot}001u''^3),$$
$$\nu_{GeS} = 32889{\cdot}5 + (375{\cdot}0u' - 1{\cdot}51u'^2) - (575{\cdot}8u'' - 1{\cdot}80u''^2).$$

66-electron emitters:

$$\nu_{SiTe} = 28663{\cdot}5 + (335{\cdot}7u' - 0{\cdot}83u'^2 - 0{\cdot}080u'^3) - (480{\cdot}4u'' - 1{\cdot}61u''^2 - 0{\cdot}008u''^3),$$
$$\nu_{SnS} = 28337{\cdot}9 + (331{\cdot}9u' - 1{\cdot}25u'^2) - (487{\cdot}7u'' - 1{\cdot}34u''^2).$$

Finally, the energies of dissociation of the ground states, as obtained by linear extrapolation by means of the expression

$$D = (\omega_e - x_e\omega_e)^2/(4x_e\omega_e \times 8106),$$

are included in table 3. It will be seen that the energies of the four silicon compounds appear to vary in quite a different manner from those of the lead compounds: in the one case there is a decrease from SiO to SiSe followed by a slight increase at SiTe, while in the other case there is a general rise from PbO to PbTe. It will be of interest to find, as a result of the work in progress, the trend of these energies in the intermediate series of Ge and Sn compounds. For the upper states of SiSe and SiTe no reliable estimates of the dissociation energies can be obtained in view of the large and rather uncertain terms in $(v' + \frac{1}{2})^3$.

§ 6. ACKNOWLEDGEMENTS

The author takes pleasure in recording his indebtedness to Prof. H. V. A. Briscoe and Dr W. Jevons for helpful discussion throughout the course of this work, and for assistance in the preparation of this paper. He would also like to thank Prof. H. Dingle for facilities in the spectroscopic laboratories of the Department of Physics.

REFERENCES

(1) Barrow, R. F. and Jevons, W. *Proc. Roy. Soc.* A, **169**, 49 (1938).
(2) Barrow, R. F. *Nature, Lond.*, **142**, 434 (1938).
(3) Barrow, R. F. *Nature, Lond.*, **142**, 536 (1938).
(4) Cameron, W. H. B. *Phil. Mag.* **3**, 110 (1927).
(5) Jevons, W., Bashford, L. A. and Briscoe, H. V. A. *Proc. Phys. Soc.* **49**, 543 (1937).
(6) Herzberg, G. *Ann. Phys., Lpz.*, **15**, 677 (1932).
(7) Almy, G. M. and Kinzer, G. D. *Phys. Rev.* **47**, 721 (1935).
(8) Walker, J. W., Straley, J. W. and Smith, A. W. *Phys. Rev.* **53**, 140 (1938).

ANALYSIS OF LIGHT SCATTERED FROM A SURFACE OF LOW GLOSS INTO ITS SPECULAR AND DIFFUSE COMPONENTS

By W. W. BARKAS, M.Sc., Forest Products Research Laboratory, Princes Risborough, Bucks

Received 23 *May* 1938. *Read in title* 28 *October* 1938

ABSTRACT. It is assumed that surfaces showing low gloss consist of small elementary facets which may be set at any angle to the mean surface. These facets may be of two types, one diffusing a proportion of the incident flux according to Lambert's law, and the other reflecting, at the specular angle, a proportion s of the incident flux, where s is determined by Fresnel's equation and is dependent on the refractive index of the material. On these assumptions formulae are obtained whereby the emergent flux E can be resolved into its diffuse and specular components R and M and from which the proportional areas B of the mirror facets, set at different angles to the mean surface, can be calculated. The use of the equations is illustrated by analysing two families of curves obtained by means of an apparatus which is described and relating to light scattered from a surface of Bristol board and from a surface of magnesium-oxide smoke deposited on plane glass.

§ 1. INTRODUCTION

According to Lambert's law, if a parallel beam of light of finite cross section falls at any angle of incidence α on to an optically rough surface, the total flux scattered at any angle of view β is proportional to $\cos\beta$. No real surfaces have been found which completely follow Lambert's law, but a layer of magnesium-oxide smoke carefully deposited on a plane glass surface approaches the ideal surface closely enough[24] for the law to be assumed to be correct.

For most materials the shape of the polar curve depends on α as well as on β. This can be illustrated most simply by referring to figure 1, which gives a family of curves obtained from a surface of Bristol board, such as is used for black-and-white drawings; it was in fact one of the surfaces used for testing the theory presented in this paper. The Bristol board would be judged visually to be of low gloss, but each curve shows an appreciably increased emission in the direction $\beta = -\alpha$, i.e. at the specular angle, which is shown by a small arrow on each curve.

A surface showing a large emission at the specular angle is said to be "glossy", though the precise definition of this term has proved to be a matter of some difficulty since it has not been found possible to associate the judged "glossiness" of a surface rigorously with the objective physical properties of the surface itself. Considerable progress has been made by Hanstock[7], who has shown the importance of the refractive index of the material in this connexion, and for a full discussion on the nature of gloss the reader is referred to publications by him and others at the

Paint Research Laboratories, and to R. S. Hunter's *Methods of Determining Gloss*[8]. The latter author says (p. 21): "Specular reflection and diffuse reflection are constantly used in technical descriptions of the appearance of articles. Unfortunately there is no general way in which the effects of these two processes may be accurately separated." The present paper attempts to furnish a method whereby this separation can be achieved, so that each of the curves in figure 1 may be resolved into its components of specular and diffuse reflection.

In figure 1 the gradual decrease in the flux on either side of the specular angle is not due to lack of angular discrimination in the apparatus, because when a plane mirror was substituted for the test surface and a parallel beam of light was reflected from it so as to enter the photocell at the specular angle, a change of as little as 2° in the angle between the illuminated and reflected beams served to cut off the light

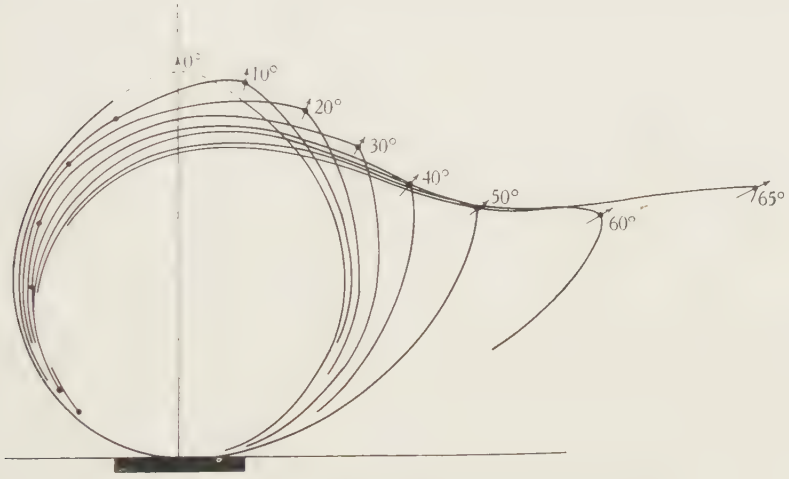

Figure 1. Bristol board. Distribution of scattered flux for various angles of incidence of a parallel beam of light.

completely from the photocell. The shape of the curves can, however, be explained on the assumption that the surface contains small mirror-like facets making various angles with the mean surface of the material. This conception is not new[3], but there appears to be a tendency, in analysing surfaces for gloss, to rely only on comparison of the light received at the specular angle to the mean surface with that received at some other angle where the light is assumed to be perfectly diffuse.

Such a method overlooks the possibility of an observer being able to appreciate the occurrence of bright reflections over a considerable range of angles on either side of the specular, and Hanstock is careful to stress the probable influence of the spatial distribution of the light on the subjective judgement of gloss. In the case of wood, for example, the inner surfaces of the cell walls, exposed by planing, are highly reflecting, and the light received from them greatly influences the visual quality of the material.

A short summary of previous research into the optical quality of surfaces is given in an appendix by Mr R. F. S. Hearmon.

§ 2. APPARATUS

Figures 2 and 3 give the essentials of the apparatus used.

In the optical system, figure 2, 1 denotes the test surface at the centre of rotation of a rotating arm 2 mounted on a cycle hub; 3 is a 30-candle power pointolite lamp; 4 a casing; 5 a projection lens with a focal length of 15 cm.; 6 are baffles to restrict the spread of the beam; 7 is a graduated table; 8 a collecting lens of large

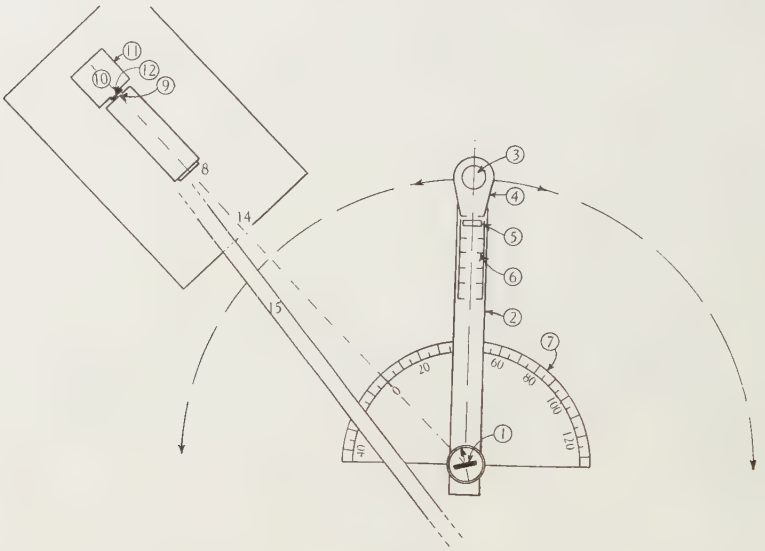

Figure 2. Optical apparatus.

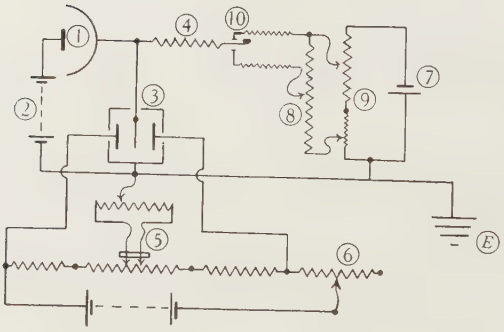

Figure 3. Electrical apparatus.

diameter and a focal length of 25 cm.; 9 an aperture of the same size as the focused image of the source; 10 a photocell; 11 an earthed casing; 12 a shutter; 14 an aperture in a shielded casing, and 15 a shielded lead to an electrometer.

The angle of illumination on the surface may be increased until the illuminated patch spreads to a width comparable with the diameter of the lens 8. In the present case, the diameter of the incident beam being about 2·5 cm., this limit was reached at an angle of 65°.

In the electrical system, figure 3, 1 is a photocell; 2 a source of anode voltage (120 v.); 3 a Lindemann electrometer; 4 a resistance of 30,000 megohms; 5 an earth-centring potentiometer; 6 a tapping for adjusting sensitivity; 7 a source of compensating voltage; 8 a 100-stud potentiometer giving flux as a percentage of the maximum, and 9 a potentiometer for compensating the maximum flux; and 10 is a switch for returning rapidly to the maximum setting of 8 when checking the maximum flux. The arrangement of the parts 3, 5 and 6 was kindly suggested to me by Dr G. M. B. Dobson, F.R.S., of Oxford.

§ 3. EXPERIMENTAL RESULTS FOR BRISTOL BOARD

The surface first used for experiment was a piece of Bristol board showing low gloss. With a strip of plane mirror held against the surface, the sample was adjusted so that the illuminating beam fell normally on it, and all angles of incidence α were measured from this position. At any setting of α, the flux was measured for all angles of view β of the rotating arm as a percentage of the maximum flux obtainable. This, for Bristol board, was found in each case to be at the specular angle ($\beta = -\alpha$), while for magnesium oxide it was found when $\beta = 0$. The relative values of these maxima were then measured so that the different curves could be correlated.

Figure 1 gives the experimental values of the flux obtained from Bristol board; those for magnesium oxide will be found in table 5.

§ 4. THEORY

Let α be the angle of illumination and β the angle of view measured with respect to the normal to the mean surface. Let i be the angle of incidence and e the angle of emergence measured with respect to the normal to a particular facet. Let μ be the refractive index of the material composing the surface, γ and θ the angles defining the inclination of a rough facet relative to the mean surface, and ϕ the angle of inclination of a mirror facet relative to the mean surface. Let A' be the total area, per cm.^{2} of mean surface, of rough facets illuminated and visible for particular values of α and β, while A is the value which A' would have on an optically equivalent surface where θ is zero. Let B be the total area, per cm.^{2} of mean surface, of mirror facets at a particular angle ϕ to the mean surface. Let I be the intensity of the illuminating beam, X the total cross section of the beam, r the proportion of incident flux scattered normally to a rough facet, and s the proportion of incident flux reflected at the specular angle from a mirror facet. Let $E_{\alpha\beta}$ be the total flux received from the surface when the latter is illuminated at angle α and viewed at angle β, while $R_{\alpha\beta}$, $M_{\alpha\beta}$ are the fluxes received from the rough elements and mirror elements respectively under the same conditions.

Rough facets. By Lambert's law, a parallel beam of light falling at angle i on a rough surface is scattered in such a way that, if *all* the light emitted at an angle e is collected, the total flux is

$$R_{ie} = XIr \cos e. \qquad \text{.....(1)}$$

It should be noted that optical roughness does not assume a macroscopic departure from a geometrical plane; a magnesium-oxide surface, for example, though macro-

scopically smooth is optically rough, whereas ground glass, though macroscopically rough, probably contains few elements of true optical roughness, since the light is scattered by a system of reflections and refractions. The surfaces here considered will be termed plane if they lie in contact macroscopically with a geometrical plane, called the "mean surface". The actual profile of a surface is called the "true surface".

Mirror facets. An ideally smooth surface illuminated at an angle i reflects light only at the specular angle $-i$. The flux reflected is

$$M_i = sXI, \qquad \text{.....(2)}$$

where s is given by Fresnel's formula[20] which, for purposes of accurate calculation from tables, may be conveniently transposed to

$$s = \frac{1}{2}\left[\left\{\frac{\mu\sqrt{\left(1-\frac{\sin^2 i}{\mu^2}\right)}-\cos i}{\mu\sqrt{\left(1-\frac{\sin^2 i}{\mu^2}\right)}+\cos i}\right\}^2 + \left\{\frac{\cos i-\frac{1}{\mu}\sqrt{\left(1-\frac{\sin^2 i}{\mu^2}\right)}}{\cos i+\frac{1}{\mu}\sqrt{\left(1-\frac{\sin^2 i}{\mu^2}\right)}}\right\}^2\right] \qquad \text{.....(3)}$$

For the paper surface here studied the refractive index has been taken as 1·55[22], and for magnesium oxide as 1·736 (p. 288).

Surfaces of low gloss. We shall suppose that a surface of low gloss contains small elementary areas, or facets, of two kinds, those which reflect the light falling on them according to Fresnel's equation and those which diffuse it according to Lambert's law. These facets may be set at any angle to the mean surface.

It is important to realize that the analysis is concerned only with the external optical behaviour of the surface. The texture of a real surface can seldom be fully resolved by the unaided eye, and we need therefore only construct an equivalent surface, consisting of the above facets, which would be photometrically indistinguishable from the real surface under test. Thus any small area in the real surface, being in fact partially a reflector and partially a diffuser, emits light which can be analysed into its specular and diffuse components, and the area itself will then appear as equivalent to two facets, of suitable areas, one reflecting and the other diffusing.

This conception of facets is not far removed from the actual structure of many real surfaces as seen in the microscope. In the case of paper, for example, complete fibres have reflecting surfaces, whereas finely divided fibres and the filling material, if any, scatter the light; in a wood surface the interiors of cells cut open are highly polished, whereas the knife leaves a surface of varying roughness cutting through the cell walls.

The parallel between real and equivalent surfaces ceases to apply when multiple reflections are considered. When a highly inclined mirror facet is illuminated, much of the light reflected will fall on other elements of the surface which, whether mirror or rough, will in general be highly curved, and will consequently distribute the light over a wider angle at each reflection. Such light on emerging will be equivalent to light from diffusing facets. Light transmitted by the surface and re-emitted will be similarly classified as coming from rough elements.

If now such a composite surface is illuminated, light will be received from all the visible rough components, but from only those particular mirror components whose normals lie in the photometer plane and which are set at an angle ϕ to the mean surface such that

$$\phi = \frac{(\alpha+\beta)}{2}, \qquad \text{.....(4)}$$

and the angle of incidence and reflection on these mirror facets will therefore be given by

$$i = e = \frac{(\alpha-\beta)}{2}. \qquad \text{.....(5)}$$

The total flux received from the composite surface is given in the above notation by

$$E_{\alpha\beta} = R_{\alpha\beta} + M_{\alpha\beta}. \qquad \text{.....(6)}$$

In cases where the angles need not be specified, the subscripts will be omitted from these symbols.

Evaluation of R. One cm.^{2} of mean surface contains dA' cm.^{2} of rough facets inclined at any given angle to the mean surface. When these facets are illuminated at i and viewed at e, the flux received is $rI \cos i \cos e\, dA'$ per cm.^{2} of mean surface and, since the area illuminated is $X/\cos\alpha$, we have that the flux received

$$dR = \frac{XrI}{\cos\alpha} \cos i \cos e\, dA'. \qquad \text{.....(7)}$$

Since the photometer plane is fixed and is perpendicular to the mean surface we may conveniently define the angle of inclination of a facet in terms of latitude θ and longitude γ; in other words, θ is the angle which the normal to the facet makes with the photometer plane and γ is the angle between the normal to the mean surface and the plane of longitude containing θ.

We thus have

$$\left.\begin{aligned} \cos i &= \cos(\alpha-\gamma)\cos\theta, \\ \cos e &= \cos(\beta-\gamma)\cos\theta, \\ dA' &= f(\gamma,\theta)\, d\gamma\, d\theta, \end{aligned}\right\}$$

and from equation (7)

$$dR_1 \cos\alpha = XrI \cos(\alpha-\gamma)\cos(\beta-\gamma)\cos^2\theta f(\gamma,\theta)\, d\gamma\, d\theta.$$

If we confine ourselves to surfaces giving a symmetrical distribution of scattered light when illuminated normally—a condition true for most manufactured surfaces such as paper, but not always for wood—there will be a corresponding equal area dA' of rough facets at an angle $(-\gamma, \theta)$ on the other side of the meridian, giving a flux

$$dR_2 \cos\alpha = XrI \cos(\alpha+\gamma)\cos(\beta+\gamma)\cos^2\theta f(\gamma,\theta)\, d\gamma\, d\theta.$$

Adding dR_1 and dR_2 and integrating we have

$$2R_{\alpha\beta}\cos\alpha = XrI\{p_1\cos(\alpha-\beta) + p_2\cos(\alpha+\beta)\}, \qquad \text{.....(8)}$$

where

$$\left.\begin{aligned} p_1 &= \iint \cos^2\theta f(\gamma,\theta)\, d\gamma\, d\theta, \\ p_2 &= \iint \cos 2\gamma \cos^2\theta f(\gamma,\theta)\, d\gamma\, d\theta. \end{aligned}\right\}$$

Equation (8) can be further simplified only in the light of experiment, because $f(\gamma, \theta)$ and the limits of γ are, for a complex surface, completely unknown. For any isolated opaque body of simple form and without re-entrant surfaces the limits to the area which is both illuminated and visible are easily determined, but although the limits of θ are $\pm\frac{1}{2}\pi$, those of γ depend on α and β so that, if such limits were applied to the present surface, both p_1 and p_2 would vary with every combination of α and β, and no solution of (8) would be possible. This insistence on limits to the area which is both illuminated and visible overlooks the numerous refractions and cross reflections which must occur in the surface, so it seems more probable that the limits of γ and θ will not be effective in practice. In support of this, figure 4, for Bristol board, shows that, provided that combinations of α and β are taken in groups

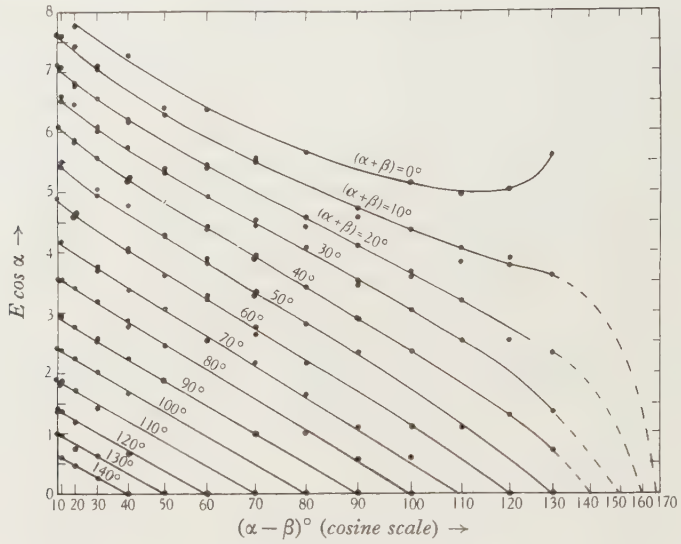

Figure 4. Bristol board. $E_{\alpha\beta}$ cos α plotted against cos $(\alpha-\beta)$.

such that $(\alpha+\beta)$ is constant, the experimental values of $E_{\alpha\beta}$ cos α in any group lie on a straight line when plotted against cos $(\alpha-\beta)$ for values of $(\alpha+\beta)$ in excess of 70°. Large values of $(\alpha+\beta)$ correspond to large inclinations of the mirror facets, if these are present, so that any light falling on them will be reflected into the surface and will suffer the scattering described above.

For cases, therefore, in which we obtain straight lines as in figure 4, we may say that, *as far as external effects are concerned*, $M_{\alpha\beta}=0$, so that

$$E_{\alpha\beta}\cos\alpha = R_{\alpha\beta}\cos\alpha = \tfrac{1}{2}XrI\{p_1\cos(\alpha-\beta)+\text{constant}\}$$

and from equation (8) this constant must be $p_2\cos(\alpha+\beta)$. Further, from the fact that no flux is emitted when $\beta=\frac{1}{2}\pi$, we find that $p_1=p_2$.

The integral p_1 cannot be evaluated unless the distribution of facets is known, but if all the facets had lain on the equator ($\theta=0$), the integral would have become $p_1=\int f(\gamma)\,d\gamma$. This is simply the total area A, which is both illuminated and visible

at given values of α and β. We may thus describe the flux from rough elements, at all angles (γ, θ) and of area A', as equivalent to the flux from an area A of rough facets in a two-dimensional case.

Thus equation (8) reduces to

$$[R_{\alpha\beta}]_{(\alpha+\beta)\text{ constant}} = \tfrac{1}{2}XrIA\{\cos(\alpha-\beta)+\cos(\alpha+\beta)\}. \quad \ldots\ldots(9)$$

Equation (9) is of course equivalent to

$$[R_{\alpha\beta}]_{(\alpha+\beta)\text{ constant}} = XrIA\cos\beta,$$

but it will be found more convenient to have it in the form given above because constancy of $(\alpha+\beta)$ determines, in cases where a specular component is present, that this component shall always come from the same facets, by equation (4), and because $(\alpha-\beta)$ determines the angle of incidence on these facets by equation (5). For an ideally rough surface rA is the same for all values of $(\alpha+\beta)$, so that the straight lines in figure 4 are parallel in this case, and equation (9) therefore reduces to

$$R_{\alpha\beta} = XrIA\cos\beta,$$

which is Lambert's law.

Evaluation of M. One cm^2 of mean surface contains B cm^2 of mirror facet set at an angle ϕ. The flux reflected at the specular angle is $sIB\cos i$ and the total area illuminated is $X\cos\alpha$, hence, since $i=\frac{1}{2}(\alpha-\beta)$, the total flux reflected is given by

$$M_{\alpha\beta}\cos\alpha = XsIB\cos\tfrac{1}{2}(\alpha-\beta). \quad \ldots\ldots(10)$$

It should be noted that s varies with the angle of incidence.

Total effect. As the measured fluxes are comparative and not absolute, XI may be omitted and the total flux may be written thus:

$$E_{\alpha\beta}\cos\alpha = \tfrac{1}{2}(rA)\{\cos(\alpha-\beta)+\cos(\alpha+\beta)\}+sB\cos\tfrac{1}{2}(\alpha-\beta). \quad \ldots\ldots(11)$$

§ 5. COMPUTATION

Equation (11) is symmetrical with respect to α and β, which provides a useful check on the accuracy of the photometer readings, since it implies that, when the directions of illumination and view for any pair of angles are interchanged,

$$E_{\alpha\beta}\cos\alpha = E_{\beta\alpha}\cos\beta. \quad \ldots\ldots(12)$$

A calculation of these two terms shows that in nearly all cases the agreement is good.

Further if, as in figure 4, $E_{\alpha\beta}\cos\alpha$ is plotted against $\cos(\alpha-\beta)$ and the points for constant $(\alpha+\beta)$ are joined, a family of curves is obtained which are so simple in form that values of $E_{\alpha\beta}\cos\alpha$, for intervals of α and β, which were not measured experimentally, may safely be obtained by interpolation.

The value of r is unknown and may vary at different depths in a real surface, so rA will appear as a product throughout, leaving in effect two unknowns, rA and B, to be found from equation (11). Equation (10), which gives M, does not stipulate

that the mirror flux should be zero when $\beta = \frac{1}{2}\pi$,* so that the final expression (11) for the emergent flux cannot be resolved into its components rA and B simply by taking pairs of simultaneous equations, since B is not independent of $(\alpha - \beta)$. In figure 4, however, straight lines result as long as mirror components are negligible, and the intercept of these lines on the ordinate $(\alpha - \beta) = \frac{1}{2}\pi$ will give values of $\frac{1}{2}rA \cos(\alpha + \beta)$, from which rA may be obtained. Figure 4 shows that straight lines can be obtained from $(\alpha + \beta) = 140°$ to $(\alpha + \beta) = 70°$. For lower values of $(\alpha + \beta)$, mirror components become appreciable and the line is no longer straight, but the following method may then be used for determining rA in these cases.

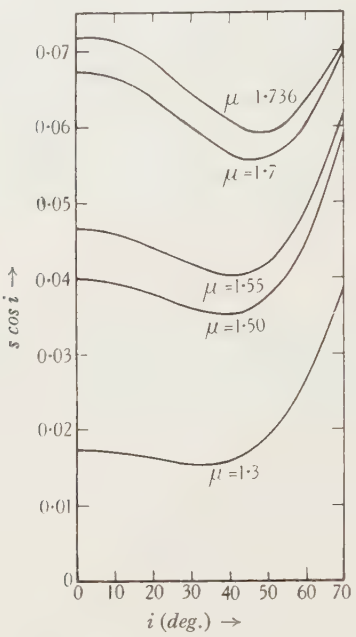

Figure 5. $s \cos i$ plotted against i.

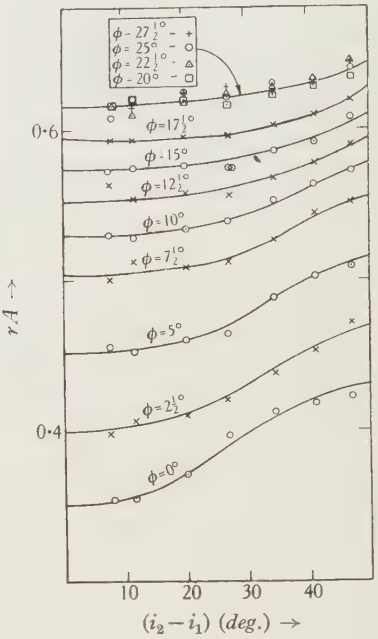

Figure 6. Bristol board. Apparent values of rA.

Figure 5 shows the values of $s \cos i$ for refractive indices of 1·3, 1·5, 1·7 and for the two special values required in this paper. These pass through a minimum, so that an approximate value of rA could be obtained from the slope of the lines in figure 4 at the point corresponding to this minimum. Greater accuracy is obtained if we choose several pairs of values of i for which $s \cos i$ are equal. Calling these paired values i_1 and i_2, where $i_1 < i_2$, we have, except for masking,

$$\frac{rA}{2} = \frac{(E \cos \alpha)_1 - (E \cos \alpha)_2}{\cos 2i_1 - \cos 2i_2}. \qquad \text{.....(13)}$$

The areas of mirror facets at any particular inclination will be progressively eclipsed as the angle of illumination increases and rA, as calculated from (13), will be larger

* That this is found experimentally is due to the masking of the small mirror elements by neighbouring projections on the mean surface. The masking effect will not affect equation (12) because it applies equally to either direction of illumination.

the greater the distance between the two chosen values of i. If now the apparent values of rA obtained from equation (13) are plotted against $(i_2 - i_1)$, a curve will be obtained from which the true value of rA when $(i_2 - i_1) = 0$ may be extrapolated with fair accuracy. The pairs i_1 and i_2 chosen for the Bristol board, for which $\mu = 1{\cdot}55$, were as shown in table 1. The apparent values of rA calculated from these pairs

Table 1

i_1 (deg.)	10	15	20	25	30	35	37
i_2 (deg.)	57	56	$54\frac{1}{2}$	$52\frac{1}{2}$	50	$46\frac{1}{2}$	45

are plotted in figure 6 for different values of ϕ up to 30°, the greatest inclination at which mirror facets are appreciable.

The values of rA which have been obtained by these two methods, for the full range of $(\alpha + \beta)$ considered, are set out in table 2.

Table 2

$(\alpha+\beta)$ (deg.)	0	10	20	30	40	50	60	70
rA	0·350	0·452	0·528	0·574	0·610	0·616	0·616	0·620
$(\alpha+\beta)$ (deg.)	80	90	100	110	120	130	140	
rA	0·620	0·588	0·580	0·572	0·560	0·560	0·546	

By taking the smoothed values of $E_{\alpha\beta} \cos \alpha$ from figure 4, and using the appropriate values of rA in each case we obtain from equation (11) the separate rough and mirror components R and M, and the comparative areas B of the mirror facets for each reading of the total flux. These resolved components R and M are shown in figure 8. The values of B are given in table 3 and show the diminution due to

Table 3. Bristol board. Comparative areas B of mirror facets at various inclinations ϕ to the mean surface, showing the masking of these areas for various angles of incidence i

i (deg.)	ϕ (deg.)					
	0	5	10	15	20	30
0	—	6·7	4·2	2·6	1·6	0·6
10	9·8	6·5	4·1	2·5	1·4	0·5
20	9·3	6·2	3·9	2·3	1·3	0·3
30	9·1	6·1	3·9	2·4	1·4	0·3
40	9·0	6·2	4·0	2·5	1·4	0·3
50	8·9	6·0	3·9	2·4	1·3	0·2
60	8·5	5·5	3·2	1·9	1·0	0

masking which was predicted above. There is a tendency for the values to rise slightly in the region of 40° incidence. This may be reduced by taking rather lower values of rA, but is probably due to the somewhat arbitrary choice of refractive index. What may be termed the "true" values of B—that is the values which obtain

when $i = 0$ (or $\alpha = \beta$) and there is no masking—are plotted against ϕ in figure 7, and give the comparative "true" areas of mirror facets at all inclinations to the mean surface. Since B is not obtainable experimentally for light at normal incidence when $\phi = 0°$, the curve for $i = 10°$ is added to show the rapid increase in area of these facets with decreasing angles of inclination. The evaluation of B is not necessary to the resolution of E into R and M. It is given here to show that although equation (10) does not allow for the masking of mirror elements, the computation leads to acceptable results for the mirror components.

Finally, figure 8 shows the polar curves for the total flux at angles of incidence differing by 10°, and the polar curves of the rough and mirror components in each case.

It is to be noted that the curves for the rough components bear no resemblance to the circle which would be predicted from Lambert's law on the assumption that

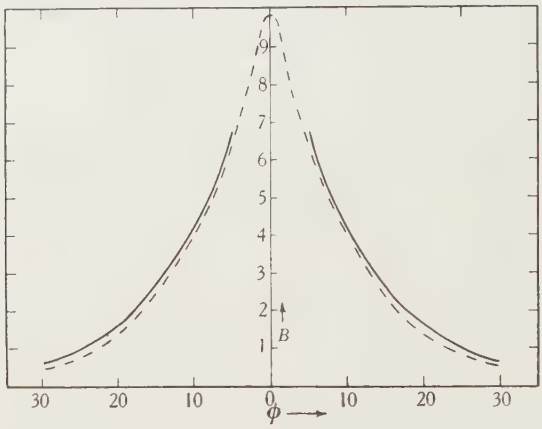

Figure 7. Bristol board. Comparative areas of mirror facets at various inclinations to the mean surface. ———— incident light normal to facet; — — — incident light at 10° to facet.

the contribution of the rough elements was equivalent to a plane rough surface parallel to the mean surface. This result is due to the fact, which is allowed for in the analysis, that the diffusing facets do not all lie parallel to the mean surface. To illustrate this most simply, take the case of a symmetrical surface under normal illumination, and imagine that all the rough facets, at a given inclination relative to the normal, lie on the surface of a circular cone of vertical angle 2η and of base area a. We may compare the effects of different values of η by keeping a constant for each cone, since the same incident flux will then be absorbed in each case. In this hypothetical case the flux will not fall to zero when $\beta = \frac{1}{2}\pi$, which is the result of the grouping of the facets on the mean surface, but it will be sufficient to show differences in the distribution of flux due to inclination of the facets.

An element of area dA on the surface of the cone is fixed by reference to the angle ψ which the radius through dA subtends with a fixed radius parallel to the photometer plane and to the circular section on which it lies. The radius of this

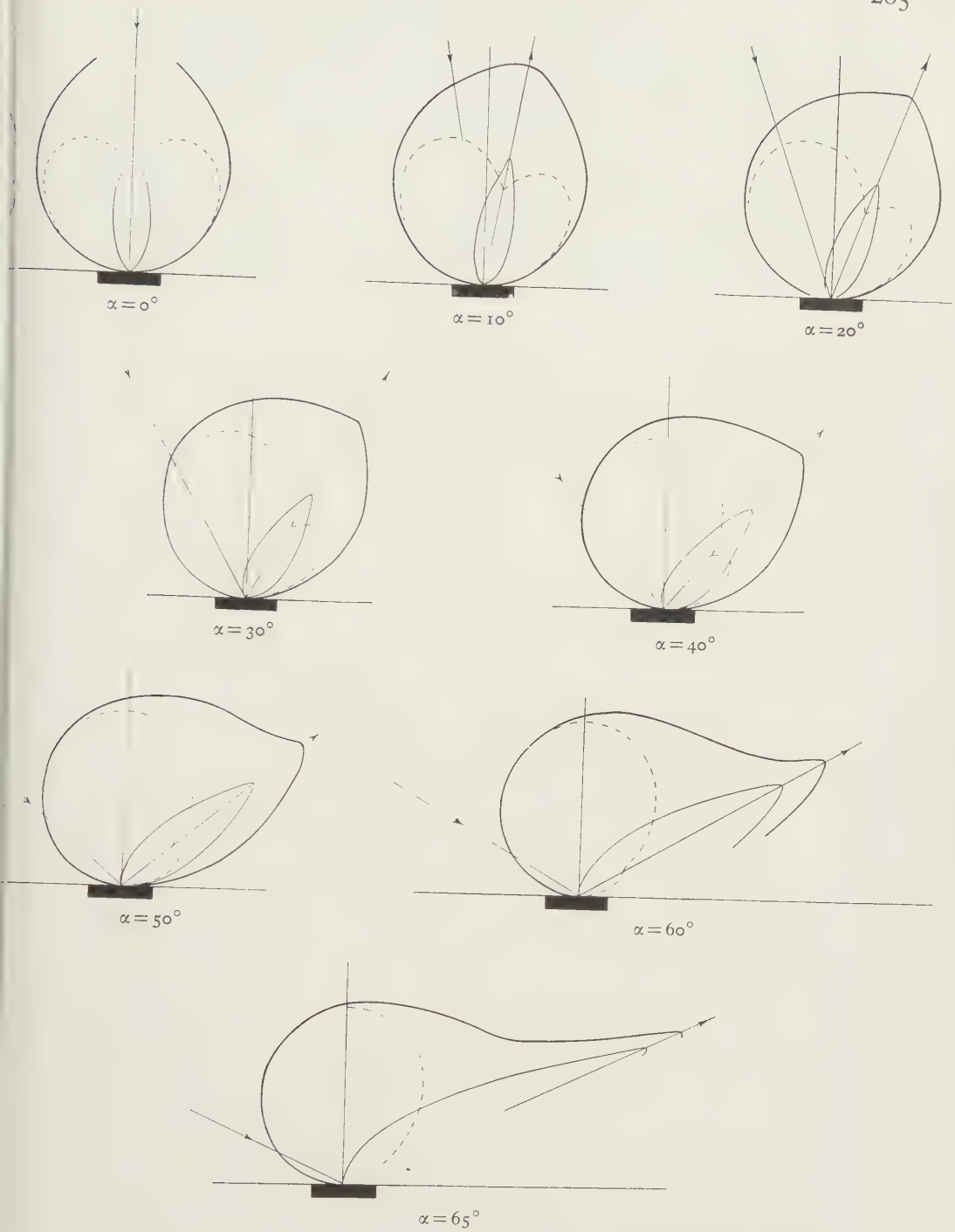

Figure 8. Bristol board. Resolution of scattered flux into diffuse and specular components.
—— total flux; – – – – diffuse flux; —— specular flux.

circle is $h \tan \eta$. If the mean surface is, as before, illuminated at α and viewed at β we have

$$\left.\begin{aligned} \cos i &= \sin \eta \cos \alpha + \cos \eta \sin \alpha \cos \psi, \\ \cos r &= \sin \eta \cos \beta + \cos \eta \sin \beta \cos \psi, \\ dA &= \frac{h \tan \eta}{\cos \eta}\, d\psi\, dh. \end{aligned}\right\}$$

If the cone has a uniformly diffusing surface and if $\alpha = 0$, the total flux scattered at angle β is given by equation (7) as

$$R = XrI \iint \{h \tan^2 \eta \,(\sin \eta \cos \beta + \cos \eta \sin \beta \cos \psi)\}\, d\psi\, dh. \quad \ldots\ldots(14)$$

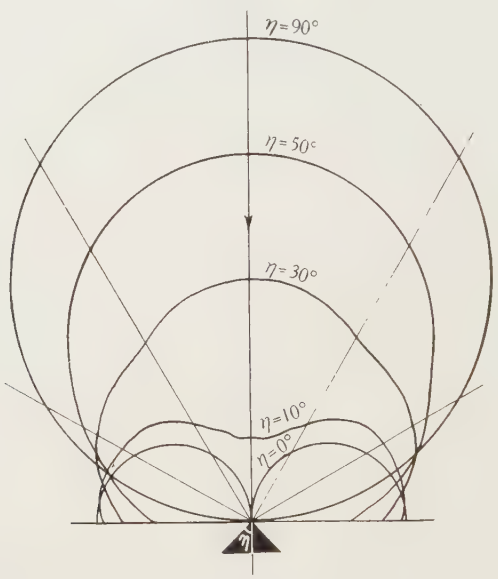

Figure 9. Distribution of scattered flux from rough cones, of various apex angles but equal base areas, under illumination parallel to the axis.

The base area a of the cone $= \pi h^2 \tan^2 \eta$ so we have by integration

$$R = \frac{XrIa}{\pi} \left[\sin \eta \cos \beta + \cos \eta \sin \beta \sin \psi\right]_{\psi_1}^{\psi_2} \quad \ldots\ldots(15)$$

and by symmetry $\psi_1 = \psi_2 = \pm \psi_L$.

There are two cases to consider for ψ_L. First, when $\beta \leqslant \eta$ and the whole surface can be seen, while $\psi_L = \pm \pi$. This gives

$$R_{(\beta \leqslant \eta)} = XrIa \sin \eta \cos \beta. \quad \ldots\ldots(15a)$$

Secondly, when $\beta \geqslant \eta$ and ψ_L is determined by the point at which $e = \frac{1}{2}\pi$ or $\cos \psi_L = \mp (\tan \eta / \tan \beta)$, whence

$$R_{(\beta \geqslant \eta)} = \frac{XrIa}{\pi} \left\{\sin \eta \cos \beta \cos^{-1}\left(-\frac{\tan \eta}{\tan \beta}\right) + \sqrt{(\cos^2 \eta - \cos^2 \beta)}\right\}. \quad \ldots\ldots(15b)$$

Figure 9 gives the polar curves of R for several values of η.

In any real surface the cone angles η have a given distribution on which the curve for the total flux will depend. If, as in Bristol board, facets nearly parallel to the mean surface ($\eta = 90°$) are scarce, owing presumably to the pressing and rolling in manufacture, the polar curve for R will as in figure 8 bear little resemblance to a Lambert's circle. Further, in any real surface, the highly inclined facets will be under a much stronger illumination than that given by the direct beam, owing to cross reflections, and will therefore have a disproportionately large influence on the shape of the polar curve. When we come to consider a magnesium-oxide surface we shall see that a nearly uniform distribution of rough facets gives a polar curve which is a Lambert's circle.

§ 6. ANALYSIS OF A SURFACE OF MAGNESIUM OXIDE

A surface of magnesium oxide was prepared by burning magnesium ribbon under a glass plate. Table 5 gives the values of the flux obtained from this surface at 10° intervals of α and β. Values which have been used in the calculations were

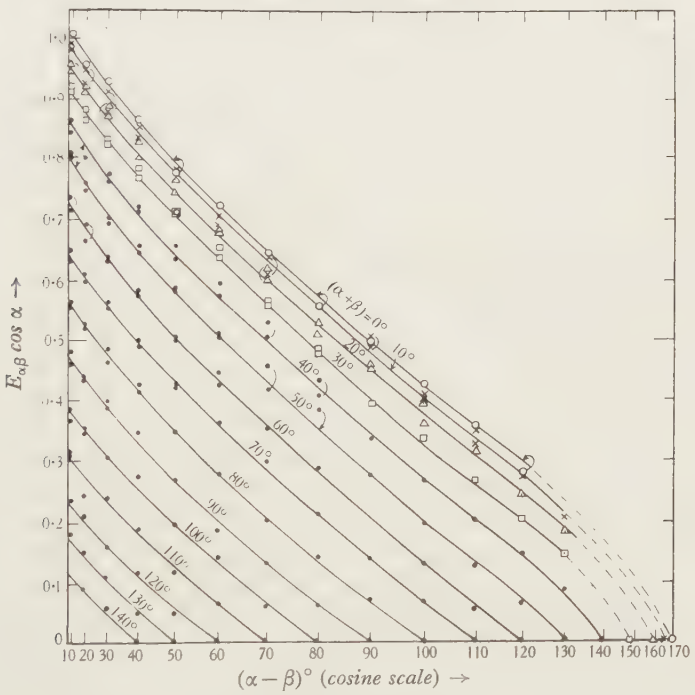

Figure 10. Magnesium oxide. $E_{\alpha\beta}\cos\alpha$ plotted against $\cos(\alpha-\beta)$. ○, $(\alpha+\beta)=0°$; ×, 10°; △, 20°; □, 30°; ●, other values.

obtained also at each 5° interval, but these have been omitted from the table. The results are in good agreement with a few measurements made by Thaler[23], who records the visual brightness of the surface and not the flux.

If the surface were a perfect diffuser, the flux scattered at any angle β, positive or negative, would be independent of α and proportional to $\cos\beta$. This is not the case

here, for the values are somewhat too high near the specular angle, but these are by no means maximum values, as they were in the case of the Bristol board. This shows that there is no marked excess of the mirror facets lying parallel to the mean surface.

These results may be analysed by the above method, and figure 10 corresponds to figure 4 in giving the graph of $E_{\alpha\beta}\cos\alpha$ against $\cos(\alpha-\beta)$. The chief difference between figures 4 and 10 is that in the latter the lines do not tend to become straight for high values of $(\alpha+\beta)$. This proves the existence of mirror facets at large inclinations to the mean surface.

On the assumption that the refractive index of magnesium oxide in the form of periclase, which is given in the *International Critical Tables* as 1·736, applies also to a smoke deposit, pairs of values of i giving equal values of $s\cos i$ were chosen from figure 5 and are given in table 4.

Table 4

i_1 (deg.)	25	30	35	37	40	$42\frac{1}{2}$	45
i_2 (deg.)	$64\frac{3}{4}$	$62\frac{1}{4}$	$59\frac{1}{4}$	$57\frac{1}{4}$	$55\frac{1}{2}$	$53\frac{3}{4}$	$51\frac{1}{2}$

By the use of equation (13), apparent values of rA could be obtained, between $(\alpha+\beta)=0°$ and 70°, from the lines in figure 10. When these were plotted as in figure 6, it was found that, within the limits of experiment, the apparent values were the same for all the lines within this range, and that the true value of rA could be taken as 0·83.

Table 5. Magnesium-oxide smoke on plane glass. The figures are correct, with few exceptions, to 1 per cent of the value obtaining when $\beta=0$ in each column. Figures denoting flux at specular angle are given in black type

β (deg.)	α (deg.)						
	0	10	20	30	40	50	60
+90	000	000	000	000	000	000	000
+80	0·139	0·130	0·147	0·134	0·150	0·163	0·176
+70	0·297	0·280	0·284	0·315	0·308	0·324	0·354
+60	0·446	0·430	0·450	0·458	0·449	0·480	—
+50	0·584	0·580	0·587	0·602	0·600	—	0·622
+40	0·733	0·700	0·734	0·745	—	0·740	0·706
+30	0·832	0·810	0·860	—	0·823	0·806	0·772
+20	0·921	0·920	—	0·928	0·870	0·868	0·822
+10	0·990	—	0·978	0·947	0·917	0·906	0·840
0	—	1·000	0·978	0·956	0·936	0·906	0·840
−10	0·990	**0·970**	0·970	0·956	0·925	0·885	0·832
−20	0·911	0·890	**0·920**	0·899	0·896	0·857	0·806
−30	0·822	0·810	0·832	**0·831**	0·832	0·815	0·772
−40	0·713	0·720	0·723	0·699	**0·795**	0·751	0·714
−50	0·584	0·600	0·596	0·583	0·653	**0·660**	0·678
−60	0·445	0·460	0·460	0·450	0·515	0·544	**0·553**
−70	0·297	0·290	0·294	0·306	0·346	0·380	0·412
−80	0·139	0·140	0·137	0·143	0·187	0·226	—
−90	000	000	000	000	000	000	—

Estimates of rA cannot be made for larger values of $(\alpha+\beta)$, because the minimum of the $s \cos i$ curve is not included in the range of $(\alpha-\beta)$, and the method is, in this respect, unsatisfactory in cases where mirror facets are found at large inclinations to the mean surface. On the other hand the light received from the surface at angles connected with large values of $(\alpha+\beta)$ is always small and contributes little to the appreciation of gloss.

For this particular surface it seems justifiable to assume that rA will also have the same value of 0·83 for those lines of constant $(\alpha+\beta)$ from which rA cannot be directly computed and, for the sake of completing the analysis, this assumption will be made. This means that the diffuse component R of the polar curve of scattered flux will be a Lambert's circle of diameter 0·83 for each angle of illumination, as shown in figure 11 for values 0°, 30° and 60° of α.

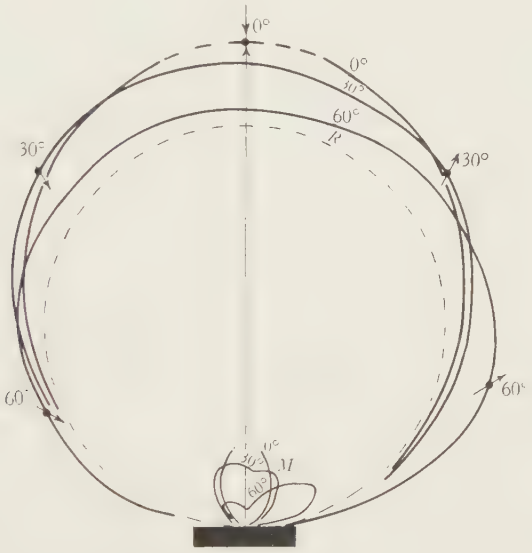

Figure 11. Magnesium oxide. Resolution of scattered flux into diffuse and specular components.

Table 6 gives the values of B calculated from equation (11), while the true values of B (those which obtain when $i=0$) at each inclination ϕ are shown in figure 12. The values of B for Bristol board are included in this graph. Though the numerical values of B for the two surfaces cannot be compared, unless the flux at some common point is measured for both in the same units, it is evident that the decrease in facet-area with inclination is much more gradual for the magnesium-oxide surface. It can also safely be inferred from the relative values rA and B in the two cases that the actual area of mirror facets parallel to the mean surface is much smaller for magnesium oxide than for Bristol board.

It was postulated above, in considering the Bristol board, that the $(\alpha+\beta)$ lines were straight owing to the occurrence of multiple refractions and reflections in the depths of the true surface. This suggestion is borne out in the case of magnesium oxide where the lines are no longer straight, because here the true surface is so

Table 6. Magnesium-oxide smoke on plane glass. Comparative areas B of mirror facets at different inclinations ϕ to the mean surface, showing the masking of these areas for different angles of incidence i

i (deg.)	ϕ (deg.)						
	0	10	20	30	40	50	60
0	—	2·1	1·9	1·6	1·1	0·7	0·4
10	2·4	1·9	1·6	1·2	0·8	0·5	0·3
20	1·9	1·4	1·0	0·6	0·3	0·1	0
30	1·6	1·2	0·7	0·3	0	0	0
40	1·3	1·0	0·5	0	−0·1	0	
50	1·3	0·9	0·3	−0·1	0		
60	1·3	1·0	0·5	0			
70	0·7	0·7	0				

nearly plane that even highly inclined facets will be able to produce external effects by single reflection. To test this idea the magnesium-oxide surface was viewed microscopically with an Ultropak illuminator at a magnification of about 1200, the

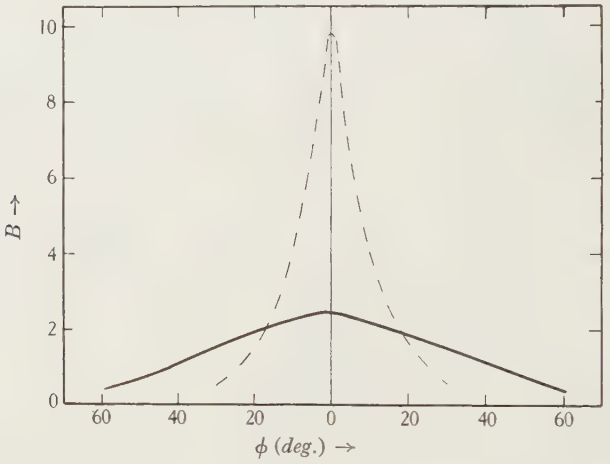

Figure 12. Magnesium oxide. Comparative areas of mirror facets at various inclinations to the mean surface. ——— magnesium oxide; — — — Bristol board.

light falling in a narrow beam from one side only. It was found that though for the most part the image could not be resolved beyond a general white haze, the surface was sprinkled all over with separate bright spots, representing presumably larger particles of smoke. There seems little doubt that it is these projecting particles that contribute the light here classed as specular and cause the departure from Lambert's law.

§ 7. DISCUSSION OF RESULTS

This development of the conception of mirror facets has been attempted in order to deal with surface structures such as wood or paper which can be resolved microscopically. The analysis seems to be successful for surfaces giving symmetrical

scattering curves for normal illumination, and the question of dealing with unsymmetrical surfaces such as those of wood is now being considered. The analysis of the magnesium-oxide surface was made with some hesitation as it was felt that spurious M components might appear in the analysis which would not be strictly related to true specular reflection in this case. The results seem to indicate that the analysis is in fact applicable even to surfaces so nearly matt as magnesium oxide because it leads to the plausible structure of a uniform surface of perfect diffusion sprinkled over with few randomly oriented mirror facets projecting from the general surface. None the less the numerical values of M, and especially of B, cannot be taken as very accurate when they are relatively so small, depending as they do on the accurate choice of rA. This in turn is somewhat sensitive to the choice of refractive index owing to the change in shape of the $s \cos i$ curves in figure 5, and in the position of their minimum value.

A source of error in the values of R and M here presented lies in the dependence of lines of constant $(\alpha+\beta)$ on the accurate correlation of the polar curves for different angles of incidence, as each point on a given $(\alpha+\beta)$ line is taken from a different experimental curve. Greater accuracy could be obtained if the successive readings of the flux could be made under conditions in which $(\alpha+\beta)$ instead of α was held constant.*

An important question in relation to the practical utility of the method is how far surfaces can be differentiated by it. To test this we may, by way of illustration, imagine a surface which is indistinguishable from an ideally rough surface when illuminated normally, in giving a flux proportional to $\cos\beta$, but is in fact composed entirely of mirror facets. We shall then see whether the method will differentiate between this surface and one ideally rough.

For normal illumination, if only mirror facets are present, $E_{\alpha\beta}=M_{\alpha\beta}=K\cos\beta$ and $R_{\alpha\beta}=0$; and when $\alpha=0$, $i=\phi$ and $\beta=2\phi$. Hence by equation (10)

$$B_\phi = K\frac{\cos 2\phi}{s_\phi \cos\phi},$$

which is the effective area of the facet when the surface is illuminated normally For a refractive index of 1·55, this expression gives for the ratios of the necessary facet-areas the values shown in table 7.

Table 7

β or 2ϕ (deg.)	0	10	20	30	40	50	60
B_ϕ	1	0·988	0·954	0·894	0·810	0·698	0·557

Owing to masking, these areas will not be the same if the facet is illuminated at some other angle, so, in order to predict the flux when α is not zero, we must adopt some arbitrary system of masking. Having chosen a refractive index equal to that of

* Since this paper was submitted the rotation of the sample has been geared to that of the arm so as to achieve this end. The determination of the complete family of curves given here is tedious and is, for practical purposes, unnecessary now that the apparatus has been modified, because the number of facet angles at which the specular component is measured can be suited to the material under examination.

Bristol board, we may conveniently assume the masking to be the same as that given in table 3 for this surface. Table 8 compares the flux at angle β when under normal illumination, which we have taken as proportional to cos β, with that found at the same angle of view when the illumination is, in each case, at $-\beta$. This is the flux which would be obtained in the cycle of readings for which $(\alpha+\beta)=0$, and corresponds to specular reflection relative to the mean surface.

Table 8. Values of $E_{\alpha\beta}$ for a surface composed of mirror facets

β (deg.)	0	10	20	30	40	50	60
$E_{\alpha\beta}$ when $\alpha=0$	1·00	0·98	0·94	0·87	0·77	0·64	0·50
$E_{\alpha\beta}$ when $(\alpha+\beta)=0$	1·00	0·98	0·94	0·94	1·01	1·24	1·77

This comparison makes it clear that a single cycle of measurements when $(\alpha+\beta)=0$ would serve to show that, in spite of the ideal distribution of flux under normal illumination, the surface was not ideally rough, because the surface contains mirror facets parallel to the mean surface. Other cycles when $(\alpha+\beta)=10°$, 20° and so on would reveal similar departures from the ideal distribution.

Thaler's results for ground glass show an approximation to this state of affairs in a real surface. His figures, when recalculated on the present system of measurement are given in table 9. These values indicate that, although, at 10° incidence the

Table 9. Thaler's values of $E_{\alpha\beta}$ for ground glass

β (deg.)	10	30	50	70	80
$E_{\alpha\beta}$ when $\alpha=10$ (deg.)	1·00	0·86	0·62	0·32	0·15
$E_{\alpha\beta}$ when $(\alpha+\beta)=0$ (deg.)	1·00	0·89	0·76	0·99	2·18

flux follows Lambert's law approximately,* there is considerable specular reflection from mirror facets parallel to the mean surface. The analysis for R and M of this surface cannot be made without knowing the refractive index of the glass.

§8. ACKNOWLEDGEMENTS

In conclusion I should like to thank Mr R. F. S. Hearmon of this Laboratory for undertaking many of the measurements and calculations and studying the literature, and Miss M. S. Smith for preparing the illustrations. I am also indebted to the Director of the Laboratory Mr W. A. Robertson for permission to publish the paper.

* Thaler does not give results for normal incidence.

APPENDIX

OUTLINE OF PREVIOUS WORK ON THE ANALYSIS OF LIGHT SCATTERED FROM MATT OR SEMI-MATT SURFACES

By R. F. S. HEARMON

The scattering of light by surfaces which are intermediate between perfect reflectors and perfect diffusers has received much attention, particularly from the technical point of view, with special reference to the problem of lustre or gloss[7, 8, 13]. It has been studied for textiles[14, 15]; for paints[7, 10, 11]; for photographic and other papers[9, 10]; and for metal surfaces[4]. Although there is a wealth of experimental material, most of it has been used empirically, but some attempts have been made to relate the scattering to the structure of the particular surface under consideration.

Barkas[1] has been able to explain the differences observed in the light scattered from a longitudinal wood surface under normal illumination when the plane of observation is respectively at right angles to, or parallel with, the direction of the grain, by calculating the light scattered from an assemblage of concave cylindrical mirrors, to which are likened the interior surfaces of the cells exposed when the wood is cut. A somewhat similar idea has been used independently by Pelton[15], who interprets the lustre of textile materials in terms of an assemblage of convex transparent cylindrical filaments.

Kubelka and Munk[11] have expressed the light received from a material consisting of superposed layers in terms of two constants, reflectivity and coefficient of scatter. They applied their theory to the covering power of paints, and it has been extended to other materials than paints by Judd[10]. Gurevich[6] has analysed the reflection and transmission of light by a material the surface of which is regarded as a layer of particles. He also concludes that scattering media can be classified on the basis of two constants, in this case the reflection coefficients of an infinitely thin and an infinitely thick layer.

Lommel[12] attempted a theoretical explanation and modification of Lambert's law by considering multiple scattering of light within the material and its subsequent re-emission. An alternative method of approach, which appears first to have been put forward by Bouguer[3] in 1760, assumes the surface to consist of elementary mirrors disposed at all possible angles; this idea has been used either qualitatively as by Thaler[23], or quantitatively as by Seeliger[21], in attempts to explain experimental deviations from Lambert's law. Seeliger, however, concluded that it was not possible to find a frequency function for the distribution of the mirrors which would give a scattering according either to Lambert's law or to the modifications of it proposed by himself or by Lommel.

This point has been taken up by Grabowski[5], who expresses both the scattered intensity and the frequency function for the distribution of the mirrors as a general function of α, β* and the angle between the planes of incidence and scattering.

* The notation used is given on p. 277.

Assuming that the emergent flux is proportional to $\cos\beta$, he finds by a process of functional analysis that

$$f(\alpha) = A \sec^{2n}\alpha,$$

where $f(\alpha)$ is the law of perfect reflection, represented by equation (3) according to Fresnel[20], and A and n are constants. This solution is impossible, because $f(\alpha)$ is known to increase with α, so that n must be positive, in which case $f(\alpha)$ given by the above equation increases without limit. Grabowski therefore concludes that Lambert's law cannot be explained on the Bouguer hypothesis.

Berry[2], however, has assumed two forms for the distribution of area of mirror elements at different slopes. The two expressions for $E_{\alpha\beta}$ which are thus obtained are compared graphically with Lambert's law, and although the discrepancies are in some cases considerable, Berry concludes that Bouguer's hypothesis need not necessarily be rejected, since the deviations can probably be explained on the basis of shadows cast by irregularities in the surface or by diffraction.

Pokrowski[16] goes a step further and divides the scattered light into two parts, so that

$$E_{\alpha\beta} = R_{\alpha\beta} + M_{\alpha\beta},$$

where $M_{\alpha\beta} = as_i$, a being a constant. The assumption that a is constant is equivalent to an assumption that the areas of the mirror elements are so distributed as to make the reflected flux dependent only on Fresnel's equation. $R_{\alpha\beta}$ is assumed to obey Lambert's law, and is thus equal to $b\cos\beta$.

The constants a and b are presumably chosen empirically, but in view of the assumption involved in a being constant, the agreement obtained by Pokrowski between observed and calculated values for $E_{\alpha\beta}$ is rather remarkable, even though figures for only one angle of incidence, 80°, were used.

Although the majority of surfaces showed reasonable agreement, magnesium oxide and lampblack did not, and Pokrowski attempted to make the agreement better by allowing for the effects of shading. In a later paper[17] he considered multiple reflection within the body and obtained a formula to allow for this effect.

Schulz[19] has criticized various points in these papers, particularly the assumption that a is constant. He also pointed out that Pokrowski himself had to make further *ad hoc* assumptions before he could obtain agreement between his theory and the experimental results, and that the latter are in any case rather meagre. Schulz gave some experimental results of his own for a number of materials, from which he concluded that the assumption of an ideal diffusing surface overlain by regularly reflecting elements, whose inclinations are uniform or distributed according to the probability law, is inadequate. Pokrowski[18] later acknowledged that Schulz's rejection of the hypothesis that a is constant is probably justified; at any rate for those surfaces which show gloss.

REFERENCES

(1) Barkas. "The scattering of a parallel beam of light by an assemblage of concave cylindrical mirrors." F.P.R.L. Project 46, Progress Report (October 1937). (Unpublished.)

(2) Berry. "Diffuse reflection of light from a matt surface." *J. Opt. Soc. Amer.* **7**, 627 (1923).

(3) Bouguer. *Traité d'Optique* (Paris, 1760), as quoted by Berry (2).
(4) Egeburg and Promisel. "Studies in evaluating the brightness of electro-deposits." *1st Int. Electrodep. Cong. London* (1937).
(5) Grabowski. "On the theoretical photometry of diffuse reflection." *Astrophys. J.* **39**, 299 (1914).
(6) Gurevich. "A rational classification of light-scattering media." *Phys. Z.* **31**, 753 (1930).
(7) Hanstock. "The measurement of gloss." *Res. Ass. Brit. Paint, Colour and Varnish Manufacturers, Bull.* no. 21 (1937).
(8) Hunter. "Methods of determining gloss." *Bur. Stand. J. Res., Wash.*, **18**, 19 (1937).
(9) Jones. "Gloss characteristics of photographic papers." *J. Opt. Soc. Amer.* **6**, 140 (1922).
(10) Judd *et al.* "Optical specification of light scattering materials." *Bur. Stand. J. Res., Wash.*, **19**, 287 (1937).
(11) Kubelka and Munk. "The optical properties of paints." *Z. tech. Phys.* **12**, 593 (1931).
(12) Lommel. "On fluorescence." *Ann. Phys., Lpz.*, **10**, 449 (1880).
(13) McNicholas. "Equipment for measuring the reflective and transmissive properties of diffusing media." *Bur. Stand. J. Res., Wash.*, **13**, 211 (1934).
(14) Naumann. "Gloss measurements on textiles." *Z. tech. Phys.* **8**, 239 (1927).
(15) Pelton. "The lustre of textile fibres and a method of measurement." *Trans. Opt. Soc. Lond.* **31**, 184 (1929–30).
(16) Pokrowski. "The theory of diffuse reflection. I." *Z. Phys.* **30**, 66 (1924).
(17) Pokrowski. "The theory of diffuse reflection. II." *Z. Phys.* **35**, 34 (1925).
(18) Pokrowski. "The theory of diffuse reflection. IV." *Z. Phys.* **36**, 472 (1926).
(19) Schulz. "Reflection from matt surfaces." *Z. Phys.* **31**, 496 (1925).
(20) Schuster and Nicholson. *The Theory of Optics*, p. 50.
(21) Seeliger. "The photometry of diffusely reflecting substances." *S.B. bayer. Akad. Wiss.* **18**, 20 (1888).
(22) Stamm. "The colloid chemistry of cellulosic materials." *Misc. Publ. U.S. Dep. Agric.* no. 240 (1936).
(23) Thaler. "Diffuse reflection of light at matt surfaces." *Ann. Phys., Lpz.*, Ser. IV, **11**, 996 (1903).
(24) U.S. Bureau of Standards Circular LC–395; quoted by Harrison, *Printing and Allied Trades Research Assn. Res. Report*, no. 1 (July 1938).

THE INVESTIGATION OF ELECTRON LENSES

By O. KLEMPERER, Ph.D., Research Department, Electric and Musical Industries Limited

AND

W. D. WRIGHT, A.R.C.S., D.Sc., Imperial College of Science and Technology

Received 22 *September* 1938. *Read in title* 20 *December* 1938

ABSTRACT. The paper describes two methods of deriving the optical constants and spherical aberration of electrostatic-lens systems. In the first, §§ 2 to 6, the electrical field is imagined to be divided into a series of equipotential surfaces at each of which there is a finite change of potential. To a first approximation these surfaces are spherical close to the axis, and the normal optical ray-tracing formulae can be used to compute the paths of electrons through the system. Results are reported for a two-tube lens for various voltage ratios, the two tubes being of equal diameter. The aberration contributions of the different refracting surfaces to the final aberration can be evaluated, and the curvature of field can also be determined by this means. In the second method, §§ 7 to 9, the Hartmann test used in glass optics has been applied to the experimental investigation of electron lenses. Narrow pencils of electrons pass through a suitable diaphragm and their course when they are focused by the lens under test is found by measurements of their intersections with a fluorescent screen placed at appropriate points along the axis. The design of an electron gun suitable for these tests is described, and results for the two-tube lens are given for various voltage ratios.

§ 1. INTRODUCTION

In geometrical electron optics, use is made of the fact that the path of an electron in electric fields is in close analogy to the path of a light-ray in refractive media. It has been shown already in many papers[1,2] that the effects of axially symmetric fields on electrons can be completely described by the location of the optical cardinal or Gaussian points (focal points, principal points and nodal points) and by the registration of the lens errors, all in complete analogy with the lens systems of glass optics.

The optical constants of electron lenses have been investigated either by the direct experimental method of measuring object and image distances, magnifications, etc.,[3] or by special ray-tracing methods. One of these ray-tracing methods starts with the plotting of a series of equipotentials in the electrolytic trough[4,5]; the path of the ray is then found by graphical methods based on the differential equation of motion of the electron through the field, together with the experimentally known potential function[6]. In another ray-tracing method, mechanical tracers for the electron trajectories, working automatically in an electrolytic trough, are employed[7,8].

We are presenting here two new methods that we have used to investigate electron lenses, both very closely allied to procedures worked out very thoroughly in the design of glass lenses[9, 10]. In the first of these, the trigonometrical ray-tracing method is employed. From a series of equipotentials as measured in the electrolytic trough, the path of the ray is traced by application of the law of refraction at successive equipotential surfaces. The other new method described here is closely analogous to the well-known Hartmann test[11]. A number of fine electron pencils emerging through a pepperpot-like diaphragm is traced through the actual electron lens by means of a sliding fluorescent target, and the path of the beam is measured up with a calibrated microscope.

The two methods are complementary, since the experimental results confirm the approximate calculations made by trigonometrical ray-tracing. Moreover, as will be explained later, the trigonometrical method is more accurate for paraxial rays while the results from electron-beam-tracing give better accuracy for zonal and for marginal rays. Further, although the experiments show the final aberrations present, the trigonometrical results indicate in addition their origin at the various refracting surfaces. As a result, the accumulated experience of ordinary optical methods can more readily be applied in the design of electron-lens systems when the aberrations are evaluated by the standard ray-tracing formulae.

§ 2. TRIGONOMETRICAL RAY-TRACING THROUGH ELECTROSTATIC LENSES

In the design of glass lenses, the fact that the shape of the lens surfaces is almost universally spherical enables formulae to be developed by which the exact path of any light-ray can be traced through the whole of a lens system, by the application of the law of refraction to each surface in succession. The aberrations, that is the deviations of the rays from their ideal paths in a perfect lens system, can be calculated and the results can be used to design the closest approach to the perfectly corrected system.

For the benefit of those readers who are not familiar with trigonometrical ray-tracing methods, it may be stated that given the necessary data defining any ray incident at a spherical refracting surface, the path of the ray after refraction can be calculated to a high degree of accuracy by applying the law of refraction under the conditions appropriate to the geometry of the particular system. By transferring the data of the refracted ray from one surface to the next, the complete ray-path through any spherical system can be determined. The accuracy of the calculations is governed by the accuracy with which the radii of the surfaces, their separation, and the refractive indices of the media, are known. For a given system, the relative positions of two or more rays can be found with high precision. This is in sharp contrast with any graphical method, in which the process of ray-tracing itself introduces errors into the ray-paths that may completely mask or alter the aberrations present.

Similar methods can be applied to the case of electron lenses. It is now well known that the path of an electron across a surface separating two fields of different

potential is exactly analogous to the refraction of a beam of light at an optical surface. This is made use of in an electron lens, by using two electrodes of some suitable shape, for example two cylinders, and applying potentials, say V and V', to them. The equipotential fields that are obtained in an electrode structure of this type are illustrated in figure 1, but although a number of individual equipotentials are shown in this diagram, the field in practice varies continuously, and the exact path of an electron through such a field can only be found by considering refraction from one potential field to the next, when the two differ in potential by only an infinitesimal amount. The integration of the path through the whole lens system leads to very elaborate formulae that do not lend themselves very readily to the design of electron-lens systems. However, if we aim at an approximate instead of an exact answer, the electron path can be determined much more conveniently by ordinary ray-tracing methods.

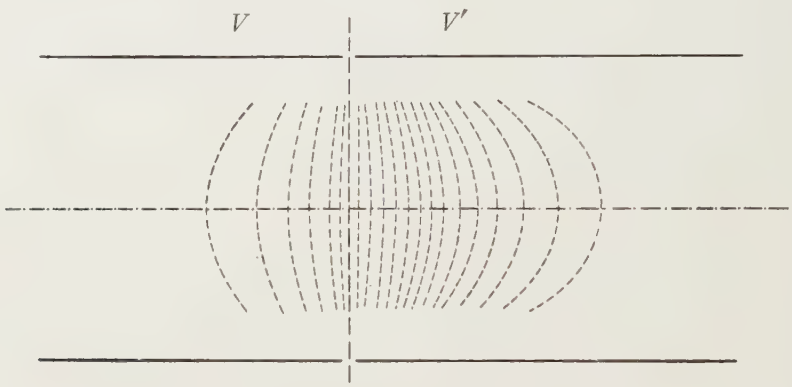

Figure 1. Equipotentials of symmetrical two-tube lens near the axis, giving equal steps in refractive index at each surface.

For this to be achieved, the continuously varying electric field must be subdivided into a finite number, say $(n+1)$, of uniform fields, bounded by n equipotential surfaces. A lens modified in this way will differ from the actual electron lens, but the difference will grow less as n increases. On the other hand, the amount of work involved in computing the aberrations will be greater, the larger the value of n that is selected.

The refraction of an electron across the equipotential surfaces separating potentials of V_p and V_q is exactly equivalent to the refraction of a light-ray from one medium to another, where the refractive indices of the two media are proportional to $\sqrt{V_p}$ and $\sqrt{V_q}$. The outstanding difficulty of applying normal optical computing formulae to the design of electron lenses is that the equipotential surfaces are not spherical. The compromise we have adopted has been to utilize the fact that the central portions of the potentials are spherical to a first order of accuracy. If we can determine their radii, the ray-paths can be traced through this approximation to the actual electron lens by use of the standard ray-tracing formulae, and from the results it is possible to deduce the Gaussian constants of the lens system and the primary, or first-order, spherical aberration. The data obtained can obviously be

only approximately correct, and will apply only to the central portion of the lens system. A method of tracing the rays through the non-spherical parts of the field has been tried, in which the radii of curvature of the equipotential surfaces were determined for a given height above the axis. The method proved, however, to be very inaccurate, largely owing to the fact that a ray entering the lens at a height Y above the axis will, after a few refractions, be at some other height $Y \pm \delta Y$. δY is not negligible, and for any reasonable accuracy it would be necessary to measure the curvature of the potential surface at the appropriate height above the axis. This could, of course, be done, but the measurement would have to be carried out graphically at each surface simultaneously with the trigonometrical work, and would be very laborious. It is shown below, however, that one of the most useful properties of the ray-tracing method is that it allows the contributions of each surface to the final aberration to be calculated. This would not be possible with the non-spherical calculations; the only answer that would be obtained would be a not very accurate determination of the final course of the ray as it emerges from the system. As the same data can now be obtained more quickly and more accurately by direct experiment, the non-spherical calculations have not been followed up.

To find the radii of the central portions of the equipotential surfaces, a series of templates was fitted to the experimentally determined equipotential surfaces, and a curve was plotted relating the curvatures measured with the distance between the surfaces along the axis of the lens. This curve was smoothed, and the radii at the required points along the axis could be found by interpolation.

§ 3. TRIGONOMETRICAL RAY-TRACING: PRELIMINARY INVESTIGATIONS

Initial calculations were made to determine the number of surfaces into which the lenses should be subdivided, the way in which the refractive indices of successive media should be chosen, and the number of rays it was necessary to trace.

It was first decided that if N is the refractive index to the left of the surface and N' that to the right, then N/N' should be the same for all the surfaces through the lens. The refraction at a surface is proportional to N/N', and this arrangement therefore subdivides the refraction equally, at least as far as the index is concerned. It will also be seen below that this choice aids the evaluation of the aberration contributions of the various refracting surfaces. Then if, with n surfaces and $(n+1)$ media, N_1 is the initial refractive index and N_n' the final index, N/N' for each surface will be given by

$$\frac{N}{N'} = \left(\frac{N_1}{N_n'}\right)^{1/(n+1)}$$

and since N is proportional to the square root of the potential of the space concerned, then

$$\frac{N}{N'} = \left(\frac{V_1}{V_n'}\right)^{1/2\,(n+1)}.$$

Since N/N' depends only on the ratio of V_1 and V_n', any calculations made for a given ratio of V_1/V_n' (the focusing ratio) will hold equally well, no matter what the absolute values of the initial and final potentials happen to be.

As the potentials at different positions along the axis are measured in the field-plotting trough, the subdivision of the field can be easily accomplished by plotting $\log \sqrt{V}$ against the axis co-ordinate. It is then only necessary to subdivide the $\log \sqrt{V}$ ordinate into a suitable number of equal steps and to read off the corresponding distances along the axis. The radii at these points are then obtained from the curve referred to above. The process is illustrated in figure 2.

Throughout this paper all lengths are measured in terms of the radius of the cylinders forming the lens. As the only case discussed is that of a lens formed by two equal coaxial cylinders, no doubts can arise as to the interpretation of this unit.

To find the minimum number of surfaces required, a lens formed from two coaxial cylinders of the same diameter and with a 5 : 1 focusing ratio was tested when subdivided into 5, 10 and 20 surfaces in turn. A paraxial ray and a marginal ray, figure 3, parallel to the axis at heights y and Y respectively from the axis and incident from the high-potential side, were traced through the system in each case and the final intersection lengths, l_n' and L_n' respectively, were determined. The focal length f' of the system was found in the usual way as

$$f' = \frac{y}{u_n'},$$

where u_n' is the angle between the paraxial ray and the axis after it has left the final, nth, surface. We can also calculate what we term the mid-focal length, ${}_m f'$, namely the distance from the mid plane, or plane of symmetry between the two cylinders, to the paraxial focus. This is, in a sense, analogous to the back focal length used in glass optics, in so far as it refers the focus to some definite part of the lens structure. The longitudinal spherical aberration LA' is given by

$$LA' = l_n' - L_n',$$

and all these quantities, the true focal length, the mid-focal length and the spherical aberration were compared for the three lenses subdivided into 5, 10 and 20 surfaces respectively. The results are given in table 1.

Table 1. Effect of subdivision of field

Number of surfaces	5	10	20
Focal length	4·00	4·00	4·08
Mid-focal length	4·97	5·37	5·76
Spherical aberration ($Y=0·50$)	0·812	1·069	1·267

With the exception of the focal length, it will be seen that these values do not converge as rapidly as could be desired and a subdivision into more than 20 surfaces would obviously represent a further improvement in the method. An increase to, say, 40 surfaces would, however, represent a very great increase in the computation work with a hardly comparable gain in the value of the numerical result. It would, of course, be possible to increase the number of surfaces in only those parts of the field which exert the greatest refracting effect on the electrodes, but this would

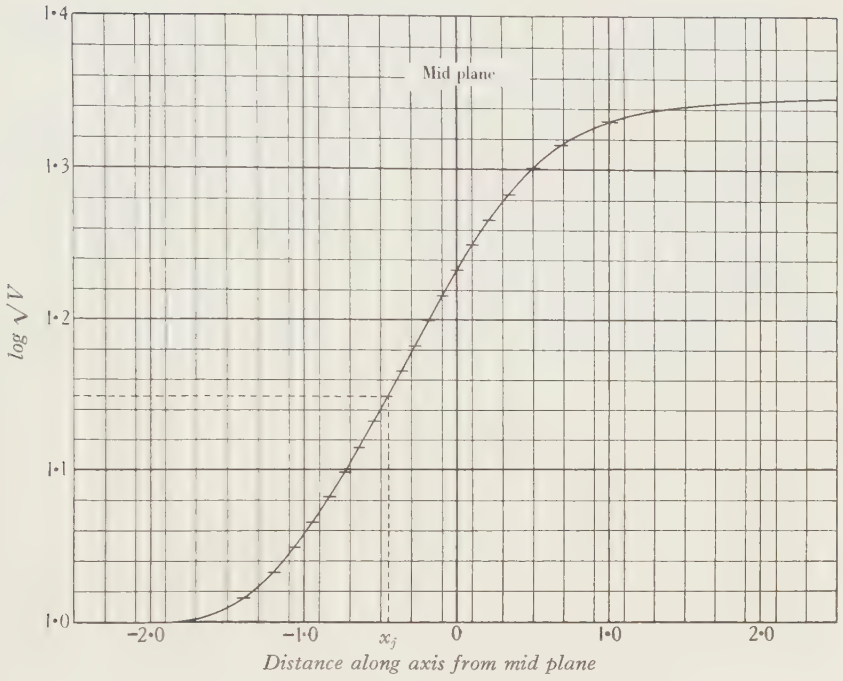

Figure 2 (*a*).

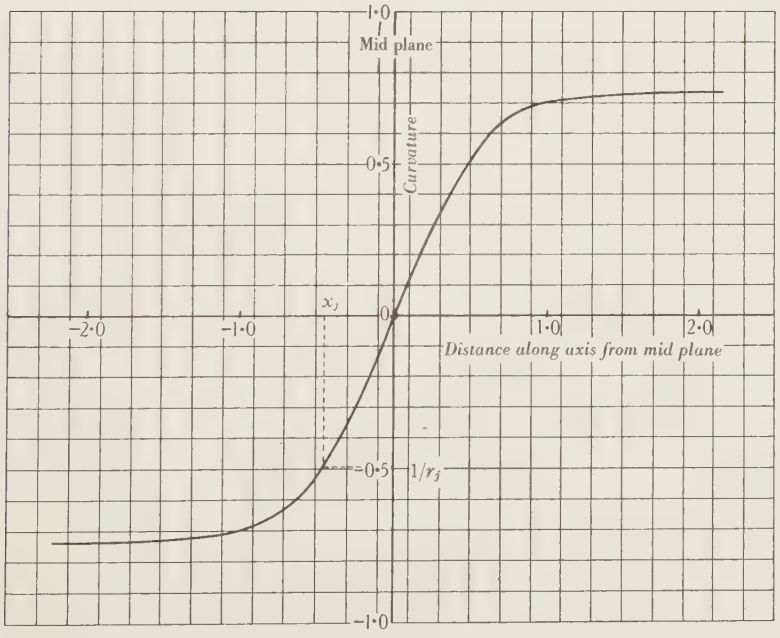

Figure 2 (*b*).

Figure 2. Derivation of the radii of curvature for trigonometrical ray-tracing. (i) log $\sqrt{V}$ plotted against distance along the axis. Total range of log $\sqrt{V}$ is divided into 21 equal parts. The distance x_j, corresponding to the jth equipotential surface, is read off this curve. (ii) Curvature $1/r$ plotted against distance along the axis. The value of $1/r_j$ at distance x_j is read off this curve.

involve sacrificing the constancy of the N/N' relation from surface to surface. A slavish adherence to this constant would be wrong if some appreciable gain were to result from varying it. We have, in fact, carried out some tests in which the field at the two extremes of the lens were more closely subdivided, but the changes in the results were not very significant. Moreover, the accuracy of the field-plotting is lowest at this part of the field, and any high degree of accuracy in the ray-tracing can therefore hardly be hoped for. This is unfortunate, since we shall see that the aberration contributions are greatest at the two ends of the field. But, as we shall point out later, we feel that the chief merit of the ray-tracing method is in indicating in a general way where the aberration arises, and the direction in which it changes as the lens structure is changed; hence any modifications of the trigonometrical method, which are aimed solely at obtaining higher accuracy, should be avoided if, at the same time, they necessitate a considerable increase in the work, or diminish the general applicability of the computing formulae, as a variation in N/N' in fact

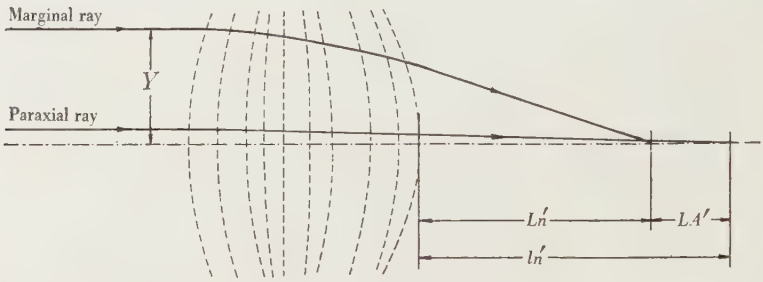

Figure 3. Calculation of spherical aberration LA'.

would do. For these reasons we have been content with a subdivision into 20 surfaces, with a constant ratio N/N' at each surface.

Finally, it had to be decided which and how many rays should be traced. The longitudinal aberration for a given ray is a series function of the type

$$LA' = a_2 Y^2 + a_4 Y^4 + a_6 Y^6 \ldots,$$

where a_2, a_4, a_6 are coefficients and Y is the semi-aperture at which the ray in question is incident on the lens system. As the number of rays that are traced increases, so the number of coefficients that can be calculated also increases. In ordinary optical systems it is unusual to consider more than the first two terms in the series, and frequently the first term alone gives a good idea of the state of correction of the lens. This depends, of course, on how much of the aberration is of the first order, and on the aperture of the system that is being used.

The question was tested by tracing a paraxial ray, a zonal ray with Y_Z equal to 0·25, and a marginal ray with Y_M equal to 0·50 through the lens already described above, when divided into 20 surfaces. These rays gave the zonal aberration as $LA_Z' = 0{\cdot}304$ and the marginal aberration as

$$LA_M' = 1{\cdot}267.$$

This gives $LA_M'/LA_Z' = 4{\cdot}12$, showing that since $Y_M = 2Y_Z$, the aberration is given to a close approximation by only one term in the series, namely

$$LA' = a_2 Y^2.$$

This, of course, is true only for the lens having the hypothetical spherical refracting surfaces. For the actual lens at $Y = 0{\cdot}50$, the aberration would be very different.

Thus the tracing of a paraxial and a marginal ray alone are sufficient to enable the paths of any other axial rays to be calculated sufficiently nearly, assuming that the equipotential fields are spherical or nearly spherical for some distance from the axis. As, in fact, the trigonometrical method can only be used safely for relatively small apertures, the first term in the aberration series is the only one that can be dealt with by this method.

§ 4. GAUSSIAN CONSTANTS AND SPHERICAL ABERRATION BY THE TRIGONOMETRICAL METHOD

Ray-tracing results are given for three focusing ratios, 2 : 1, 5 : 1 and 10 : 1, for two equal cylinders, and the data are tabulated in table 2. In this table the positions of the focal points, the principal points and the nodal points are given relative to the mid plane of the lens, distances to the right of the mid plane being taken as positive, to the left negative. In addition the paraxial focal lengths and the primary spherical aberration are tabulated, the latter being represented by the magnitude of the coefficient a_2 referred to above and calculated for parallel electrons incident from the left.

Table 2. Optical constants of two-tube lens, when diameters of tubes are equal. All lengths are in terms of the radius of each tube as a unit

Lens focusing ratio V/V'	Focal length f'	Focal points		Principal points		Nodal points		Spherical aberration a_2
		F	F'	P	P'	K	K'	
Accelerating 1 : 2	25·0	−20·3	20·9	−2·3	−4·1	4·7	2·9	15·7
Decelerating 2 : 1	18·0	−20·9	20·3	4·1	2·3	−2·9	−5·7	31·8
Accelerating 1 : 5	8·9	−5·7	6·2	−1·6	−2·7	3·2	2·1	3·3
Decelerating 5 : 1	4·1	−6·2	5·7	2·7	1·6	−2·1	−3·2	5·5
Accelerating 1 : 10	3·9	−2·9	1·3	−1·6	−2·7	1·0	0·0	2·6
Decelerating 10 : 1	1·3	−1·3	2·9	2·7	1·6	0·0	−1·0	3·4

It will be seen that each lens system has been tabulated twice, once for the electrons travelling from the low-potential space to the high-potential space (an accelerating lens) and again for the electrons travelling from the high to the low potential (a decelerating lens). The position is somewhat different from the analogous glass system because, although all the lenses discussed here are equivalent to

immersion lenses, the speed of the electrons is an important property of the system, whereas in glass lenses the velocity of light is of no account except in so far as it affects the refractive index. We therefore feel that it is more useful to regard the

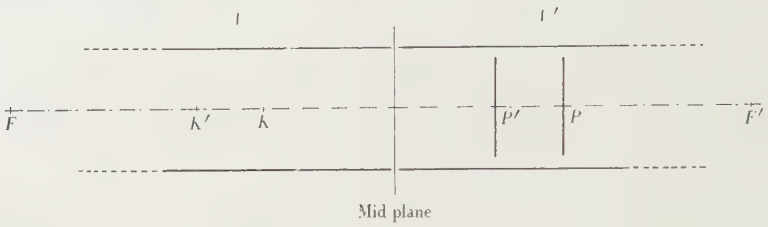

Figure 4 (*a*). $V = 5V'$.

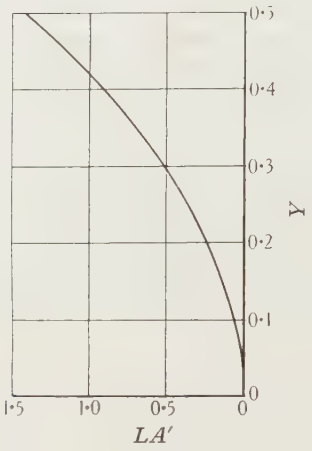

Figure 4 (*b*).

Figure 4. Data for decelerating lens with focusing ratio of 5 : 1. (*a*) Gaussian constants. (*b*) Spherical aberration.

accelerating and decelerating lenses as two distinct systems and we have accordingly tabulated them as such.

To illustrate the results, we have shown in figure 4*a* the relative positions of the Gaussian points of the system for the decelerating lens with a focusing ratio of 1 : 5. Figure 4*b* shows the spherical aberration LA', plotted against the semi-aperture Y when evaluated from the equation $LA' = a_2 Y^2$.

§ 5. THE ABERRATION CONTRIBUTIONS. SPHERICAL ABERRATION

By considering the amount of aberration that is produced at each refracting surface and then applying the ordinary laws of magnification through successive surfaces until the final image plane is reached, Conrady* has developed formulae from which the final primary aberrations can be calculated as the sum of the components arising at each surface. These can be very usefully employed here either as

* See p. 314 of reference (9).

an alternative method of finding a_2, or, more especially, for finding at what points in the system the aberration contributions are greatest.

The contributions have been calculated for the six lenses referred to in table 2, and curves showing the relative distribution of the contributions amongst the 20 surfaces are shown for all six lenses in figure 5.

It will be seen that in all cases the contributions are greatest from the surfaces at the two ends of the field. They are positive on the low-potential side and negative on the high-potential side, and the removal of the aberration becomes a question of

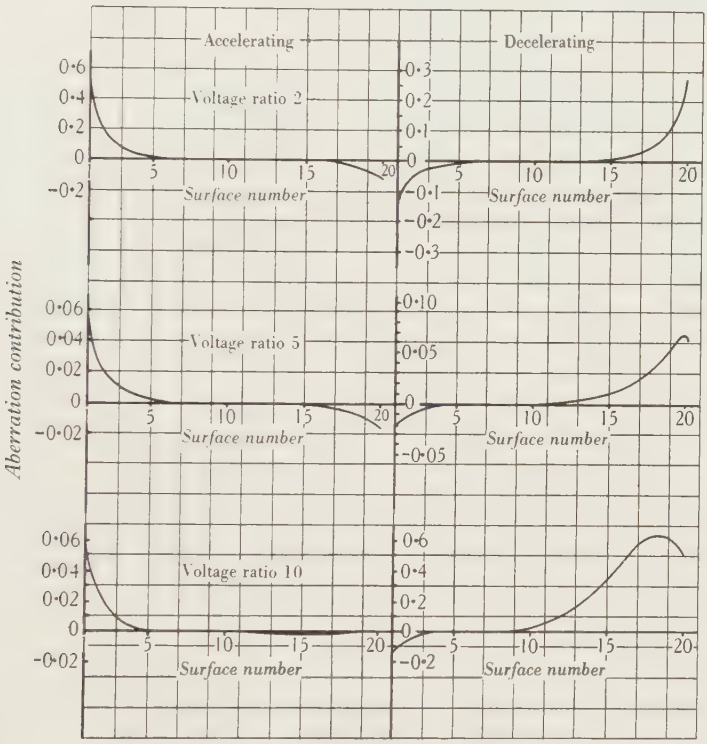

Figure 5. Curves showing aberration contribution.

matching the positive against the negative component by some modification of the equipotential surfaces. This in turn depends on the shape of the electrodes and the distribution of the voltages applied to them. Thus it is possible, by changing the electrodes, to reduce the steepness of the extreme equipotential surfaces and so change the aberration contributions. This would also have the effect of modifying the power of the system, but that again could be compensated for by adjustment of the focusing ratio. It is the interplay of such factors as these that has to be considered in designing electron lenses, and the advantage of knowing, even approximately, the distribution of the aberrations among the equipotential surfaces can readily be appreciated.

It is of interest to speculate on the effect on the curves in figure 5 of increasing

the number of equipotential surfaces. As the number increases the curves tend to approach a differential form, from which, by integration, the final aberration could be derived; we have no doubt that such a differential curve could be formulated from the exact mathematical formulae that are available for tracing the electron path through the continuously varying field, quite apart from any trigonometrical ray-tracing. We have made no attempt to do this, but it is easy to see that the curves in figure 5, which are still increasing at the two ends, would rise to a maximum (lower than their present height) and then diminish towards zero, if the number of refracting surfaces were very considerably increased.

§ 6. PETZVAL CURVATURE

One of the most important developments that follows from a knowledge of these aberration contributions is the determination of the curvature of field which an electron lens will introduce. In certain types of electronic device an image of an extended electron object, usually a photoelectric surface, has to be focused on to a flat screen. It is found in general that with a flat object the image lies on a very steep, round field. Aberrations in this type of device are not usually of much importance unless they are of very great magnitude, owing to the narrowness of the pencils of electrons in the image space and the consequent large depth of focus. (Distortion is, of course, an exception, since this is not primarily affected by considerations arising out of depth of focus.) But the curvature of field is so large that a very marked deterioration in the sharpness of the image is produced.

The cause of this large curvature is immediately apparent if we evaluate the first-order contributions to the final curvature, to give the so-called Petzval curvature. It was shown by Petzval that, in the absence of other aberrations, the radius of curvature C of the final image surface is given to a first approximation by the equation*

$$\frac{1}{C}=N_n'\,\Sigma\,\frac{N_j'-N_j}{N_jN_j'r_j},$$

where N_n' is the index of the final medium in which the image is formed and N_j, N_j' are the indices on either side of the jth refracting surface of radius r_j. This reduces to

$$\frac{1}{C}=\Sigma N_n'\,\{1-N_j/N_j'\}\,\frac{1}{N_jr_j},$$

and since N_j/N_j' is constant in the method we have adopted in subdividing our refracting surfaces, the equation becomes

$$\frac{1}{C}=N_n'\,\{1-N_j/N_j')\,\Sigma\,\frac{1}{N_jr_j}$$

for our system.

The calculation necessary to determine C is thus very straightforward; it amounts to little more than summing $1/N_jr_j$ for the 20 refracting surfaces we have used. But as important as a knowledge of the actual magnitude of this curvature is

* See p. 288 of reference (9).

the realization of the extreme difficulty of ever trying to flatten the field. This can be appreciated by considering the ordinary two-tube lens, in which the positive refracting surfaces occur at the low-potential side of the lens; that is to say, N will be small when r is positive, but large when r is negative. Hence $1/C$ will be a large positive sum, giving C as a small radius corresponding to a steeply rounded field. The position is very much more serious in the case of an electron system using a photoelectric cathode as object, because, owing to the initial velocity of the electrons, which is of the order of only a volt or so, the refractive index is very low indeed and the large positive curvature becomes correspondingly great.

The problem of correcting this field curvature is very closely analogous to the design of anastigmat photographic lenses. These were not produced until flint glasses, having a lower refractive index than the crown glasses, had become available so that an achromatic combination could be made with a negative lens of low index and a positive lens of high index. This effectively reduced the Petzval curvature to manageable proportions. In the electron lens, in order to flatten the field, it becomes necessary to have the negative refracting surfaces at the low-potential side of the field and the positive surfaces at the high-potential side. Unfortunately, when this is attempted three other troubles arise. In the first place the electrons tend to diverge and may fail altogether to get through the lens; if they do succeed in getting through, the amount of distortion introduced will be very large. Secondly, the power of the lens system is reduced and it may be very difficult to focus an image at a reasonable distance along the tube. Thirdly, the system tends to become a kind of immersion telephoto lens, in which the two principal planes are close to the object plane and the two nodal points are close to the image plane. When this occurs the size of the image is small compared to the object, unless the system is lengthened to unmanageable proportions to provide a long image-distance.

The position is to some extent retrieved by the large difference in refractive index at the object plane as compared with the image plane. This is admittedly the origin of the whole trouble, but it also means that a comparatively small curvature of the cathode surface will compensate for a very much larger curvature in the image space. In the case of a curved cathode the glass-optical designer is left with the problem of forming a sharp image on the hollow field which the curved cathode surface will present to a glass lens used to focus an image of a scene on the cathode.

§ 7. AN EXPERIMENTAL METHOD USING PEPPERPOT-DIAPHRAGM, SLIDING TARGET AND MICROSCOPE. THE ELECTRON SOURCES

To trace the path of actual electron beams through an electron lens a number of fine pencils has to be produced. The path of these pencils has to be observed by means of a sliding fluorescent target. Two different sets of measurements can be taken, the first with strictly parallel beams, and the second with divergent beams corresponding to a finite object-distance.

For the first set of measurements the production of a strictly parallel electron beam of very wide cross section is essential. The voltage of this parallel beam has to

be controllable within a rather wide range in order that it may be possible to investigate the lens at different electron-velocities and at all focusing ratios which are important for practical use. To satisfy all requirements the new electron gun which is shown in figure 6 has been developed. Electrons emitted from the concave cathode *Ca* are focused through the mouth of the accelerating funnel *Fu*. An electron lens between *Fu* and a converger electrode *Cv* reduces the divergence of the beam, and a further lens between *Cv* and the final electrode *Z* refracts the beam, so that the electrons leaving *Z* are parallel. *Z* carries a pepperbox-like diaphragm *Pp*, which is shown in outline in figure 7 *a*. *Pp* contains two or more circles of holes 0·5 mm.

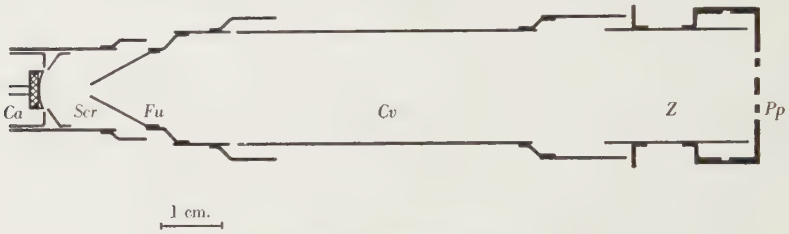

Figure 6. Electron gun.

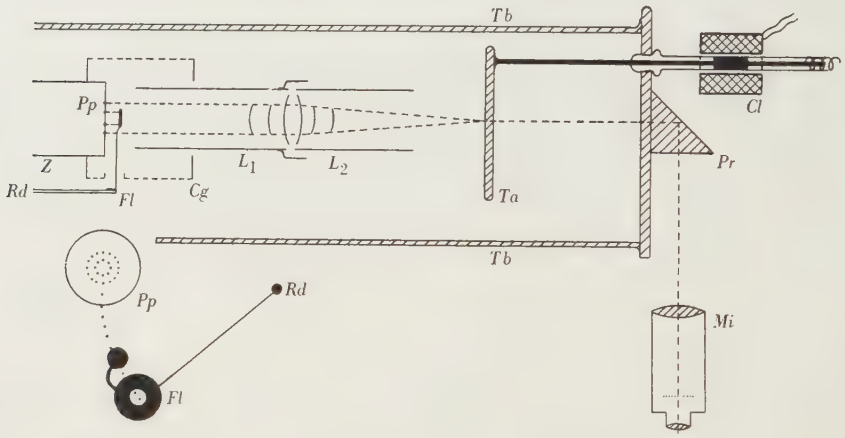

Figure 7 *a*.

Figure 7. Gear for measuring aberrations.

wide, cutting out two circles of pencils from the wide, parallel electron beam. By a movable flap *Fl*, all but one of the circles of holes can be completely covered at a time. *Fl* can be rotated round the axis *Rd*. *Rd* represents a long metal rod sealed in a glass ground joint so that it is movable from outside the vacuum. As shown in figure 7, *Pp* and *F* are electrostatically shielded by the metallic cage *Cg*. Projecting partially into this cage is the lens under investigation, which consists of the two tubes L_1 and L_2. By means of this lens the electrons are focused on the sliding target *Ta* made from glass covered with wire gauze and carrying the fluorescent screen. This target is movable from outside by means of the electromagnetic coil *Cl*, pulling along a small iron bolt inside a glass tube. The focus of the electron pencils on the target is observed from the back, the light being reflected by the rectangular prism

Pr into the measuring microscope *Mi* which has an ocular scale and magnifies about twenty times. The whole apparatus is wrapped in a sheet of 0·25-mm. mumetal.

The actual measurements start with a check of strict parallelism of the test beam. For instance the funnel electrode is kept at 250 v., the converger electrode at 1300 v., and the anode Z at about 4000 v., the latter voltage being however adjusted in such a way that the diameter of the circle of fluorescent spots on the target has exactly the same value as the diameter of holes in the pepperpot lid; this adjustment should be checked for different positions of the target. As the gun cannot be made free of aberration, the voltage of the anode Z required to produce a strictly parallel beam is a function of the radius of the circle of pencils which is employed.

There are two series of parallel beams, with anode-potentials of about 4000 and about 400 v., respectively corresponding to an acceleration or a deceleration of the electrons leaving the converger electrode. The great importance of having strictly parallel beams appears from the following example. Assume a lens free from spherical aberration, with focal length of 20 cm., and assume the divergence of all beams to be $\delta = 0{\cdot}0025$. As a consequence, for the semi-apertures 2 mm. and 4 mm. respectively, wrong focal lengths of 23 cm. and 26 cm. would be found. The parallelism of the beams used here was much better, as δ could be adjusted to be smaller than $\pm 0{\cdot}0005$. With the smallest semi-apertures and the largest focal lengths here used, the maximum error of focal lengths measured would be of the order of ± 2 mm. or about ± 2 per cent. This fits in well with the accuracy of the voltage-measurements. With any cylinder of pencils which are travelling exactly parallel, mid-focal lengths and principal points can readily be measured, as will be explained in the next paragraph. But some precautions might be mentioned here which are necessary in order to obtain reproducible and accurate results. (1) The lengths of the lens tubes should be at least equal to three tube-radii. An investigation in the field-plotting trough showed that the position of the 97·5 per cent equipotential surface changes remarkably with the lengths of the tubes until a distance of $2{\cdot}7R$ is reached. A direct measurement of mid-focal length and spherical aberration made with the electron beam confirmed that the results were exactly identical whether the tubes were 3 or 6 tube-radii long. (2) The gap between the tubes has to be small in comparison with the tube-radius. Identical results were obtained with $\frac{1}{2}$-in. tubes whether the gap was $\frac{1}{2}$ mm. or whether it was 1 mm. wide. (3) The gap between the lens tubes has to be shielded electrostatically. The shield actually used can be seen in figure 7 fixed at the tube L_1. Special experiments were made to study the influence of the position of the shield. It was fixed either at the first or at the second tube of the lens, i.e. either with L_1 or with L_2 in figure 7. It could be proved that mid-focal length and spherical aberration of the lens were independent of this position when the lens was an accelerating one, but that the spherical aberration was slightly larger at the decelerating lens if the shield was connected with L_1, i.e. with the high-voltage side. This difference was very small but was just noticeable at the higher voltage ratios. In the present measurements the shield has been always connected with L_1.

For the second set of measurements, those with divergent beams corresponding

to finite object-distance and image-distance, the development of a point source was necessary. It was found that a concave cathode with funnel-shaped accelerator, as shown in figure 6, emits divergent electrons which generally do not cross over at a common point but give an intersection characterized by some spherical aberration. Systematic experiments showed that this aberration can largely be avoided by choosing the proportionally correct geometric dimensions with respect to the curvature of the cathode, the inclination of the screen, and the distance between cathode and funnel accelerator. In this way was developed a point source producing a circular object of radius $\frac{1}{4}$ mm. nearly homogeneous intensity-distribution over an angle of about 45°, and with no measurable spherical aberration.

§ 8. MEASUREMENTS WITH PARALLEL BEAMS: MID-FOCAL LENGTHS, SPHERICAL ABERRATION, PRINCIPAL POINTS

Measurements on mid-focal lengths as functions of the voltages at the lens tubes could be obtained in the following way. The target *Ta* in figure 7 was placed at any

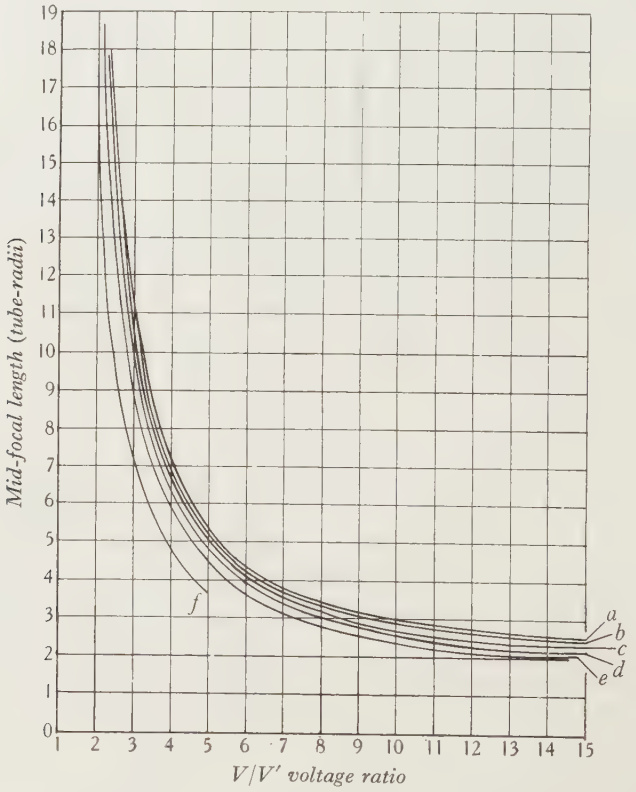

Figure 8. Measurements of spherical aberration. Parallel electrons decelerated. Semi-aperture Y/R of rays: (*a*) 0·08, (*b*) 0·16, (*c*) 0·24, (*d*) 0·32, (*e*) 0·40, (*f*) 0·63.

given position, and the potential of L_2 was changed until a sharp focus appeared at the target. The minimum size of this focus could be recognized in the microscope. Results of such measurements are represented in figure 8 for decelerated parallel

beams and in figure 9 for accelerated parallel beams. The plots show curves of mid-focal lengths ${}_mf'$ against the voltage ratio applied to the tubes, the fixed parameter of each curve being the semi-aperture of the beam, designated in the figure by Y_1R. Experiments proved that ${}_mf'$ was independent of the absolute voltages applied to the tubes, and that the voltage ratio alone was the controlling factor. Moreover, ${}_mf'/R$ was independent of the tube-radius R; thus it can be seen that the curves taken with $\frac{1}{2}$-in. tubes and 1-in. tubes strictly coincide as soon as Y/R, the ratio of semi-aperture and tube-radius, is the same for both. Therefore, in order to obtain mid-focal

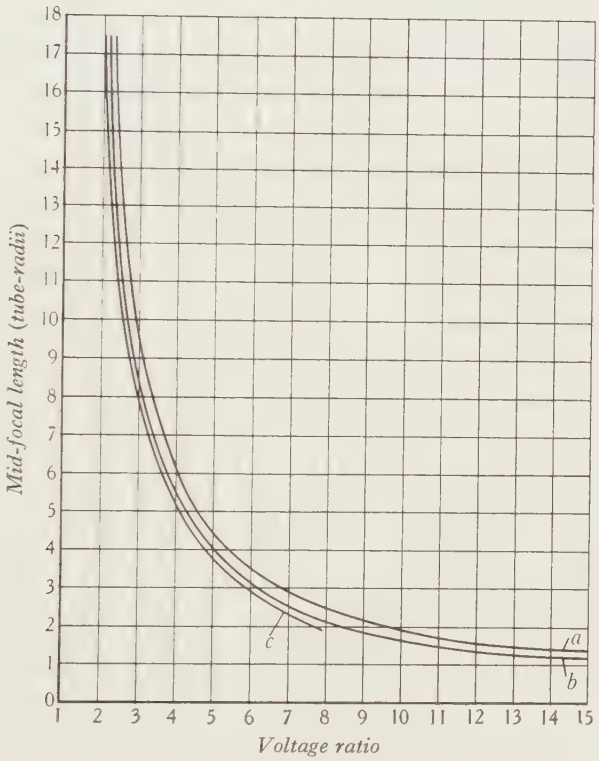

Figure 9. Measurements of spherical aberration. Parallel electrons accelerated. Semi-aperture Y/R of rays: (*a*) 0·16 and 0·32, (*b*) 0·48, (*c*) 0·63.

lengths as a function of the semi-aperture, in many experiments ${}_mf'/R$ was measured with the same diameter of the electron beam but with lens tubes of different sizes.

The method of observing the electron focus directly on the target can be well applied to measure mid-focal lengths between about 20 and 3 tube-radii. Measuring a focus $20R$ distant from the mid plane is already rather difficult, the divergence of the beam becoming very small and the depth of focus considerable, and therefore the accuracy is not good for mid-focal lengths which are too long. On the other hand, for reasons already explained, the lens tubes have to be at least 3 tube-radii long and the sliding target should not be moved inside the tube since it would then modify the field-distribution. However, mid-focal lengths shorter than $3R$ can be

traced in the following way, which is shown in figure 10. The radii of the circles of fluorescent spots $y_1, y_2, y_3, \ldots$ are measured at several positions of the sliding target $x_1, x_2, x_3, \ldots$. The straight path of the beam can therefore be traced outside the lens tube, and the focus of the beams F' which occurs inside the tube can be extrapolated. In this way mid-focal lengths and spherical aberration were measured between 1 and 3 tube-radii. Of course the foci extrapolated in this way do not coincide with the actual intersection of the beams with the axis, as the electrostatic field after the intersection acts on the beam so as to make it more divergent in the accelerating case and more convergent in the decelerating case. Therefore the actual cross-over F_0' would be closer to the mid plane in the accelerating case and farther away in the decelerating case than the extrapolated focus F' of figure 10.

There is only one particular case where the intersection F_0' can actually be located, and that is when it falls just in the mid plane. In this case, the second lens tube can be dispensed with, and the mid plane of the lens can be replaced by the

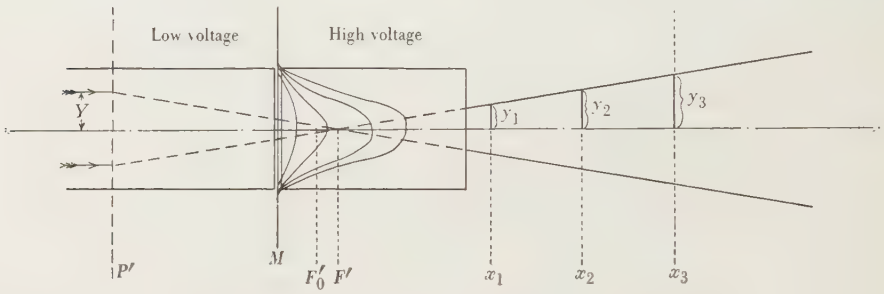

Figure 10. Measurement of very short mid-focal lengths.

sliding target. From reasons of symmetry, the voltage-difference between the first lens tube and the mid plane is always equal to the voltage-difference between the mid plane and the second tube. Therefore one can find out the voltage ratio of the two-tube lens at which the actual intersection occurs in the mid plane, by measuring the voltage at the sliding target when the beam is focused on it. This particular voltage ratio of the two-tube lens, where the originally parallel beam crosses over in the mid plane, was found to be 70.

The results on extrapolated mid-focal lengths are plotted together with the other results in figures 8 and 9. The accelerating lens, figure 9, appears to be better corrected than the decelerating one, figure 8, for with the accelerating lens the mid-focal lengths for any given voltage ratio seem to coincide up to a semi-aperture Y of at least $0{\cdot}32R$, whereas in the decelerating lens there is already a just observable difference of mid-focal length for semi-apertures $0{\cdot}08R$ and $0{\cdot}16R$. Results may be judged more easily if they are plotted as shown in figures 11 and 12. There, mid-focal lengths are plotted against semi-apertures, the fixed parameter for any curve being the voltage ratio. It appears that all accelerating lenses are corrected up to nearly 0·4 tube-radii, whereas the decelerating lenses have rather large aberrations over the whole range of values.

Although all the measurements are performed with as high an accuracy as possible, the results, more especially those for the paraxial beams, tend to give too short a mid-focal length. This follows from the fact that in an actual experiment both the holes in the pepperpot-diaphragm and the original source of electrons are of finite size. When the pencils are focused on the target by controlling the voltage of the lens tubes, adjustment is made for the smallest possible circle of confusion. It can be shown quite easily that, if the lens suffers from positive spherical aberration, with pencils of finite aperture the disc of least confusion will lie nearer the

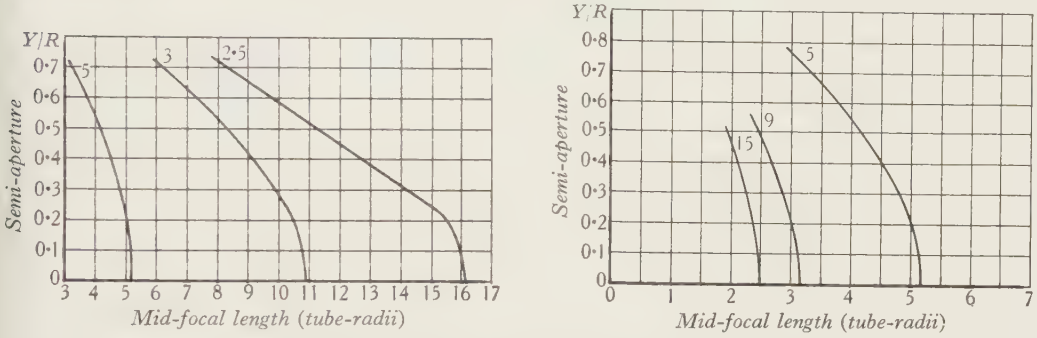

Figure 11. Aberration curves for parallel electrons decelerated. The figures on the curves indicate the appropriate voltage ratios.

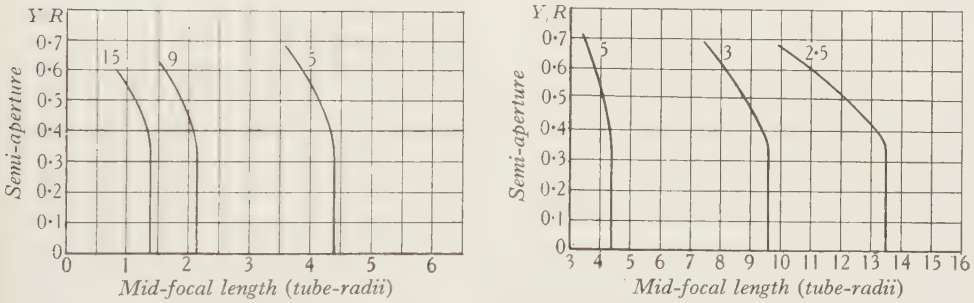

Figure 12. Aberration curves for parallel electrons accelerated. The figures on the curves indicate the appropriate voltage ratios.

lens than the true focus. Hence the aberration curves shown in figures 11 and 12 may be slightly erroneous, and experiments made with apparatus having a higher resolving power might be expected to show slightly more aberration than is indicated in these diagrams.

The measurements of real focal length and of principal points were made in the following way, as illustrated in figure 13. L_1 and L_2 represent the two tubes forming the electron lens with the mid plane M. A bundle of electron pencils El forms a hollow cylinder with the radius Y, which is produced by the gun with the pepper-box lid, figures 6 and 7. This bundle enters the lens and is refracted through the focal point F'. The voltages at the lens tubes are kept as constant as possible during the whole measurement. The sliding target is put into the positions $X_1, X_2, X_3, \ldots$

and the corresponding radii of the circles of dots are measured as semi-apertures of the beam $y_1, y_2, y_3, \ldots$. In order to obtain sufficient accuracy for each principal-plane measurement, about five different readings of x and y are found to be necessary. The divergence of the beam is obtained as the average of $y_1/X_1F', y_2/X_2F', \ldots$. The position of the focus F', which is needed in order to obtain the denominator XF', can be measured in principle as the interpolated position of the sliding target where the beam is crossing over and shows a minimum cross section. However, better results are obtained if F' is taken from the graphs of figures 8 and 9, which give ${}_mf' = MF'$ with highest accuracy.

The measured divergence y/XF' is equal to Y/f_0', where Y is the radius of the circle of holes in the pepperbox lid, which is known, and f_0' is the projection of f' on the axis, f' being the real focal length of the lens for the zone of radius Y and equal to $\sqrt{(Y^2+f_0'^2)}$. In figure 13 the lower part of the diagram shows f_0' equal to $F'P'$,

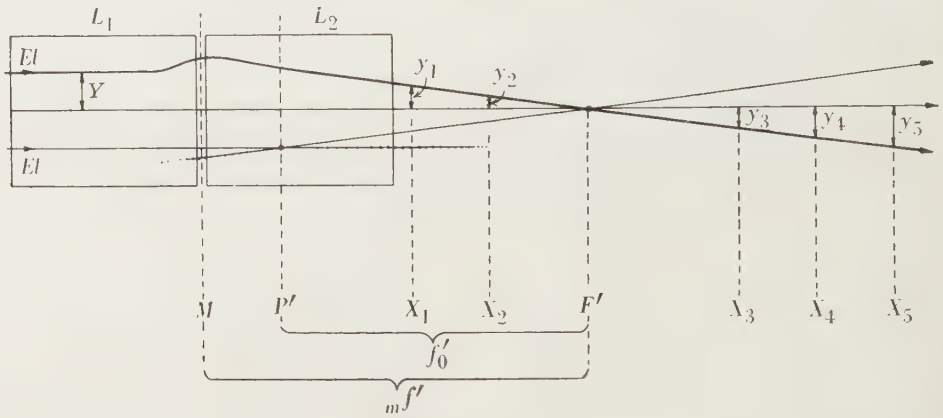

Figure 13. Measurement of principal plane.

where P', the principal plane, is seen to be defined as the plane where the entering and the leaving rays intersect. The upper part of the diagram illustrates the actual path of the beam, which is assumed to be decelerated in the given example. The originally parallel beam diverges when leaving the first tube and becomes convergent in the second tube. Therefore it is obvious that the principal plane should lie in the second tube.

The results of the actual measurements are plotted in figure 14 as crosses. As a rather surprising result it appears that the curves representing the distance between mid plane and principal planes as a function of the voltage ratio are parallel to the voltage axis over a very long range. Therefore the position of the principal points depends very little on the voltage ratio.

An attempt has been made to measure the points of intersection between the focused beams and the corresponding parallel incident beams of different semi-aperture, in order to define the principal surface. A knowledge of the shape of the principal surface might give interesting information on the coma of the lens. According to the sine condition for a coma-free lens the real focal length should be

constant. For a lens without spherical aberration the principal surface should be a sphere with the radius f'. In the case where spherical aberration is present, the coma would be obtained by subtracting the spherical aberration from the focal length along the various rays. However, the experimental accuracy is not yet good enough, as the location of the points of intersection for beams of different apertures lie within the range of fluctuation of the results.

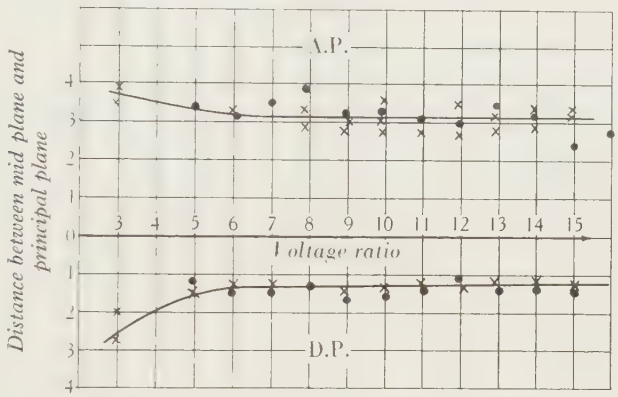

Figure 14. Positions of principal points.

§ 9. MEASUREMENTS OF PRINCIPAL POINTS WITH DIVERGENT BEAMS

The investigations described as having been made with parallel beams can be made with divergent beams also. The aberration results may be expected to lie somewhere between the values for parallel beams in each direction. As the results have no fundamental novelty, we have refrained from reporting them. On the other hand, it is interesting to compare the location of the principal planes by means of divergent beams with the results obtained with parallel beams. For this purpose the divergence δ of the beam at the object side and δ' at the image side have to be measured. We obtain the two focal lengths from Lagrange's equation

$$\delta \times I \times N = \delta' \times I' \times N'$$

by replacing the ratio I/I' of object-size to image-size by the ratio of the distances of the object and the principal plane P from the focus F, according to the relation

$$I/I' = \frac{\mathrm{IF}}{\mathrm{FP}},$$

and replacing the refractive indices N by the square roots of voltage V, thus

$$\mathrm{F'P'} = \frac{\delta'}{\delta}\sqrt{\frac{V'}{V}} \times \mathrm{I'F'},$$

$$\mathrm{FP} = \frac{\delta}{\delta'}\sqrt{\frac{V}{V'}} \times \mathrm{IF}.$$

The position of the focus F′ is known from curves of the kind shown in figures 8 and 9, and the positions of the object I and the image I′ can be measured. One obtains a new set of results for the location of the principal planes, plotted in figure 14 as solid dots. The results confirm, within the limits of the errors of measurement, those obtained by the parallel-beam method, which have been plotted in the same figure as crosses.

§ 10. COMPARISON BETWEEN TRIGONOMETRICAL AND EXPERIMENTAL METHODS

We do not propose to discuss the relative merits of the different lenses that have been investigated. Those concerned with the actual problem of electron-lens design will be able to utilize the data we have given to test the magnitude of the aberrations for any particular case in which they are interested. We would, however, point out that the aberration curves cannot be directly compared to deduce the state of correction for the different focusing ratios. Those familiar with ordinary optical problems will appreciate that the linear aberration is not necessarily a direct measure of the seriousness of the defect; the aberration has to be estimated in relation to the focal length and aperture of the system, the conjugate distances of object and image, and so on.

One obvious point of interest is the comparison between the experimental and the trigonometrical results. So far as the position of the Gaussian points is concerned, the agreement between table 2 and the data of figures 11 and 12 is on the whole quite good.

It is of a different order from the very close agreement found in the corresponding tests in glass optics, but that is to be expected. As has been suggested earlier, the values of the mid-focal length extrapolated from the electronic measurements shown in figures 11 and 12 are likely to be smaller than those obtained by trigonometrical ray-tracing, and the latter should, therefore, be closer to the true values. Comparing the aberration curves shown in figure 4*b* with those shown in figures 11 and 12, the agreement is almost better than could be expected and is, in fact, rather better than in the case of the other lenses. In addition to the agreement between particular curves, both methods show that the decelerating lens has less aberration than the accelerating lens of the same focusing ratio, and that lenses with smaller focusing ratios have greater aberration.

The trigonometrical results obviously cannot be applied over large apertures because they are based on the assumption, which is only approximately valid, that the refracting surfaces are spherical. For wide-aperture beams, the experimental ray-tracing obviously gives the more useful results. For small apertures, on the other hand, it is likely that the trigonometrical method may be the more valuable in cases where small amounts of aberration are important. For the construction of most electron guns, the aberration found in the accelerating lens is negligible up to a semi-aperture of about 0·3 tube-radii; in fact, experimentally, little aberration was observed. Probably a little aberration exists even for very small apertures, but is less than the experimental error of the observations; the accuracy of measurement inevitably falls off at small apertures because of the small inclination of the electron

beams to the axis, and the consequent difficulty of locating their intersections with the axis. It is, moreover, impossible to determine the axial focus at all by direct observation. As this is precisely the region in which the trigonometrical method is most reliable, it is likely that where high resolution is being sought after, as in the electron microscope, and where the use of wide-aperture beams is not necessarily required, the method will find its most useful field of application.

§ 11. ACKNOWLEDGEMENTS

The research was carried out in the Laboratories of the Electric and Musical Industries Ltd., and acknowledgements are due to Mr I. Shoenberg, Director of Research and to Mr G. E. Condliffe and the staff of the Research Department.

We are especially indebted to Mr G. E. Waters for his careful and precise measurements with the electron-tracing apparatus, and to Mr G. C. Newton for his assistance with the trigonometrical work.

We should also like to thank Dr Ruth Lang for her help with the ray-tracing calculations.

NOTE ADDED IN PROOF

While this paper was in the press, an article by L. Jacob[12] was published on "Field distribution and graphical ray tracing in electron optical systems". Jacob used a subdivision of the field into a number of finite steps, but traced the electron paths by a graphical method of applying the law of refraction. We referred in § 2 to the inaccuracies inherent in graphical methods of ray-tracing, but in spite of these Jacob concluded that the results were considerably more accurate than those obtained by the method developed by Maloff and Epstein[6], a method using the axial potential distribution and its derivatives which he also tested. This conclusion provides further justification for our belief in the value of the purely trigonometrical method, especially in deriving the optical constants of any electron lens. An abstract of our paper was first published in March 1938[13].

REFERENCES

(1) Brüche, E. and Scherzer, O. *Geometrische Elektronenoptik* (Berlin, 1934).
(2) Busch, H. and Brüche, E. *Beiträge zur Elektronenoptik* (Berlin, 1937).
(3) Epstein, B. W. *Proc. Inst. Radio Engrs, N.Y.*, **34**, 1095 (1936).
(4) Fortescue, C. L. and Farnsworth, S. W. *Proc. Amer. Inst. Elect. Engrs*, **32**, 757 (1913).
(5) McArthur, E. D. *Electronics*, **4**, 192 (1932).
(6) Maloff, I. G. and Epstein, D. W. *Proc. Inst. Radio Engrs, N.Y.*, **22**, 1386 (1934).
(7) Gabor, D. *Nature, Lond.*, **139**, 373 (1937).
(8) Langmuir, D. B. *Nature, Lond.*, **139**, 1066 (1937).
(9) Conrady, A. E. *Applied Optics and Optical Design* (Oxford Univ. Press, 1929).
(10) Steinheil, A. and Voit, E. *Applied Optics* (London, 1918).
(11) Hartmann, J. *Z. InstrumKde*, **24**, 1 (1904).
(12) Jacob, L. *Phil. Mag.* **26**, 570 (1938).
(13) Klemperer, O. and Wright, W. D. *Proc. Roy. Soc.* A, **166**, 58 (1938).

DISCUSSION

(*See page* 376.)

THE ADSORPTION OF OXYGEN AND HYDROGEN ON PLATINUM AND THE REMOVAL OF THESE GASES BY POSITIVE-ION BOMBARDMENT

By C. W. OATLEY
University of London, King's College

Received 11 *October* 1938. *Read in title* 20 *December* 1938

ABSTRACT. An account is given of the results of measurements of the contact potential-difference between a tungsten filament and a platinum anode after the latter has been subjected to various treatments. It is shown that a clean platinum surface can be obtained by successive bombardments of the anode with positive ions of oxygen and of argon. The work function of a surface so prepared is found to be in good agreement with the most recent values obtained by thermionic measurements on clean platinum. Values are obtained also for the work functions of oxygen on platinum, hydrogen on platinum, and mixed layers of oxygen and hydrogen on platinum. The bearing of these results on the structure of the mixed layers is discussed.

§ 1. INTRODUCTION

The thermionic and photoelectric properties of a metal are governed to a great extent by the value of its work function, and the determination of this quantity is therefore of considerable intrinsic importance. Furthermore, the value of the work function is particularly sensitive to the presence on the surface of the metal of adsorbed films of other substances, and studies of the variation of the work function with changing conditions have, in the past, provided valuable information concerning the properties of such films. The application of this method of investigation clearly requires a knowledge of the work function of the clean metal and, on account of the difficulty of removing adsorbed films, this knowledge has been obtained with certainty only for comparatively few metals.

The usual method of obtaining a clean surface is to subject the metal to a prolonged heating in a good vacuum, or to form a new surface by distilling some of the metal on to an electrode which is generally made of another metal of higher melting point. While these methods have proved very satisfactory in some cases, in others they are either inapplicable or are so laborious that the further study of adsorbed films after the metal has been cleaned is extremely difficult. It has often been suggested that metal surfaces might be cleaned by bombardment with positive ions of some gas which, itself, is not adsorbed. This method, if successful, could be used in many cases where heating cannot be employed, and would thus open up several new fields of investigation.

In order to test this new method, it is desirable to experiment with some metal whose work function is already accurately known, and the test will be all the

more severe if, in addition, the metal is difficult to clean by the ordinary process of heat treatment. These conditions are fulfilled by platinum, for there is every reason to believe that the most recent values of the work function of this metal are substantially correct. At the same time the latest investigations have shown that, when platinum is cleaned by heat treatment alone, adsorbed films persist unless the temperature is raised to within some 30° C. of the melting point.

The experiments described below were carried out to investigate the possibilities of removing adsorbed films from a platinum surface by bombardment with positive ions of argon. This gas was chosen because it was less likely to be adsorbed than most others and also because the work of Langmuir and Kingdon[1] had shown positive ions of argon to be particularly effective in removing a monomolecular layer of thorium from the surface of a tungsten filament.

Thermionic measurements of the work function were unsuitable in the present experiments because the necessarily high temperature of the platinum would have caused diffusion of gaseous impurities from the interior of the metal to the surface, and it would thus have been very difficult to interpret results obtained by this method. The work function might have been determined from photoelectric measurements, but it was considered simpler to measure the contact potential-difference V_c between the cold platinum surface and a hot tungsten filament and then to calculate the work function ϕ_A from the equation

$$V_c e = \phi_W - \phi_A, \qquad \ldots\ldots(1)$$

where ϕ_W is the work function of tungsten at the temperature of the filament and e the electronic charge. V_c is to be taken as positive when the platinum surface is positive with respect to the tungsten. A further advantage of this method is that the resulting value of the work function is affected far less by traces of electro-positive contamination on the platinum surface than it would have been had the photoelectric method been used.

In a recent paper[2] I have described a new method of measuring contact potential-differences which involves the determination of the velocity acquired by electrons which pass from a straight tungsten filament to a coaxial cylindrical anode made of the metal under investigation. The determination is carried out by measuring the magnetic field parallel to the axis of the filament which is just sufficient to reduce the electron current to some specified fraction of its initial value. This method is particularly suitable for determining the absolute value of the work function of a surface and was therefore used in the present experiments.

As will be seen later, bombardment with positive ions of argon proves to be a most effective method of removing adsorbed gases from a platinum surface. Despite this fact, however, bombardment frequently does not result in the production of a clean surface, because gas diffuses from the interior of the metal and replaces the adsorbed surface atoms as fast as these are removed by the argon ions. Since different gases diffuse through platinum at very different rates, the importance of the above effect depends on the nature of the gas and, in particular, is very much greater for hydrogen than it is for oxygen. In order to obtain further information

on this matter, a series of experiments was carried out in which an adsorbed layer of oxygen or of hydrogen was first formed on platinum and an attempt was then made to clean the platinum by bombardment with positive ions of argon. As a result of these experiments, it was found possible to adopt a procedure which prevents diffusion of gas from the interior to the surface and, when this was done, subsequent bombardment with argon ions produced a clean platinum surface. During the course of this investigation, values were obtained for the work functions of oxygen on platinum and hydrogen on platinum respectively.

§ 2. APPARATUS

The apparatus was essentially the same as that described in the previous paper[2], but the design was modified to enable the electrodes to be given a much more thorough outgassing than had previously been possible. The general electrode assembly is shown in figure 1. With the exception of the platinum anode *A*, the platinum support wire *G*, the tungsten filament *BB* and the tungsten

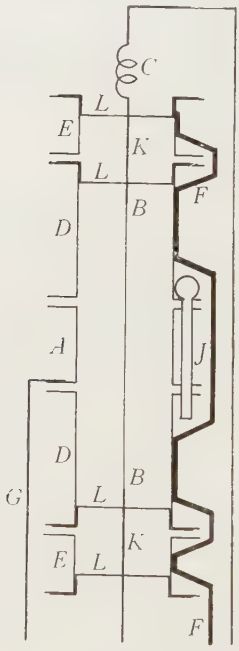

Figure 1.

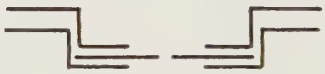

Figure 2.

spring *C*, all the metal parts were made of constantan. The four flanged cylinders *D*, *D*, *E*, *E*, were fastened together by four bent supporting wires, of which only one, *FF*, is shown. To ensure that the cylinders should be mounted coaxially, they were placed in position on a closely fitting machined copper rod which formed one electrode of the spot welder with which the joints to the supports were made. The anode *A* was 1·74 cm. in diameter and 1·3 cm. long. It was constructed from pure platinum sheet 0·013 cm. thick, and was kept in position by three silica pins,

one of which is shown at *J*. These pins, which were about 0·2 cm. in diameter, passed through holes in the flanges attached to *A* and to the nearer ends of the guard rings *D*, *D*. The filament *BB* was welded to wires *K*, *K* which were kept in an axial position by the plates *L*, *L*, *L*, *L* attached to the cylinders. The detailed construction of one of these plates is shown in figure 2. Each consisted of two thin plates of constantan with central holes about 0·5 cm. in diameter, which fitted one inside the other. Between them was clamped a circular disc of mica and, when the component parts had been tightly pressed together, the flanges of the metal plates were welded to each other. Finally, a central hole, just large enough to allow passage of the filament-supports, was punched in the mica. By using suitable jigs in the construction of the apparatus, it was possible to ensure accurate fitting of the various parts, and it is probable that in the final assembly the filament and anode were coaxial to within one or two tenths of a millimetre.

The whole electrode system was cleaned with carbon tetrachloride in order to remove grease, and all metal parts were vacuum-furnaced at bright red heat for several hours. The apparatus was then mounted in a pyrex tube, the connecting leads being taken out through tungsten seals, and the tube was attached to a vacuum system consisting of a liquid-air trap, mercury cut-off, McLeod gauge, mercury diffusion pump, and rotary oil pump. When necessary, hydrogen was admitted to the system through a palladium tube, while oxygen could be produced by gently warming a side tube containing crystals of potassium permanganate. Argon was contained in a glass cylinder connected to the vacuum system through two taps. This gas was supplied commercially and was reputed to be spectroscopically pure.

To avoid the effects of potential-drop due to the filament-heating current, a rotating commutator was used to make and break this current 50 times per second and to isolate the anode during the periods when the filament current was flowing. The mean anode current was usually about 2 microamperes and was measured with a reflecting galvanometer. Anode potentials varying between 0 and 10 volts were used, and these, as well as the currents flowing through the Helmholtz coils which surrounded the tube, were measured on a Crompton potentiometer.

§ 3. EXPERIMENTAL PROCEDURE

Before any measurements were made, the experimental tube, liquid-air trap and connecting tube were baked out at 480° C. for about one hour. All the electrodes were then heated to bright redness by eddy currents. This process was repeated from time to time during the course of the experiments when it seemed desirable. From the nature of the work measurements of contact potential-difference were necessarily made immediately after gas had been present in the system to a pressure of at least 0·1 mm. of mercury. When this gas had been pumped off, no attempt could be made to remove adsorbed gas from the walls of the apparatus because any such attempt might have resulted in contamination of the anode surface. During a run, therefore, a continual slow evolution of gas from the walls must have been taking place. An estimate of the magnitude of this effect

was made by raising the mercury cut-off and so isolating the system from the pump. At the end of 5 min. the pressure was still too low for accurate measurement on the McLeod gauge, but was in the neighbourhood of 3×10^{-6} mm. of mercury. It seems safe to conclude therefore, that, while the pump was running, the pressure in the system was always well below 10^{-6} mm. of mercury. Furthermore, the results of the measurements of contact potential-difference showed that this pressure was sufficiently low to prevent appreciable contamination of the anode surface during the time taken to make a measurement.

At the beginning of the experiments the filament was aged for several hours at about 2200° C. with occasional short flashings at 2900° C. After this treatment the electron-emission was steady and repeatable. The procedure in determining the work function of the anode surface was as follows. A known potential-difference V_a was applied between anode and filament, and the corresponding anode current i_a was observed. The current through the Helmholtz coils was then switched on and a measurement was made of the value i_H which caused a reduction of the anode current to one-half of its previous value. The current through the Helmholtz coils was then reversed and a second value of i_H was obtained. By taking the mean of these two values the effect of the earth's magnetic field was eliminated. The relation between i_H and V_a is given by[2]

$$V_a + V_c + V_T = eR^2p^2i_H^2\,8m, \qquad \text{.....(2)}$$

where V_c is the contact potential-difference between filament and anode, V_T a correction for the initial velocities of the electrons, R the radius of the anode, p the magnetic field produced by unit current in the Helmholtz coils, and e and m the charge and mass respectively of an electron. When, therefore, the observed values of i_H^2 are plotted against V_a, a straight-line graph is obtained which has a slope equal to $8m/eR^2p^2$ and an intercept on the axis of V_a equal to $-(V_c + V_T)$. As was shown in the previous paper[2], V_T can be calculated from a knowledge of the filament temperature, so that V_c can be obtained from the intercept. The value of ϕ_A then follows from equation (1), since ϕ_W is known. In practice, since the linear relation between i_H^2 and V_a had previously been accurately verified, it was unnecessary to take a series of readings of these quantities, and the intercept was often obtained from a pair of points on the graph, though readings were sometimes taken for three or four points.

When it was desired to bombard the anode with positive ions, gas was admitted to the system and the anode was connected to the negative terminal of a high-tension unit through a resistance of about 30,000 ohms. The positive terminal was joined to the filament. Bombardment of the guard rings might have resulted in the sputtering of some metal from them on to the anode, so they also were joined to the positive terminal of the supply unit. It was found convenient to use a discharge current of about 1 ma. with 1000 v. across the tube, and the gas pressure necessary to secure these conditions was about 0·1 mm. of mercury. Each discharge was continued for a period which varied from a few minutes to one hour, an average discharge lasting about 10 min.

§ 4. PRELIMINARY EXPERIMENTS

The method of calculating the correction term V_T to allow for the initial velocities of the electrons was discussed in the previous paper[2], where curves were given showing how the value of V_T depends upon the temperature of the filament and on the fractional reduction of anode current which occurs when the magnetic field is switched on. As a check on the accuracy of these curves, the contact potential-difference between filament and anode was measured three times, the anode currents being reduced to two-thirds, one-half and one-third of their initial values respectively in the three experiments. The calculated values of V_T for these three cases were 0·13, 0·21 and 0·31 v. respectively, and with these values the measured contact potential-differences were 0·10, 0·07 and 0·07 v. In this particular instance the contact potential-difference happened to be very small and, in consequence, there was a rather large percentage difference between the three values obtained for it. However, the contact potential-difference itself is of interest only in so far as it enables us to calculate from equation (1) the work function of the anode. Since this work function will always be several electron-volts in magnitude, the 0·02 v. by which the above three values differ from their mean is of no account and is, in fact, within the limits of experimental error. In general, reduction of the anode current to half-value is best because this gives the most sensitive setting of i_H.

When the apparatus was designed, it was erroneously assumed that any difference in contact potential between the anode and the guard rings, owing to the fact that these electrodes were made of different metals, would have a negligible effect on the results obtained with the apparatus. However, preliminary experiments showed that this was not the case and the problem was therefore investigated more fully. It was then found that no allowance need be made for the effect so long as the slope of the $\{i_H^2, V_a\}$ curve does not differ by more than 2 or 3 per cent from the theoretical value calculated from the constants of the apparatus. An abnormally high slope indicates that the anode is effectively positive with respect to the guard rings, and in such cases the difficulty can be overcome by applying to the guard rings a potential 1 or 2 v. above that of the anode.*

* Detailed consideration of the effect of a small difference of potential between anode and guard rings on the distribution of current between these two electrodes leads to the conclusion that, so long as the anode is negative with respect to the guard rings, the values of i_H required to reduce the anode current to half-value will be the same as if anode and guard rings were at the same potential. On the other hand, when the anode is positive with respect to the guard rings the values of i_H will be affected and, under these conditions, the slope of the $\{i_H^2, V_a\}$ curve will be abnormal; that is to say it will differ from the theoretical value deduced from equation (2).

The theoretical slope was calculated from the constants of the apparatus and a series of experiments was carried out in which readings of i_H and V_a were taken when the potential applied to the guard rings differed from that applied to the anode by various definite amounts. The results of these experiments were entirely in accordance with the above conclusions and showed that the slope of the $\{i_H^2, V_a\}$ curve is, in fact, a very sensitive indicator of the relative effective potentials of anode and guard rings. They showed, moreover, that when the anode is negative with respect to the guard rings, the intercept of the $\{i_H^2, V_a\}$ curve is not affected by this difference of potential even when it amounts to some 2 or 3 v.

§ 5. RESULTS

For a proper understanding of the results set out below, it must be realized that bombardment of a metal with positive ions affects only those atomic layers of the metal which lie close to the surface. Since, in the present experiments, it was impossible to heat the anode to a sufficiently high temperature to rid it of all occluded impurities, contamination was certainly present in the interior of the metal, even when the surface was clean. Of the possible contaminants the most important is hydrogen, on account of the ease with which it diffuses through platinum. Hydrogen was certainly present in the anode during all of the experiments which were carried out after this gas had been admitted to the tube, and the results suggest that it was also present to a less extent when the electrodes were first mounted in the tube. It was found that under certain conditions the formation of a surface film as a result of the diffusion of hydrogen from the interior was quite rapid even at room temperature, and thus the success of any attempt to clean the surface depended to a considerable extent on the previous history of the anode. For this reason, before dealing with the production of a clean surface, it is convenient to describe the results obtained when the surface was purposely covered with a complete film of either oxygen or hydrogen.

In all the experiments the filament was run at a temperature of about 1900° K. In accordance with the work of Riemann[3] the work function of tungsten at this temperature may be calculated from its known electron-emission by assuming a surface-roughness factor of 1·3 and a transmission coefficient of unity. In this way ϕ_W is found to be 4·67 ev. The filament was always flashed at 2600° K. before any readings were taken and, throughout the experiments, there was no evidence of any subsequent contamination. At 1900° K. the correction V_T for initial velocities is 0·20 v. and, to avoid confusion, the results are given directly in terms of the work function of the anode surface.

Oxygen on platinum. After the anode had been standing in contact with hydrogen, diffusion of this gas from the interior to the surface was so rapid that, even if oxygen was admitted to the system as soon as possible after the surface had been cleaned by an argon discharge, a complete film of oxygen could never be obtained. It was therefore necessary to adopt some alternative procedure, and the most convenient method was to bombard the anode with positive ions of oxygen. When this was done, a surface was eventually formed which was stable and reproducible. This surface was independent of the previous history of the anode and was not affected by standing in oxygen or by further discharges in oxygen. Values for the work function of such a surface, obtained on different occasions after the anode had been subjected to various intermediate treatments, were 6·51, 6·55, 6·55, 6·52 and 6·58 ev., giving as the mean value for oxygen on platinum, 6·55 ev.

Hydrogen on platinum. A hydrogen on platinum surface was formed most conveniently by running a discharge with a mixture of argon and hydrogen in the tube. This method was preferred to the use of a discharge with hydrogen alone, since this gas is known to be inefficient as a sputtering agent, and bombardment

with positive ions of hydrogen might not have removed traces of other gases, such as oxygen, from the platinum surface. In one or two instances the same final surface was obtained by cleaning the platinum by bombardment with positive ions of argon and then admitting hydrogen to the tube as soon as the argon had been withdrawn. In this case, of course, diffusion of hydrogen from the interior did not matter. The surface formed by either of these two methods was independent of the previous history of the anode, could be repeated at will, and was not affected by running a discharge with pure hydrogen in the tube. Values of the work function of such surfaces, formed at different times, were 4·25, 4·15, 4·24, 4·21 and 4·22 ev., giving as the mean value for hydrogen on platinum, 4·21 ev.

Clean platinum surfaces. When the anode had been standing in contact with hydrogen, attempts to clean it by bombardment with argon ions were always unsuccessful. Readings taken as soon as possible after the discharge sometimes gave values for the work function approaching that for a clean platinum surface, but there was always a drift towards the value for hydrogen on platinum, and this drift was often quite rapid. An attempt was made to reduce the concentration of hydrogen in the metal by simultaneous eddy-current heating and bombardment, but this only served to decrease the subsequent rate of drift of the work function towards the value for hydrogen on platinum.

On the other hand, if an oxygen film had previously been formed on the platinum by bombardment with positive ions of oxygen, it was found possible to remove this film by bombardment with argon ions, and the surface then formed was quite stable and was unaffected by further moderate bombardment with argon ions. For reasons to be discussed later this surface was taken to be clean platinum, and values for its work function, obtained at different times, were 5·39, 5·41, 5·34, 5·40 and 5·24 ev., giving as the mean value for clean platinum, 5·36 ev. When a surface formed in this way was subjected to a sufficiently long discharge in argon, the effects of diffusion of hydrogen once again became noticeable.

Mixed films on platinum. It had been intended to make observations on various mixed gaseous films on platinum, but the premature failure of the apparatus during a period of too severe eddy-current heating terminated these experiments. The results given below are however of considerable interest, though too much weight must not be attached to them until they have been confirmed.

A hydrogen on platinum surface was prepared in the usual way, and was then allowed to stand in contact with oxygen at a pressure of a few millimetres of mercury. After 5 min. the work function had not changed appreciably, so oxygen was again admitted to the apparatus and left for 3 hr. The work function had then risen to 5·25 ev. After a further 15 hr., during which, however, liquid air had been removed from the trap so that traces of other gases were present, the work function was found to be 5·37 ev.

An oxygen on platinum surface was formed and then exposed for about 15 hr. to hydrogen at a pressure of a few millimetres of mercury. Once again liquid air was not used. The final value of the work function was 5·37 ev., that is, almost exactly the same as when the gases were used in the reverse order.

§6. DISCUSSION OF RESULTS

In the above work certain assumptions have been made. Thus, in equation (1) a term due to the Peltier effect is omitted. Its inclusion could hardly have affected the results by an amount exceeding the unavoidable experimental error. Again, it has been assumed throughout that there were no effects due to adsorption of argon. This seems justifiable, since numerous workers in this field have shown that adsorption of argon is always of the reversible Van der Waals type and, furthermore, that even this adsorption is extremely small at room temperature. Throughout the present experiments no effects were noticed which could reasonably be attributed to adsorption of argon.

One of the most interesting of the results is the unexpected stability of the surface when an oxygen layer, formed by exposing the anode to an oxygen discharge, is subsequently removed by bombardment with positive ions of argon.

It is known that large quantities of gas can be absorbed by the cathode in an electric discharge. Thus, when a platinum surface is bombarded with positive ions of oxygen a considerable quantity of this gas will accumulate in the layers near the surface, and since the diffusion of oxygen through platinum is extremely slow at room temperature the accumulation will persist for long periods after the discharge has ceased. It seems very probable that the presence of these oxygen atoms or ions will hinder the diffusion of hydrogen through the platinum and we make the assumption that, in fact, hydrogen is unable to pass through those parts of the metal where the concentration of oxygen is high. Since there is good reason to believe that hydrogen diffuses not only along the grain-boundaries but also through the lattice itself, the hypothesis involves the assumption that the oxygen ions themselves occupy positions within the lattice.

Consider now the effect of bombarding with oxygen ions an anode which has hydrogen distributed throughout its volume as well as on its surface. Since the oxygen ions are efficient sputtering agents, surface hydrogen atoms will quickly be removed and their places will be taken by oxygen atoms. As the discharge proceeds, a considerable concentration of oxygen will be built up in the layers just below the surface, and it is reasonable to suppose that the hydrogen will be removed from these layers also. Thus, after a time, there will be a complete film of oxygen on the surface and a barrier of the same gas immediately below the surface.

Suppose now that when the anode is in this condition it is bombarded with positive ions of argon. The surface layer and some of the oxygen beneath the surface will be removed, but so long as the oxygen barrier is not completely destroyed no rapid diffusion of hydrogen from the interior can take place. Thus, since any adsorption of argon is completely reversible, a clean platinum surface should be obtained when this gas is finally pumped off. As was recorded above, the work function for a surface prepared in this way was found to be 5·36 ev., and the most direct test of the foregoing hypothesis is to compare this value with that found by other methods. Of the previous determinations we need consider only those due to Van Velzer[4] and Whitney[5]. Both of these experimenters used the

thermionic method and, unlike earlier workers, they obtained values in good agreement with theory for the emission constant A in Richardson's equation. They also showed that the failure of earlier workers to do so was due to insufficient outgassing of the platinum. Their final values for the work function of platinum are 5·29 and 5·32 ev. respectively, and these are in excellent agreement with the value obtained in the present experiments.

Further evidence in favour of the hypothesis is provided by the behaviour of a clean platinum surface, prepared in the manner described, when it is subjected to further prolonged bombardment with positive ions of argon. We should expect that such treatment would eventually remove the barrier of oxygen from the surface layers of the metal, and that diffusion of hydrogen from the interior would then begin once more. This is precisely what was found to occur.

Turning now to the effects on a platinum surface of adsorbed gaseous films, it appears from the above results that oxygen raises the work function by 1·19 ev. while hydrogen lowers it by 1·16 ev., which is nearly the same amount. It is known that when oxygen or hydrogen is adsorbed on tungsten the gas is present in the adsorbed layer in atomic form, with one atom of gas to each surface atom of tungsten. It is reasonable to suppose that this is also the case when either of these gases is adsorbed on platinum, since the adsorption forces are even greater with this metal. We may then regard the change in work function of the surface as being due to a separation of charges within the atoms to form a dipole layer. If, then, V is the change in work function, σ the number of atoms per square centimetre of the surface, and μ the dipole moment of an adsorbed atom,

$$V = 2\pi\sigma\mu \qquad \text{.....(3)}$$

so that our assumption of the equality of σ for the two gases, combined with the experimental fact that they produce equal and opposite changes of work function, leads to the conclusion that the atomic dipole moments themselves are equal and opposite.

This result is very suggestive and throws light on the formation of mixed films of oxygen and hydrogen on platinum. Suppose atoms of each of these gases to be adsorbed on platinum; one very stable arrangement would clearly be that in which the two kinds of atom alternate in a two-dimensional lattice, so that equal numbers of the two kinds are present. Since the dipole moments of oxygen and hydrogen atoms on platinum are opposite in sign, each atom in such an arrangement would be strongly attracted to its immediate neighbours. Furthermore, since the numerical values of the dipole moments are equal, the average moment of the whole film would be zero, so that the work function of such a surface should be the same as that of clean platinum. This, however, is precisely what was found when a film of either oxygen or hydrogen was first formed on platinum and then left in the presence of an excess of the other gas until equilibrium had been attained. It thus seems likely that the equilibrium mixed layer is, in fact, that in which equal numbers of atoms of the two gases are present.

The present experiments do not give any information as to the way in which

the equilibrium mixed film is formed. In considering this question it must be remembered that the method adopted to form a complete surface layer of the first gas was in each case such as to ensure that this gas should also be present in the atomic layers immediately below the surface. When, therefore, this complete surface layer was left in contact with the second gas, there was, in effect, an excess of each gas within reach of the surface. It is probable, therefore, that the equilibrium layer formed under these circumstances is the same as that which would be formed if completely outgassed platinum were exposed to an excess of a mixture of oxygen and hydrogen. It is at least possible that the composition of the final equilibrium-layer would have been different if an excess of the first gas had not been present in the layers below the surface.

Whether or not the two gases combine chemically during the formation of the equilibrium layer, there can be no doubt that the final arrangement of the atoms in the layer is such as to facilitate chemical combination, and it seems more than likely that the catalytic activity of platinum in promoting the combination of oxygen and hydrogen in bulk must be ascribed to this fact.

§ 7. ACKNOWLEDGEMENT

I wish to thank Prof. C. D. Ellis, F.R.S., for the great interest he has taken in the work and for the helpful advice which I have received from him.

REFERENCES

(1) Langmuir, I. and Kingdon, K. H. *Phys. Rev.* **22**, 148 (1923).
(2) Oatley, C. W. *Proc. Roy. Soc.* A, **155**, 218 (1936).
(3) Riemann, A. L. *Proc. Roy. Soc.* A, **163**, 499 (1937).
(4) Van Velzer, H. L. *Phys. Rev.* **44**, 831 (1933).
(5) Whitney, L. V. *Phys. Rev.* **50**, 1154 (1936).

THE BAND SPECTRUM OF ANTIMONY FLUORIDE (SbF)

By H. G. HOWELL, Ph.D., University College, Southampton

AND

G. D. ROCHESTER, Ph.D., University of Manchester

Received 11 *October* 1938. *Read in title* 20 *December* 1938

ABSTRACT. The spectrum of SbF has been produced in active nitrogen and also by means of a high-frequency discharge. It consists of three groups of bands lying in the regions 3600 to 5000, 2600 to 2700, and 2200 to 2430 A. Most of the bands in the first region had already been shown by Rochester to belong to two systems; the remaining bands in this group are here allocated to a third system. As the vibrational constants of these three systems are very nearly the same they are considered to be due to transitions between triplet electronic levels. Similarly, the ultra-violet bands form a triplet system, one component being in the region 2600 to 2700 A. and the other two between 2200 and 2430 A. The final state is common to both triplet systems and is probably $^3\Pi$. The multiplet separations of the states are not known nor is the nature of the other electronic levels. The vibrational constants of all the SbF systems are given in the paper.

§ 1. INTRODUCTION

THE emission spectrum of SbF was obtained independently by the authors in 1935. Rochester[1], using the active-nitrogen method of excitation, found the spectrum to consist of an intense band system in the visible region and a wide system in the ultra-violet region. Howell, using a high-frequency discharge through the vapour of SbF_3, found that the system in the ultra-violet region was well developed but that the visible region of the spectrum was overlaid by a continuum. The bands in the visible region were later allocated by Rochester to two systems A_1 and A_2 having almost the same vibrational constants and two short progressions. It was considered possible that the two fragmentary progressions were parts of a third system A_3, with the same vibrational constants as A_1 and A_2, the whole forming one large triplet system.

The present paper gives an account of new data for the system A_3, and the analysis of the band system in the ultra-violet region.

§ 2. EXPERIMENTAL

The high-frequency discharge was produced in a 30-cm. length of Pyrex tubing 1 cm. in diameter having a quartz window cemented on to one end. External iron electrodes wound round the tube about 5 cm. apart supplied the excitation energy from a $\frac{1}{2}$-kw. oscillator working at a frequency of 10^7 c. sec. SbF_3 was distilled into the discharge tube from a short side limb by utilizing the heat generated by the

discharge. The vapour pressure of SbF_3 was kept low by continuous pumping with a Cenco Hyvac oil pump, a tube containing calcium metal filings and a liquid-air trap preventing F_2 from reaching the pump.

The ultra-violet part of the spectrum from 2200 to 2700 A. was photographed on a Hilger E 1 spectrograph with an average dispersion of 3 A./mm. in that region. Exposures which ranged from 15 min. to 1 hr. were made on Ilford Double Express and Monarch plates.

The active-nitrogen method of exciting the SbF spectrum, as described by Mulliken[2], was adopted. Photographs of the visible region of the spectrum were also taken with the Hilger E 1 spectrograph on Monarch plates with exposures up to 4 hr. Throughout this work iron arc lines served as wave-length standards. Wave-number measurements are consistent to 1 $cm.^{-1}$ Weaker bands which could not be studied in this way were photographed on a Hilger small quartz spectrograph against internal Sb 1 standards. Their wave-numbers are probably correct to 5 $cm.^{-1}$ Intensities were assigned visually on a 0-to-10 scale.

§ 3. VIBRATIONAL ANALYSIS

A photographic reproduction of both systems has been given by Rochester[1]. It will here be shown that all the bands can be arranged into two electronic systems each of which is a triplet system.

(1) *The ultra-violet triplet system.* The ultra-violet bands stretch from 2200 to 2450 A. and appear to consist of one large system. There is also a group of bands lying at 2650 A. All of these bands are degraded to the violet and most have sharp heads and short branches. In the case of the strong bands Q heads can be detected very close to the P heads. The separations between P and Q heads are small, being of the order of 2 to 4 $cm.^{-1}$, and consequently the P-head measurements which are used here are good substitutes for band-origin measurements.

All the bands in the 2650-A. region have been fitted into the quantum scheme given in table 1, the intensity-distribution of the bands is shown also.

Table 1

Vibrational analysis

v' \ v''	0		1		2		3
0	37978·3	610·1	37368·2	603·2	36765·0		
	695·7		695·4		693·8		
1	38674·0	610·4	38063·6	604·8	37458·8	600·1	36858·7
	692						694·0
2	39366						39552·7

Intensity-distribution

v' \ v''	0	1	2	3
0	10	9	3	
1	2	8	6	1
2	1			0

The vibrational constants have been determined by plotting the interval $\Delta G\,(v+\frac{1}{2})$ against $2\,(v+1)$, the following quantum formula being derived for the band heads:

$$\nu = 37937{\cdot}6 + (696{\cdot}9u' - 1{\cdot}09u'^2) - (616{\cdot}6u'' - 3{\cdot}19u''^2),$$

where $u = v + \frac{1}{2}$.

The agreement between the wave-numbers of the heads as calculated from this formula and those actually measured can be judged from table 5 which contains all the classified bands.

Of the 21 bands in the region 2200 to 2450 A., 18 have been fitted into the quantum scheme shown in table 2. Their heads are represented by the formula

$$\nu = 43513{\cdot}7 + (698{\cdot}8u' - 1{\cdot}93u'^2) - (612{\cdot}6u'' - 2{\cdot}63u''^2).$$

Table 2

Vibrational analysis

v' \ v''	0		1		2		3		4		5		6		7
0	43557·0	607·9	42949·1	600·1	42349·0	593·8	41755·2								
	697·0		699·0		694·4		689·0								
1	44254·0	605·9	43648·1	604·7	43043·4	599·2	42444·2	590·1	41854·1	585·9	41268*	584	40684*		
			687·1				691·3		691·3		690		692		
2			44335·2				43135·5	590·1	42545·4	587·1	41958·3	582	41376*		
													688		
3													42064*	578	41485*

* Measured with small quartz spectrograph.

Intensity-distribution

v' \ v''	0	1	2	3	4	5	6	7
0	10	8	3	1				
1	6	7	8	4	2	1	0	
2		2		5	4	2	0	
3							1	0

The vibrational frequencies are thus almost the same as those of the previous system, suggesting that the two systems form part of a multiplet system. As SbF has an even number of electrons, a triplet system is to be expected. If all the bands measured had been found to fit into table 2 it would have been assumed that the third component of the triplet would lie in the Schumann or vacuum region, i.e. below 1900 A. However it is considered that the three unallocated bands in table 3 are part of this third system, for their differences 609 and 697 are of the same order as ω_e' and ω_e'' of the previous systems. In all probability these bands are the $1 \to 0$, $0 \to 0$ and $0 \to 1$ bands of this third system, for the intensity-distributions of the previous systems given in tables 2 and 3 are such as would lead

Table 3. Remaining SbF bands

44801	609	44192
697		
45498		

one to expect that these bands would be the strongest. It is impossible to derive the vibrational constants of this third system in the usual way, but an estimate of their magnitude will be given later.

(2) *The visible triplet system.* 76 red-degraded bands have been measured in the region 3200 to 5000 A., and of these 61 have already been allocated by Rochester to two systems, represented by the formulae

$$A_1\nu = 21887{\cdot}5 + (411{\cdot}3u' - 1{\cdot}71u'^2) - (616{\cdot}9u'' - 2{\cdot}89u''^2),$$

$$A_2\nu = 23992{\cdot}5 + (420{\cdot}0u' - 1{\cdot}75u'^2) - (612{\cdot}6u'' - 2{\cdot}58u''^2).$$

The additional 15 bands have now been fitted into the quantum scheme given in table 4, and the following formula has been derived for their R heads:

$$\nu = 27912 + (412{\cdot}0u' - 2{\cdot}35u'^2) - (612{\cdot}5u'' - 2{\cdot}55u''^2).$$

The intensity-distribution also of these bands is shown in table 4.

Table 4

Vibrational analysis of system A

v' \ v''	0		1		2		3		4		5		6		7
0	27815*	612	27203	602	26601	597	26004	591	25413	588	24825				
	406		408								409				
1	28221	610	27611								25234	580	24654	579	24075
	400														
2	28621*														
	398														
3	29019*														
	396														
4	29415*														
5			29204*												

* Measured with small quartz spectrograph.

Intensity-distribution

v' \ v''	0	1	2	3	4	5	6	7
0	3	4	5	5	4	2		
1	3	3				2	1	1
2	2							
3	1							
4	0							
5		0						

It will be noted that all three systems, A_1, A_2 and A_3, have almost identical values of ω_e' and ω_e''. They constitute therefore a second triplet transition, and as the values of ω_e'' correspond with those of the ultra-violet system, the final electronic state is common to both systems.

§ 4. DISCUSSION OF RESULTS

The multiplet separations in the visible triplet system are very large and unequal, viz. 3919 and 2105 cm.$^{-1}$, and may belong to the upper or lower state or be

due to a splitting of both states. The values of ω_e'' and ω_e' in this system are 612·6, 616·9 and 612·5 cm.$^{-1}$ and 411·3, 420·0 and 412·0 cm.$^{-1}$ respectively. The fact that differences in both ω_e'' and ω_e' occur is considered significant, and suggests that

Table 5. Classification of SbF bands

λ (A.)	Intensity	ν (cm.$^{-1}$)	o–c	v' v''
		The A_3 system		
4152·5	(1)	24075	1	1, 7
4055·0	(1)	24654	3	1, 6
4027·1	(2)	24825	−1	0, 5
3961·8	(2)	25234	1	1, 5
3933·9	(4)	25413	0	0, 4
3844·5	(5)	26004	−1	0, 3
3758·2	(5)	26601	−1	0, 2
3675·0	(4)	27203	−2	0, 1
3620·7	(3)	27611	−1	1, 1
3594·2	(3)	27815	3	0, 0
3542·4	(3)	28221	2	1, 0
3492·9	(2)	28621	−1	2, 0
3445·0	(1)	29019	−1	3, 0
3423·3	(0)	29204	10	5, 1
3398·7	(0)	29415	2	4, 0
		The ultra-violet system		
2719·18	(3)	36765·0	0·8	0, 2
2712·26	(1)	36858·7	−2·7	1, 3
2675·28	(9)	37368·2	0·1	0, 1
2668·63	(6)	37458·8	0·0	1, 2
2632·30	(10)	37978·3	0·0	0, 0
2626·40	(8)	38063·6	0·9	1, 1
2584·94	(2)	38674·0	1·1	1, 0
2539·5	(1)	39366	1	2, 0
2527·5	(0)	39554	−1	2, 3
2457·2	(0)	40684	−3	1, 6
2422·43	(1)	41268·2	0·3	1, 5
2416·12	(0)	41376·0	−1·8	2, 6
2409·74	(0)	41485·6	−3·7	3, 7
2394·19	(1)	41755·2	4·5	0, 3
2388·52	(2)	41854·1	0·1	1, 4
2382·59	(2)	41958·3	−0·6	2, 5
2376·59	(1)	42064·2	−0·9	3, 6
2360·62	(8)	42349·0	1·5	0, 2
2355·31	(4)	42444·2	−0·5	1, 3
2349·71	(4)	42545·4	0·2	2, 4
2327·62	(8)	42949·1	−0·5	0, 1
2322·52	(8)	43043·4	0·9	1, 2
2317·56	(5)	43135·5	−1·2	2, 3
2295·13	(10)	43557·0	0·0	0, 0
2290·34	(7)	43648·1	−3·5	1, 1
2259·01	(6)	44254·0	2·0	1, 0
2254·84	(2)	44335·2	4·2	2, 1
2262·1	(3)	44192	—	0, 1
2231·4	(5)	44801	—	0, 0
2197·2	(2)	45498	—	1, 0

both the upper and lower states are multiple. That the differences observed in ω_e'' are real and not due to experimental error is supported by the fact that the ω_e'' values calculated from the ultra-violet systems show the same variation. Thus

although only two values of ω_e'' are known definitely, viz. 612·6 and 616·6, the value of $\Delta G''$ for the third system is 609, and it is very probable that ω_e'' for this state is about 612. Values of ω_e' for the ultra-violet system are 698·8, 696·9, and as $\Delta G'$ is 697 for the third member, ω_e' for this may be taken as 700. With these values it is possible to estimate that ν_e for this system is approximately 44750 cm.$^{-1}$

The three values of ν_e being 44750, 43508·7 and 37937·6, the multiplet separations are 1241 and 5571, again very large and even more unequal than for the visible system.

When the inequality in the separations is marked, splitting in both final and initial states is probable. It is impossible to draw an energy diagram of these systems as the absolute separations of the levels are not known, but certain suggestions as to the nature of the states may be made on the assumption that the lower state common to both systems dissociates into normal atoms. This state must be of the electronic type $^3\Sigma$, $^3\Pi$, $^5\Sigma$ or $^5\Pi$. It has already been remarked that Q heads are observed in the ultra-violet system, and the heads in the visible system are line-like, indicating the presence of a Q branch, and so the upper states must be $^3\Pi$, $^5\Pi$, $^3\Delta$ or $^5\Delta$. In view of these various possibilities it is clear that no satisfactory conclusion can be drawn as to the identification of the states without a rotational analysis. Whatever be the correct allocation, however, it is certain that the multiplet separations of at least one of the states are widely unequal.

§ 5. ACKNOWLEDGEMENT

It is a pleasure to record our thanks to Prof. W. E. Curtis for the facilities for photographing the spectrum placed at our disposal at King's College, Newcastle.

REFERENCES

(1) Rochester, G. D. *Phys. Rev.* **51**, 486 (1937).
(2) Mulliken, R. S. *Phys. Rev.* **26** (1925).

EMISSION OF NEGATIVE IONS FROM OXIDE CATHODES

By L. F. BROADWAY, Ph.D.

AND

A. F. PEARCE, Ph.D., A.Inst.P.

Electric and Musical Industries Limited

Received 8 *September* 1938. *Read in title* 20 *December* 1938

ABSTRACT. A beam of negative ions has been detected in cathode-ray tubes by the darkening effect produced on the fluorescent screens of the tubes. The beam has a number of components, of which the following seven ions have been identified: H_1^-, C_{12}^-, O_{16}^- (or O_{32}^{--}), Cl_{35}^-, Cl_{37}^-, Br_{80}^-, I_{127}^-. Two other ions having mass-to-charge ratios of 26 and 42 are thought to be CN^- and CNO^- respectively. The negative-ion current has been measured and found to be of the order 10^{-9} amp., about 10^5 to 10^6 times smaller than the corresponding electron current. The results are discussed in connexion with various processes by which ions may be produced, and conclusions relating to the origins of the various ions are drawn.

§ 1. INTRODUCTION

During the last few years a negative-ion component of the cathode-ray beam in cathode-ray tubes of the high-vacuum type has been reported by several writers[1,2]. The investigation of the nature and mode of formation of these ions described in this paper has been carried on over the last two years. During preparation of the paper a publication on the same subject has been made by Bachman and Carnahan in America[3]. Some of their observations are confirmed in the present paper which also gives further experimental results and concludes with a discussion of the origin of the ions.

The usual manifestation of the presence of the ions in a cathode-ray tube is the gradual appearance of a dark or discoloured area on the screen during the normal operation of the tube. The discoloration, which has a very variable rate of growth on different tubes, is centred around the point at which the electron gun is directed. In the case of a tube having its electron beam focused on the screen entirely by electrostatic fields and scanned electromagnetically (as in these experiments) the darkening takes approximately the shape and size of the focused stationary electron spot. If the scanning and focusing are both electrostatic, the darkening is distributed over the whole screen. The discoloured area, the so-called "black spot", is generally apparent only whilst the screen is being excited to fluorescence, being invisible under other conditions of illumination. It would thus seem to be a surface destruction or modification of screen fluorescence.

A great range of susceptibility to discoloration is shown by the various fluorescent materials. Willemite for instance is comparatively resistant, while the less stable sulphides are particularly vulnerable; screens of zinc cadmium sulphide were for this reason used throughout the experiments. Many of the experiments were carried out with tubes of the type used for television reception, but a number of special tubes also were made; a demountable tube too was occasionally employed.

§ 2. ANALYSIS OF THE BEAM OF IONS

The partial destruction of fluorescence of the screen in the region of the black spot is clearly due to the bombardment of that region with negatively charged particles; for firstly the localization of the spot indicates a focusing action exerted on the particles by the electrostatic fields of the gun, and secondly the screen is at a higher positive potential than any other electrode of the tube. Moreover the particles are relatively heavy, since no appreciable deflection is produced by weak magnetic fields such as those used in scanning. Their origin must be at or near the cathode since their focusing point is the same as that of the electrons.

The next step is to discover the nature of these negative ions. An electron gun employing only electrostatic fields exerts the same focusing action on all charged particles, irrespective of their charge or mass. Hence the observed spot may be due to the aggregate effect of a number of types of ion or various masses and charges. These may, however, be sorted out by deflecting the beam, after it has passed through the final lens, by means of a transverse magnetic field, when the various component beams are deflected to varying extents depending upon the charge-to-mass or e/m ratio of the ions. Since all the focused ions start at or near the cathode they have very nearly equal energies on entering the magnetic field, so that this arrangement constitutes a mass spectrograph without the need of the customary velocity filter. From the radial line of black spots or ionic spectrum so formed the ions present may be identified by the methods described later. A high accuracy and resolving power are attainable if suitable conditions of fineness of gun focus and intensity of magnetic field are chosen. In addition the method of ion-detection by formation of a black spot is very sensitive, so that only short exposures are necessary.

The dependence of the deflection upon the e/m value of the ion can be readily calculated in the simple case of a magnetic field which is of uniform strength H over a distance l but terminates sharply at its edges (the planes AB and CD, figure 1). The deflection is given by

$$d=\frac{HlL}{\sqrt{(2V)}}\sqrt{\frac{e}{m}}, \qquad \text{.....(1)}$$

where V is the voltage through which the ion has been accelerated and L is the distance of the screen from the deflecting point. If the intensity of the magnetic field instead of being uniform over a finite distance varies along the path of the beam, the deflection d is given by substituting $\int H\,dl$ for Hl in this equation, provided that the field is not too extensive.

This equation shows that the deflections produced on the various ions are directly proportional to $\sqrt{(e/m)}$, or, for the singly charged ions most frequently encountered in practice, to $1/\sqrt{m}$.

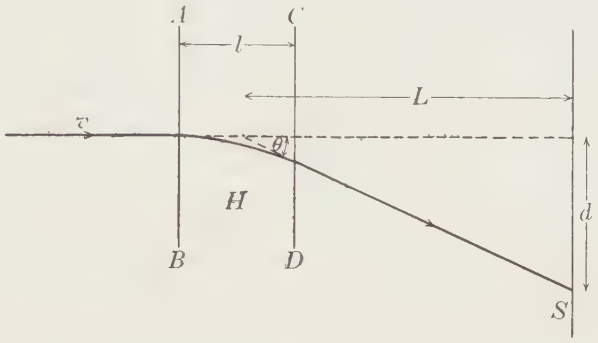

Figure 1.

§ 3. EXPERIMENTAL

(i) *The electron gun.* An axially symmetric gun of the hexode type, represented in figure 2, was generally used. Electrons from the cathode C are accelerated by the potential on the accelerator A and brought to a first focus at F near the modulating electrode M. After this the beam diverges in the first anode A_1 and is finally focused upon the screen by the lens formed between the first and second anodes, the latter being held at a high positive potential. The oxide cathode was of the indirectly heated type, the oxide being applied to the nickel core without binder. It was thoroughly degassed and the carbonates were broken down before removal from the

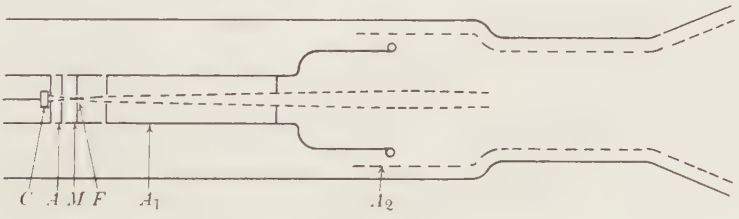

Figure 2.

pump. The tubes were gettered with barium to ensure a good vacuum throughout their lives.

(ii) *Experimental arrangement.* The arrangement is shown diagrammatically in figure 3. The horseshoe electromagnet NS, having an adjustable pole-piece separation, was placed as far from the gun as was convenient in order to avoid magnetization of the nickel. A mumetal shield was put around the gun as an additional precaution. In the early experiments the gun was further removed from the magnet by extending the length of the neck of the bulb, but this arrangement was later found to be unnecessary. In the designing of the magnet, the order of field required was estimated from equation (1). A field of about 700 gauss between pole pieces of

two-inch-square section, separated by about 6 cm., was frequently used and gave a good resolution.

The pole spacing was chosen large enough to go over the scanning coils, which were of non-magnetic material, so that the screen could be scanned for viewing purposes, after ion-deflection, without disturbance of the set-up.

(iii) *Spotting procedure.* When a tube was examined for negative-ion components the following procedure was adopted. The second anode voltage being kept constant, usually at 4 kv., the first anode voltage was adjusted until the electron spot was focused on the screen, as viewed either on the lines during scanning or on the stationary spot. Care was taken in the latter case not to cause an electron burn near the centre of the screen. Tests have shown that the ion spot also is focused at this focusing ratio. The magnetic field was then applied for a brief period, say 1 min., after which the screen was examined while being scanned with electrons of lower velocity to increase the contrast and make the black spots more plainly visible. In order to obtain a more accurate measure of the deflections this procedure was

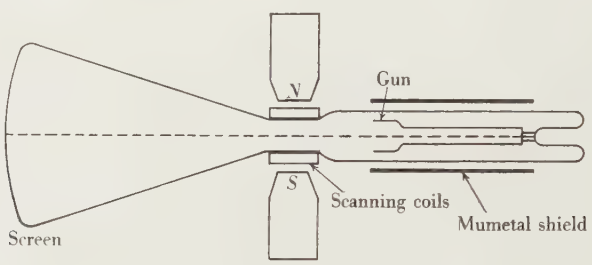

Figure 3.

usually repeated with the magnetic field reversed so that the spectrum was formed on both sides of the central undeflected spot. The linear deflections were usually large enough for a reasonably accurate measurement to be made by rule, but for greater accuracy, especially in the measurement of relative deflections, a photograph was taken and the negative was measured. The negatives were also occasionally analysed by means of a Moll microphotometer. One such tracing, figure 4, taken at low resolution shows hydrogen, oxygen and chlorine ions. The isotopes of the latter are unresolved in this particular case.

The analysis could be repeated if desired by rotating the tube slightly with respect to the magnetic field, so as to expose a fresh area of screen on which to form spots.

(iv) *Identification of ions.* The components of the ion beam were identified from values of e/m derived from the deflections of the various spots of the mass spectrum. The following four methods were available.

(1) The use of equation (1). The distribution of magnetic field along the axis of the tube was found by means of a search coil, and e/m calculated from this and the known geometrical constants. This is only an approximate method since the measured field-distribution was disturbed by the introduction of the gun and screening. It was found however that the equation written in the form $d \propto \sqrt{(e/m)}$

was accurate within experimental error; tests also showed that the deflection was proportional to the field applied for any one ion.

(2) Extrapolation from the deflections produced on an electron beam by small magnet currents, the relationship between magnetic field and current supplied having previously been determined. The accuracy of this method is limited by residual magnetism of the core of the magnet, which may produce relatively large deflections of the electron beam.

(3) Comparison of the squares of the deflections (proportional to e/m) of the various ions simultaneously present in one tube. Since the ionic masses must be whole numbers (of atomic units) and the charges most probably single, this is very useful with the lighter ions. For instance, in the early tubes two ions with deflections in the ratio 4 : 1 frequently appeared, giving a mass ratio of 1 : 16 if both are singly charged. With method (1) the measured deflections led to masses of

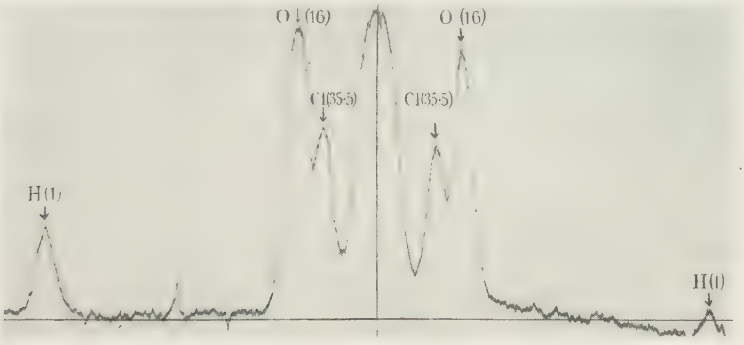

Figure 4.

about 1 and 16, so these ions were assumed to be due to singly charged atomic hydrogen and oxygen respectively.

(4) The introduction of a known contaminant into the tube in order to identify one particular ion. The suspected hydrogen ion, for instance, was confirmed in this manner by introducing hydrogen through a palladium side seal, whereupon the spot under consideration became much denser. It was also used for the halogens by introduction into the cathode coating.

All these methods were used for the initial calibration with the several types of tube employed, and gave results in mutual agreement. Thereafter an ion could be identified merely from its deflection, the comparison with any others also present being used as a check.

(v) *Effect of potential of screen.* Some difficulty in maintaining the screen at the appropriate potential during the deflection of ions was experienced. Normally, under electron bombardment, as in scanning, the screen takes up a potential nearly equal to that of the anode by emitting secondary electrons which return to the second anode. On application of the magnetic field, however, the electrons are deflected off the screen, which is then virtually insulated from the anode. Since also the screen material is a poor conductor, those areas on which negative ions fall will

lose positive charge rapidly until eventually the potential becomes so low that no further negative charges can arrive, and black-spotting ceases, making analysis impossible. Sometimes the ions are not completely cut off but are deflected radially by the local potential hump, causing the spots to have tails. The effect is not serious at relatively low strengths of magnetic field, giving small deflections, presumably because a sufficient number of electrons to maintain its potential reach the screen after being scattered from the neck of the bulb, so that testing at low resolution is possible without precaution; but for higher resolutions special measures are necessary.

Two methods were found to be satisfactory up to the highest resolutions. The first consisted in settling the screen on a thin semitransparent film of lead sulphide which was in contact with the anode, so that there was metallic contact between the two. In the second the screen was bombarded by electrons from an auxiliary cathode sealed into the tube near the screen; this was very effective and much used. These expedients were applicable only to special tubes. For standard tubes, the maximum resolution obtainable could be somewhat increased by moving the magnet with an increased pole gap towards the screen, when more scattered electrons than in the normal position could reach the screen. Another method depending upon photo-conduction of the screen under ultra-violet radiation was ineffective because the screen material is apparently non-photoconductive unless bombarded by electrons at the same time. It is evident from the existence of this effect that the ions are very inefficient producers of secondary electrons at the screen.

§ 4. RESULTS

(i) *Ions present.* A total of nine kinds of negative ions have been detected in cathode-ray tubes. They have the values of m/e shown in table 1, m being in atomic units:

Table 1

m/e	Ion
1	Singly charged atomic hydrogen H^-
12	Singly charged carbon C_{12}^-
16	Singly charged atomic oxygen O_{16}^- or possibly doubly charged molecular oxygen O_{32}^{--}
26	Not positively identified, but probably CN^- or $C_2H_2^-$
32	Singly charged molecular oxygen O_{32}^-
35, 37	Singly charged atomic chlorine Cl^- (two isotopes)
42	Not positively identified—may be CNO^- or a hydrocarbon such as $C_3H_6^-$
80	Singly charged atomic bromine Br_{79}^- and Br_{81}^- (isotopes unresolved)
127	Singly charged atomic iodine

A badly focused ion with m/e about 8 has also occasionally been seen; it is probably O_{16}^{--}. A suspicion of another ion with m/e about 48 also exists. Two typical ionic spectra are shown in figures 5 (*a*) and 5 (*b*). These are photographs, about two-thirds full size, of the screens of a demountable tube and a 9-in. tube respectively, taken whilst the tubes were fluorescing under low-velocity electron

scanning. The spot spectra have been formed on both sides of the centre; figure 5*b* shows a second reproduction of the system obtained by rotating the tube slightly. Both photographs show the isotopes of chlorine clearly resolved, especially figure 5*b*, in which special care was taken to produce small well-focused spots. Near the centre of figure 5*a* the spots of the system are shown at lower resolution, the hydrogen spot being just perceptible. The carbon spot was visible on the screen but is almost imperceptible in the print owing to loss of contrast. Figure 5*b* shows clearly the fine focus of the chlorine ions as compared with the others; this is referred to later.

The hydrogen and oxygen ions appear most strongly in soft (i.e. gassy) tubes, the former usually disappearing rapidly with ageing. The 32 ion has been observed only in extremely soft tubes, at a pressure of about 10^{-3} mm. Carbon appears

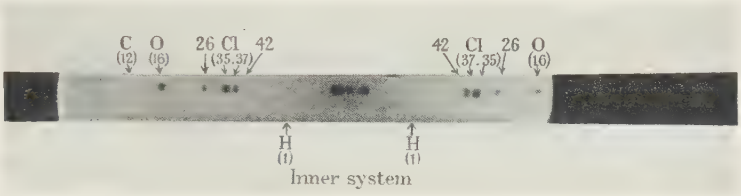

Figure 5 (*a*).

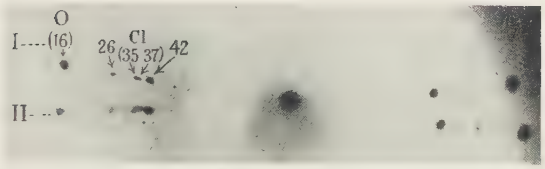

Figure 5 (*b*).

strongly only in tubes in which the cathode has been insufficiently degassed, and is probably associated with the incomplete breakdown of the carbonates used to form the oxide cathode. The 26 and 42 ions appear most strongly in the presence of wax and grease vapours as in the demountable gear, although their intensities do not appear to be mutually dependent.

The halogens—chlorine, bromine and iodine—are sometimes present in the tube as impurities, but only the chlorine ion appears regularly. The resolved isotopes of masses 35 and 37 appear with an intensity ratio of about 3 : 1, as we should expect from the known composition of natural chlorine. All three halogen ions appeared simultaneously when common salt containing bromine and iodine as impurities was added to the cathode coating.

Some of the ions listed above have been reported in the literature. J. J. Thomson[4] observed the negative ions of atomic hydrogen, molecular and atomic oxygen, carbon and chlorine in his positive-ray-parabola experiments many years ago; he mentions also C_2^-, OH^- and H_2^-, but these have not been observed in cathode-ray tubes. Freisewinkel[5] observed H^- in a high-voltage oscillograph.

Barton[6] recorded O_{32}^- emitted by an oxide cathode, but failed to find O_{16}^-; Blewett and Jones[7] also have recently observed O_{32}^- from a barium-oxide emitter at a high temperature. Reimann[8] is of the opinion that Barton's cathode must have been in some peculiar condition; the possibility of the ion really being Cl^- also exists, since Barton's resolution was not particularly great.

An empirical relationship between ion-emission and electron-emission that has been established may be mentioned here. From an examination of a number of tubes it has been found that the ionic current is in general roughly proportional to the electron-emission.

The relationship with screen voltage has not been fully investigated but it is known that the spot becomes relatively less conspicuous as the voltage is increased at constant current above about 4 kv.

On tubes with intense ion-emission, fluorescence caused by the impingement of the ions on the screen has sometimes been observed during the brief period before the fluorescing power of the screen has been destroyed by the development of a black spot. For ions of equal black-spotting intensity, the luminosity increases as we go from the heavy to the light ions. This may be due either to the screen-destructive power (black-spot formation) of an ion increasing with its mass, or to the luminous efficiency decreasing with increase of mass, or more probably to both.

As a matter of interest a brief search for positive-ion-emission from an oxide cathode was made by reversing all the tube potentials. No such ion-emission could be detected up to a filament temperature of about 1000° C., although barium and strontium ions have been reported. Screen-potential trouble may account for this negative result.

§ 5. MEASUREMENT OF INTENSITY OF ION BEAM

An absolute measurement of the intensity of the ion beam was made electrically by collecting the focused components of the beam in turn in a Faraday collector, and measuring the current. The arrangement is shown in figure 6. The Faraday collector F, with a defining slit A about 1 mm. wide before it, was placed a few centimetres off the centre of the screen S, so that the various component ion beams could be brought into it in turn by varying the analysing magnetic field. The ion current was measured with a sensitive galvanometer G. The upper half of the screen S was coated with fluorescent material so that by reversing the magnetic field the black-spotting effect of the various ions could be seen.

The results at two different filament temperatures are given in figure 7. In this particular tube chlorine was the only strong ion present. The graph shows that the ion current is about 6×10^{-10} amp. at the normal running temperature of 800° C.; this was sufficient to produce an appreciable black spot on the screen in about 1 min. The cathode used had an emitting area of approximately 2 mm^2 and was operating under space-charge conditions.

This measurement is only approximate, for the currents involved are near the lower limit of sensitivity of the galvanometer and the special tube used is not necessarily representative of the usual types of cathode-ray tube. It serves however

to show the minute order of the ionic emission involved in cathode-ray tubes, and also the sensitivity of the screen to bombardment by ions. The ionic current is about 10^5 or 10^6 times smaller than the corresponding electron current.

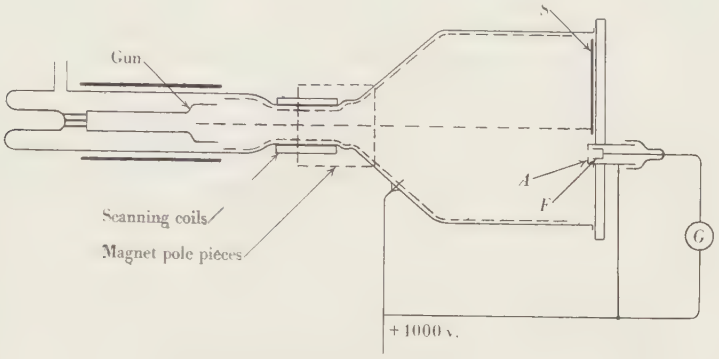

Figure 6.

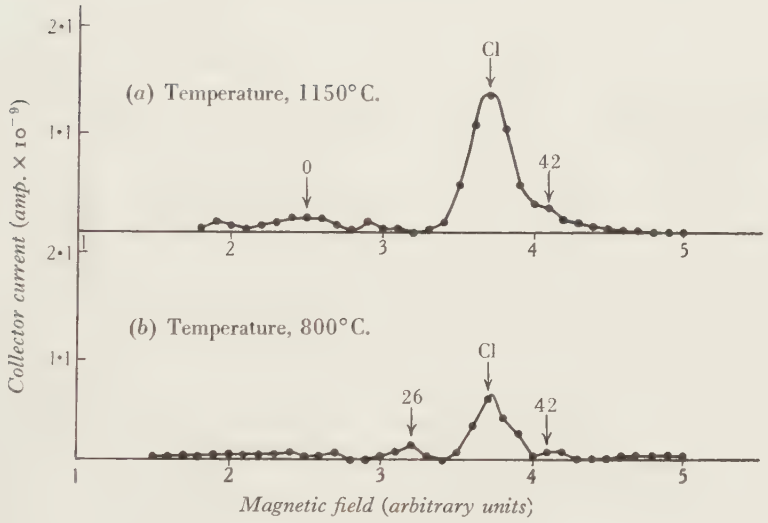

Figure 7.

§ 6. DISCUSSION OF RESULTS

(i) *The mechanism of emission.* Certain atoms and molecules of an electronegative nature are capable of readily attaching an electron and so forming a stable negative ion. They are said to have an "electron-affinity", energy being released when attachment occurs. We should consequently expect all the observed ions to fall into this class, and that the most intense ones would have high affinities. Some electron affinities already published are collected in table 2.

Ions of nitrogen have never been observed in these experiments; this would be expected from its low affinity. Fluorine also has been absent in spite of its high affinity, probably because of its sparsity of occurrence in nature. Sulphur might

Table 2

Atom	Electron-affinity ev.	Author
H^-	0·7	Glockler[9]
C^-	1·37	Glockler[9]
N^-	0·04	Glockler[9]
O^-	3·8	Glockler[9]
Cl^-	3·6–3·7	Glockler[9], Verwey and Boer[10]
Br^-	3·3	Verwey and Boer[10]
I^-	3·0	Verwey and Boer[10]
F^-	4·0	Verwey and Boer[10]
S^-	2·1	Glockler[9]
CN^-	4·0	Lederle[11]

have been expected, since it is a tube constituent, but the evidence indicates that the 32 ion when present is wholly due to oxygen.

From the fact that the ion beam is focused at the same focusing ratio as the electron beam, it is evident that both have a common origin, i.e. the ions originate at or near the cathode. The ions may be divided broadly into three classes as follows, according to their possible modes of formation: (1) ions emitted as such by the cathode; (2) ions formed outside the cathode by attachment of electrons to atoms emitted by the cathode; and (3) ions due to the presence of residual gas in the tube. Group (3) may be subdivided into (*a*) ions formed by direct attachment of an electron to an atom or molecule of gas in a low-velocity region of the gun; (*b*) ions formed by conversion of positive gas ions at the cathode; (*c*) ions formed by the enhancement of the direct-cathode ion-emission postulated in process (1) by bombardment of the cathode surface with positive ions of the gas. These possible processes will now be discussed in more detail.

Process (1) is somewhat analogous to the emission of electrons. The generally accepted view of the operation of the mixed-oxide cathode is the barium circulation theory of Becker, which may be briefly stated as follows. During activation, free barium and strontium are produced in the oxide; these may subsequently diffuse to and fro between the surface and the core until an equilibrium concentration of barium is set up both in the oxide and in a layer on the outer surface of the cathode. This layer lowers the work function and accounts for the enhanced activity of the oxide cathode. Becker's theory, for which there is considerable experimental evidence, requires that some of the conduction in the oxide shall be electrolytic, positive barium ions moving in towards the core while negative oxygen ions move out towards the surface. The ratio of ion current to total current is very dependent upon conditions of temperature, current drawn from the cathode, degree of activation, etc., but in one experiment was found to be of the order 1/200. Becker[12] and others[13] have also shown that oxygen is evolved when space current is drawn from the cathode; most of this oxygen is uncharged, but a small fraction may be emitted as ions. This may account for some of the observed oxygen-ion current, although it must be remarked that the observed ions are either singly charged atoms or

doubly charged molecules, these being indistinguishable, while the electrolytic ions are presumably doubly charged atoms.

If an electrolyte such as sodium chloride were present in the cathode we might expect it to electrolyse in the same way as the oxide. The negative ion would be brought to the surface where an equilibrium layer of atoms and ions would be formed; some of these might evaporate as ions. Such a process would account for the halogen ions if the corresponding halides were present as impurity in the cathode. The experimental evidence supporting this view is (1) the fact already mentioned that the halogen ions can be brought to as small a focus as the electron beam, in contradistinction to some of the other ions which always have a larger focus; and (2) the fact that addition of halide impurity to the oxide of the cathode results in an emission of the corresponding halogen.

It is evident that any emission of negative ions from the cathode will be strongly influenced by the state of the surface, as electron-emission is. Oxide cathodes are notorious for their ready adsorption of atoms of an electronegative nature. The surface layer so formed is extremely stable, and has the effect of increasing the work function and so diminishing electron-emission. Any intrinsic emission of ions by the cathode would be expected to be similarly affected. It is probable, however, that some re-evaporation of atoms of the adsorbed layer takes place and that some of these are negatively charged. Consequently in the case of a cathode which is partially poisoned by the presence of gas, we may have an emission of negative ions of the gas by the process of adsorption on the cathode with a subsequent re-evaporation as ions.

Process (2). The ionization in this case takes place outside the cathode, the element or radical having previously been emitted in the uncharged state. No evidence for the existence of this process has been found.

Process (3*a*). When a beam of electrons is fired into a gas, direct attachment of an electron to an atom or molecule may take place by one of two mechanisms. In attachment to an atom the excess energy (the electron affinity and the kinetic energy of the electron before impact) must be radiated, which makes the process somewhat improbable; in the molecular case dissociation into an ion and an atom may occur, the excess energy being carried off in the kinetic form. These processes have been investigated in detail by Bradbury and co-workers[14, 15, 16], Bailey and co-workers[17], Massey and Smith[18], Hogness and Harkness[19], Hogness and Lunn[20], and others, for a number of gases. The last-named observers find in the case of oxygen that the atomic ions are more abundant than the molecular ions.

The probability of attachment at a collision depends upon the energy of the electron as well as upon the nature of the gas; for molecular gases in which dissociation occurs it usually has a minimum at about 1 ev., increasing rapidly as zero energy is approached and more slowly with increase of energy above 1 ev. In oxygen, however[14], after passing through this minimum as the energy is increased from zero, the probability reaches a maximum at 1·6 ev., thereafter decreasing continuously as far as it has been investigated up to about 10 ev. Sufficient data are not available to allow of an accurate calculation of the negative-ion current that we

might expect in a cathode-ray tube from this process, but a very rough estimate can be made. For this purpose we may take from Bradbury's results a value of 3×10^{-4} for the average probability of attachment in oxygen for all electrons of energies up to 10 ev., neglecting those of higher energy for which data are not available but which are likely to have a lower probability. Assuming further that the pressure in the tube is 10^{-5} mm., at which the mean free path of an electron is about 4×10^{3} cm., and that the electron current is 1 ma. with an effective path-length of 1 cm., we compute that the negative-ion current is about 10^{-10} amp.

This is rather smaller than the observed ion current but is not of a very different order, and might account for some of the ions that are known to be due to the presence of gas. The process could account, especially when dissociation occurs, for the large focus observed at, for instance, the oxygen spot, since the ions would start off after formation with energies of various magnitudes and directions.

Process (3 *b*). A new process for the formation of negative ions has recently been formulated by Arnot [21] to account for his experimental observations. According to this the positive ions normally formed in a gas by electron-impact may be converted into negative ions by impinging upon a negatively charged electrode such as the cathode and extracting therefrom two electrons. Experiments in mercury vapour, hydrogen, oxygen, nitrogen and carbon dioxide have led to the conclusion that the process has a comparatively high probability, and that most of the negative ions observed in these gases were so formed, a very small fraction only being formed by the process of direct attachment discussed above.

The probability of conversion depends upon the work function of the surface concerned and upon the ionization potential, electron affinity, and energy of the incident ionized atom. It decreases with increase of the first factor but increases with increase of the other three. Arnot has found the probability for a nickel surface (with a work function 5·03 ev.) for ions of energy up to 200 ev. For an oxide cathode (with a work function about 1 ev.) the value is probably considerably greater than this. Lacking this datum, however, we may use the probability for nickel to obtain a rough estimate of the order of ion current that could be expected in a cathode-ray tube. We may consider the first anode, in which most of the effective positive ions will be created, to be 10 cm. long and at a potential of say 800 v., the electron current being 1 ma. Then taking the efficiency of ionization of electrons in oxygen at a pressure 10^{-5} mm. to be 4×10^{-5}, and the probability of conversion to be 10^{-3} (extrapolated from Arnot's results), we compute the negative-ion current to be about 4×10^{-10} amp.

This might be increased by a considerable factor by conversion on an oxide instead of a nickel surface, but losses must be allowed for, since not all of the positive ions created will strike the cathode, and of those converted not all will be focused on the screen, owing to the fact that they may leave the cathode with considerable energy.

This current however is of the observed order. It is interesting to note in connexion with the oxygen spot that the probability of formation of O_{16}^{-} ions from carbon dioxide is relatively high. This gas, which is evolved in large quantities

when the cathode oxide is formed by the breaking down of the carbonate, is likely to be the main constituent of the residual gas of the tube.

Process (3*c*): enhancement of ion-emission from the cathode by bombardment with positive gas ions. It is well known that bombardment by positive ions may dislodge and remove particles adsorbed on surfaces, as, for instance, when argon is used in the reactivation of oxygen-poisoned cathodes; hence it might be expected to enhance at least temporarily the intrinsic emission of negative ions by a cathode. The magnitude of the effect on cathode-ray tubes has been found to be somewhat variable, and to depend on the kind of gas present and on its pressure as well as on the state of the cathode surface. In a normally hard tube the effect is probably very small.

(ii) *Experimental applications and conclusions.* We can now see how far these processes are in accordance with the experimental results. The appearances and intensities of the various components of the beam of ions have been found to be very erratic, so that the results are largely of a qualitative rather than a quantitative nature. Moreover, some of the ions can be accounted for only by the simultaneous operation of two or more processes. The following conclusions may however be drawn:

(1) Some of the ions, notably the halogen ions, are emitted directly by the cathode by process (1). This follows from (*a*) the smallness of the focus and (*b*) the fact that addition of halide impurity to the cathode enhances emission of the corresponding halogen.

(2) The ions H^-, O^-, 26^- and 42^- are due to the presence of the appropriate gas or vapour in the tube, being formed in the main by processes 3 (*a*) and 3 (*b*). The evidence for this view is briefly that (*a*) the focus is large and (*b*) the ions usually weaken progressively as the tube is hardened. No discrimination between these two processes can at present be made.

A proportion of each of these ion components is probably formed by surface adsorption of atoms with subsequent re-emission as ions, in the manner outlined in connexion with process (1). Some evidence for this is that occasionally the emission continues after the tube has been hardened.

(3) The ion for which $m/e = 26$ is probably due to the electronegative radical CN^-. This is known to have a high electron-affinity (see table 2), whereas the alternative C_2H_2 exists as a molecule and is reported to have a low electron-affinity.

(4) The ion for which $m/e = 42$ may be due to CNO^- rather than to a hydrocarbon, since CNO^- is known in chemistry to exist as an electronegative radical.

(5) The C^- ion, which is only prominent when the cathode has been incompletely broken down, is probably formed from carbon dioxide by dissociation accompanied by ionization.

§ 7. ACKNOWLEDGEMENTS

The work described in this paper was carried out in the Research Laboratories of Electric and Musical Industries, Ltd., and the authors desire to express their thanks to Mr I. Shoenberg, Director of Research, to Mr G. E. Condliffe, to their colleagues of the Research Department, and in particular to Dr F. H. Nicoll for his suggestions in this investigation.

REFERENCES

(1) Von Ardenne. *Arch. Electrotech.* **29** (Nov. 1935); also *Television* (Nov. 1936).
(2) Levy and West. *J. Instn Elect. Engrs*, **79**, 11 (1936).
(3) Bachman and Carnahan. *Proc. Inst. Radio Engrs, N.Y.*, p. 529 (May 1938).
(4) Thomson. *Conduction of Electricity through Gases*, **1**, 274.
(5) Freisewinkel. *Arch. Electrotech.* **29** (April 1935).
(6) Barton. *Phys. Rev.* **26**, 360 (1935).
(7) Blewett and Jones. *Phys. Rev.* **50**, 464 (1936).
(8) Reimann. *Thermionic Emission*, p. 208.
(9) Glockler. *Phys. Rev.* **46**, 111 (1934).
(10) Verwey and Boer. *Rec. Trav. chim. Pays-Bas*, **55**, 431 (1936).
(11) Lederle. *Z. phys. Chem.* B, **17**, 362 (1932).
(12) Becker. *Phys. Rev.* **34**, 1323 (1929).
(13) Horton. *Philos. Trans.* A, **207**, 149 (1907). Detels. *Jb. drahtl. Telegr.* **30**, 50 (1927).
(14) Bradbury. *Phys. Rev.* **44**, 883 (1933).
(15) Bradbury. *J. Chem. Phys.* **2**, 827, 835 (1934).
(16) Bradbury and Bloch. *Phys. Rev.* **48**, 689 (1935).
(17) Bailey. *Phil. Mag.* **50**, 825 (1925); and others.
(18) Massey and Smith. *Proc. Roy. Soc.* A, **155**, 472 (1936).
(19) Hogness and Harkness. *Phys. Rev.* **32**, 784 (1928).
(20) Hogness and Lunn. *Phys. Rev.* **27**, 732 (1926).
(21) Arnot. *Proc. Roy. Soc.* A, **158**, 137 (1937); also **156**, p. 538 (1936).

THE CONDUCTIVITY OF THIN FILMS OF THALLIUM ON A PYREX GLASS SURFACE

By J. R. BRISTOW
H. H. Wills Physical Laboratory, University of Bristol

Communicated by Prof. A. M. Tyndall, F.R.S., 7 October 1938.
Read in title 20 *December* 1938.

ABSTRACT. Thin films of thallium have been prepared by condensation of the metal on a cooled pyrex surface at a pressure of 10^{-7} mm. of mercury or less. At a thickness of more than 40 A. the films show a resistivity only about three times greater than that of the bulk metal. The results tend to substantiate the views of Appleyard and Lovell that evaporated films do not differ radically in structure from the bulk metal, at least after the first few atomic layers. The thallium films described here differ in an important respect from both the alkali films and from mercury. Unlike the alkali-metal films they show no conductivity until the film is about five atomic layers in thickness; and unlike mercury films, which show a similar delayed conductivity, they have a finite range of thickness in which the resistivity is very high. It seems possible that the material is only semiconducting in this range, possibly owing to distortion of the normal metallic lattice by the atoms of the substrate.

Deposition of films in a poor vacuum, between 10^{-7} and 10^{-5} mm. of mercury, has demonstrated the far-reaching effects of occluded gas in the films. This may raise the resistivity at a given thickness by a factor of 10^4 or more, and also alter the temperature coefficients from the consistent positive values obtained in a good vacuum to large and variable negative values.

§ 1. INTRODUCTION

THIN films of thallium have been obtained by evaporative deposition on pyrex glass at various temperatures of condensation and in vacua varying between 10^{-5} and less than 10^{-7} mm. of mercury.

It has been possible to demonstrate the effect of occluded gas on the electrical properties of thin films, the results obtained being similar to those of earlier investigators (e.g. Reinders and Hamburger[1]), which show marked variations under what appear to be similar experimental conditions. The main characteristic of the films of earlier workers, thinner than 100 A., is the possession of resistivities which are greater than that of the bulk metal by a factor of at least 10^3, and show an irreversible change on treatment with heat, and negative temperature coefficients.

The properties of relatively gas-free films, deposited under carefully controlled conditions as described by Lovell[2] and by Appleyard[3] in their examination of the thin films of the alkali metals, have also been studied. Unlike those of alkali films, however, the first few atomic layers of thallium films appear to be only semiconducting if not non-conducting. Further, the films are not unstable.

§ 2. EXPERIMENTAL DETAILS

The experimental tube and method of working are similar to Lovell's[4] except for the oven (Q in Lovell's figure 1), which, as the melting point of thallium is about 300° C., had to be entirely re-designed, figure 1.

The thallium was evaporated from a small cylindrical crucible of iron and molybdenum. It was not possible to use an iron crucible, apparently owing to the iron dissolving in the metal. Neither could a molybdenum crucible be used, as the thallium creeps over its surface. The crucible was therefore of molybdenum inside and iron outside. As it was found impracticable to purify the metal by distillation in a vacuum, it was melted in a vacuum and run off through several narrow constrictions into small tubes and sealed off. The small tubes were coated

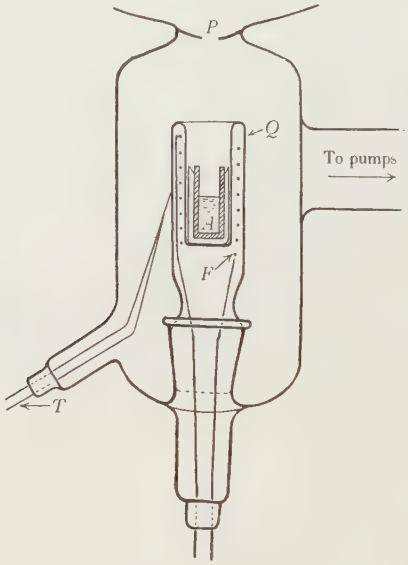

Figure 1.

with colloidal graphite to prevent the thallium from sticking to the glass, which it slowly attacks. The tubes were also of such a size and shape that the small cylinders of metal contained by them easily slipped out and fitted the crucible. The crucible was held in the quartz pocket Q and heated by the tungsten spiral F, the temperature being measured by the platinum platinum-rhodium thermocouple T.

The beam of thallium atoms issuing from the crucible passes from the oven to the experimental tube proper through the hole P which is about 2 mm. in diameter. This hole is closed by a steel ball which is moved by an electromagnet in order to start the deposition. The beam is then defined by cooled pyrex slits so that the patch of thallium, formed by condensation on the cooled pyrex surface, overlapped end-contacts made of graphite baked on to the glass over a layer of platinum paint which had previously been burnt into the glass.

The apparatus was continuously evacuated by a mercury diffusion pump backed by a Hyvac pump. Considerable difficulty was experienced in obtaining a vacuum of less than 10^{-7} mm. of mercury, the pressure always tending to be locally high in the oven during evaporations.

A bake-out of the apparatus would easily produce a pressure of less than 10^{-7} mm., which would deteriorate as soon as the thallium was heated. Only after evaporating for over 20 hr. at a temperature corresponding to a deposition rate of 1 A. per min. (about 350° C.) could the pressure be reduced below 10^{-7} mm. and consistent results be obtained.

The production of reproducible films is also complicated by the fact that, when attempts were made to clear the surface by heating, the thallium attacked the glass, giving it a frosted appearance; and only two or three similar films could be obtained without permanent alteration in the properties of the surface.

The intensity of the beam was determined by a method described fully by Powell and Mercer[5], namely, by measuring the emission of positive ions from a tungsten-oxide filament placed in the beam. The measured beam-intensities are consistent to ±10 per cent. With the various beam-intensities used, the film thickness increased by $\frac{1}{2}$ to 1 A. per minute.

The resistance of the films was measured by several methods: for very high values by measurement of the current produced by a known potential, for intermediate values by means of a Wheatstone Bridge, and for very low resistances by means of a potentiometer.

The results may conveniently be considered in two groups: firstly, those relating to films deposited in vacua lying between 10^{-5} and 10^{-7} mm. of mercury, and, secondly, those relating to films deposited in vacua below 10^{-7} mm. of mercury.

§ 3. RESULTS OBTAINED UNDER POOR VACUUM CONDITIONS

Once the thallium had been thoroughly degassed, enough gas was allowed back into the tube, from the backing, to give pressures as high as 10^{-5} mm. of mercury. The results obtained at various pressures are summarized in figure 2, in which the common logarithm of the resistivity is plotted against the thickness.

The films show, as do the films deposited in good vacua, an initial thickness in which no conductivity is detected. It is clearly shown that the higher the residual pressure in which the films are prepared, the slower the decrease in resistivity as the films thicken. Further, the temperature coefficients are smaller, being in many cases negative (see table 1), as the resulting resistivity increases, for depositions in

Table 1

Pressure (mm. of mercury)	Resistivity at 90° K. for films 50 A. thick (Ω.-cm.)	Temperature coefficient ($\rho_{90}-\rho_{64}$)	Graph
10^{-5}	$2{\cdot}37\times10^{-2}$	−20	*A*
5×10^{-6}	$6{\cdot}32\times10^{-4}$	−8	*B*
5×10^{-7}	$2{\cdot}82\times10^{-4}$	0	*C*
2×10^{-7}	$1{\cdot}26\times10^{-4}$	+0·50	*D*
Less than 10^{-7}	$15{\cdot}8\times10^{-6}$	+0·67	*E*

the poorer vacua. No variation of temperature coefficient with thickness could be detected.

As has been observed by other workers[6], if the films with negative temperature coefficients are allowed to warm up to room temperature they lose a considerable amount of their high resistivity, which is reduced by a factor of 10 or more, and they then have positive temperature coefficients of the same order as that of the bulk metal. This rise in temperature and the subsequent return to liquid-oxygen temperatures must be carried out very slowly, for otherwise the films disintegrate, probably as a result of differential expansion between the film and the glass.

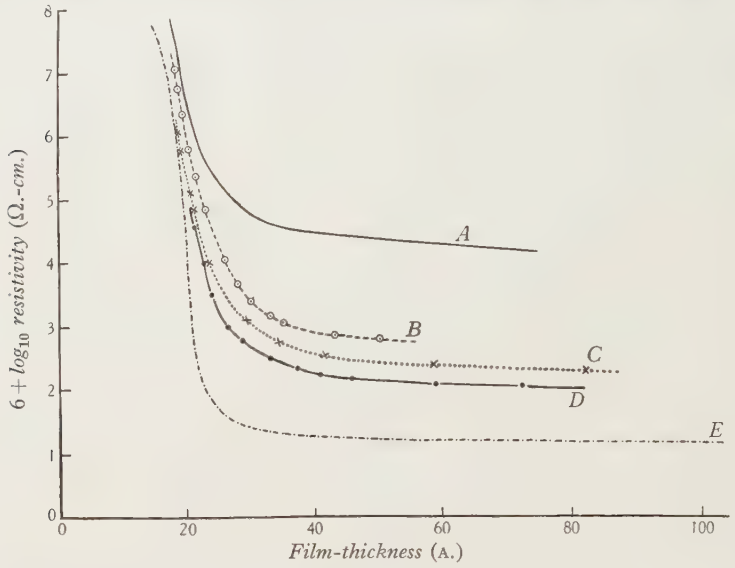

Figure 2. Films deposited at 90° K. in vacua of *A*, 10^{-5} mm.; *B*, 5×10^{-6} mm.; *C*, 5×10^{-7} mm.; *D*, 2×10^{-7} mm.; *E*, less than 10^{-7} mm.

§ 4. DISCUSSION

It seems reasonable to suppose that the higher the pressure in which deposition of the films takes place the more gas the film will contain. From the results obtained, therefore, it seems quite obvious that high resistivities and negative temperature coefficients can be attributed to gas occluded in the metal films, as was proposed by Appleyard[7]. It is tentatively suggested that the high resistivities and negative temperature coefficients observed by earlier workers, apparently working in good vacua, are due to a relatively high local gas pressure in the beam itself, resulting from gas occluded in the evaporating metal. If gas is occluded in the evaporating metal the beam of metal atoms travelling at high thermal velocities to the cooled surface will be accompanied by a similar beam of gas atoms. A fast pump capable of maintaining a good vacuum cannot remove gas atoms from the beam itself, but only those which are scattered from the surfaces on which the atoms impinge.

It has been suggested that the irreversible change in resistivity which occurs

when the temperature of the films is raised is due to recrystallization[6]. But in view of the reversal in sign of the temperature coefficient which accompanies it, it seems more probably due to some, if not all, of the gas coming out of the films. Recrystallization will occur, but cannot account for a factor of more than 8—the change in resistivity on heating from 90° K. and melting—whereas the actual change can be by a factor of more than 10. Moreover the results appear to indicate that, in continuous films more than a few atomic layers in thickness, it is the presence of gas occluded in the films, rather than an inherent high degree of disorder in thin metal films, that accounts for the very high resistivities.

§ 5. FILMS DEPOSITED IN HIGH VACUA

Figure 3 shows two typical experimental curves produced by depositions at 90 and 64° K. in vacua of less than 10^{-7} mm. of mercury. It can be seen that both curves are characterized by a finite range of thickness in which the resistivity is very high, followed by a long range in which the resistivity falls gradually to a value about

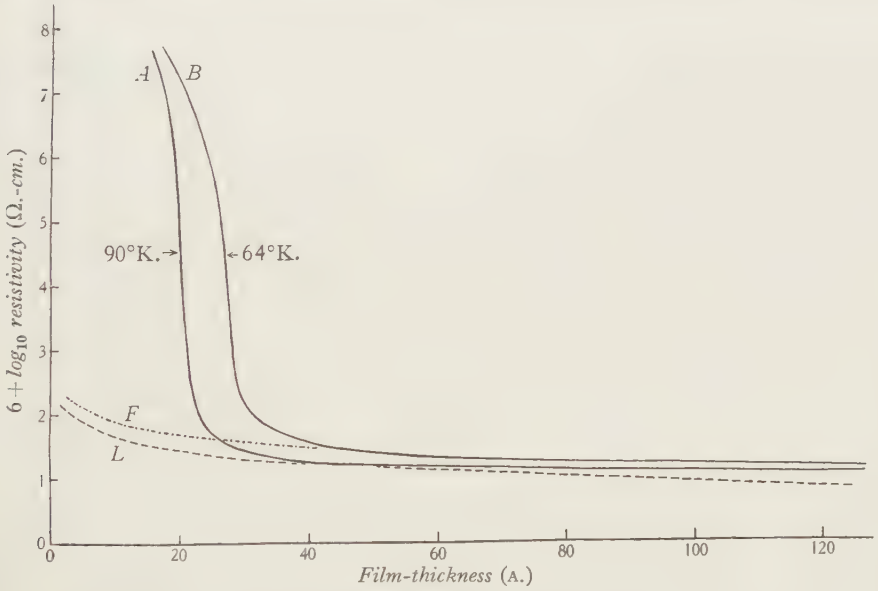

Figure 3. For films deposited in vacua lower than 10^{-7} mm. of mercury. *A*, deposited at 90° K.; *B*, deposited at 64° K.; *F*, theoretical curve from Fuchs' formula; *L*, theoretical curve from Lovell's formula.

three times that of the bulk metal at the same temperature. Even after the pyrex surface had been decomposed visibly by successive distillations, all the curves obtained showed the above characteristics, though in that case the critical thickness at which conductivity was first detected was considerably increased.

One is naturally tempted to attribute the initial high resistance to agglomeration of the material of the film, an explanation which seems quite satisfactory in the case of mercury and alkali films[7]. It is disproved, however, by the observation that the critical thickness, as well as the range of thickness showing high resistivity, increases

very considerably as the temperature of deposition is lowered. It seems possible, therefore, that the initial layers of thallium are deposited with a lattice structure much distorted by the underlying substrate, and that they may in this case show semiconducting properties, as was suggested by de Boer[8] in the case of molybdenum films. Unfortunately in this range of thickness the films show a secular change of resistance which makes the determination of a temperature coefficient impossible, and so it was not practicable to test whether they showed the negative temperature coefficient to be expected on this hypothesis.

Not much can be said about the absolute magnitude of the resistivities. In figure 3 the theoretical curves of Lovell[2] and the modified curve of Fuchs[9] have been drawn in for comparison. Both are calculated on the assumption that the increased resistance of a thin film is to be attributed entirely to the shortening of the mean free path of the conduction electrons by inelastic collisions with the boundaries. There is fair agreement in the range between 40 and 80 A. We believe, however, that this must be attributed to accident, for both theoretical formulae give a temperature coefficient considerably greater for the film than for the bulk metal, whereas the value given by experiment is about three times less; see table 1.

The low experimental value of $\delta\rho/\delta\tau$ obtained for these films equally prevents us from assuming that the excess of their resistivity above that of the bulk metal is attributable entirely, as in films of the alkali metals, to simple strain in the lattice. It seems probable that, even when they are deposited in vacua of 10^{-7} mm. of mercury or less, some gas absorption still persists, and that this reduces the temperature coefficient below the value for the bulk metal. Thallium therefore seems to be more sensitive to traces of residual gas than were the alkalis, for pressures as high as 5×10^{-7} mm. of mercury made no appreciable difference to the properties of these alkali films. Reference to table 1 shows that a residual pressure of this magnitude reduces the temperature coefficient to zero in the case of the thallium films.

To test this hypothesis it would be necessary to deposit films in vacua lower than 10^{-8} mm. of mercury, and these are not yet available with contemporary vacuum technique.

§ 6. ACKNOWLEDGEMENTS

In conclusion I wish to express gratitude to Prof. A. M. Tyndall for his encouragement, to Dr E. T. S. Appleyard for his invaluable advice, and to Mr J. H. Burrow for his skilled construction of glass apparatus. I am also indebted to the Department of Scientific and Industrial Research for a maintenance grant.

REFERENCES

(1) Reinders and Hamburger. *Rec. Trav. chim. Pays-Bas*, **50**, 441 (1931).
(2) Lovell. *Proc. Roy. Soc.* A, **157**, 311 (1936).
(3) Appleyard and Lovell. *Proc. Roy. Soc.* A, **158**, 718 (1937).
(4) Lovell. *Proc. Roy. Soc.* A, **166**, 271 (1938).
(5) Powell and Mercer. *Philos. Trans.* A, **235**, 101 (1935).
(6) Fukuroi. *Sci. Pap. Inst. Phys. Chem. Res., Tokyo*, **32**, 196 (1937).
(7) Appleyard. *Proc. Phys. Soc.* **49** (extra part), 128 (1937).
(8) de Boer and Kraak. *Rec. Trav. chim. Pays-Bas*, **55**, 941 (1936).
(9) Fuchs. *Proc. Camb. Phil. Soc.* **34**, 100 (1938).

THE SCATTERING OF FAST β PARTICLES BY XENON NUCLEI

By R. L. SEN GUPTA, M.Sc.

Communicated by Prof. P. M. S. Blackett, F.R.S., 2 September 1938.
Read in title 25 *November* 1938

ABSTRACT. The nuclear scattering and energy-loss of fast β particles with energy about 2×10^6 ev. has been studied, using a cloud chamber filled with a xenon-oxygen mixture. A radon source in conjunction with an electron lens was used to provide a fairly homogeneous beam of electrons. The results obtained for the angular distribution of scattering are in agreement with Mott's formula. The collisions in which the particles lose 50 per cent or more of their original energy are found to be about six times more frequent than the theoretical number for energy-loss by emission of collision radiation.

§ 1. INTRODUCTION

THE nuclear scattering of fast β particles has been the subject of many investigations, but the results have been somewhat discordant. In the work of Neher[7], Champion[2], Skobeltzyn and Stepanowa[8], Klarmann and Bothe[4], Stepanowa[10] and Zuber[12], the observed angular distribution of scattering was compared with the formula deduced by Mott[6] for the wave-mechanical scattering of β particles, on the assumption that the interaction force is Coulombian. When this formula is integrated over the angles θ_1 to θ_2, it can be written in the form

$$n(\theta_1\theta_2) = \pi N t \left(\frac{Ze^2}{m_0c^2}\right)^2 \left(\frac{1-\beta^2}{\beta^4}\right) \left[\left\{\cot^2\tfrac{1}{2}\theta_1 - \cot^2\tfrac{1}{2}\theta_2 - 2\beta^2 \log\frac{\sin\frac{1}{2}\theta_2}{\sin\frac{1}{2}\theta_1}\right\} + \frac{2\pi\beta Z}{137}\{\sin\tfrac{1}{2}\theta_1 - \sin\tfrac{1}{2}\theta_2 + \operatorname{cosec}\tfrac{1}{2}\theta_1 - \operatorname{cosec}\tfrac{1}{2}\theta_2\}\right],$$

where n is the number of scattered particles between θ_1 and θ_2, β the ratio of the velocity of the particle to that of light, t the total length of the track, N the number of nuclei per cm.^{3} of the scatterer, and Z the atomic number.

Neher worked with relatively slow electrons, with energies up to 145 kv., using an aluminium foil as scatterer, and observed that the number of particles scattered between 95° and 172° was about 20 or 30 per cent higher than that given by Mott's formula. Champion using β particles from *RaE* with an upper energy-limit of $1{\cdot}2 \times 10^6$ ev., and a nitrogen-filled cloud chamber, found a satisfactory agreement between his results and Mott's formula in the entire range of angles between 20° and 180°. Skobeltzyn and Stepanowa on the other hand, using β rays of energy between $1{\cdot}5 \times 10^6$ and 3×10^6 ev., found the scattering in nitrogen between 40° and 180° to be about 40 times the theoretical value. This work has been repeated by Stepanowa[10], who has observed the distribution curve to be considerably above the theoretical curve calculated from Mott's formula. The discrepancy was particularly large for particles whose energy lay between $1{\cdot}5 \times 10^6$ and 3×10^6 ev., where the

observed scattering at angles greater than 90° was 30 or 35 times greater than that calculated. Klarmann and Bothe have studied the nuclear scattering of fast β particles in the energy interval $0{\cdot}5 \times 10^6$ to $2{\cdot}6 \times 10^6$ ev. by krypton and xenon, and have found only about one-fifth of the scattering predicted by the theory. Zuber, however, working with an argon-filled Wilson chamber and electrons whose energy lay between $1{\cdot}7 \times 10^6$ and $2{\cdot}4 \times 10^6$ ev., observed a fair agreement with the theory. Further experiments were clearly required to resolve some of these discrepancies.

§ 2. THE EXPERIMENTAL METHOD

An investigation similar to that made by Zuber was carried out about a year ago with an argon-filled chamber, an electron lens being used for obtaining a homogeneous electron beam with a mean energy of 2×10^6 ev., and a rough agreement with the theory was found. Further experiments were then undertaken with xenon in the chamber. The use of such a heavy gas gives much greater numbers of scattering and energy-loss processes, and so facilitates the work. An electron lens of the type used by Klemperer[14] and by Davies and O'Ceallaigh[3] was used in this investigation to give a fairly homogeneous beam, a radon tube with a strength of a few millicuries being used as the source. The mean energy of the electrons was $2{\cdot}1 \times 10^6$ ev., corresponding to a value of 0·981 for β. The mean spread of energy in the beam was about $\pm$ 10 per cent.

The chamber worked automatically, and stereoscopic photographs of each expansion were taken on cinematograph film with a pair of 35 mm. Ross X-press $F/1{\cdot}9$ lenses. The xenon used in the chamber was diluted with 48 per cent of oxygen. The scattering by the oxygen is negligible as compared with that by xenon, while the total scattering is reduced to a convenient value. This amount of oxygen is also quite sufficient to ensure sharp tracks.

§ 3. RESULTS

Two series of measurements were made to determine the scattering. In the first series an equivalent length of 64 m. of track in 100 per cent of xenon at atmospheric pressure was used to study the angular distribution, and in the second series, an equivalent length of 172 m. of track in 100 per cent of xenon was used to extend the results between 40° and 180°.

In tables 1 and 2 the experimental results have been compared with the theoretical values deduced from Mott's formula.

Table 1. 64 m. of track in xenon

Angular intervals (deg.)	Number of tracks	
	Observed	Deduced from Mott's formula
20 to 30	88	106
30 to 40	45	40
40 to 180	28	45
20 to 180	161	191

Table 2. 172 m. of track in xenon

Angular intervals (deg.)	Number of tracks	
	Observed	Deduced from Mott's formula
40 to 50	50	50
50 to 60	16	28
60 to 70	15	16
70 to 80	5	10
80 to 180	15	14
40 to 180	101	118

§ 4. DISCUSSION OF RESULTS

The experimental values of the scattering between 40° and 180° in the first series are somewhat below the theoretical values, and thus suggest a possible anomaly such as has been reported by Skobeltzyn and Stepanowa, and Klarmann and Bothe. However, the additional data of the second series show no sign of this anomaly. On the contrary, when the statistical error and the error in the measurement of the length of the tracks are taken into account, the agreement between the theoretical and experimental values is as good as could have been expected.

In 330 m. of track, in the xenon-oxygen mixture, 30 collisions have been observed in which electrons lost 50 per cent or more of their initial energy, 12 being completely stopped in the gas. The theoretical number of such energy losses, if they occur by the emission of collision radiation, is about 5[1]. Thus the experimental number is about six times the theoretical value. A discrepancy of this type has already been reported by Skobeltzyn and Stepanowa[9], Leprince Ringuet[5], Klarmann and Bothe[4], and Turin and Crane[11]. The number of such collisions being relatively small, their influence on the distribution of scattering is negligible.

No evidence has been obtained for the creation of pairs by fast β particles in nuclear collisions.

§ 5. ACKNOWLEDGEMENTS

The work was carried out at Birkbeck College, London. I wish to express my thanks to Prof. P. M. S. Blackett, F.R.S., for suggesting the problem, and for his continued interest and advice during the progress of the work.

NOTE ADDED IN PROOF

After the submission of the present paper, Fowler and Oppenheimer[13] published results of a cloud-chamber investigation of the scattering and energy-loss of fast electrons, with energies ranging from 5×10^6 to 17×10^6 ev., in a thin lamina of lead. They found, in agreement with the author's results, a scattering-distribution consistent with the theory. The mean energy-loss was observed to be about 1·5 times the theoretical value, but, owing to difference in the experimental arrangement, it is difficult to relate this result to the observation, mentioned above, of an abnormal number of large losses.

REFERENCES

(1) Bethe and Heitler. *Proc. Roy. Soc.* A, **146**, 83 (1934).
(2) Champion. *Proc. Roy. Soc.* A, **153**, 353 (1936).
(3) Davies and O'Ceallaigh. *Proc. Camb. Phil. Soc.* **33**, 540 (1937).
(4) Klarmann and Bothe. *Z. Phys.* **101**, 489 (1936).
(5) Leprince Ringuet. *C.R. Acad. Sci., Paris,* **201**, 712 (1935).
(6) Mott. *Proc. Roy. Soc.* A, **124**, 426 (1929).
(7) Neher. *Phys. Rev.* **38**, 1321 (1931).
(8) Skobeltzyn and Stepanowa. *Nature, Lond.*, **137**, 456 (1936).
(9) Skobeltzyn and Stepanowa. *Nature, Lond.*, **137**, 234 (1936).
(10) Stepanowa. *Phys. Z. Sowjet.* **12**, 550 (1937).
(11) Turin and Crane. *Phys. Rev.* **52**, 610 (1937).
(12) Zuber. *Helv. phys. Acta,* **11**, 370 (1938).
(13) Fowler and Oppenheimer. *Phys. Rev.* **54**, 320 (1938).
(14) Klemperer. *Phil. Mag.* **20**, 545 (1935).

DISCUSSION ON ELECTROACOUSTICS

Opening remarks by C. V. Drysdale, D.Sc., C.B., O.B.E.

Greatly as I appreciated the honour of being invited to open this discussion, I accepted it only after considerable hesitation as it is many years since I was actively engaged in acoustic problems and I felt that the task should have been entrusted to someone who has kept abreast with the recent rapid developments. I propose therefore to confine my remarks to a few fundamental points which seem to me of importance for future progress.

The title "electroacoustics" seems to me happily chosen, for the two sciences are becoming more and more closely associated and the more we consider electroacoustic devices as a whole rather than as separate electrical and acoustic components the better. Nearly 40 years ago when I first tried to teach alternating-current theory to evening students, I soon saw the advantage of employing mechanical analogies and equations; and the modern treatment of electroacoustic devices as

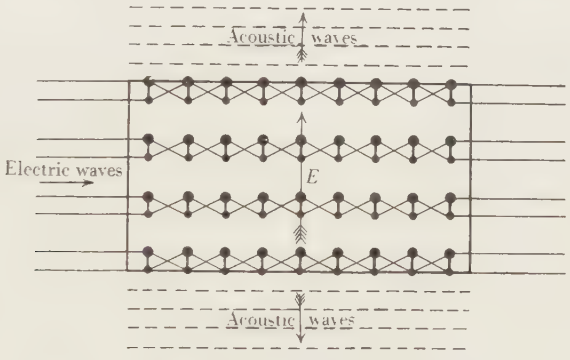

Figure 1. Conversion of electric to acoustic waves.

equivalent to electrical circuits has been of great assistance towards their complete understanding and design. But the connexion between electric and acoustic waves goes much deeper, and as wireless telephony or broadcasting now forms such an important part of the subject, a few words on this connexion and its practical implications may be of interest.

Relation between electric and acoustic waves. According to the Maxwellian theory, electric waves consist of transverse electrical displacements travelling with the velocity of light, and when they pass through a material dielectric the protons and electrons forming its molecules are displaced and vibrate transversely in opposite senses as shown in figure 1. Acoustic waves on the other hand consist of vibrations of the molecules as a whole in the line of propagation of sound. If the protons and electrons were of equal mass and vibrated in opposite phase with equal amplitude when subjected to an alternating electric stress, no acoustic effect would be produced; but as the mass of the molecules resides almost entirely in its protons,

it seems reasonable to suppose that their motion has a preponderating effect and hence produces acoustic waves transverse to the electric waves. This supposition is confirmed by the fact that a block of dielectric material subjected to a high alternating electric stress of sonic frequency emits an audible note; and in certain crystals, notably quartz, tourmaline and Rochelle salt, this effect is sufficiently large to be of service for both acoustic transmitters and acoustic receivers, especially if the crystal is cut to such dimensions as to be in resonance. If the whole power of a broadcasting station could be radiated at sonic frequency, it seems likely that it would be heard to a considerable distance simply by the vibration of the molecules of the air, in spite of their relatively small number; but, fortunately for our already tortured ears, high-power electrical radiation involves frequencies far above the audible limit and this high frequency requires rectification of modulated waves to render them audible, which is a very inefficient process. Even the old crystal sets, however, did good service in their time, and it is easy to see that if all the energy from a broadcasting station which enters an average room could be efficiently transformed, good audibility should be obtainable at ranges of hundreds of miles.

Until a few years ago we had only a very rough idea of the power required for audition, but thanks to the pioneer work of Fletcher in 1925 and to subsequent work, we now have a useful practical standard and scale of sound-intensity. The unit or minimum audible intensity, the phon, has been defined by the British Standards Institution as an r.m.s. pressure of 2×10^{-4} dyne/cm^2, which corresponds to an r.m.s. displacement velocity of about 5×10^{-6} cm./sec., a displacement of about 10^{-9} cm. at a frequency of 1000 c./sec., and a power of about 10^{-16} W. per cm^2. For ordinary conversation in quiet surroundings, an intensity of 40 phons, or decibels above the threshold, is sufficient, which requires a power W of $10^{-16} \times 10^4 = 10^{-12}$ W. or one $\mu\mu$W. per cm^2. Since $W = P/4\pi r$, where P is the total power emitted by a source and r is the distance,

$$r = \sqrt{\frac{P}{4\pi W}} = 9 \times 10^7 \text{ cm.}$$

or 900 kilometres, if P is 100 kW.; and as the electric radiation is somewhat concentrated towards the surface of the earth it appears that 100 kW. of electrical radiation should provide satisfactory audition up to a radius of 1000 kilometres if it could be completely transformed into acoustic energy.

Although there is no prospect at present of such perfect transformation it is of interest to consider a possible application. In figure 2, suppose we have two flat horizontal plates, *ab* and *cd*, say on the ceiling and floor of a room, and a very thin sheet of rubber or cellophane *ef* in contact with the lower surface of the plate *ab* which should be perforated to ensure equal air pressure on both sides of the film. The lower surface of the film *ef* should be silvered to render it conducting and be connected to the bottom plate *cd* through a tuning inductance L, while *ab* is connected to *cd* through a choke coil and high-tension battery giving an e.m.f. E which can be varied to cause the film *ef* to be attracted against *ab* with a very ligh pressure. If electric waves traverse the space between the plates, L can be adjusted

to resonance, and if v is the induced voltage, the attractive force varies proportionally to Ev, tending to cause the film to vibrate with the frequency of the waves and with amplitude proportional to v. Owing to the high frequency of the carrier waves, their effect on the film would be inappreciable and in any case inaudible, whether the wave is modulated or not, if the film is equally free to move up or down, but if the film is just in contact with the plate it is free to move downwards but not upwards, and this should give a rectifying effect and an audible response to modulated waves.

Whether such a device would be of any practical use or not is open to question, and it would hardly be welcomed by valve manufacturers, but it is extremely simple and clearly shows the basic requirements of a broadcasting receiver: (*a*) electrical resonance to collect all the available power in a given volume, (*b*) transformation of electrical to acoustic power, and (*c*) rectification to separate the modulated from the supersonic vibrations. The unsymmetrical motion of the film is the mechanical equivalent of the rectifying crystal or valve, and it exists to a small extent even in

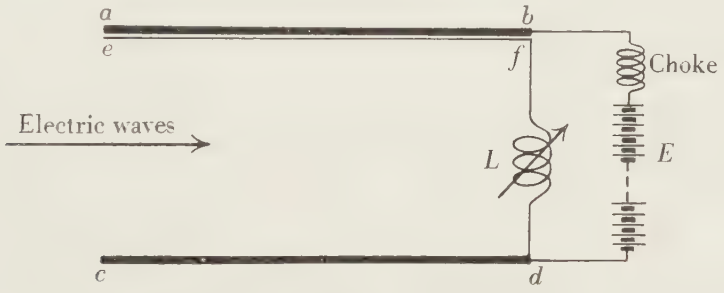

Figure 2. Schematic broadcast receiver.

our ears, as a result perhaps of the articulation of the ossicles, so that we can hear modulations of powerful supersonic waves.

Incidentally it seems possible that a large metal plate covered with a thin layer of soft fibrous material such as silk chiffon and a conducting film would make an excellent condenser microphone or loudspeaker for use with ordinary receiving sets, as the extreme lightness of such a film and the small amplitude needed with a large area should render it uniformly responsive to all acoustic frequencies. Such a device could be fixed as a flat panel on a wall or ceiling, or form the surface of a sound-picture screen. It seems quite likely that it will be true before long that "walls have ears" and also tongues, whether the prospect is pleasing or not.

The physical nature of electric waves. There is another connexion between acoustic and electric waves, however, which greatly assists the comprehension of the latter. Although the Maxwellian theory is supposed to be well known and many are able to handle its equations with enviable facility, its physical basis and implications seem to be little understood—so much so that its validity is now disputed. During the last few years I have been trying to simplify the Maxwellian theory and get down to its physical foundation, and have found that both the Maxwellian equations and the fundamental equations of acoustics can be reduced

to simple and similar algebraic equations from which the phenomena of electric and acoustic waves can be easily developed and made physically intelligible. One example may interest radio engineers.

If we agitate one end of a cord, transverse waves travel along it, and in any textbook of acoustics it is shown that the velocity V of propagation of these waves is

$$V = \sqrt{\frac{T}{m}},$$

where T is the tension in the cord and m its mass per unit length. Now opposite charges attract one another as if they were connected by elastic contractile threads which become thinner as their length is increased, and the attractive force or tension T in the thread between a proton and electron, of charges $+e$ and $-e$ respectively separated by a distance r in a medium of permittivity k, is e^2/kr^2. But a moving charge is equivalent to a current element and produces a magnetic field which possesses energy, and since it is due to the motion of the charge it is sometimes called electrokinetic energy, in correspondence with the kinetic energy of a moving mass. This implies that an electric field has mass or density, so that a charged body has what we call electromagnetic mass; and if we consider an electric field as being made of fibres or bonds, a simple calculation shows that the mass m of a bond connecting a proton and electron in a medium of permeability μ is $\mu e^2/r^2$ per unit length. Hence if either the proton or the electron is agitated, waves should travel along the bond with a velocity V such that

$$V = \sqrt{\frac{T}{m}} = \sqrt{\frac{e^2/kr^2}{\mu e^2/r^2}} = 1/\sqrt{(k\mu)},$$

and this is Maxwell's formula for the velocity of propagation of electric waves. In space, k and μ have certain absolute values k_0 and μ_0 which we have not been able to determine separately, but we can measure their product $k_0\mu_0$ by simple electrical measurements, and $1/\sqrt{(k_0\mu_0)}$ comes out to exactly the velocity of light as determined by direct measurements, or very nearly 3×10^{10} cm./sec.

This gives one illustration of the assistance which can be given by acoustics or mechanics towards the understanding of electric waves, and its practical value may be considerable as it indicates that we can determine and visualize the transmission from an oscillator by the help of simple models with stretched strings.

Acoustic measurements. Progress in science and its technical applications depend enormously upon measurement, but in this respect acoustics has been seriously hampered and it is remarkable how much has been achieved in spite of this obstacle which has only recently been partially overcome. Within a couple of decades after the advent of electric generators, motors and transformers, we had fairly accurate units and primary standards of p.d. and current, and ammeters, voltmeters and wattmeters of high sensitivity and wide range; but it is only a few years since we have settled on a definite unit and scale of acoustic intensity and have developed instruments capable of measuring intensities directly and conveniently.

On fundamental grounds it seems that acoustic measurement is the most difficult of all technical measurement problems. As was mentioned above, the

power in acoustic waves is extremely minute—only about 1 $\mu\mu$W./cm.^{2} for ordinary speech—and it is extremely difficult to collect the power from a definite area and concentrate it on the measuring element, owing to the disturbance of the waves by the presence of the measuring instrument itself. Moreover all solid substances reflect sound, so that laboratory acoustic measurements resemble photometry in a room in which the walls, ceiling, floor, furniture and observers are all mirrors; while in the open they are liable to serious disturbance by air currents which cannot easily be shielded. In all these respects acoustic measurements are at a great disadvantage compared with electrical measurements, but there is one matter in which the advantage is on their side—they are nearly always made in one medium, so that the power can be determined from measurements of pressure or displacement alone and there is no need for phase-measurements or wattmeters.

Before the advent of thermionic valves the Rayleigh disc and acoustic pendulum were almost the only devices which enabled acoustic power to be directly measured, but they were so delicate that they were very rarely used, and the only portable instrument was the Webster phonometer, which was probably insufficiently sensitive for all but loud sounds. Now we have several types of direct-reading valve instruments of ample sensitivity, but they all require calibration, and the two main desiderata now appear to be a simple standard source of sound, and more effective acoustic absorbing materials.

As regards the standard source, the ideal would be a sphere expanding and contracting over its whole surface with a known uniform amplitude, and some years ago I suggested covering a solid metal sphere with a layer of quartz crystals; but this would only give a very small amplitude for an inconveniently high voltage, and I am inclined to think that the best standard would be a solid metal sphere say 10 cm. in diameter covered with a layer of fibrous material about 1 mm. thick like a tennis ball and having a thin rubber envelope gilded on the outside. I rejected this idea earlier on account of the difficulty of measuring the amplitude of a delicate film, but Prof. Andrade has since shown that the amplitude of vibration of the air itself can be measured by observing fine smoke particles through a microscope, and moreover since the acoustic absorption of a thin layer of fibrous material should be extremely small, the radiated power should be directly measurable with a wattmeter. A sphere 10 cm. in diameter vibrating with an amplitude of 2×10^{-4} mm. should give an acoustic intensity of about 50 phons at a distance of 3 m. for a frequency of 1000 c./sec. and a total power of about 10 μW.; and with an alternating p.d. of 1000 v. between the sphere and film, the maximum electrostatic force would be nearly 0·2 g./cm.^{2}, so that it should not be difficult to find a material which would yield sufficiently under this pressure to give the above displacement.

Acoustic absorption and noise-reduction. The problem of noise-reduction has become one of ever-increasing urgency, and although a great deal of work has been done on it lately with encouraging results, especially as regards comfort in air and railway travel, there is great need for further improvement, for the sake not only of general comfort but also of facilitating acoustic measurements. Reduction of noise to 10 or 20 phons would give great relief, but for acoustic measurements

almost complete suppression with a minimum thickness of sound-absorbing material is desirable. Up to the present, investigations appear to have been confined to testing the acoustic absorption of various materials, and I do not think the scientific aspect of the problem and its possible application to the production of absorbent materials has received much attention.

The obvious means for absorbing sound is to communicate the acoustic vibrations to small granules or fibres which dissipate the energy in friction, but the density or inertia of solid particles is so high compared with that of air that their direct response is very small, and hence the attenuation is low and a large thickness of material is required for effective absorption, as can be seen in certain acoustic laboratories. But since the energy of a vibratory motion is proportional to the square of its amplitude, a tenfold increase of the amplitude of the particles would dissipate a hundred times the energy, and the simplest way of increasing their amplitude is by resonance.

According to the famous optical dispersion theory of Drude this is the way in which light is absorbed. Reverting to figure 1 it will be noticed that the protons and electrons of the dielectrics are shown as being coupled by elastic bonds, and since the protons and electrons have unequal masses each atom will have two resonance frequencies for either of which the amplitude or electric displacement will build up to a high value if excited by a continuous train of electric waves. This is equivalent to a great increase of the permittivity k of the dielectric, and hence causes a great reduction of the velocity of propagation V, equal to $1/\sqrt{(k\mu)}$, for waves of either of these frequencies. Hence if there were no dissipation of energy, light of either of these frequencies would be unable to pass through the medium, and the spectrum of the transmitted light would be crossed by two dark lines or absorption bands; but if the dielectric is slightly conducting, energy is dissipated and the bands become broader. In complex molecules, represented by lattice models with a dozen or more balls, the number of degrees of freedom and resonance frequencies is very large, and hence the absorption bands are very numerous; and if they are sufficiently broad and evenly spaced, a thin layer of the material may be practically opaque to all waves over a wide range of frequencies, although even in a solid material the space occupied by the molecules is a very small fraction of the total volume.

This indicates that an acoustic absorbing medium should have (*a*) a large number of resonance frequencies fairly evenly spaced over the frequency range to be covered, and (*b*) sufficient internal friction to broaden the bands and dissipate the energy without overdamping and unduly reducing the resonance. It is far too much to expect to find such a combination of properties in any natural material, but it does not seem as if it should be very difficult to produce one artificially.

Suppose we have a couple of sheets of thin cellophane, press them between dies so as to cover them with indentations of various sizes and shapes, put a little light powder in each indentation and then stick them together so as to form a single sheet covered with partially dust-filled cavities or bubbles having different resonance frequencies. If the sizes of the bubbles were suitably graded and the

quantity of powder in each were suitable, a single sheet of this kind would have the desired characteristics and should have considerable absorptive effect with almost negligible weight. Of course a considerable amount of experiment would be required to produce sheets which would absorb nearly uniformly over the large frequency range (nearly 14 octaves) of audible sound, but a start could be made with bubbles of a single size and determining the frequency of the sound which they refuse to pass, and from a few such experiments the required form of the dies could be designed with sufficient accuracy. As the bubbles could be very close together it seems possible that a few sheets of such material mounted nearly in contact would give a high degree of absorption for a small thickness. They should be sufficiently transparent for use with office windows in noisy streets, and a grid of strips of the material an inch or so wide mounted fairly close together would probably give considerable acoustic absorption with little interference with light or ventilation.

Although these remarks and suggestions have been based purely on theory and I have not kept in touch with recent developments sufficiently to know whether any of them may have been made by others, I hope they may be of some service both for future progress and for stimulating this discussion.

DISCUSSION

Mr W. West. The oldest of all acoustical measuring devices is the human ear. In recent years apparatus for objective measurements has taken much of the burden of testing away from the ear. But subjective testing still is, and is likely to remain, of basic importance to progress in electroacoustics. The proper functions of subjective and of objective tests are, in fact, complementary. The ear is the final arbiter and the main responsibility rests on the results of subjective tests. Subjective tests are essentially comparison tests, and the ear requires a real and relevant standard for comparison. For example, if two transmission systems with loudspeakers are to be compared for quality, it is I think insufficient merely to ask the observers which they judge to be the better. Instead, a comparison with the original source of sound, heard in the same room under natural listening conditions, would give the ear a chance to decide which transmission is more like the original. The ear is so adaptable that small details of the technique of testing can introduce an unwanted influence on the result; moreover the avoidance of conscious or unconscious personal bias by the observers often requires careful study. Time does not permit me to do more than draw attention to the importance of subjective tests and to the need for continued scientific study of the methods whereby the most relevant and reliable information can be obtained therefrom.

Mr G. C. Marris. The achievements of research in electroacoustics have been so considerable in recent years, and their practical embodiments so important, that some of the weak points still outstanding may get overlooked.

On the radio-engineering side, more particularly in the broadcast-receiver field, many difficulties exist. For example in the design of loudspeakers it has apparently

been impossible for mathematical science to deal with the problem of the typical vibrating paper cone of a loudspeaker. This seems to be due to the existence of so many degrees of freedom in the parts that are coupled together and the difficulty of specifying boundary conditions. The cone is coupled at its centre to a moderately stiff coil and is constrained at its outer edge; it is the aim of most designers to make the outer edge of the cone extremely flexible, while the centre is sometimes stiffened with dope, in order to get a good response at low frequency. As is well known, the

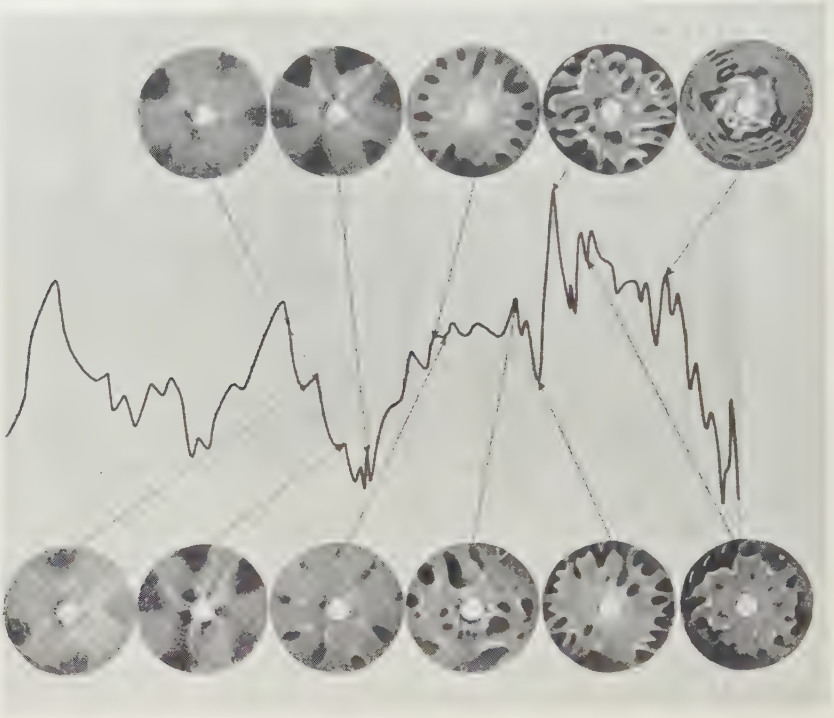

Figure 3.

cone vibrates as a whole or in other modes according to the frequency, and as a result of an immense amount of empirical work designers are able to make loudspeakers with a variety of frequency-response characteristics. It is unfortunate that there seems to be no theory for use as a guide to any further advance, and empirical methods still hold the field. Figure 3 shows the frequency-response characteristic of a typical loudspeaker with a number of photographs of the vibration pattern on the cone at certain points along the curve.

Even when a particular frequency-response characteristic can be attained at will, we have to face a very difficult problem in interpreting the behaviour of the loudspeaker with actual speech or music and appraising its value as a reproducer. In the first place there arises the difficulty of the reverberation time and natural frequencies of the room in which the loudspeaker is tested. These characteristics

of the room may markedly affect the reproduction, and the fact that loudspeakers are used in cabinets of various sizes adds in effect another resonator to the long chain of coupled systems. Various methods for obtaining useful objective measurements in such conditions have been used, and I would like in particular to refer to one which has been developed by my colleague Mr Brittain and demonstrated

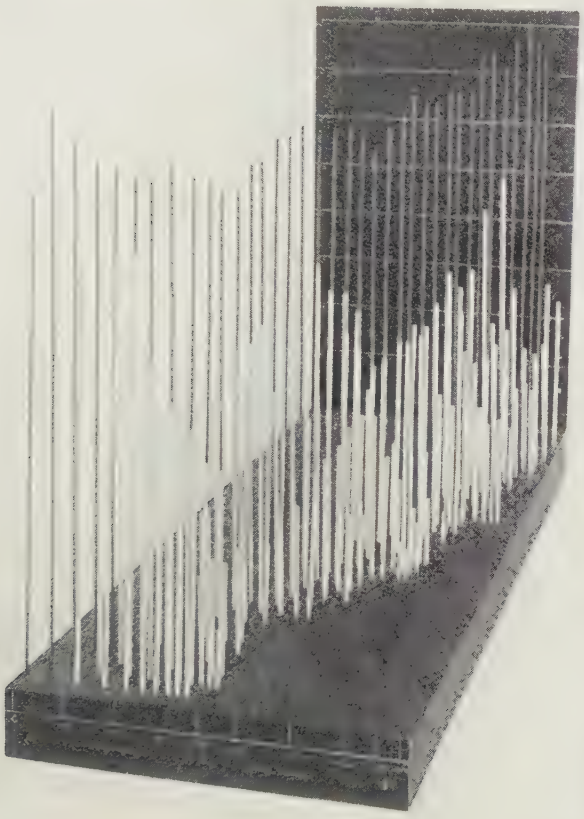

Figure 4.

at the Physical Society's exhibition. A description appears in the *Wireless Engineer* of January 1938.* This we have found very useful. It consists briefly in feeding the loudspeaker with a source containing, in effect, components of all frequencies in a band and analysing the loudspeaker output with a sharply tuned analyser. The noise is the shot noise from a saturated diode, and experience shows that this method can be used in a normal room to give results closely comparable with those obtained by measurements of single frequencies in a damped room or in the open

* Brittain and Williams, "Loudspeaker reproduction of continuous spectrum input", *Wireless Engr* (January 1938).

air. It is of particular use when a loudspeaker is in a cabinet, for measurements in damped rooms, unless these are inconveniently large, are unsatisfactory in such a case. It is also useful where extraneous noises are large, and a current issue of *Electronics* describes how our method is being used in America inside aeroplane cabins. The effect of peaks and cut-off shown in a response curve can be roughly estimated, so that we can by inspection of such a curve see what will be the general performance of the loudspeaker and what difference would be made by shifting a peak, say, $\frac{1}{5}$ of an octave, or altering its amplitude by 3 db. or so. Major errors can thus be avoided. There remain, however, a large number of cases in which listeners find important differences which are very difficult to trace to particular electroacoustical sources. One that immediately presented itself was the generation of harmonics, and we have devoted much time to this. There are, of course, cases in which, owing to the low radiation efficiency of a small cabinet, a bass note is so cut that the harmonics, those natural to the original musical instrument or voice, may have their relative intensity increased to several hundred per cent. In addition to these well-known cases we have made an estimation of the audibility of the whole range of harmonics in the presence of the fundamental, for loudspeakers under conditions of use. This involved an immense amount of work as a large number of fundamentals must be chosen and harmonics up to the 10th must be searched for; tests must be made at various levels of output and with different types of loudspeakers. One immediate difficulty is that the results are very voluminous. They have been demonstrated in the form of models at the Physical Society's exhibition; figure 4 shows a model, which indicates the nature of the problem; the dark rods represent fundamentals and the white rods in the same rows represent the corresponding harmonics.

It has been known for some time that very small percentages of higher harmonics will be noticed by a listener in comparing two loudspeakers. Our attempt was to carry this observation further so that one might be able to say if a harmonic of measured percentage at a particular frequency or band of frequencies was in fact the cause of the users' criticism in a particular case. The attempt has not been carried on long enough to enable the question to be answered fully, and there are undoubtedly inconsistencies. It is necessary to take into account the whole tonal balance of the loudspeaker and set, and possibly the effect on transient sounds of any peaks in the response curve and, as Mr West said, of intermodulation products. Meanwhile for practical purposes an assessment of quality by measuring and weighting certain harmonics is in actual use in the radio industry as an aid to the specification of performance, but then it is doubtful whether this method is of any use to the design engineer.

Dr Phyllis Kerridge. For the appreciation of even the most perfect electroacoustics, both the ear and the brain are necessary. The ear is a physiological mechanism, which, like a physical mechanism, occasionally goes wrong: and is like a physical mechanism again, in that one can learn about its working by finding out why it goes wrong, and how it can be put right.

Electroacoustics has already invaded otology. We have hearing aids, and also audiometers. It is still quite exceptional to be able to get any figures concerning the physical characteristics of hearing aids. This elementary lack is a real bar to progress. I would like to take the opportunity afforded by this occasion of stressing the problem of audiometers, which are now available for testing the auditory threshold of deaf persons. They would be more generally used in clinical practice if they were cheaper. But the essence of the present difficulty is the variety of audiometers which is offered. The otologist cannot by himself decide between a good and an indifferent instrument, and cannot state the minimum physical standards to which such instruments should be made. When I plead for co-operation between the physicist and the otologist I do not wish to seem ungrateful to the many physicists (several of whom are present to-day) who have helped me in the past. I think there is a good case for a permanent coalition.

We all know that knowledge is worth seeking for its own sake, and that one cannot tell what pure knowledge gained by this generation may not result in material benefits to the next. But there is no reason for avoiding a research which would quite certainly benefit the present generation.

Mr S. Hill. The subject is very wide, embracing much of the field of communication engineering. In a certain sense, telephony is just two electroacoustic problems joined by a transmission problem. There is a tendency among electrical engineers to be biased towards the electrical side and to regard acoustics rather as the nuisance side. After a famous definition of early medicine, public-address engineering might once have been described as the art of putting electrical apparatus of which we knew little into buildings of which we knew nothing. Though this state of ignorance has passed, many acoustic problems remain and they are the more awkward because they are partly aesthetic. The technical and the aesthetic can only be wedded if technician and artist co-operate from the earliest stage of design. They should work together to make their building independent of public-address aid, but should nevertheless make provision for public-address systems which special circumstances may always make necessary. The electroacoustic expert is too often called on to provide solutions that basic design has made impossible. I would like to see reverberation-meters and noise-meters popularized. For this they need to be much simpler and more workable. We might then have fewer of those unpractical acoustic surveys which are performed in an empty (and quiet) hall, both the absorbing and the emitting functions of the audience being neglected. Measured results in halls must be treated with caution, as any engineer will see if he calculates the required acoustic power in terms of the reverberation time for a room for which his experience tells him a 10 w. amplifier is needed. He will probably calculate a few milliwatts.

Dr L. E. C. Hughes. A subjective method of estimating the quality of reproduction of broadcast programme receivers has been in use by the Apparatus (Approval) Subcommittee of the Central Council for School Broadcasting for about 6 years; the committee has trained itself to assess quality of reproduction on a scale, which

has been shown to be consistent, and to say whether or not the receiver under test is of adequate quality for use in receiving broadcast lessons in schools. For the speech test, a local studio and modulating system uses the type of apparatus used in normal transmission. The characteristics of the speakers, both male and female, are studied by the non-technical members of the committee before the quality on a standard reference receiver and loudspeaker, which are always maintained, are judged. The reference receiver is to assist the members of the committee in recollecting the desirable characteristics of the speakers' voices, and so estimating the degree of defect in receivers under test, a special regime of testing between the standard and test being maintained. The reference standard is not the best that could be obtained, otherwise the members of the committee would not be able to recognize receivers which might be better in performance than the standard, which is definitely better than the minimum tolerated for class-room purposes.

By making tests on receivers, which have been independently measured in the manner laid down in the Radio Manufacturers' Specification for receiver testing, it was hoped to correlate the objective tests with the subjective rating, but there appeared to be no correlation and further experiments must be made.

There is no doubt that the final test of a reproducing system is an aural comparison of the reproduction with the original, but the instances where this is possible are comparatively rare and have to be specially arranged. There are no means whereby the public can assess the value of high-grade reproduction under suitable conditions. The special technical tests are to satisfy the designers that the apparatus is functioning as intended, and to enable them to chase faults. The final test must be a subjective one, so that it may be possible to recognize the commercial tolerance of departures from the ideal specification of reproduction.

Mr L. C. Pocock. The connecting link which unites an electric to a mechanical or acoustic system is a transfer impedance and is often called the "force factor"; it has interesting similarities to and differences from an electrical transformer. For example, for maximum transfer of energy from an electrical resistance containing an e.m.f. to a mechanical resistance, the force factor should be equal to the geometric mean of the two resistances. Reactances of the same sign in the two systems neutralize each other under certain conditions; for example, if there is an electrical inductance on one side and a mass reactance on the other side and the force factor is the geometric mean of the resistances, the frequency characteristic is as at (*a*), figure 5, with maximum efficiency at zero frequency where reactance is zero. If the force factor is progressively increased, characteristics like (*b*) and (*c*) emerge, having maximum efficiencies at certain frequencies where the electrical and mechanical reactances neutralize; thus with a slight loss of maximum efficiency a flatter response curve is obtained with a higher force factor.

As an example of modern application of this and other acoustic principles, I will refer to a recent improvement in telephone receivers.* New magnetic materials

* J. S. P. Roberton, "An improved quality commercial telephone receiver", *Elect. Commun.* **17**, no. 2, p. 116.

have enabled an increase of 100 per cent to be obtained in force factor with resultant advantages in frequency characteristic as has already been described. In addition, the acoustic side of the instrument, which has long been neglected, has now been designed on sound principles analogous to those encountered in electrical networks;

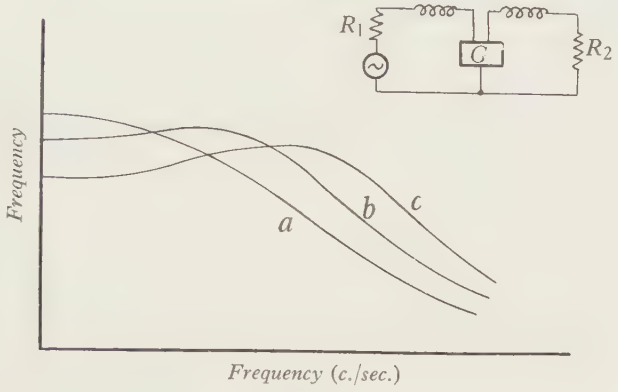

Figure 5.

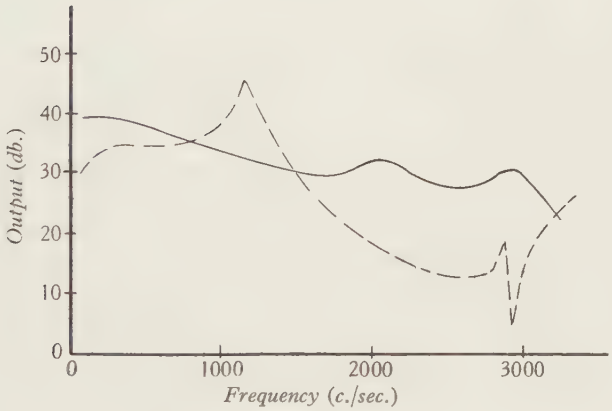

Figure 6.

the resultant improvement in frequency characteristic is shown in figure 6. From the transmission point of view the high peak in the old characteristic was prejudicial in reinforcing unduly the vowel sounds, which are already high in energy-content and masking to some extent the higher speech frequencies. The gain in output at the higher frequencies with the new design enables the new receiver to produce substantially the same speech loudness as the old receiver.

Mr H. A. M. Clark. I should like to describe the underlying principle of a device used at the E.M.I. laboratories for recording the results of electroacoustic calibrations. The main features of the instrument are the accuracy of the logarithmic law to which the scale conforms and the use of a robust meter, of comparatively low current-sensitivity, for chart recording. The meter is controlled by the automatic adjustment, by means of a series of relays, of a resistance attenuator, the

deflection being proportional to the attenuation required to keep the output level of the attenuator constant.

Mr John McLaren. Although this discussion is primarily on electroacoustics, I am not going to talk on that subject, but on architectural acoustics, since I am responsible for the acoustical design of the studios of the British Broadcasting Corporation. But since I have been given a lead by Dr Drysdale, who mentioned the subject of absorption by resonance, I feel justified in my choice of subject. Dr Drysdale mentioned that electroacoustics was the bringing together of electricity and acoustics, and in a similar way I can say that architectural acoustics brings together acoustics and architecture.

In the laboratories of the B.B.C. Research Department we are carrying out an extensive research on absorption by resonance, and we have found that to obtain absorption in the lower frequencies it is preferable to use this means rather than an excessive thickness of porous absorbent, which is very clumsy from the architectural point of view. It is one of the most important points in architectural acoustics that the treated studio should be pleasing aesthetically and not look like a warehouse or a packing shed. Natural structural features, such as can be constructed by normal building-construction methods, are always used to obtain this resonant effect. Anything in the nature of accurately designed resonant chambers are strictly barred by reason of the cost and difficulty of construction.

The first element which gives considerable resonant absorption is the ceiling, which is of normal lath and plaster on wood joist construction. This has a natural resonant period far down in the scale, and gives good absorption in the region of 50 c./sec. The next element is lath and plaster, which consists of wood or other non-metallic lathing spiked to battens spaced with from 14 to 18 in. between their centres and rendered with lime and hair plaster. This has a fairly wide absorptive region up to about 250 or 350 c./sec. Finally, there is wood panelling of studio construction, which gives further resonant absorption in the same region of the frequency spectrum. It has a further use in enriching the tone from orchestral music. For the upper frequencies a 1 in. thickness of rock wool, asbestos, or felt is used. These materials have a fairly straight absorption characteristic for frequencies above 500 c./sec. Below this frequency the absorption drops off until it is very small at 50 c./sec. By careful proportioning of the quantities and by suitable placing of these elements, an overall flat characteristic up to about 3000 c./sec. is obtained. There is generally a falling off in the reverberation time for the higher frequencies, which is due in a great measure to air absorption in large halls, and also to the generally increased absorptive value of the materials for the highest frequencies.

In the design of these studios, it has been found that it is impossible to calculate even approximately the reverberation time from absorption coefficients which have been measured in the reverberation chamber. This is probably due to two effects, firstly that the conditions of measurement in the reverberation chamber are not the same as those used in the studio, and secondly that it does not seem correct

to add porous absorption, which is resistive, arithmetically, to resonant absorption, which is reactive. It is considered that these should be added vectorially, in analogy with electrical impedances, and it is hoped in due course to be able to evolve a new reverberation formula which will take into account the presence of reactive and resistive absorbents.

Mr R. A. Bull. The problem of obtaining high acoustic absorption is particularly acute in the design of rooms to simulate the condition of a free sound field. To obtain a high ratio between direct and reverberant sound for measurement purposes, the surface area of the room should be large and the average absorption coefficient should approach unity. An interesting form of wall treatment has been suggested by Bedell* consisting of multiple layers of muslin and flannel spaced at unequal intervals from the wall. Such a structure can give a substantially uniform absorption coefficient of 0·98 over the frequency range 250–5000 c./sec.

In a room having a high absorption coefficient, I have found that the average pressure generated by a small source may fall at a greater rate than would be anticipated from the inverse square law at frequencies at which the air absorption should have been negligible. This is particularly true if the measurement is made adjacent to one of the boundary walls. It has been suggested that this may be due to the wave-front being bent towards the absorbing surface, with the result that more energy strikes the surface than if the wave-front remained plain.

There is one aspect of equivalent-loudness measurements by objective noise-meters which I should like to mention. The noise-meter, in its usual form, measures the quantity $\surd(\Sigma P^2)$, where P is a pressure component at a given frequency of a complex sound field. If a weighting characteristic simulating a constant-loudness contour of the ear is used in the meter, the quantity measured is modified by suppression of the contribution of low-frequency and high-frequency components. Since, on a loudness basis, the appreciation by the ear of the contribution of a given component does not bear a simple relationship to the pressure of that component, the noise-meter is open to a fundamental error. This was emphasized to me recently by the following experiment. A pure tone was produced in a highly damped room, the tone having an intensity corresponding to the intensity of the loudness contour used for the weighting network in the meter. The equivalent loudness of the pure tone was measured by the subjective technique recommended for the establishment of the phon, and also with the meter. The meter had previously been calibrated on a single tone. A second tone, also having an intensity corresponding to the loudness contour, was then added at such a frequency that masking should have been negligible. The measurements were repeated. This process was continued up to a total of five tones. As the number of tones increased, there was an increasing discrepancy between the objective and subjective measurements, and a smooth curve drawn through the measured points showed that the objective meter, when measuring five components, was reading some 8 db. lower than the subjective estimation of equivalent loudness.

* *J. Acoust. Soc. Amer.* (October 1936).

This emphasizes that the objective noise-meter cannot, with a single calibration, be used for the universal measurement of equivalent loudness, but requires calibration in a laboratory by a primary method against a sound whose spectrum is similar to that of the sound to be measured.

Dr A. H. Davis. Dr Drysdale has referred to the use of resonance in the design of acoustically absorbent materials. He may be interested to know that E. Meyer* and others have discussed acoustical absorbents composed of layers of foil or other thin material with resonant layers of air.

A standard source of sound would of course be useful as Dr Drysdale suggests, but it should be remembered that a standard source probably had more importance in the early days of optics than it has now in acoustics, where the sound emitted from a source may be measured in absolute mechanical units, without the use of a standard source.

I wish to refer also to one or two general aspects of electroacoustical measurements, and to one or two particular problems presented at the terminal points of electroacoustical systems. In general, sound-intensity measurements are on an exact basis. Methods exist for measuring the sensitivity of microphones and loudspeakers over the frequency range. At the National Physical Laboratory two distinct bases are employed for calibrations of microphones; one employs the Rayleigh disc as the ultimate standard of sound measurement, and the other uses known pressure variations set up by a controllable piston in an enclosed space of known volume. The two methods agree excellently and thus show that intensity measurements are on a safe foundation.

Certain special questions arise when the output of telephone receivers and similar devices is considered; for telephone receivers are used, in practice, with the human ear as a terminating impedance, and their output depends upon the nature of this impedance. Human ears vary enormously, and the question arises: What should be the characteristics of an artificial ear intended to represent the average human ear as a terminating impedance when the pressures set up in the ear by the receiver are being measured? To a large extent this problem has been solved, and we know the relation between the acoustical pressures exerted in the ear canal and the resultant loudness of the sound concerned. But an analogous case arises in assessing the output of hearing aids of the bone-conduction type, in which the receiver is a vibrating point or button which is applied not to the ear but to the mastoid bone. In this case what terminating impedance corresponds to the average skin-covered bone of the human head? What are the real thresholds from which one should measure?

The question of measuring the distortion which arises in any electroacoustical system from lack of proportionality between the stimulus and the response has been much discussed, but still seems to be somewhat open. One can measure the total production of harmonics consequent upon the distortion of a pure tone input; one can go further and weight the harmonics before summation on the ground that

* *Elect. Nachr.-Tech.* **13**, 95 (1936).

they are not all equally loud to the ear. On the other hand one can take the view that these harmonics themselves are not seriously detrimental in the reproduction of sound, but that what matters is the extent to which undesirable difference tones are produced when a sound composed of two or more components is injected into the system. Only experiment can decide which criterion, if any, gives the most useful figure, and it would be very interesting to hear the views of those who have had practical experience of any correlation between the effects of distortion and numerical estimates of its magnitude.

Two important recent achievements in electroacoustical instruments relate to measurements on noise. One is the production of an analyser whereby one can record, on a cinema camera, the changing constitution of sounds, a cathode-ray screen showing instantaneously the intensity of sound in the various audiofrequency bands. The other is the development of objective noise-meters for determining the equivalent loudness of sounds by means of an indicating instrument, and without suspicion of personal bias. Since the ear is not equally sensitive to sounds of all pitches the sensitivity of the meter has to vary with pitch in the same manner as that of the ear. Without certain additional adjustments, however, such a meter will not normally measure repeated impulsive sounds. For dealing with them the meter needs to be given appropriate electrical characteristics which are equivalent to a certain amount of transient memory. I will not go into details, but a recently published paper* gave particulars of the development of such a meter at the National Physical Laboratory, for moderate and loud noises, and showed the wave-forms of varied types of noise for all of which the meter gives results in satisfactory agreement with subjective measurements of loudness.

* A. H. Davis, *J. Instn Elect. Engrs*, **83**, 249 (1938).

THE INVESTIGATION OF ELECTRON LENSES

By O. KLEMPERER, Ph.D., Research Department, Electric and Musical Industries Limited

AND

W. D. WRIGHT, A.R.C.S., D.Sc., Imperial College of Science and Technology

(*Continued from* p. 317)

DISCUSSION

Prof. L. C. Martin. The authors of this paper have shown successfully that familiar optical methods can be usefully employed in new investigations, and they are to be congratulated on several achievements of obvious value. I shall be glad, however, if they can deal more specifically with a difficulty which I feel in relation to the basis of the aberration calculations in the earlier part of the paper.

They point out that the equipotential surfaces are non-spherical; hence if the typical equation of such a surface in terms of the generating curve

$$x = ay^2 + by^4 + cy^6 + \dots$$

is considered, we find that the coefficients of the terms in y^4 and y^6 etc. will differ from those characteristic of a sphere of the same axial curvature. The coefficient of primary spherical aberration due to the surface will depend on the term in y^4. When y is so small that the term in y^4 is inappreciable, we have reduced the consideration to the paraxial case.

In the paper it appears to be argued that since on the drawing-board we can fit a spherical curve to an equipotential trace fairly well if we neglect the outer parts of the curve, we shall obtain a true measure of the spherical aberration by assuming the sphericity of the surfaces and applying formulae appropriate to a sphere but using very small values of y. This does not seem to be valid, unless it can be shown independently that the equipotential surfaces near the axis are spherical to a second degree of approximation.

The confirmation of the results by practical tests does not reassure me as much as it might, since, as the authors point out, the accuracy of the Hartmann test for the paraxial region is very low, and the form of the aberration curve in the neighbourhood of the axis is not easy to make sure of. On the other hand a knowledge of the true primary aberration is essential for the small-aperture beams employed in electron microscopy.

The whole subject is of such great importance that a thorough analysis of the question I have raised is very desirable. If the determination of the spherical aberration of electron-optical systems can be effected without most laborious integrations it will be a great gain to practice.

AUTHORS' reply: We appreciate Prof. Martin's point and agree that it is probably rather rash to conclude that the trigonometrical method would give an accurate value of the spherical aberration occurring in the narrow pencils of electrons used in electron microscopy. However, in view of the inevitable approximations in almost any method of evaluating the aberration, we feel that the main value of theoretical calculations lies in the extent to which they can be used as a tool for improving the design of electron lenses. Thus it is extremely useful to know in what direction a certain change in the shape of the equipotential surfaces will tend to modify the positive and negative contributions to the final aberration. For this purpose we believe that in the general case the trigonometrical method is eminently suitable. Examination of the experimentally determined equipotential surfaces shows that at either end of the field plot, where the aberration contributions are greatest, the curvature of the surfaces increases at a short distance from the axis, a deviation that in general will increase the arithmetical value of the aberration arising at each surface. Hence the error introduced in the trigonometrical method is one of degree rather than of kind, and will not appreciably affect its value as a designing tool. It is, of course, true that with certain types of electrode structure the equipotential surfaces might be distorted in such a way that the positive surfaces would introduce negative aberration and vice versa; in that case the main application of the trigonometrical method would have to be confined to the determination of the optical constants of the system.

It is worth pointing out that, although the primary spherical aberration depends on the y^4 term in Prof. Martin's equation, the Petzval curvature depends on the y^2 term. The evaluation of this quantity is not, therefore, in question.

REVIEWS OF BOOKS

Physical Science in Modern Life, by E. G. Richardson. Pp. 256. (London: The English Universities Press.) 8*s*. 6*d*. net.

It is refreshing to find a book on physics intended primarily for the layman which does not give the impression that physics is synonymous with "atom-splitting and electron-chasing". In fact Dr Richardson in this book has "set his back to the atom and the molecule" and deals with macroscopic, not microscopic, phenomena. It is not generally realized how much advance there has been in recent years in the less spectacular branches of physics; for example recent work on convection has done much to foster improvements in engines, cooling and ventilation, and there is an interesting section on this topic. Dr Richardson concerns himself with those recent advances in physics which make contact with our everyday existence and which have specially interested him. Among these are sound and supersonics, sensation and reaction, items about heat and light, and the exploration of the stratosphere. On the whole the style is pleasing and the diagrams and photographic reproductions are excellent. The printing and production of the book leave nothing to be desired.

H. R. L.

The Amplification and Distribution of Sound, by A. E. Greenlees, A.M.I.E.E. Pp. xiii + 254, with 82 diagrams. (Chapman and Hall, Ltd., 1938.) 10*s*. 6*d*. net.

In recent years the artificial reproduction of speech and music has found extensive application in many fields. In auditoria too large for the unaided voice to reach remoter members of the audience, amplification can provide satisfactory hearing for all, and even where defective hearing is due to bad acoustical properties of the auditorium, some improvement may usually be obtained by the use of a suitably designed public-address system. In the open air the amplified voice may address large crowds, as for instance at sports meetings, or may be used for the control of traffic, or for the direction of passengers at railway stations. The amplification of music is used to raise the volume of sound from a small orchestra, or to enable it to serve several rooms at the same time, while the reproduction of music from disc or film records has largely replaced the cinema orchestra. Even the steam organ of the roundabout is being ousted by the loudspeaker.

The design of amplifying equipment is governed by the purpose for which it is to be employed, and correct choice or design requires both a proper understanding of the acoustical considerations involved and a knowledge of the characteristics of the various types of microphones, amplifiers and loudspeakers which are available. The author has sought to bring together in this volume all the relevant information required for the specification, lay-out and operation of sound-amplifying equipment. He deals with the component parts of equipment for operation from microphones, from disc or film records, and from radio receivers, and describes the planning of complete installations for various purposes and their operation and maintenance. On the practical side the choice of material is good and fairly complete, though some reference might have been made to the high-frequency type of loudspeaker, and to the power microphone which can operate a loudspeaker directly without the need for an intermediate amplifier. Of necessity little detail is given of the various types of components which may be employed, but the book provides an adequate summary of the essential features which govern the choice of the appropriate type and, to some extent, the general lay-out of the equipment for the particular purpose in view. In the chapter on fundamentals the choice of material is not so good. Indeed, the questions dealt with are entirely electrical, and no reference is made

to acoustics, a subject on which one might expect the average reader to be more in need of instruction. The text is well illustrated with diagrams, and numerical examples are freely used. In converting power ratios to decibel changes and vice versa, however, the practice of quoting the result to an accuracy entirely unwarranted by the data should have been avoided. The acoustical engineer is rarely interested in any fraction of a decibel, and never in a thousandth part.

The book can be strongly recommended to those engaged or interested in the planning, installation or operation of sound-amplifying equipment. N. F.

The Perception of Light: An Analysis of Visual Phenomena in Relation to Technical Problems of Vision and Illumination, by W. D. Wright, D.Sc., A.R.C.S. Pp. 100. (London and Glasgow: Blackie and Son, Ltd.) Price 6*s*. net.

This little book of 95 pages is a valuable addition to the literature of vision. The author has made a useful selection of his material, and the amount of space given to various subjects, though necessarily limited in a book of this size, is well balanced, with the result that the reader is left with the impression that far more ground has been covered than is accomplished by many books of more pretentious dimensions.

The scope is indicated by the chapter headings—General account of visual phenomena; Vision at low intensities; Vision at high intensities; Glare; Visual sensations; Recent researches—and under each of these heads much useful information is given. The book forms an excellent introduction to the study of vision for students or others who wish to be launched well into the subject with a minimum of reading. The writers of text-books usually, and very naturally, have views of their own on those problematical aspects of their subjects which are still controversial, and it is important that the reader should not be led by the method of presentation to regard as a generally accepted doctrine some speculation or theory which has not yet acquired this status. Dr Wright gives exceptionally little ground for complaint in this respect but, probably through inadvertance, his treatment of the vexed and difficult question of the quantitative relatedness of sensations is open to criticism. For example, he states that within the range of intensities for which $\Delta I/I$ (the Weber fraction) is approximately constant, and for which also brightness-contrast is largely dependent on ratio of intensities, the integrated curve of $\Delta I/I$ will correspond to a sensation-interval scale. The statement is made as though there were no doubt about the conclusion following from the postulated facts, whereas there are many authorities who would deny the validity of the conclusion. In later editions, for which there will no doubt be a demand, the author should remedy this defect, not necessarily by retracting such views as he may hold, but by giving some account of the philosophical difficulties which have arisen in connexion with this part of the subject, and indicating the conflict of views which at present exists on the applicability of quantitative concepts to sensations.

But we must not end on a note of criticism where so much is deserving of commendation: all who are interested in the subject of visual perception will find both profit and pleasure in reading Dr Wright's book. J. G.

Ferromagnetism: The Development of a General Equation to Magnetism, by J. R. Ashworth, D.Sc., formerly Hon. Research Fellow of the University of Manchester. Pp. xiii + 97. (London: Taylor and Francis, Ltd.)

For many years Dr Ashworth has been the leading exponent of the idea that the variation of the intensity of magnetization of a ferromagnetic is closely analogous to the changes of density of a fluid under similar conditions of temperature. In his view, the

relation between the intensity of magnetization, applied field and absolute temperature takes the same form as Van der Waals' equation for a gas, the quantity H replacing p, an expression containing the intensity of magnetization replacing the a/v^2 term, and the reciprocal of the maximum intensity of magnetization at low temperatures replacing the b term of the more familiar gas equation.

Now it is obvious that such analogies have an individual rather than a general appeal, and it is possible that, in the modern literature, they have not been given as careful a consideration as they deserve. Consequently, the monograph before us may be treated as a complete, authoritative exposition of these analogies, which should rectify any lack of treatment elsewhere, and each physicist can judge for himself whether they are likely to assist him in his outlook on magnetic problems. At any rate, he can assess for himself the experimental facts bearing upon the subject which the author surveys. But the author does not introduce modern quantum conceptions into his work, and the reviewer feels that very much experimental and theoretical work has been done in the last ten years in connexion with magnetostriction and energy changes associated with ferromagnetism which the author should have taken into account. L. F. B.

Gaseous Electrical Conductors, by Prof. E. L. E. Wheatcroft. Pp. xi+265. (Oxford Engineering Science Series. London: Humphrey Milford, Oxford University Press.) 21*s*. net.

It is fitting that the Oxford Engineering Science Series should include a volume on gaseous conduction, a subject which now interests engineers as well as physicists. The fact that gases can become relatively good conductors creates difficulties for the engineer interested in high voltages and in switch design, but it also gives us the mercury arc rectifier, the thyratron, and the luminous discharge tube. Prof. Wheatcroft's book contains much information on this subject in a compact form and it will be of value both to the physicist and to the engineer. A considerable portion of the book deals with the various fundamental phenomena involved, and this makes it suitable for the reader with but little previous knowledge. The essentials of the kinetic theory of gases, thermionic and photoelectric emission, secondary electron emission, motion of ions in electric and magnetic fields, and space charge effects are treated adequately and give the book a wider appeal than it might otherwise have. Then follows a discussion on the nature of the glow, corona, arc and spark. The second part of the book is concerned mainly with practical applications; vacuum technique, vacuum and gas-filled tubes, circuit breakers, and luminous discharge tubes are amongst the subjects discussed. Throughout the book a considerable amount of mathematical treatment has been given without making it too heavy for non-mathematical readers. It is well balanced in this respect.

It is surprising to find that the author has used for the quantum of energy emitted the symbols hf instead of the very widely accepted notation $h\nu$. One would like to have seen more consideration of the breakdown of various gases under high pressures, with mention of the case of freon. Although considerable attention has, very properly, been given to thyratrons, no reference is made to their de-ionization time. It is a pity that a book of this type should not have a more adequate index. The entries amount only to about one per page, but this deficiency is offset to some extent by the clearly set-out table of contents. This volume can be recommended without hesitation as a good general text-book on the subject with which it deals. E. T. S. W.

The Properties of Glass, by GEORGE W. MOREY. Pp. 561. (New York: Reinhold Publishing Corporation; London: Chapman and Hall.) Price 62*s.* 6*d.*

Glass is such a common substance and has such diverse uses that a collected and critical account of its properties is certain to be appreciated by many readers. Dr Morey evidently knows his subject, and must have given years to the collection, not merely of such obviously useful data as the refractive index, but also of incidental references in non-technical literature, both ancient and modern. It thus comes about that chapter 1, on the history and definition of glass, is good reading, however superficial our interest may be. We learn how the Assyrians made glass, taking care to use styrax wood which had been cut in the month of Ab as fuel, and in addition we are shown the results of modern analyses of glasses made as early as the fifteenth century B.C. Apparently the definition has always given trouble. Merrett in 1662 set out 26 properties which jointly defined the material, of which a few are worth quoting: "20 'Tis the most plyable and fashionable thing in the world, and best retains the form given. 21 It may be melted but 'twill never be calcined. 22 An open glass fill'd with water in the summer will gather drops of water on the outside, so far as the water reacheth, and mans breath blown upon will manifestly moisten it."

After this introduction, the book deals with the chemical side of its subject, and proceeds to mechanical aspects such as viscosity, the annealing process, and surface tension. Then follow thermal conductivity, heat capacity and thermal expansion, and elasticity, strength and hardness. A long chapter is naturally devoted to the optical properties, and here one misses any reference to British optical glass. The value of the data is greatly enhanced by the fact that the chemical composition is given for each glass as well as the optical properties.

Chapters 17 to 19 are occupied with data and discussions on electrical and magnetic properties, and the final chapter, headed "The constitution of glass", includes both the X ray and other evidence. There is a large index, and the blank pages at the end headed "memoranda" should be very useful.

The book is beautifully produced, and the high cost is doubtless justified by the expense of production and the smallness of the probable market. Nevertheless, the cost is to be regretted, for it must put the work out of the reach of most individuals, restricting the possible market almost entirely to libraries. J. H. A.

The Physical Properties of Colloidal Solutions, by E. F. BURTON. Pp. viii + 235. (London: Longmans, Green and Co. 1938. Third edition.) Price 15*s.* net.

The preface to the third edition begins as follows: "On completion of the manuscript for this edition it was found that somewhat over one-half was completely new matter. There has been considerable rearrangement of the material and orientation of emphasis." Notwithstanding these changes, the book is still far from fulfilling the promise of its title: it deals exclusively with suspensoid (or lyophobic) sols and does not discuss the larger and, as most people will think, more important class of emulsoid (or lyophilic) colloids. The preference thus shown is perhaps natural in a physicist, whose "aim has been to accentuate the contribution of the study of colloidal solutions to the confirmation of the basic principles of the kinetic theory of matter". The Brownian movement, the distribution of particles, and the determination of Avogadro's number certainly receive very full treatment, but it seems doubtful whether this will be of any satisfaction to the reader who may reasonably expect to find information on silicic acid, proteins, or rubber in a book on colloidal solutions.

Optical properties, electrokinetic phenomena, and electrolyte coagulation are treated adequately on recognized lines; brief reference only is made to modern theories (such as

Pauli's) of the origin of the charge on colloidal particles. The account of Smoluchowski's work on coagulation-velocity does not give the simple formula for the number of primary particles surviving after a time t, though it is the one most easily verified experimentally.

A brief concluding chapter again emphasizes the importance of the contributions made to physics by the study of suspensoid sols, and a number of outstanding problems, exclusively connected with these systems, are defined.

"The phenomena of adsorption which *is* of the very greatest moment..." (p. 225; the italics are the reviewer's) must be an unfortunate oversight on the part of the proof-reader. E. H.

Ultrasonics, by L. BERGMANN, translated by H. S. HATFIELD. Pp. viii+264. (London: G. Bell and Sons, 1938.) Price 16*s*.

The applications of supersonics have so multiplied since the piezoelectric oscillator came into being, that the English-speaking reader will welcome the appearance of this textbook. It contains five chapters. The first deals with various types of generator, including the mechanical precursors of the magneto-strictive and piezoelectric sources, and includes some useful practical data in the form of circuits and coil-sizes for the latter, not forgetting hints on persuading a stubborn crystal to oscillate. The second chapter deals with the various methods for detecting the radiation, including the now well-known one by which the supersonic beam is made to act as an optical grating. In the third and fourth chapters we find comprehensive accounts of experiments on the propagation of waves in fluids and solids. The final chapter deals with the more spectacular effects and technical applications. In the bibliography which follows a number of important British and American papers have been overlooked, whereas some French papers have crept in which should surely not have been admitted, since they deal with sound measurements in the audible region or with *ondes de choc* which are not usually classified under ultrasonics; this is, however, a venal fault, and does not detract from the value of the first general account of the subject in the English language. Actually this is the second book in the German tongue, another on similar lines having appeared in 1934. The publishers have naturally selected Dr Bergmann's more up-to-date book for translation. Dr Hatfield's translation is uniformly good. E. G. R.

Under the general heading *Actualités Scientifiques et Industrielles* we have received the monographs listed below. Each is written by an authority on his subject and the treatment is, in general, concise and clear. The publishers are Hermann and Co., 6 Rue de la Sorbonne, 6, Paris.

562. B. CABRERA. *Dia- et Paramagnétisme et Structure de la Matière.* 20 fr.
569. W. JEUNEHOMME. *Calcul des Équilibres Physico-Chimiques.* 20 fr.
574. F. BEDEAU. *Théorie et Technique du Bruit de Fond.* 25 fr.
613. S. RYTOV. *Diffraction de la Lumière par les Ultra-sons.* 15 fr.
626. MAURICE PROST. *Travaux Pratiques de Physique. I. Mesures. Chaleur.* 25 fr.
627. PIERRE DUBOIS. *Les Cristaux Mixtes et leur Structure.* 12 fr.
635. JULIEN PACOTTE. *L'Espace Hermitien Quantique.* 12 fr.

PRINTED IN GREAT BRITAIN BY WALTER LEWIS, M.A., AT THE UNIVERSITY PRESS, CAMBRIDGE